

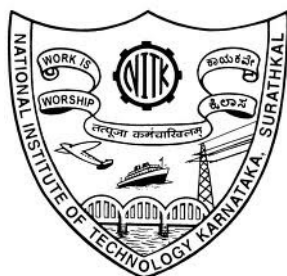
DESIGN AND SYNTHESIS OF NEW DONOR-ACCEPTOR TYPE CONJUGATED POLYMERS FOR PHOTONIC APPLICATIONS

Thesis

Submitted in partial fulfillment of the requirements for the degree of
DOCTOR OF PHILOSOPHY

by

VISHNUMURTHY K. A.



DEPARTMENT OF CHEMISTRY

NATIONAL INSTITUTE OF TECHNOLOGY KARNATAKA

SURATHKAL, MANGALORE – 575 025

July - 2012

DESIGN AND SYNTHESIS OF NEW DONOR-ACCEPTOR TYPE CONJUGATED POLYMERS FOR PHOTONIC APPLICATIONS

Thesis

Submitted in partial fulfillment of the requirements for the
degree of

DOCTOR OF PHILOSOPHY

by

VISHNUMURTHY K. A.

(CY08F09)

Research supervisor

PROF. A. VASUDEVA ADHIKARI



DEPARTMENT OF CHEMISTRY

NATIONAL INSTITUTE OF TECHNOLOGY KARNATAKA

SURATHKAL, MANGALORE – 575 025

July - 2012

DECLARATION

By the Ph.D. Research Scholar

I hereby *declare* that the Research Thesis entitled “**Design and synthesis of new donor-acceptor type conjugated polymers for photonic applications**” which is being submitted to the **National Institute of Technology Karnataka, Surathkal** in partial fulfillment of the requirements for the award of the Degree of **Doctor of Philosophy in Chemistry** is a *bonafide report of the research work carried out by me*. The material contained in this Research Thesis has not been submitted to any University or Institution for the award of any degree.

Vishnumurthy K. A.

Reg. No. CY08F09

Department of Chemistry

Place: NITK – Surathkal

Date: 27 - 07 - 2012

CERTIFICATE

This is to *certify* that the Research Thesis entitled “**Design and synthesis of new donor-acceptor type conjugated polymers for photonic applications**” submitted by **Mr. Vishnumurthy K. A.** (Register Number: CY08F09) as the record of the research work carried out by him is *accepted as the Research Thesis submission* in partial fulfillment of the requirements for the award of degree of Doctor of Philosophy.

Prof. A. Vasudeva Adhikari

Research Guide

Date: 27 - 07 - 2012

Chairman – DRPC

Date: 27 - 07 - 2012

DEDICATED TO MY

BELOVED PARENTS

ACKNOWLEDGEMENTS

I would like to express my deep sense of gratitude to my research supervisor Prof. A. Vasudeva Adhikari, Department Chemistry, NITK for his invaluable guidance and help rendered throughout the course of this investigation, without which I would not have completed this thesis successfully. The direction he gave and knowledge he shared in each and every single step of this work made it all possible. I am extremely thankful to him for all the help he rendered during my research.

I am thankful to Prof. Sandeep Sancheti, Director, NITK and Prof. A.C. Hegde, Head, Chemistry Department for providing necessary facilities to carry out this research work.

My special thanks are due to Dr. Reji philip, Associate Professor, LASER, Optics group, Raman Research Institute, Bangalore for providing laboratory facilities for NLO studies. Also I thank his group members Smijesh N. A. and Safakath K, for their support for analyzing samples for Z-scan study.

I thank Prof. A.N. Shetty, Dr. B.R. Bhat, Dr. D.K. Bhat, Dr. A.M. Isloor and Dr. Udaya Kumar for their constant support. I also thank RPAC members Dr. Uday Bhat and Dr. D.R. Trivedi, for giving valuable suggestions towards my research.

My special thanks to NMR Research Centre, IISc, Bangalore, SAIF Gujarat and RRI Bangalore, for providing instrumental analysis data of my samples.

I have to remember always and thank my friends Manjunath M.G, Pramod Hegde, Ravi K., Sumesh E., Thomas K.D, Sunitha M.S, Shrikanth U and Ahipa T.N for their regular help, suggestions and company.

I would like to thank all the research scholar friends of Chemistry and Physics Department, NITK, for their help and support. I also thank non-teaching staff members of Chemistry Department, Mrs. Kasthuri Rohidas, Mr. Prashanth, Mr. Pradeep, Mr. Ashoka, Mrs. Sharmila, Ms. Deepa and Mr. Harish for their help in the department.

Finally, I would like to thank my father, K. N Ananthapadmanabha Bhat and mother, Satyavathi, for their constant support and encouragement. Also, I thank all of my family members for their love and constant support.

Vishnumurthy K. A.

ABSTRACT

In recent years, a great deal of interest has been focused on the synthesis of novel D-A type conjugated polymers because of their excellent photonic properties. Recently, lots of attentions have been dedicated towards the development of new D-A type polymers with desired properties through proper structural modifications. In this context, the proposed research work has been aimed at design and synthesis of new D-A type conjugated polymers with improved photonic properties. Based on the literature review, five new series of D-A type conjugated polymers (**P1-P20**) carrying various electron donors and acceptor moieties have been designed.

Seven series of bi-functional monomers required for the synthesis of new polymers have been prepared using appropriate synthetic procedures. Structures of new intermediates and monomers have been evidenced using spectral and elemental analyses. Starting from these monomers, five new series of target polymers, viz. (i) poly(3,4-ditetradecyloxythiophene)s carrying thiophene, naphthalene, isophthalyl, vinyl and pyrazole moieties as π -conjugated spacers (**Series 1, P1-P5**), (ii) poly(cyanopyridines) containing phenyl, carbazole, alkoxythiophene phenothiazine and diphenyl amine based electron donating bridges (**Series 2, P6-P10**), (iii) poly(3,4-ditetradecyloxythiophene)s involving vinylene π -conjugated spacers (**Series 3, P11-P14**), (iv) poly(3,4-ditetradecyloxythiophene)s carrying aromatic conjugated cyclic imides (**Series 4, P15 and P16**), and (v) poly(3,4-ditetradecyloxythiophene)s with imine functionalized electron donors as π -conjugated bridges (**Series 5, P17-P20**), have been successfully synthesized and their synthetic protocols have been established. Their structures have been confirmed by different spectroscopic and elemental analyses. Their molecular weights have been determined by GPC technique and thermal properties have been evaluated by TGA studies. Electrochemical properties have been studied using CV experiments. The linear optical characteristics have been estimated by UV-visible absorption and fluorescence emission spectroscopy. Their fluorescent quantum yields and solvatochromic behavior have been determined. Finally, their third-order NLO properties have been investigated using open aperture Z-scan technique to investigate their optical limiting behavior. Most of the polymers have exhibited promising results.

Key words: D-A type Conjugated polymers, Fluorescence, Solvatochromism, NLO.

CONTENTS

	Page No.
CHAPTER 1	
GENERAL INTRODUCTION	
1.1. INTRODUCTION	1
1.2. HISTORY	1
1.3. ORGANIC CONJUGATED POLYMERS	2
1.4. DOPING	3
1.5. SYNTHESIS	4
1.5.1. Chemical polymerization	4
1.5.2. Electrochemical polymerization	4
1.6. CONDUCTION MECHANISM	5
1.6.1. Band theory	5
1.6.2. Polaron-bipolaron model	6
1.7. BAND GAP	8
1.7.1. Factors affecting band gap	8
1.8. DONOR ACCEPTOR APPROACH	10
1.9. APPLICATIONS OF CONJUGATED POLYMERS	12
1.9.1. Polymer light emitting diodes (PLED)s	13
1.9.2. Polymer photovoltaics (PV)	15
1.9.3. Nonlinear optics (NLO)	17
1.9.3.1. Polymer nonlinear optics	20
CHAPTER 2	
LITERATURE REVIEW, SCOPE, OBJECTIVES AND DESIGN OF NEW CONJUGATED POLYMERS	
2.1. INTRODUCTION	23
2.2. LITERATURE REVIEW	23
2.2.1. Thiophene based conjugated polymers	24
2.2.2. Conjugated polymers containing 1,3,4-oxadiazole units	32
2.2.3. Cyanovinylene based conjugated polymers	37

2.2.4. Pyridine based conjugated polymers	40
2.2.5. Pyrazole based conjugated polymers	43
2.2.6. Naphthalene based conjugated polymer	45
2.2.7. p-Phenylenevinylene based conjugated polymers	46
2.2.8. Carbazole containing conjugated polymers	49
2.2.9. Conjugated cyclic polyimides	52
2.2.10. Phenothiazene and diphenylamine based conjugated polymers	55
2.3. SCOPE AND OBJECTIVES OF THE PRESENT WORK	58
2.4. DESIGN OF NEW CONJUGATED POLYMERS	60

CHAPTER 3

SYNTHESIS OF MONOMERS

3.1. INTRODUCTION	68
3.2. MATERIALS AND INSTRUMENTATION	68
3.3. SYNTHESIS OF 3,4-DIALKOXYTHIOPHENE-2,5-CARBOXYDI HYDR- AZIDES (6a,b)	69
3.3.1. Chemistry	69
3.3.2. Synthesis and characterization	70
3.3.3. Results and discussion	71
3.4. SYNTHESIS OF THIOPHENYL TRIPHENYLPHOSPHENE DERIVATIVE (10)	72
3.4.1. Chemistry	72
3.4.2. Synthesis and characterization	73
3.4.3. Results and discussion	76
3.5. SYNTHESIS OF DITHIOPHENE DICARBOXALDEHYDE (13)	77
3.5.1. Chemistry	78
3.5.2. Synthesis and characterization	78
3.5.3. Results and discussion	82
3.6. SYNTHESIS OF 3,4-DIDOCYLOXYTHIOPHENE -2, 5-DICARBOX ALDE- HYDE	82
3.6.1. Chemistry	82
3.6.2. Synthesis and characterization	83

3.6.3. Results and discussion	84
3.7. SYNTHESIS OF CYANOPYRIDINE TRIPHENYLPHOSPHINE SALT (19)	85
3.7.1 Chemistry	85
3.7.2 Synthesis and characterization	86
3.7.3 Results and discussion	89
3.8. SYNTHESIS OF N-TETRADECYLSUBSTITUTED PHENOTHIAZINE-/ CARBAZOLE-/ DIPHENYLAMINE DICARBALDEHYDES (20, 22, 24)	90
3.8.1. Chemistry	90
3.8.2. Synthesis and characterization	91
3.8.3. Results and discussion	94
3.8. SYNTHESIS OF DIAMINE MONOMER CARRYING THIOPHENE AND OXADIAZOLE RINGS	94
3.9.1. Chemistry	94
3.9.2. Synthesis and characterization	95
3.9.3. Results and discussion	98
3.10. CONCLUSIONS	99
 CHAPTER 4	
 SYNTHESIS OF NEW CONJUGATED POLYMERS	
4.1. INTRODUCTION	100
4.2. MATERIALS AND INSTRUMENTATION	100
4.3. SYNTHESIS OF DIALKOXYTHIOPHENE BASED POLYMERS (SERIES 1, P1-P5)	101
4.3.1. Chemistry	102
4.3.2. Synthesis and characterization	102
4.3.3. Results and discussion	107
4.4. SYNTHESIS OF CYANOPYRIDINE BASED POLYMERS (SERIES 2, P6-P10)	108
4.4.1. Chemistry	109
4.4.2. Synthesis and characterization	110
4.4.3. Results and discussion	111

4.5. SYNTHESIS OF OXADIAZOLE BASED POLYMERS	
(SERIES 3, P11-P14)	114
4.5.1. Chemistry	115
4.5.2. Synthesis and characterization	116
4.5.3. Results and discussion	119
4.6. SYNTHESIS OF CYCLIC IMIDE POLYMERS	
(SERIES 4, P14 AND P15)	120
4.6.1. Chemistry	120
4.6.2. Synthesis and characterization	121
4.6.3. Results and discussion	123
4.7. SYNTHESIS OF IMINE CONTAINING POLYMERS	
(SERIES 5, P17-P20)	124
4.7.1. Chemistry	124
4.7.2. Synthesis and characterization	124
4.7.3. Results and discussion	128
4.8. CONCLUSIONS	129

CHAPTER 5

ELECTROCHEMICAL STUDIES OF THE POLYMERS

5.1. INTRODUCTION	130
5.2. CYCLIC VOLTAMMETRY	130
5.3. EXPERIMENTAL PROTOCOLS FOR ELECTROCHEMICAL STUDIES	131
5.4. RESULTS AND DISCUSSION	132
5.5. CHARGE CARRYING PROPERTIES	144
5.6. CONCLUSIONS	149

CHAPTER 6

OPTICAL STUDIES OF THE POLYMERS

6.1. LINEAR OPTICAL PROPERTIES	150
6.1.1. UV-visible absorption and fluorescence emission spectral studies of polymers P1-P20	150

6.1.1.1. Instrumentation, materials and methods	151
6.1.1.2. Results and discussion	152
6.1.2. Solvatochromism study of cyanopyridine based polymers (P6-P10)	159
6.2. NONLINEAR OPTICAL PROPERTIES	162
6.2.1. Z-scan technique	162
6.2.2. Instrumentation, materials and method	163
6.2.3. Results and discussions	165
6.2.4. Conclusions	174
CHAPTER 7	
SUMMARY, CONCLUSIONS AND SCOPE FOR FUTURE WORK	
7.1. SUMMARY	175
7.2. CONCLUSIONS	177
7.3. SCOPE FOR FUTURE WORK	178
REFERENCES	180
LIST OF PUBLICATIONS	197
CURICULUM VITAE	199

LIST OF FIGURES, DESIGNS, SCHEMES AND TABLES

FIGURES

- Figure 1.1** Structures of some important conjugated polymers
- Figure 1.2** Types of doping in conjugated polymers and its applications
- Figure 1.3** Mechanism of electrochemical polymerization
- Figure 1.4** Illustration of band structure of various materials
(VB: valence band, CB: conduction band)
- Figure 1.5** Formation of polaron and bipolaron in poly(pyrrole)
- Figure 1.6** Formation of mid band-gap stages in doped polymers
- Figure 1.7** Factors affecting band gap
- Figure 1.8** Intra annular rotations in conjugated polymers
- Figure 1.9a** Structures of different electron donors
- Figure 1.9b** Structures of various electron acceptors
- Figure 1.10** Applications of conjugated polymers
- Figure 1.11** Schematic representation of polymer light emitting diode
- Figure 1.12** Different parts of polymer light emitting diodes
- Figure 1.13** Schematic representation of polymer solar cell
- Figure 1.14** Charge separations in a photovoltaic device
- Figure 1.15** Behaviour of linear and nonlinear optical materials
- Figure 1.16** Three level model for reverse saturable absorption
- Figure 3.1** FTIR spectrum of dihydrazide **6a**
- Figure 3.2** ¹H NMR spectrum of dihydrazide **6a**
- Figure 3.3** FTIR spectrum of biscarbohydrazide **7**
- Figure 3.4** FTIR spectrum of bisoxadiazole **8**
- Figure 3.5** ¹H NMR spectrum of bisoxadiazole **8**
- Figure 3.6** ¹H NMR spectrum of triphenylphosphene salt **9**
- Figure 3.7** FTIR spectrum of bisoxadiazole **12**
- Figure 3.8** ¹H NMR spectrum of bisoxadiazole **12**
- Figure 3.9** FTIR spectrum of dicarbaldedhyde compound **13**
- Figure 3.10** ¹H NMR spectrum of dicarbaldedhyde compound **13**

- Figure 3.11** ^1H NMR spectrum of dimethanol **14**
- Figure 3.12** ^1H NMR spectrum of dicarbaldedhyde **15**
- Figure 3.13** FTIR spectrum of cyanopyridine **17**
- Figure 3.14** ^1H NMR spectrum of cyanopyridine **17**
- Figure 3.15** FTIR spectrum of dibromomethylcyanopyridine **18**
- Figure 3.16** ^1H NMR spectrum of dibromomethylcyanopyridine **18**
- Figure 3.17** ^1H NMR spectrum of cyanopyridine wittig salt **19**
- Figure 3.18** FTIR spectrum of N-tetradecyldiphenylamine-3,6-dicarbaldehyde **24**
- Figure 3.19** ^1H NMR spectrum of N-tetradecyldiphenylamine-3,6-dicarbaldehyde
- Figure 3.20** Reaction mechanism of reduction of dinitro derivative **26**
- Figure 3.22** ^1H NMR spectrum of dinitro compound **26**
- Figure 3.21** FTIR spectrum of dinitro compound **26**
- Figure 3.24** ^1H NMR spectrum of diamine **27**
- Figure 3.23** FTIR spectrum of diamine **27**
- Figure 4.1** FTIR spectrum of polymer **PH1**
- Figure 4.2** ^1H NMR of polymer **PH1**
- Figure 4.3** FTIR spectrum of polymer **P1**
- Figure 4.4** ^1H NMR spectrum of polymer **P1**
- Figure 4.5** Thermogravimetric traces of polymers **P1-P5**
- Figure 4.6** FTIR spectrum of polymer **P8**
- Figure 4.7** ^1H NMR spectrum of polymer **P8**
- Figure 4.8** FTIR spectrum of polymer **P10**
- Figure 4.9** ^1H NMR spectrum of polymer **P10**
- Figure 4.10** Thermogravimetric traces of polymers **P6-P10**
- Figure 4.11** FTIR spectrum of polymer **P12**
- Figure 4.12** ^1H NMR spectrum of polymer **P12**
- Figure 4.13** FTIR spectrum of polymer **P14**
- Figure 4.14** ^1H NMR spectrum of polymer **P14**
- Figure 4.15** Thermogravimetric traces of polymers **P11-P14**
- Figure 4.16** FTIR spectrum of polymer **P15**
- Figure 4.17** ^1H NMR spectrum of polymer **P15**
- Figure 4.18** Thermogravimetric traces of polymers **P15** and **P16**

- Figure 4.19** FTIR spectrum of polymer **20**
- Figure 4.20** ^1H NMR spectrum of polymer **20**
- Figure 4.21** Thermo-gravimetric traces of conjugated polymers **P17-P20**
- Figure 5.1** Electrochemical reactions on electrode surface
- Figure 5.2** Structures of polymers **P1-P5**
- Figure 5.3** Cyclic voltammograms of polymers **P1-P5**
- Figure 5.4** Structures of polymers **P6-P10**
- Figure 5.5** Cyclic voltammograms of polymers **P8-P10**
- Figure 5.6** Structures of polymers **P11-P14**
- Figure 5.7** Cyclic voltammograms of polymers **P11-P14**
- Figure 5.8** Structures of polymers **P15** and **P16**
- Figure 5.9** Cyclic voltammograms of polymers **P15** and **P16**
- Figure 5.10** Structures of polymers **P17-P20**
- Figure 5.11** Cyclic voltammograms of polymers **P7-P20**
- Figure 5.12** Band diagram of polymers **P1-P5** with aluminum and ITO electrodes
- Figure 5.13** Band diagram of polymers **P6-P10** with aluminum and ITO electrodes
- Figure 5.14** Band diagram of polymers **P11-P15** with aluminum and ITO electrodes
- Figure 5.15** Band diagram of polymers **P16-P20** with aluminum and ITO electrodes
- Figure 5.14** Band diagram of **P8, P9, P13, P14**, CN-PPV, Th-CN-PPV and PCBM with aluminum, ITO electrodes
- Figure 6.1** Fluorescence emission process in conjugated polymers
- Figure 6.2a** UV-vis absorption spectra of polymers **P1-P5** in THF solution
- Figure 6.2b** Fluorescence emission spectra of polymers **P1-P5** in THF solution
- Figure 6.3a** UV-vis absorption spectra of polymers **P6-P10** in THF solution
- Figure 6.3b** Fluorescence emission spectra of polymers **P6-P10** in THF solution
- Figure 6.4a** UV-vis absorption spectra of polymers **P11-P14** in THF solution
- Figure 6.4b** Fluorescence emission spectra of polymers **P11-P14** in THF solution
- Figure 6.5a** UV-vis absorption spectra of polymers **P15-P16** in THF solution
- Figure 6.5b** Fluorescence emission spectra of polymers **P15-P16** in THF solution
- Figure 6.6a** UV-Vis absorption spectra of polymers **P17-P20** in THF solutions

- Figure 6.6b** Fluorescence emission spectra of polymers **P17-P20** in THF solutions
- Figure 6.7a** Fluorescence emission spectra of polymers **P6** and **P9** in different polar solvents
- Figure 6.7b** Fluorescence emission spectra of polymers **P10** in different polar solvents
- Figure 6.8** Experimental setup of open aperture Z-scan technique
- Figure 6.9a** Open aperture Z-Scan traces of polymers **P1**, **P2** and **P4**
- Figure 6.9b** Open aperture Z-Scan trace of polymer **P5**
- Figure 6.10a** Open aperture Z-Scan traces of polymers **P6** and **P8**
- Figure 6.10b** Open aperture Z-Scan traces of polymers **P9** and **P10**
- Figure 6.11** Open aperture Z-Scan traces of polymers **P12-P14**
- Figure 6.12** Open aperture Z-Scan traces of polymers **P15** and **P16**
- Figure 6.13** Open aperture Z-Scan traces of polymers **P17** and **P18**
- Figure 6.14** Open aperture Z-Scan traces of polymer **P19-P20**

DESIGNS

- Design-1** 3,4-Dialkoxythiophene based conjugated polymers **Series 1 (P1-P5)**
- Design-2** Cyanopyridine based conjugated polymers **Series 2 (P6-P10)**
- Design-3** Vinylic linkage containing polymers **Series 3 (P11-P14)**
- Design-4** Polymers with imide functionality **Series 4 (P15-P16)**
- Design-5** Polymers with imine functionality **Series 5 (P17-P20)**

SCHEMES

- Scheme 3.1** Synthesis of dihydrazide monomers **6a, b**
- Scheme 3.2** Synthesis of thiophenyl triphenylphosphene **10**
- Scheme 3.3** Synthesis of dithiophene-2-carbaldehyde **13**
- Scheme 3.4** Synthesis of 3,4-dialkoxythiophene 2,5-dicarbaldehyde (**15**)
- Scheme 3.5** Synthesis of cyanopyridine triphenylphosphine salt **19**
- Scheme 3.6** Synthesis of dicarbaldehydes of phenothiazene, carbazole, and diphenylamine (**20, 22, 24**)
- Scheme 3.7** Synthesis of diamine monomer **27**

- Scheme 4.1** Synthesis of polymers **P1-P2**
Scheme 4.2 Synthesis of polymers **P3-P5**
Scheme 4.3 Synthetic schemes for polymer **P6 - P10**
Scheme 4.4 Synthesis of polymers **P11-P14**
Scheme 4.5 Synthesis of polymers **P15** and **P16**
Scheme 4.6 Synthesis of polymers **P17-P20**

TABLES

- Table 5.1** Electrochemical characterization data of polymers **P1-P10**
Table 5.2 Electrochemical characterization data of polymers **P11-P20**
Table 5.3 Barrier energies of polymers **P1-P20**
Table 6.1 Linear optical characterization data of polymers **P1-P20**
Table 6.2 Solvatochromic behaviour of polymers **P6-P10**

ABBREVIATIONS

PLEDs	Polymer light emitting diodes
TPA	Two photon absorption
CV	Cyclic voltammetry
D-A	Donor-acceptor
EDOT	Ethylenedioxythiophene
ESA	Excited state absorption
FTIR	Fourier transform infra Red
NMR	Nuclear magnetic resonance
GPC	Gel permeation chromatography
FET	Field effect transistor
HOMO	Highest occupied molecular orbital
TFT	Thin film transistor
LUMO	Lowest unoccupied molecular Orbital
ITO	Indium tin oxide
NLO	Nonlinear optics
OLEDs	Organic light emitting diodes
PA	Poly(acetylene)
PEDOT	Propylenedioxythiophene
PPP	Poly(p-phenylene)
PPV	Poly(p-phenylenevinylene)
PPy	Poly(pyrrole)
PTh	Poly(thiophene)
TGA	Thermo gravimetric analysis
UV	Ultra violet
PDI	Poly dispersity index
M_w	Weight average molecular weight
M_n	Number average molecular weight
PS	Poly(styrene)
VB	Valance band
CB	Conduction band

E_g	Band gap
ICT	Intra molecular charge transfer
PV	Photovoltaic
χ⁽³⁾	Third order nonlinear optical susceptibility
RSA	Reverse saturable absorption
PBD	2-(4-tert-butylphenyl)-1,3,4-oxadiazole
PCE	Power conversion efficiency
β	Two photon absorption coefficient
THF	Tetrahydrofuran
DMF	N,N-Dimethylformamide
PL	Photo luminescence
EL	Electro luminescence
T_g	Glass transitions temperature
DDQ	Dichloro dicyano quinone
LAH	Lithium aluminium hydride
NMP	N-methylpyrrolidone
NBS	N-bromosuccinimide
BPO	Benzoyl peroxide
SCE	Standard calomel electrode
CNPPV	Poly(cyanoterephthalylidene)
DMSO	Dimethyl sulfoxide
CHCl₃	Chloroform
CDCl₃	Deuterated chloroform
DMSO D⁶	Deuterated dimethyl sulfoxide
RT	Room temperature
BPO	Benzoyl peroxide

CHAPTER 1

GENERAL INTRODUCTION

CHAPTER 2

LITERATURE REVIEW, SCOPE AND OBJECTIVES, AND DESIGN OF NEW CONJUGATED POLYMERS

CHAPTER 3

SYNTHESIS OF MONOMERS

CHAPTER 4

SYNTHESIS OF POLYMERS

CHAPTER 5

ELECTROCHEMICAL CHARACTERIZATION OF POLYMERS

CHAPTER 6

OPTICAL STUDIES OF POLYMERS

CHAPTER 7

SUMMARY AND CONCLUSIONS

Abstract

This chapter deals with a brief introduction to conjugated polymers covering important aspects of their properties. Also it explains the concepts of bandgap tuning, donor-acceptor approach and their major applications in various optoelectronic and photonic fields.

1.1. INTRODUCTION

Polymers are usually considered to be good insulators and the insulating properties of polymers are used in various applications of plastics. But some of the polymers show unique electronic properties because of the presence of delocalized π -electron system, which have a framework of alternating single and double carbon-carbon bonds. Such polymers are termed as conjugated polymers. Although the chemical structure of these materials is represented as alternating single and double bonds, in reality, the electrons that constitute the π -bonds are delocalized over the entire molecule. Although this class of polymers is in its infancy in between 1930's and 60's, the potential use of these polymers are discovered after 1960's.

1.2. HISTORY

Research on conducting polymers has roots back to the 1960s where Pohl, Katon and others first synthesized and characterized poly(sulfurnitride) (SN), which is a polymeric inorganic explosive. The discovery of the high thermal conductivity and interesting electrical properties of SN was a step towards conducting polymers as they are known today.

The beginning of conducting polymer research started nearly a quarter of century ago, when films of poly(acetylene) were found to exhibit profound increase in electrical conductivity when exposed to iodine vapor. This was the first report of polymers with high electrical conductivity (7×10^{-11} to $7 \times 10^{-3} \text{ Sm}^{-1}$). The procedure for synthesizing poly(acetylene) was based upon a route discovered in 1974 by Shirikawa and coworkers through serendipitous addition of 1000 times the normal amount of catalyst during the polymerization of acetylene, these films were also semi conductive and had bandgap energy of 1.4 eV. This work eventually resulted in the award of Nobel Prize in Chemistry in the year 2000 (Paoli et al. 2002).

1.3. ORGANIC CONJUGATED POLYMERS

Conjugated polymers are organic macromolecules consisting at least one chain of alternating double- and single bonds. These polymers are characterized by a conjugated π -electron system formed by the overlap of p_z orbitals of the sp^2 hybridized carbon atoms in the molecules. As compared to the σ -bond linkages in the backbone of the conjugated polymers, the π -bonding is significantly weaker. As a result, the lowest electronic excitations of conjugated molecules are the π - π^* transitions, which leads to light absorption or emission corresponding to the molecular energy bandgaps. Consequently these conjugated polymers find applications in the field of optical, optoelectronics and photonics. Some of the common conjugated polymers are poly(acetylene) (PA), poly(thiophene) (PT), poly(pyrrole) (PPy), poly(*p*-phenylene) (PPP), poly(*p*-phenylenevinylene) (PPV) and poly(fluorene) (PF). Their structures are given in **Figure 1.1**.

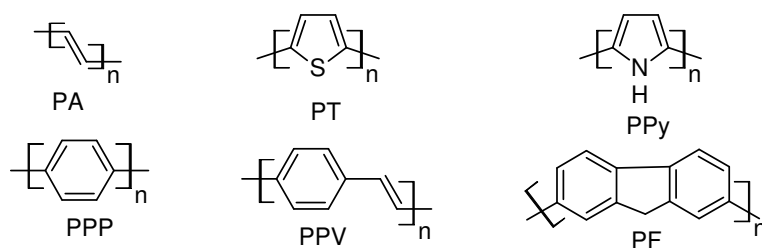


Figure 1.1: Structures of some important conjugated polymers

A number of conjugated polymers that studied in the early 1980s were based on heterocyclic compounds, which were synthesized using chemical and electrochemical polymerization techniques (Tourillon et al. 1986). Chemically synthesized conjugated polymers resulted in powders, which were insoluble and uncharacterizable (Diaz et al. 1979). The major interest in these polymers was their electrical conductivity and their corresponding electronic structure. On the other hand, electrochemical synthesis of conjugated polymers was a more attractive approach in which the synthesized polymer can form films on the surface of working electrode. Significant research on these polymer films was therefore performed to understand their spectro-electrochemical properties. In the mid 1980s, Elsenbaumer reported the groundbreaking synthesis of soluble conjugated polymers by attaching an alkyl side chain on poly(thiophene). Their solubility allowed structural characterization and easy processing using spin or drop cast methods (Miller et al. 1986).

In recent years, an extensive research on soluble conjugated polymers is growing in, due to their potential applications in electronic devices, such as field effect transistors (FETs), (Ong et al. 2004), light emitting diodes (LEDs) (Akcelrud et al. 2003), actuators, (Smela et al. 2003) and solar cells (Xue et al. 2004). The development of these soluble conjugated polymers has led to significant improvement in their properties such as high electrical conductivity (up to 2000 S/cm) (Kohler et al. 2002), high field effect mobilities ($\sim 0.12 \text{ cm}^2 \text{ V}^{-1} \text{ s}^{-1}$), LED efficiencies (up to 10%), and solar energy conversion efficiencies (4.2 %, Xue et al. 2004).

1.4. DOPING

Charge injection onto conjugated semiconducting macromolecular chain is termed as doping. This leads to the change of physical, chemical, electrochemical, and optical properties of a conjugated polymer (Heeger et al. 2000). Doping can be achieved by number of ways. Some of the methods are given below:

- i) Chemical doping by charge transfer, e.g. doping by iodine
- ii) Electrochemical doping, e.g. electrochemical polymerization
- iii) Doping by acid or base, e.g. doping of poly(aniline) by sulfuric acid
- iv) Photo doping, eg. doping by sunlight

Generally, doping of polymer chain leads to change in the chemical structure of conjugated polymer. Some of the applications of conjugated polymers according to its method of doping are given in **Figure 1.2**.

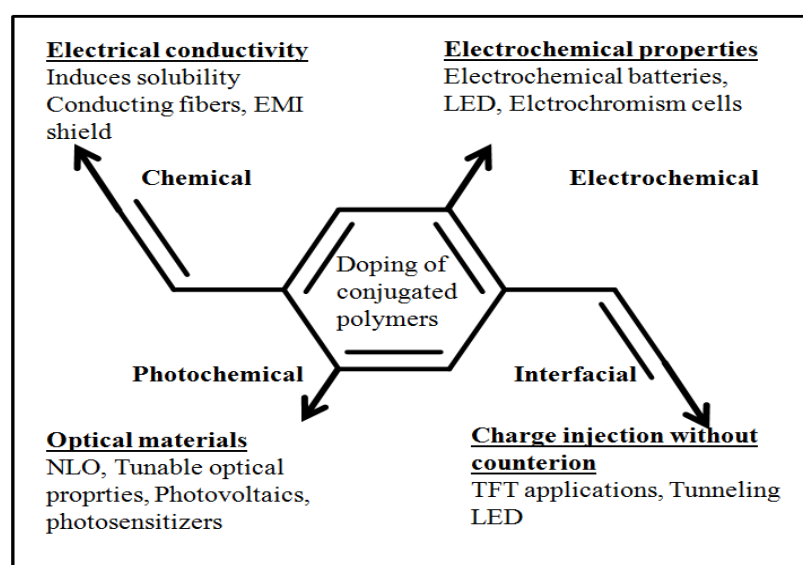


Figure 1.2: Types of doping in conjugated polymers and its applications

1.5. SYNTHESIS

Synthetic routes to conjugated polymers are extremely versatile and may involve classical polymer chemistry method such as coordination polymerization, typical organic chemistry procedures or electrochemical techniques. In general, conjugated polymers are synthesized by two different methods, viz.

- a) Chemical polymerization
- b) Electrochemical polymerization

1.5.1. Chemical polymerization

Chemical polymerization technique involves different methods of polymerization such as condensation polymerization, addition polymerization, oxidative polymerization etc. Some of the chemical polymerization methods make use of different types of well-known organic reactions like Suzuki-polymerization, Oxidative polymerization, Gilch polymerization, Knoevenagel polymerization, Wittig polymerization, Sonogoshira coupling, Yamamoto polymerization, Zigler-Nutta polymerization, Grignard polymerization etc. for which details are given in Chapter 2.

1.5.2. Electrochemical polymerization

Electrochemical polymerization technique has gained much attention because of its simplicity and the added advantage of obtaining a conductive polymer being simultaneously doped. Normally, this polymerization carried out in a single or dual compartment cell by adopting a standard three-electrode configuration in a supporting electrolyte, both dissolved in an appropriate solvent. It can be carried out potentiometrically by using a suitable power supply. Following this technique, conjugative conducting polymers such as poly(pyrrole), poly(thiophene), poly(furan) and their derivatives can be synthesized by their monomers in a single step. Simultaneously, the obtained polymer would be in its doped state and hence the polymer thus obtained is pure and homogeneous. The mechanism of electrochemical polymerization involves the following steps:

- i) Oxidation of monomer molecules to generate corresponding radical cation
- ii) Dimerisation of radical cations followed by a proton loss to yield a neutral dimer
- iii) Oxidation of dimer to obtain its radical cation

iv) Reaction of dimer radical cation with another radical cation

Finally the growing chain terminates via exhaustion of reactive radical species accompanying oxidative or other chain termination process in the vicinity of the electrode. Mechanism of electrochemical polymerization is illustrated in **Figure 1.3**.

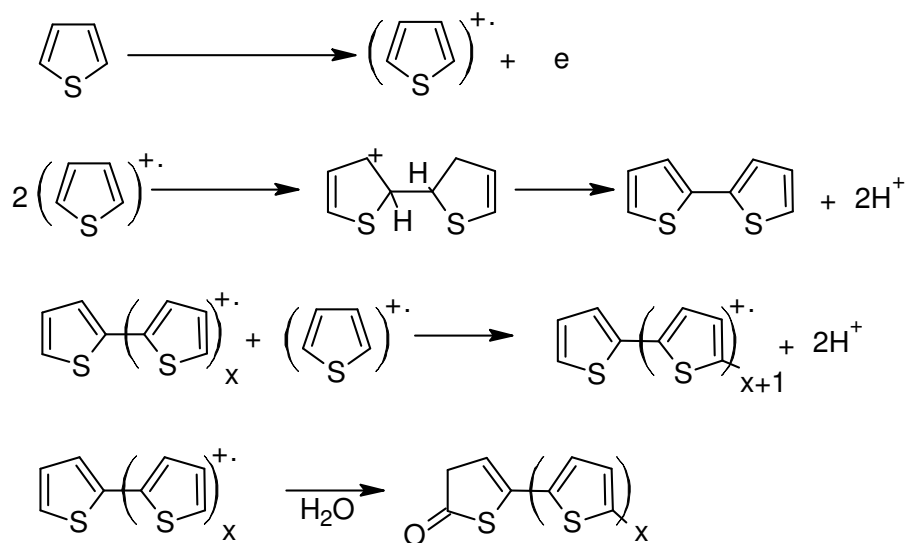


Figure 1.3: Mechanism of electrochemical polymerization

1.6. CONDUCTION MECHANISM

Conduction in conjugated polymers can be easily explained on the basis of band theory through polaron-bipolaron model.

1.6.1. Band theory

The band theory explains the conduction in various types of materials (Walton 1990). The electronic band structures of different types of materials are illustrated in **Figure 1.4**. In organic molecules, generally the highest occupied bands constitute the valance band (VB) and the lowest unoccupied bands represent the conduction band (CB). In such molecules, the energy spacing between the highest occupied molecular orbital (HOMO) and the lowest unoccupied molecular orbital (LUMO) is known as bandgap energy (E_g). For metals, the VB and CB overlap and the intrinsic conductivity is attributed to the zero bandgaps. In case of semi-conductors, the

narrow bandgap energy enables the electrons to jump to CB by thermal excitation even at room temperature to render the material conductive. Further, materials where the energy separation is too large for thermal excitation to promote electrons to CB are termed as insulators.

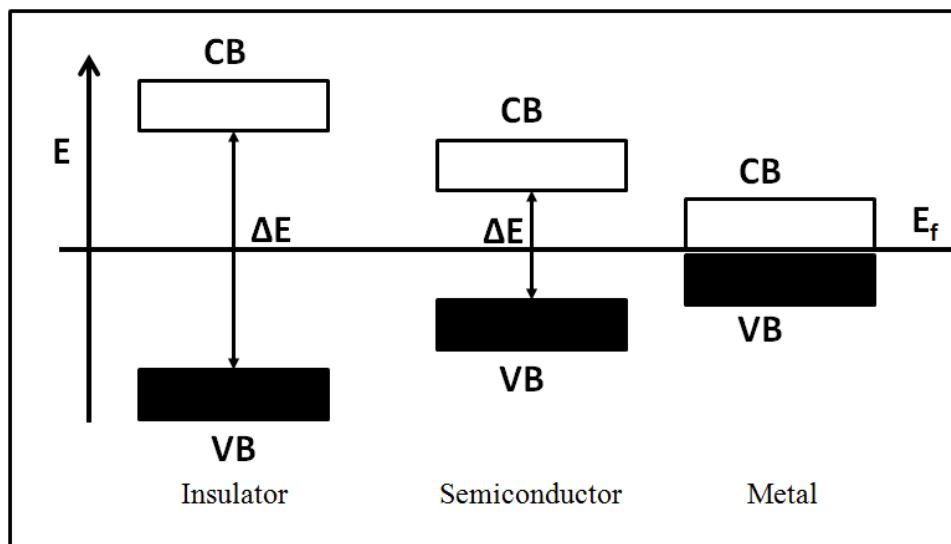


Figure 1.4: Illustration of band structure of various materials (VB: valence band, CB: conduction band, E_f , Fermi energy level)

1.6.2. Polaron and bipolaron model

The conventional doping process in the semiconductor generates intermediate energy levels within the bandgap and these mid-gap states exist as either a hole for ‘p’ doping or electrons for ‘n’ doping. Either holes or electrons contribute to the electrical conductivity of semiconductors, as charge carriers. A conducting polymer is an organic semiconductor whose bandgap is usually above 1 eV and its intrinsic conductivity is low. The process of doping (oxidation or reduction in chemistry terms) is necessary to produce higher conductivity in them.

The conduction mechanism of the doped conjugated polymer can be explained using polaron-bipolaron model. This model has been widely applied to conjugated polymeric systems. The concept of polaron and bipolaron are originated from solid-state physics. From the chemistry point of view, a polaron is a radical cation that stabilizes itself by polarizing the polymer chain. The formation of polaron and bipolaron in poly(pyrrole) has been explained in **Figure 1.5**.

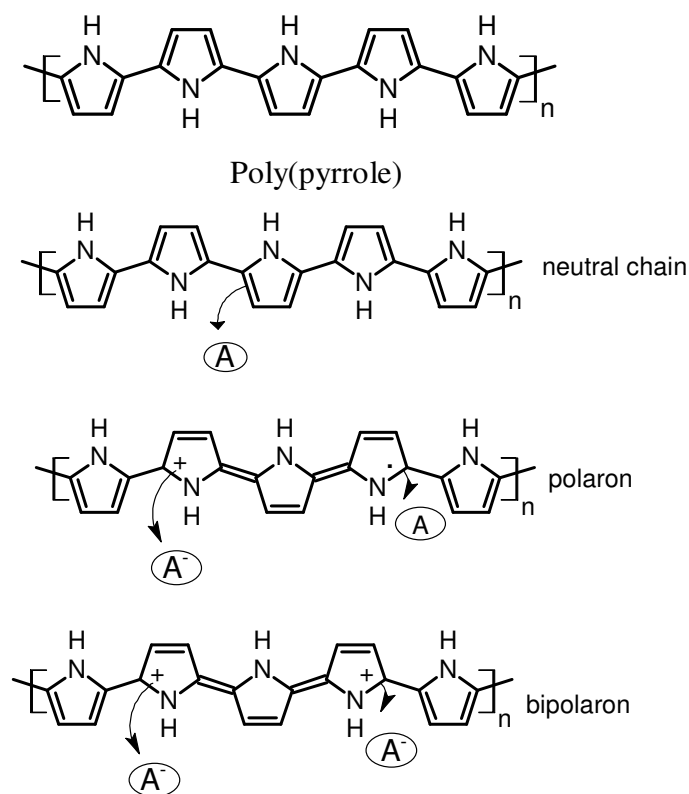


Figure 1.5: Formation of polaron and bipolaron in poly(pyrrole)

On oxidative doping of poly(pyrrole), an electron is removed from the p-orbital of the backbone producing a free radical and a spinless positive charge. The combination of a charge site and a radical is called a polaron, which has a spin of $\frac{1}{2}$. This polaron creates new localized electronic states in the bandgap, with the lower energy states being occupied by single unpaired electrons. The polaron state of poly(pyrrole) is symmetrically located about 0.5 eV from the band edges. The partial delocalization of polaron across several monomeric units leads to structural distortion in the polymer. The distortion is caused by the existence of two non degenerate ground states, namely aromatic and quinoid state. Upon further oxidation, the free radical of the polaron is removed, creating a new spinless defect called a bipolaron. This is of lower energy than the creation of two distinct polarons. Further, at higher doping levels it becomes possible that two polarons combine to form a bipolaron (Bredas et al. 1985). Thus at higher doping levels the polarons are replaced with bipolarons. The bipolarons are located symmetrically with a bandgap of 0.75 eV for poly(pyrrole). Theoretical studies have proved that the formation of bipolarons via the combination of polarons is energetically favorable, eventually leading to continuous

bipolaron band with continued doping. Their bandgap also increases as newly formed bipolarons are made at the expense of the band edges. For a very heavily doped polymer it is conceivable that the upper and the lower bipolaron bands will merge with the conduction and the valence bands, respectively to produce partially filled bands and metallic like conductivity. This concept has been illustrated in **Figure 1.6**.

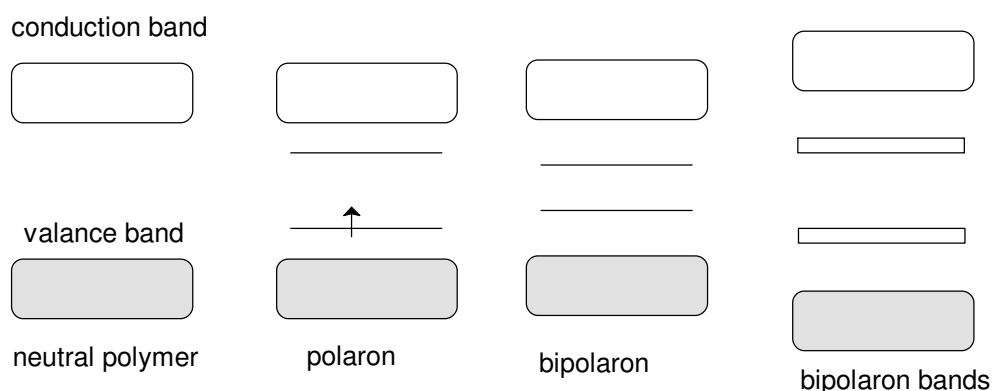


Figure 1.6: Formation of mid bandgap stages in doped polymers

1.7. BANDGAP

Bandgap of a polymer is nothing but the difference in HOMO and LUMO energy levels. It has been observed that the electronic and optoelectronic properties of the π -conjugated system depend on bandgap. Evidently, conjugated polymers offer a broad range of attractive features for use in a variety of device architectures. Therefore various strategies have been developed to control the magnitude of bandgap in conjugated polymers. One such approach involves the introduction of a flexible long chain into polymer backbone that decreases the bandgap. This approach also increases the solubility of the resulting polymer.

1.7.1. Factors affecting bandgap

The bandgap of the polymer can be tuned by various techniques. Structural modification is one of the methods. Factors that affecting bandgap in conducting polymers are mainly bond length alternation ($E^{\Delta r}$), the mean deviation from planarity (E^{Θ}), the aromatic resonance energy (E^{res}), the inductive and mesomeric electronic effects of substituents (E^{sub}) and the inter-chain interactions (E^{Int}) as shown in equation (1.1) and **Figure 1.7**.

$$E_g = E^{\Delta r} + E^{\Theta} + E^{\text{res}} + E^{\text{sub}} + E^{\text{Int}} \dots \dots \dots (1.1)$$

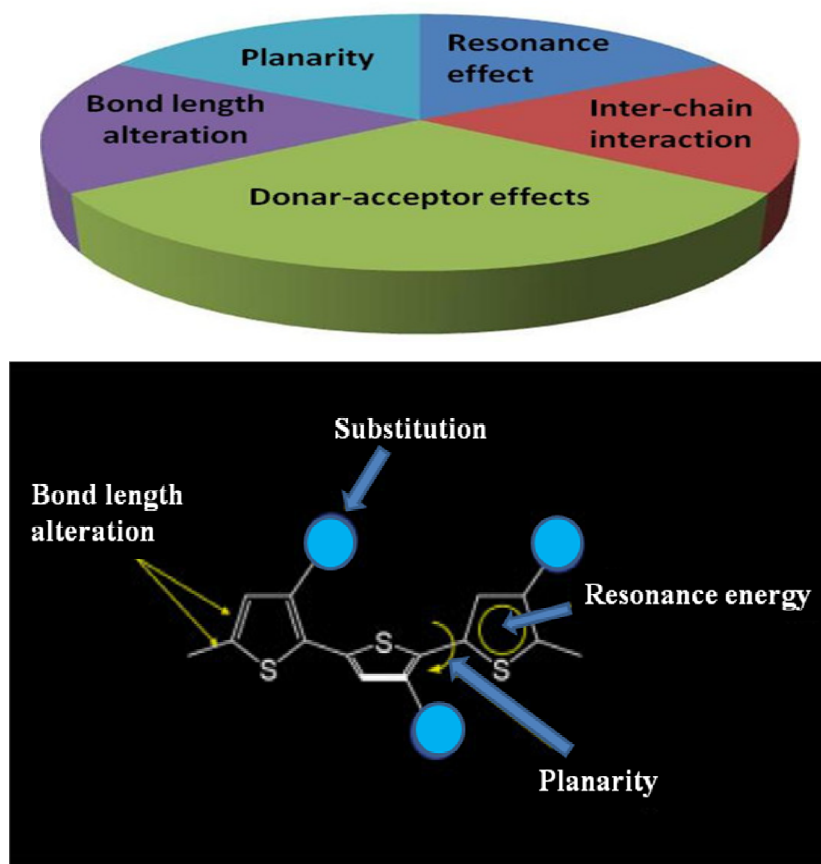


Figure 1.7: Factors affecting bandgap

Bond length alternation is defined as the difference between single and double bond lengths in poly(acetylene) molecule. However this definition cannot be used for poly(aromatic)s such as poly(thiophene) that differ from poly(acetylene) by their non-degenerate ground state. In poly(aniline), there are two mesomeric forms, viz. aromatic and quinonoid which are not energetically equivalent (Lowe et al. 1984). So, a new theory was proposed by Bredas et al. (1985); it states that bond length alternation is the maximum difference between the lengths of C-C bond inclined relative to the chain axis and C-C bond parallel to the chain axis (Bredas et al. 1985). The authors have observed that the bandgap decreases as the contribution of the aromatic geometry decreases or quinoid geometry increases.

According to Liu et al. (2001), the existence of single bond between the aromatic hetero-cycles causes inter-annular rotations in conjugated polymeric backbone (**Figure 1.8**). This induces a rotational distortion around the single bonds that leads to reduction in the effective conjugation along the polymer backbone with

the decline in the extent of overlap. Therefore any deviation in the co-planarity would results in an enhancement of the bandgap.

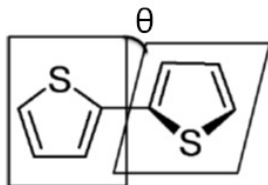


Figure 1.8: Intra annular rotations in conjugated polymers

The bandgap of conjugated polymer generally decreases with decrease in the resonance energy per electron. This results in a competition between π -electron confinement within the rings and delocalization along the chain. In general, incorporation of various substituents along the polymeric back bone has a great effect on the magnitude of bandgap. Also, the character and position of substituent plays important role. Normally, electron donating groups increase the energy of HOMO and electron withdrawing groups lower the energy of LUMO.

1.8. DONOR-ACCEPTOR APPROACH

The conventional conjugated polymers have several drawbacks. To overcome these difficulties a new concept called Donor-Acceptor (D-A) approach has been developed. This strategy induces minimum twisted arrangements between consecutive repeating units in conjugated polymers. It involves construction of D-A type systems where the donor unit has strong electron-donating and the acceptor unit has strong electron-withdrawing properties. Normally, interaction of the donor-acceptor moieties enhances the double bond character between the repeating units, which stabilizes the low bandgap quinonoid-like forms within the polymer backbones. Hence, a conjugated polymer with an alternating sequence of the appropriate donor and acceptor units through conjugation in the main chain can induce a reduction in its bandgap energy. Recently, molecular orbital calculations have shown that the hybridization of the energy levels of the donor and the acceptor moieties result in D-A systems with unusually low HOMO-LUMO separation (Sonmez et al. 2003).

Interestingly, a combination of electron rich (donor) and electron deficient (acceptor) moieties in the polymer chain is the most successful approach to obtain low bandgap polymers. The interaction between the electron donor and acceptor moieties

in such an alternating donor-acceptor conjugated system can result in the hybridization of the high-lying HOMO energy level of the donor and low-lying LUMO energy level of the acceptor, leading to a relatively small bandgap polymer with novel electronic structure and ambipolar charge transport properties (Pai et al. 2006). Alternation on the polymer backbone causes intramolecular charge transfer (ICT) from the donor to the acceptor. As a result, an absorption band at lower energy is generated. Thus, the strength of intramolecular charge transfer can be tuned through a careful selection of the donor and acceptor moieties in the polymer chain that leads to new design. Evidently, the main reason behind the donor-acceptor-donor (D-A-D) approach is that the existence of high energy HOMO of the donor and low energy LUMO of the acceptor increases double bond character which leads to broadening of valence and conduction bands and inducing small bandgap (E_g). Such D-A-D type conjugated polymers can behave as bipolar charge transfer materials for their applications in light-emitting diodes (Tarkka et al. 1996).

Electron donating units along the conjugated polymers are generally constituted by electron rich hetero-aromatic rings such as thiophene, pyrrole, phenothiazine, carbazole etc. The use of rigid aromatics like oxadiazole, benzothiadiazole etc. as an electron acceptor unit, is one of the effective ways to design these systems. As a result, a D-A-D arrangement in the polymer backbone brings about much more red-shifted absorption spectra with low bandgaps. Also it has been proven that the D-A-D polymers possess novel physical properties that could lead to applications in devices requiring high charge storage capability such as batteries and super capacitor applications (Akoudad et al. 1998). Some of the well known donor and acceptor aromatic and hetero-aromatic moieties are depicted in **Figures 1.9a** and **1.9b**.

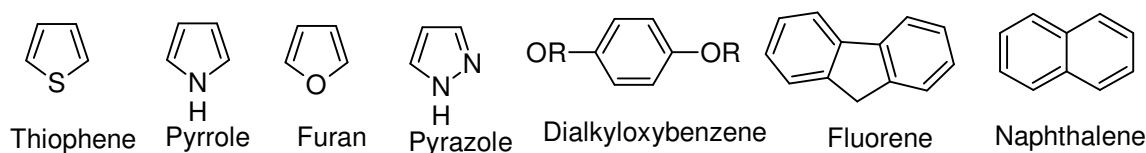


Figure 1.9a: Structures of different electron donors

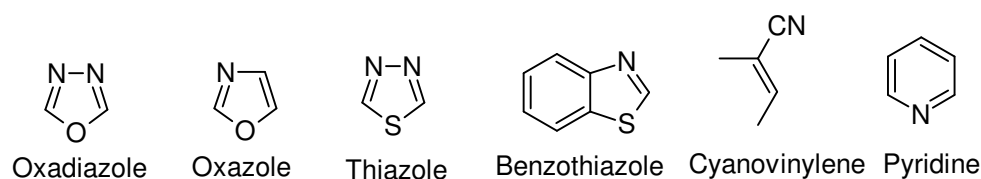


Figure 1.9b: Structures of various electron acceptors

1.9. APPLICATIONS OF CONJUGATED POLYMERS

During the past three decades electrically conducting or semiconducting conjugated polymers have attracted an overwhelming interest around the globe. These polymers exhibit novel properties which are not typically available in other materials and these unique properties enable a large number of applications for them. These numerous applications of conjugated polymers can be divided into three main classes. The first class includes conjugated polymers, which find applications in their neutral form, taking the advantages of semiconducting and luminescent properties. The second important class of applications involves the doped conjugated polymers, which have potential utilities in the field of electromagnetic shielding, selective anionic membranes and as electrode materials for capacitors (Ling et al. 2008). The third category of these conjugative polymers depends on their reversible switching between its conducting and reduced forms. This property of conjugated polymer leads to various applications such as battery electrodes (Baibarac et al. 2007), mechanical actuators (Rosso et al. 2011), sensors (Yang et al. 2011), drug delivery, and electrochromics (Dyer et al. 2010).

Now, conjugated polymers are rapidly gaining attraction in new applications due to their stability, processability, physical properties, optical properties and optoelectronic properties. The extended π -systems of conjugated polymer back bone are highly susceptible to chemical or electrochemical oxidation or reduction, which leads to the change in its electrical and optical properties. Since these reactions are often reversible, it is possible to control the electrical and optical properties with a great deal of precision. It is even possible to switch from a conducting state to an insulating state. The electronic characteristics of these materials are primarily governed by the nature of the molecular conjugation; but intermolecular interactions also exert a significant influence on the macroscopic materials properties. The flexibility in the properties of these polymers attributed to a wide range of

applications in electronic and optoelectronic devices such as biosensors, plastic batteries, polymer solar cells, field effect transistors, optical data storage devices, organic electro-luminescent devices, switching devices, and many more. Various applications of conducting polymers have been summarized in **Figure 1.10**.

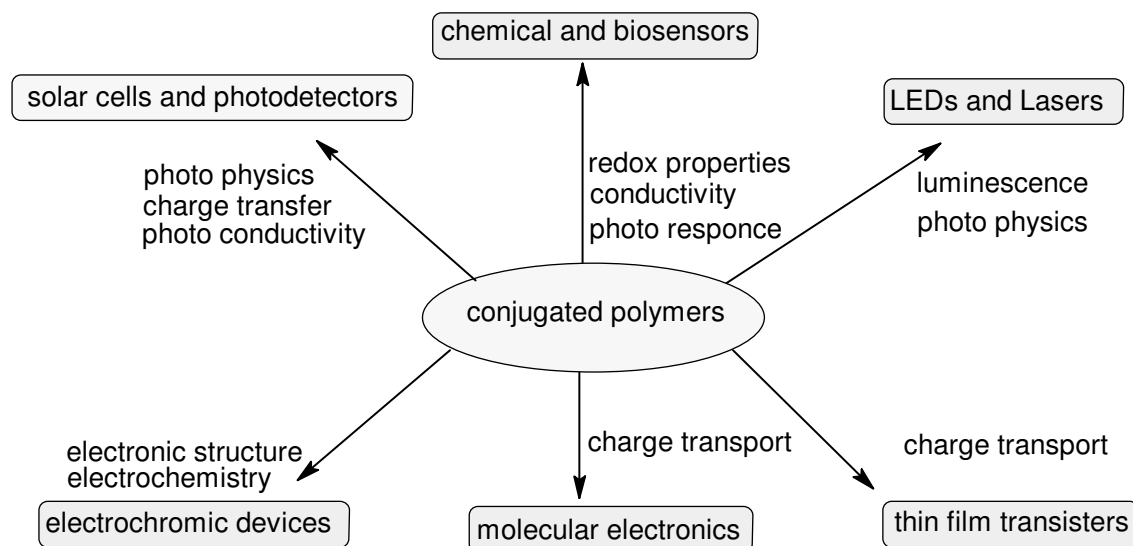


Figure 1.10: Applications of conjugated polymers

1.9.1. Polymer light emitting diodes (PLED)

Electroluminescence (EL) is an electro-optical phenomenon in which a material emits light in response to an electric current passed through it, or to a strong electric field. The electroluminescence requires injection of electrons from one electrode and holes from the other, the capture of oppositely charged carriers (so-called recombination), and the radiative decay of the excited electron-hole state (Exciton) produced by this recombination process. Since the report of metallic conductivities in 'doped' polyacetylene, conducting polymers has advanced very rapidly. Recently, much of interest is shown in LED (light emitting diode) containing conducting polymers due to their potent applications in the field of optoelectronics.

It is evident that conjugated polymers derive their semiconducting properties by having delocalized π -electron bonding along the polymer chain. Here the π (bonding) and π^* (anti bonding) molecular orbital form delocalized valence and conduction wave functions, which support mobile charge carriers. The property, electroluminescence was first reported in 1990, using poly(p-phenylenevinylene),

(PPV), as the single semiconductor layer between metallic electrodes, as is illustrated in **Figures 1.11** and **1.12**. In this structure, the ITO layer functions as a transparent electrode, and allows the light generated within the diode to leave the device. The top electrode is conveniently formed by thermal evaporation of a metal. LED operation is achieved when the diode is biased sufficiently to achieve injection of positive and negative charges carriers from opposite electrodes. Capture of oppositely charged carriers within the region of the polymer layer can then result in photon emission.

Polymer LEDs operate on the principle involving the injection of electrons and holes from negative and positive electrodes, respectively. Electrons and holes combine each other within the polymer film, and form neutral bound excited states (termed excitons). Excitons in conjugated polymers are generally considered to be more strongly localized than excitons in three-dimensional semiconductors. The spin wave function of the exciton, formed from the two spin $-1/2$ electronic charges, can be either singlet ($S = 0$) or triplet ($S = 1$), and a consequence of the confinement of the excitation is that the energy difference between singlet and triplet (the exchange energy) may also be large. Then spin-allowed radiative emission (fluorescence) is from the singlet only, and when the exchange energy is large, cross-over from triplet to singlet is unlikely, so that triplet excitons do not produce light emission, other than by indirect processes such as triplet-triplet annihilation or by phosphorescence.

PLED operation is achieved when the diode is biased sufficiently to achieve injection of positive and negative charge carries from opposite electrodes. Capture of oppositely charged carriers within the polymer layer can result in photon emission through transparent electrode. The wavelength and intensity of emitted light photon is measured by the detection system, thereby the device efficiency of PLED (polymer light emitting diodes) can be calculated.

Polymer LEDs presently showing attractive device characteristics, including efficient light generation in all color, and there are several development programs now set up to establish procedures for manufacture of these devices. The principal interest in the use of polymers lies in the scope for low-cost of manufacturing, using solution-processing of film-forming polymers. These polymer light emitting diodes can be used in several devices such as digital display, lighting, TV and computer screens etc.

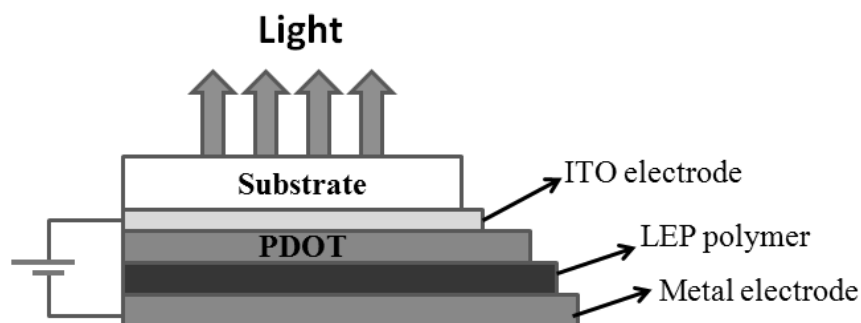


Figure 1.11: Schematic representation of polymer light emitting diode

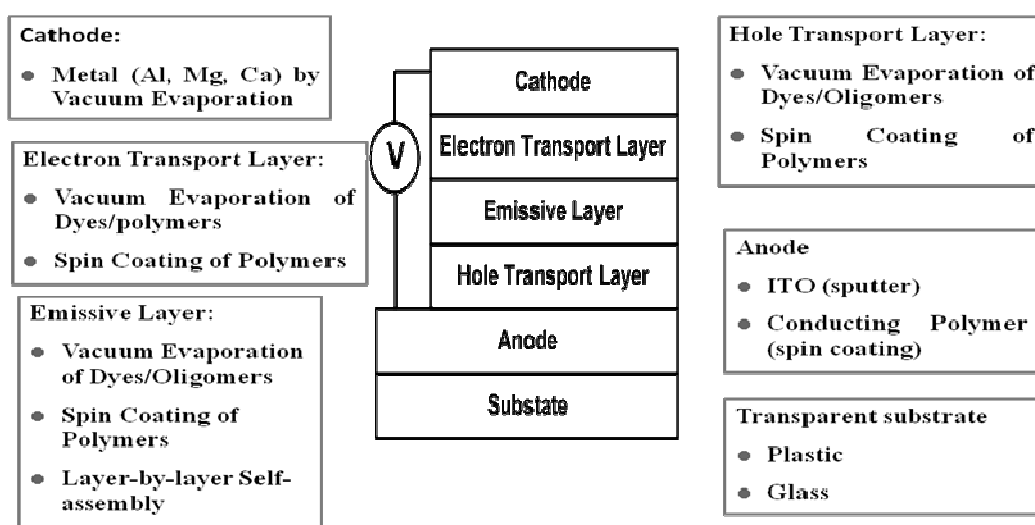


Figure 1.12 Different parts of polymer light emitting diodes

1.9.2. Polymer Photovoltaics (PV)

Recently, conjugated polymers with semiconductor-like behavior have gained their importance in devices for harvesting solar energy. This is because such materials are not only able to function in a similar manner to the inorganic semiconductors but also have important advantages such as low cost, light weight, ease of fabrication and the possibility of large area coatings. In fact, their use as photoactive electrodes is of increasing interest, as the processing possibilities of conjugated polymeric materials become more developed. Further, the high absorption coefficients of these materials and the possibility of varying the bandgap by molecular engineering have opened up new options for solar energy conversion.

Polymer solar cells (**Figure 1.13**) typically consists of a photon absorbing active layer sandwiched between two electrodes and placed on a substrate of glass or clear plastic foil (Spanggaard et al. 2004). One of the electrodes is transparent in order to allow photons to penetrate into the absorbing layer. Indium tin oxide (ITO) is commonly used as transparent electrode and metals like aluminum, calcium or magnesium as the other electrode.

The absorbed photons excite electrons in the active layer and thereby promoting them from the highest occupied molecular orbital (HOMO) to the lowest unoccupied molecular orbital (LUMO) within the polymer (Spanggaard et al. 2004). The excitation of an electron leaves behind an empty electron space in the HOMO level called “a hole”. The hole and the excited electron are not totally independent but associated to one another in a form called an exciton. In most organic molecules excitation is followed shortly by relaxation, typically in the form of recombination when the excited electron falls back into the hole. This releases the absorbed energy as either radiative or non-radiative energy which cannot be utilized for electricity generation. In polymer solar cells, the exciton is separated into a free hole and a free electron which are then transported to different electrodes due to differences in the electrodes ionization energy. The phenomenon of charge separation in organic photovoltaic cell is depicted in **Figure 1.14**. The electron is then forced to travel from one electrode through an external circuit to the other electrode in order to recombine with the hole. The absorbed energy can then be utilized in the external circuit. The separation of the electron from the hole in polymer solar cells is achieved by utilizing an electron accepting material along with the electron donating polymer (Günes et al. 2007). The electron donor and acceptor are mixed to form a heterogeneous active layer. This type of device is known as a bulk hetero-junction solar cell (Günes et al. 2007). The charge separation occurs when an exciton has diffused to the donor/acceptor interface (Kroon et al. 2008). Here a difference in potential of the two phases pulls the electron into the electron accepting phase leaving behind the hole in the electron donating phase. The electron and the hole are then free to move through their respective phases to the electrodes.

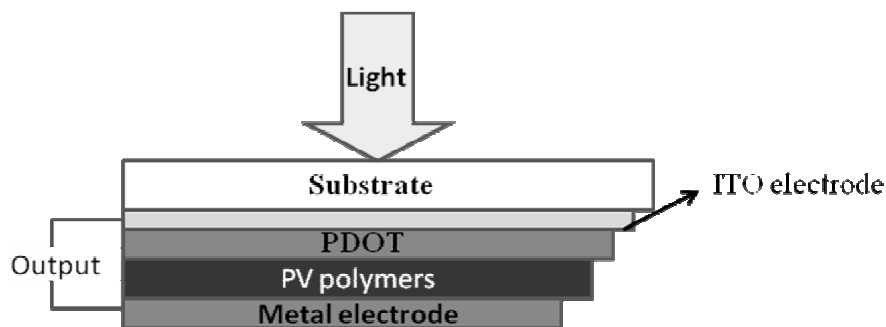


Figure 1.13: Schematic representation of a polymer solar cell

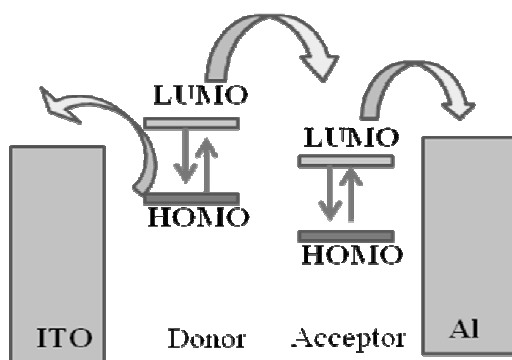


Figure 1.14: Charge separations in a photovoltaic device

1.9.3. Nonlinear Optics (NLO)

“Nonlinear optics” is the branch of optics, which deals with the phenomena that occurs as a consequence of modification of the optical properties of materials with the incident light wave. This deals with the interactions of applied electromagnetic fields in various materials, to generate new electromagnetic fields altered in phase, frequency, amplitude and various other physical properties.

In a nonlinear optical phenomenon, the response of a material to an applied optical field depends on the strength of the optical field in a nonlinear manner. In case of nonlinear optics, i.e. when the applied electric field is high, the induced polarization has a nonlinear dependence on the electric field and can be expressed as a power series with respect to the electric field, as given in equation 1.1.

$$\mathbf{P} = \chi^{(1)} \cdot \mathbf{E} + \chi^{(2)} \cdot \mathbf{E} \cdot \mathbf{E} + \chi^{(3)} \cdot \mathbf{E} \cdot \mathbf{E} \cdot \mathbf{E} + \dots \quad (\text{Eq 1.1})$$

where \mathbf{P} is induced polarization, $\chi^{(1)}$ is the linear susceptibility, $\chi^{(2)}$ is the second order nonlinear susceptibility and $\chi^{(3)}$ is the third order nonlinear susceptibility. The term $\chi^{(1)}$ is responsible for linear absorption and refraction and it reflects the linearity between the induced polarization and the incident electric field. The term $\chi^{(2)}$ is present only in

noncentrosymmetric materials, i.e. materials without inversion symmetry. This $\chi^{(2)}$ is responsible for sum and difference frequency mixing, optical rectification and the electro-optic effect. Third order nonlinear optical interactions, which are described by the term $\chi^{(3)}$, can take place in any material. The value of $\chi^{(3)}$ is related to the nonlinear index of refraction and implicitly to the optical limiting phenomenon.

Optical limiting

The optical limiting is a nonlinear effect leading to saturation in the transmittance of the NLO material under high intensity (energy) laser pulse. Thus the transmittance of the optical limiter is high at the normal light intensities and low for the intense laser beams. The transmitted energy for an ideal optical limiter increases linearly with input intensity until the threshold is reached. An important application of this phenomenon is the protection of optical materials and sensors against damage by sudden exposure to high energy light beams. In general the optical limiting phenomenon arises due to following nonlinear mechanisms.

- Two-photon absorption
- Reverse saturable absorption
- Nonlinear refraction
- Excited state absorption

The behavior of a NLO material under different laser intensities is as shown in

Figure 1.15.

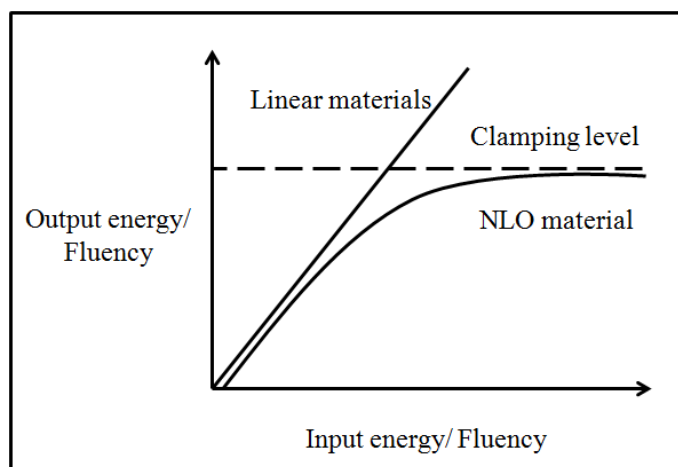


Figure 1.15: Behavior of linear and nonlinear optical materials

An optical limiter must provide protection over a wide range of incident intensity or fluence. Thus if the input-output slope is non zero, at some input above the threshold the device will fail to provide protection. In some cases, the material itself may be damaged if its damage threshold is below this point, or the intensity/fluence dependent transmittance may approach a constant asymptote so that the input-output slope again increases. Any one of these situations will define a maximum input for which the device will provide effective limiting. The ratio of this input value to the threshold is called the dynamic range of the limiter.

Reverse saturable absorption (RSA)

Reverse saturable absorption is a nonlinear optical process in which excited state absorption cross section is larger than that of ground state absorption cross section. This process can be explained by considering three energy level diagram (**Figure 1.16**), where σ_1 is the absorption cross section for ground state **1**, the σ_2 is the absorption cross section from excited state **2** to second excited state **3**, τ_1 and τ_2 are the life times for excited state **2** and excited state **3**, respectively.

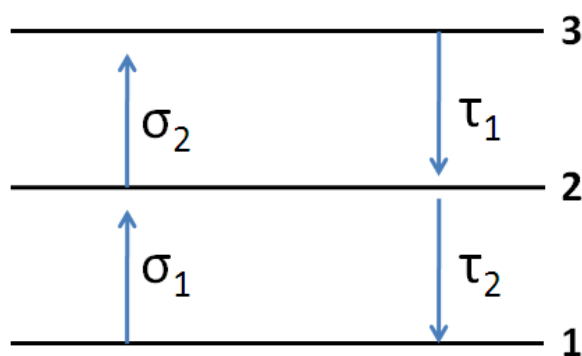


Figure 1.16: Three level model for reverse saturable absorption (RSA)

As the material absorbs light, the first excited state (**2**) begins to populate and contribute to the total absorption cross section. If σ_2 is smaller than that of σ_1 , then the material becomes transparent and behaves as a saturable absorber. Similarly, if σ_2 is larger than σ_1 , then that material is termed as reverse saturable absorber.

Two photon absorption (TPA)

Two photon absorption is a process by which the energy gap between two real states in a material is bridged by simultaneous absorption of two photons. In this case each photon has insufficient energy to complete the transition state. According to quantum mechanics, after the irradiation with laser, the first photon makes a virtual transition to a virtual state between upper and lower energy levels. If the second photon appears within the life time of the virtual state, the absorption to the upper state can be completed, otherwise it collapses to ground states without the absorption of the photon. To attain good TPA absorption, photons must be supplied at a high rate.

When the linear absorption is high, there is a very small ground state absorption; but as the intensity increases, two photons can together promote to higher excited state, then the intensity of the beam is given by,

$$\frac{dI(z)}{dz} = -\alpha I(z) - \beta I^2(z) - \gamma I^3(z) \dots \dots \dots \text{(eq. 1.2)}$$

where, $I(z)$ is the intensity of the incident beam moving along z -axis, α is the linear absorption coefficient, β is the two photon absorption coefficient, and γ is the three photon absorption coefficient. In moderate intensity of light, two photon absorption predominates. Also, the material behaves as transparent at low intensities of light, i.e. $\alpha = 0$. Then equation 1.2 becomes,

$$\frac{dI(z)}{dz} = -\beta(z)I^2 \dots \dots \dots \text{(eq. 1.3)}$$

The solution for equation 1.3, by separation of variables yields

$$I(l) = \frac{I_0}{(1 + I_0 \beta l)} \dots \dots \dots \text{(eq. 1.4)}$$

where, l is the sample length and I_0 is the input intensity. This equation 1.4 shows that, there is inverse relation between transmittance and the intensity of the incident radiation. Thus, TPA coefficient of any material depends on its transmittance and sample thickness. Generally, good optical limiting materials exhibit high β values.

1.9.3.1 Polymer nonlinear optics

In recent years, polymeric materials exhibiting strong nonlinear optical properties (NLO) have attracted a considerable interest because of their possible

applications in optoelectronic and optical devices such as optical limiters, optical switches and optical modulators. Conjugated polymers are promising class of third-order nonlinear materials because of their large third-order susceptibilities associated with fast response time in addition to their variety and good processability (Chi et al. 2008). The strong delocalization of π -electrons in the polymeric backbone determines a very high molecular polarizability and hence imparts a remarkable third-order nonlinearities (Samoc et al. 1998 and Cassano et al. 2002). These polymeric materials have advantages like easy fabrication, integration into device and intrinsic tailorability, which help in tuning their structure and also their NLO properties. Besides these, they possess low dielectric constant, inherent synthetic flexibility, high optical damage thresholds, and large NLO response over a broad frequency range comparable to those of inorganic materials.

Thiophene is a potential heterocyclic system for NLO applications, as its presence in a conjugated system has been found to be much more effective than that of a phenyl ring or other hetero aromatic system such as furan, pyridine, pyrrole etc. in increasing nonlinearity (Hao et al. 2008). This effect may be due to the participation of the sulfur d-orbital and the ease of polarization of electrons in sulfur atoms. Further the literature reports on thiophene based polymers reveal that increasing planarity and rigidity would help to enhance third-order susceptibilities as it optimizes the overlap of π -orbitals and hence enhances the electron delocalization. On the other hand, the electron-donating property, electron density and hole-transport ability of thiophene molecule in polymer back bone will enhance the third-order optical nonlinearity. A detailed explanation on NLO is given in **Chapter 5**.

Due to the increasing demand of novel materials for photonic devices, it is necessary to design new conjugated polymers with high thermal stability, damage threshold, and better optoelectronic properties. The research program that forms the basis of this thesis has been directed towards the design, synthesis and characterization of twenty new D-A type conjugated polymers derived from 3,4-dialkoxythiophene. Also, it has been aimed at investigation of their electrochemical, optical and nonlinear optical properties in order to find their applications in photonic devices.

The thesis has been divided into seven chapters. **Chapter 1** comprises a brief account on general introduction to conjugated polymers highlighting their important properties and applications. In continuation, **Chapter 2** deals with a concise survey on various types of conjugated polymers reported in the literature. Also, it describes the main objectives of the present research work and design of new D-A type conjugated polymers. Further, a detailed account of synthetic protocols of various intermediates and monomers along with their structural characterization data has been discussed in **Chapter 3**. The details of synthetic procedures for polymerization and characterization data of new polymers have been described in **Chapter 4**. Further, electrochemical properties of the polymers have been explained in **Chapter 5** and their linear and nonlinear optical studies have been discussed in **Chapter 6**. Towards the end, **Chapter 7** summarizes the conclusions and outcome of the research work.

Abstract

This chapter includes a brief discussion on literature reviews related to important donor-acceptor type π -conjugated polymers. Also, it comprises a concise account on scope and objectives of the present research work based on literature survey. At the end, design of five new series D-A type conjugated polymers with various electron releasing and electron withdrawing systems in the main chain has been described.

2.1. INTRODUCTION

Conjugated polymers have attracted widespread interest during the last three decades, because of their useful electronic, optoelectronic, electrochemical and non-linear optical properties. Since these polymers show unique physical properties, significant research efforts directed to better understanding of their chemistry, physics and engineering have been undertaken. Their interesting properties, particularly electrical conductivity along with luminescence and electroluminescence, attracted them in several applications as organic conductors and semiconductors, light-emitting diodes, sensors, and photo-detectors (Epstein et al. 1996, Akcelrud et al. 2003, Ong et al. 2004, and Xue et al. 2004). Literature reports clearly reveal that the molecular structure of conjugated polymers plays an important role in the tuning of their physical and electrochemical properties. Among various conjugated polymers, those carrying D-A type architecture are gaining much more attention in recent times. The most striking fact is that the type and arrangement of donor and acceptor moieties in the polymer chain can lead to remarkable enhancement in the electronic and photonic properties of these novel materials.

2.2. LITERATURE REVIEW

In recent years several donor-acceptor type conjugated polymers were designed and synthesized for allied applications. In the design of conjugated polymers molecular engineering plays vital role. Generally, molecular engineering begins with the synthesis of homogeneous structures. A crucial step towards the engineering of conjugated polymers basically involves designing of donor-acceptor type arrangement and macroscopic assembly of polymer in order to achieve expected properties.

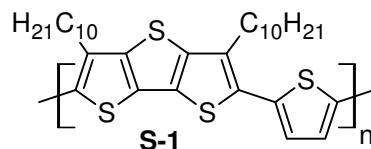
In the following section, brief descriptions on literature reports available on the important donor-acceptor type conjugated polymers carrying different kinds of

moieties have been discussed. These polymers mainly consist of thiophene, naphthalene, pyrazole, phenylene, phenothiazine and pyrazole as powerful electron donor groups and 1,3,4-oxadiazole, cyanovinylene, cyanopyridine and cyclic diimide units as strong electron acceptor systems in their chains. Further, their synthetic methodologies and effect of various functional groups on physical, optical, and electrochemical properties of the conjugated polymers have been emphasized in the literature review.

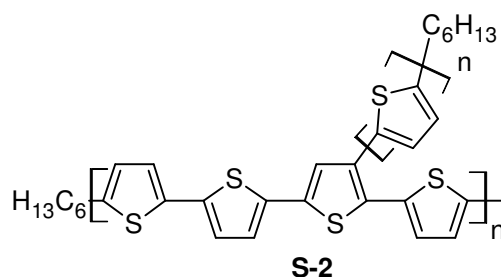
2.2.1. Thiophene based conjugated polymers

Literature survey reveals that thiophene based conjugated polymers are currently under intense research investigation. Thiophene based polymers are promising materials for optoelectronic properties, due to their easy processability, chemical stability, readiness of functionalities, good film forming characteristics, optical transparency, adequate mechanical strength and solubility in common organic solvents (Elsenbaumer et al. 1986 and Miller et al. 1986). According to the recent reports, optical and electrochemical properties can be synthetically tuned in poly(thiophene)s by modifying their structure into donor acceptor type conjugated polymers using electron releasing and electron accepting segments in the polymer chain. This would result in improved delocalization in the molecule and hence the enhancement of the required properties.

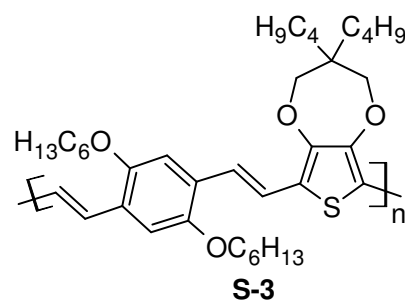
In an important study, Zhang et al. (2009) synthesized a conjugated polymer (**S-1**) with thiophene as repeating unit via palladium (0)-catalyzed Stille coupling reaction. The molecular weight of the polymer was found to be 62,000 Da and it was thermally stable with decomposition temperature of 340 °C and glass-transition temperature of 136 °C. The polymer shows strong absorption peak at 505 nm in dilute solution and 518 nm in thin film with an optical bandgap of 2.0 eV. The polymer exhibits intense emission located at 550 nm in solution and 603 nm in film state. Cyclic voltammetric study revealed that the HOMO and LUMO energies of the polymer were -5.4 and -3.4 eV, respectively. Polymer solar cells, fabricated based on the blend of the polymer showed the power conversion efficiency of 0.7 % with polymer: PCBM (1:4, w/w) as active layer.



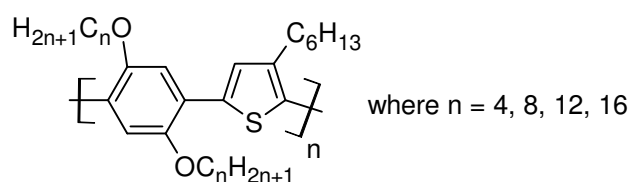
In another study, Yu et al. (2009) synthesized two-dimensional polythiophene (**S-2**) carrying alkyl-thiophene side chains by Stille coupling reaction. Optical measurements indicated that the bandgap of this polymer was in the range of 1.98-1.77 eV. The power conversion efficiency (η) of the polymers was found to be 2.5 % under simulated solar illumination (AM 1.5 G, 100 mW) from a polymer solar cell comprising an active layer containing 25 wt % polymer and 75 wt % (6,6)-phenyl-C71 butyric acid methyl ester (PC71BM).



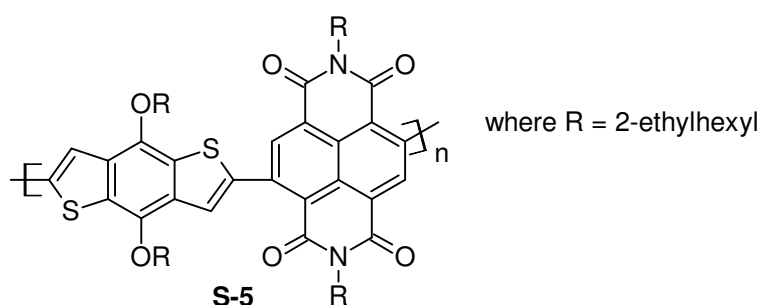
A research group led by Baek, in an attempt to obtain low bandgap material, synthesized a new thiophene/phenylene vinylene-based conjugated polymer (**S-3**) from simple alkoxythiophene derivative (Baek et al. 2009). In solution state, the polymer showed an absorbance in the range of 400-600 nm and, exhibited bandgap energy of 1.8 eV. Its UV-vis absorption and PL emission maxima in solid state were red shifted compared to that of its solution. This bathochromic shift is resulted from the closer intermolecular electronic interactions in the solid state. However, the polymer displayed slightly higher power conversion efficiencies (PCE, 0.30 %) of photovoltaic devices, fabricated using this polymer and (6, 6)-phenyl-C61-butyrac acid methyl ester (PCBM) than that of reported PCE (0.15 %) devices fabricated in the same configuration.



Yu and coworkers synthesized four new poly(1,4-phenylene-2,5-thiophene)s **S4** as potential third-order nonlinear optical materials via Stille poly-condensation reaction. These, polymers were soluble in common organic solvents and they exhibited high thermal stability. Also, polymers showed good third order nonlinear optical properties with susceptibility (χ^3) values of 1.77×10^{-13} esu. This was determined in chloroform solution with a concentration of 0.527 g/L using degenerate four-wave mixing technique.

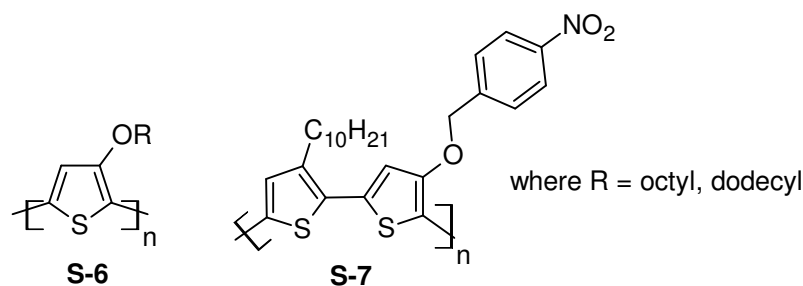
**S-4**

Recently, Chen et al. (2010) designed and synthesized three novel conjugated polymers (**S-5**), via the alternative copolymerization of the electron-donating monomer benzodithiophene (BDT) with three different electron accepting monomers. Amongst them naphthalenediimide (NDI) based conjugated polymer exhibited very low bandgap of 1.63 eV with HOMO and LUMO energy levels -5.62 and -3.99 eV respectively. The results suggest that the absorption range and the electrochemical properties of the conjugated polymers can be tuned by appropriate molecule-tailoring, which will help exploring ideal conducting polymers for potential applications in polymer optoelectronics, especially in polymer solar cells.

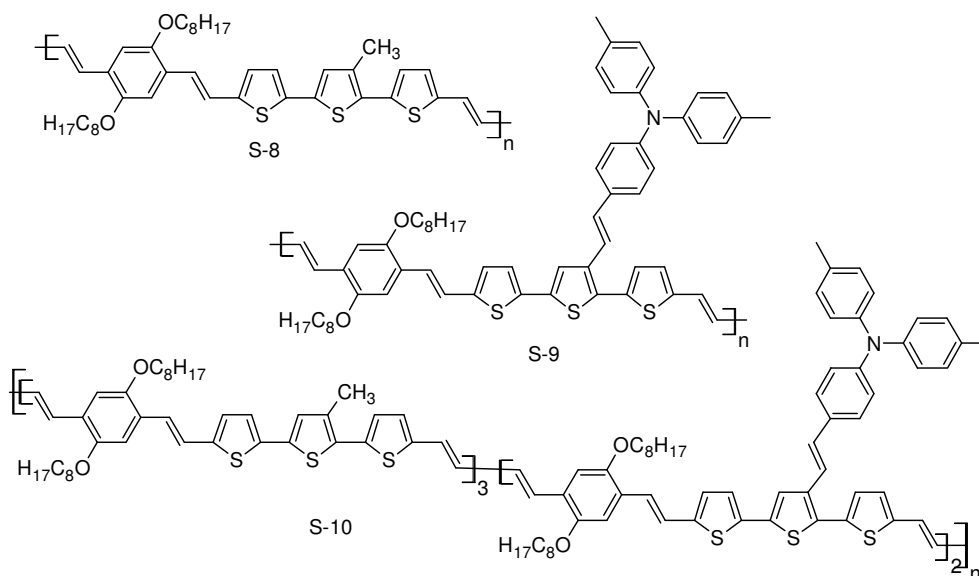
**S-5**

Poly(3-alkoxythiophene) (P3AOT) derivatives were synthesized with octoxyl, dodecaoxyl (**S-6**) and 4-nitro-benzyloxyl (**S-7**) as side-chains (Yanamo et al. 2010) as possible optical limiting materials. The absorption spectra of polymers indicated that length of the side groups affect the electrochemical and optical bandgap of poly(thiophene)s. The nonlinear optical (NLO) properties of these polymers were

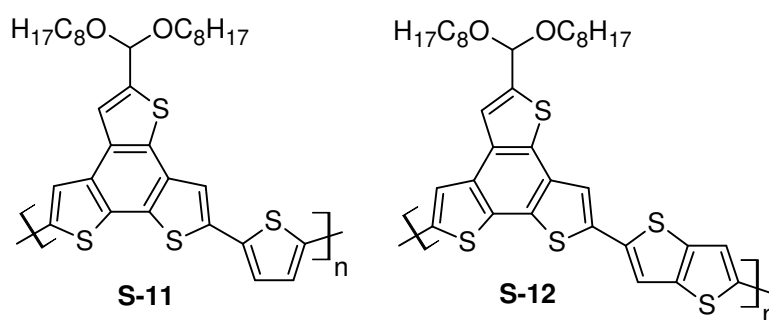
investigated using Z-scan method and results of their third-order NLO studies showed that the optical nonlinearity has a strong dependence on the length of the alkoxy side chains and polarity of polymers, which affect the intra- and intermolecular charge transfer. So, this type of poly(thiophene) derivatives can be conveniently used in optical limiting devices.



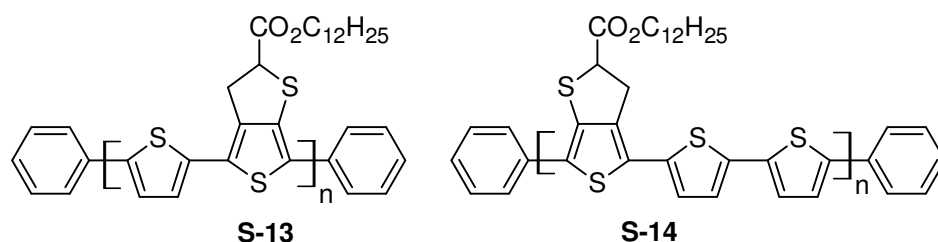
Three novel conjugated polymers (**S-8** - **S-10**) consisting of 2,5-dioctyloxy-1,4-phenylenevinylene and terthiophene systems with/without di(p-tolyl)phenylamine (TPAV) and oxadiazole (OXD) pendent groups (Chen et al. 2010) were synthesized via the Wittig-Horner reaction. It was observed that the introduction of TPAV and OXD pendent groups enhanced their optical properties. Interestingly, the polymer with triphenyl amine substitution showed low bandgap when compared to the remaining. The photovoltaic cells were fabricated with these polymers as the donors and (6, 6)-phenyl-C61-butyric acid methyl ester (PCBM) as the acceptor in a 1:4 weight ratio. The device based on polymer with triphenylamine substitution showed maximum power conversion efficiency of 1.75 % under simulated AM 1.5 G solar irradiation (100 mW/cm^2).



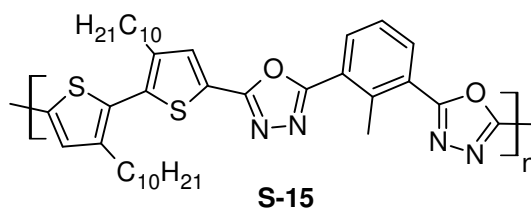
In a very recent study, Schroeder et al. (2011) synthesized two novel thiophene based conjugated polymers (**S-11** and **S-12**) with benzotrithiophene (BTT) moiety in their backbone. These two polymers showed promising organic field-effect transistor (OFET) performance. The authors found that the choice of co-monomer is very important in determining the inter-chain interaction and polymer solubility. According to them, regio-random nature of the alkyl-bearing BTT unit is quite remarkable and these polymeric materials are very good semiconductors. Despite molecular disorder introduced by a branched solubilizing alkyl chain and a region-random polymerization of the asymmetric benzotrithiophene unit, these co-polymers exhibit hole mobility as high as $0.24 \text{ cm}^2/(\text{V s})$.



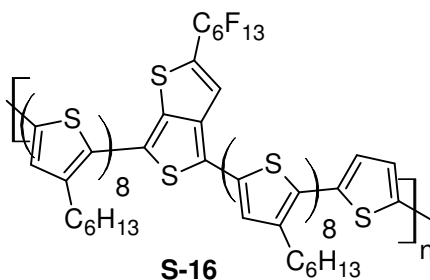
A series of low bandgap conjugated polymers (**S-13** and **S-14**), consisting of alternating 3,4-dodecylthienothiophene-2-carboxylate with one/two thiophene rings were synthesized by Myung-Jin et al. (2010) via Gilch polymerization technique. The bandgap and HOMO energy levels of these polymers were found to be $-1.58/1.61$ and $-5.15/-5.20 \text{ eV}$, respectively. Here, introduction of thiophene units along the polymer backbone reduced the bandgap considerably. Photovoltaic devices were fabricated using DTT-T2 and a fullerene derivative (PCBM), and whose power conversion efficiency was 0.21% under the illumination of AM 1.5 (100 mW/cm^2). It was found that the introduction of thiophene ring increased the conjugation path length, solubility as well as the power conversion efficiency.



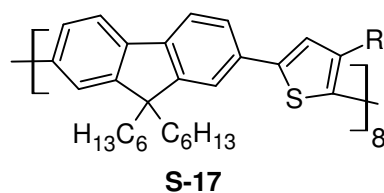
Yu et al. (1998) synthesized a new light-emitting polymer (**S-15**) carrying alternating segments of 3,3c-didecyl-2,2c-bithiophene and 2,6-bis(1,3,4-oxadiazolyl)-toluene, which are *p*-dopable and *n*-dopable, respectively. Synthesized polymer was found to be electro-active, both in the cathodic region and in the anodic region. Further, it showed green emission in its film state and displayed strong solvatochromism both in absorption and emission processes.



In an interesting study, Liang et al. (2009) synthesized a new regio-regular polymer (**S-16**) containing a thieno(3,4-b)thiophene segment. The presence of thieno(3,4-b)thiophene extends the absorption of the polymer molecule to longer wavelength region. The polymer showed higher solar energy conversion efficiency in bulk heterojunction (BHJ) solar cell. The polymer showed strong absorption peak at 575 nm in thin film with an optical bandgap 1.62 eV and exhibited intense fluorescence emission at 800 nm. The HOMO energy level of the polymer was found to be -4.92 eV.

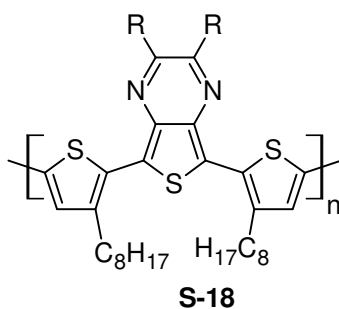


A series of novel conjugated polymers (**S-17**) comprised of 9,9-dihexylfluorene and thiophene or substituted thiophene moieties (Pal et al. 2007), were synthesized via the palladium-catalyzed Suzuki coupling reaction. In their design, both electron-donating and electron withdrawing substituents were incorporated. The steric effects of the bulkier substituents influenced the absorption and photoluminescence properties of the polymers. These polymers showed very good solubility and thermal stability. Polymer having ester substitution on thiophene ring displayed low bandgap compared to other polymers.



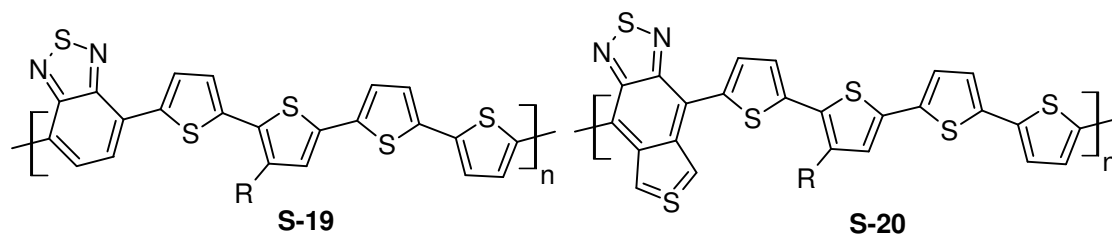
where R = C₆H₁₃, -CH₂OC₆H₁₃, -COOC₆H₁₃, -CN

Zoombelt et al. (2008) synthesized three low bandgap conducting polymers (**S-18**) carrying alternating dithiophene and thienopyrazine units via Yamamoto coupling polymerization. The polymers showed an optical bandgap of about 1.3 eV in the solid state. The solubility of the polymer was achieved by varying the chemical nature of the side chains. These polymers showed good solar cell performance with short-circuit currents of 5.2 mA/cm². An efficiency of 0.8 % was achieved under estimated standard solar light conditions, (AM 1.5 G, 100 mW/cm²) with spectral response up to 950 nm.



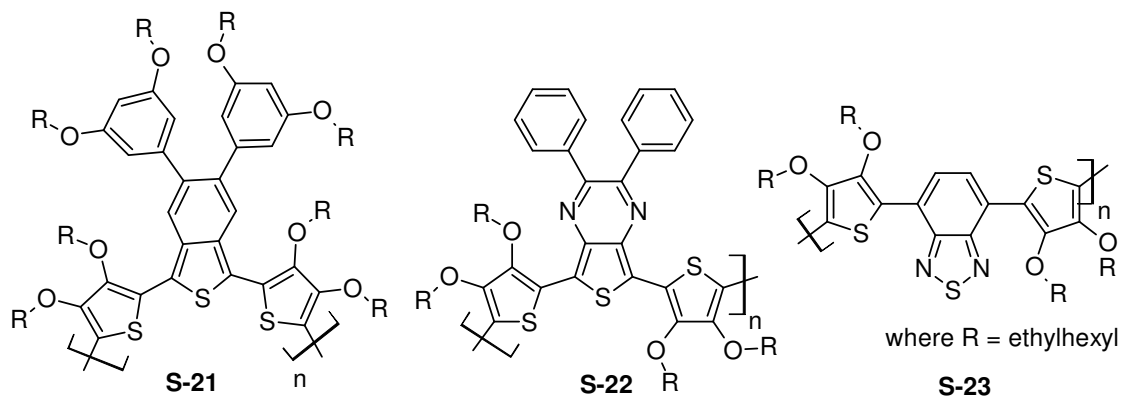
where R = 2-ethylhexyl, octyl

In recent times, Bundgard's research group (2007) synthesized thiophene based conjugated polymers (**S-19** and **S-20**) with benzothiazole and benzothiadiazole as acceptor units. According to authors, incorporation of 3,7,11-trimethyldodecyl side chains improved their solubility and better film forming properties than the use of 2-ethylhexyl, hexyl, or dodecyl as side chains. The HOMO and LUMO levels were determined to be 5.2 and 3.6 eV with a bandgap of 1.65 eV for benzothiadiazole containing polymer (**S-19**) and at -5.1 and -4.4 eV for benzo-bisthiadiazole containing polymer (**S-20**). The electrochemical results indicated that these acceptor units effectively lower the LUMO level of the polymer keeping the HOMO level more or less constant. These polymers showed good photovoltaic performance in devices.

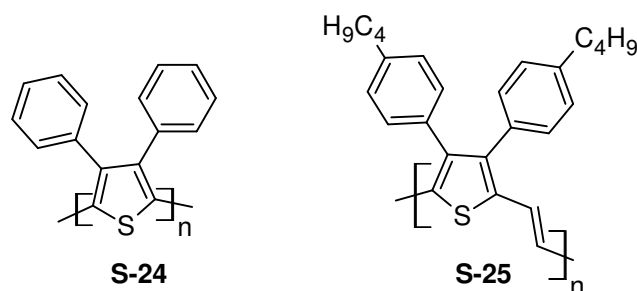


where R = 2-ethylhexyl, hexyl, or dodecyl

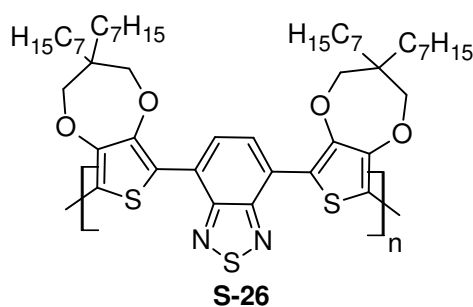
Three new conjugated polymers (**S-21** - **S-23**) carrying electron accepting benzothiadiazole and electron donating alkoxythiophene were synthesized (Wienk et al. 2006). Here alkoxy side-chains resulted in enhancement of electron donating nature of the thiophene ring with increased solubility of the polymers. The optical bandgap of polymer **S-21** was found to be 1.55 eV in the solid state. This polymer was further modified, using a different type of acceptor unit, i.e. a diphenylthienopyrazine unit. Then the bandgap of the polymer **S-22** decreased to 1.28 eV. Also they observed the shift in the HOMO and LUMO levels of the polymers when the alkyl chains were replaced by phenyl groups. Its bandgap was found to be 1.20 eV in thin film.



Two interesting conjugated poly(thiophene)s, i.e. 3,4-diphenyl substituted poly(thienylene vinylene)s (DP-PTV) (**S-24** and **S-25**) were synthesized (Chan et al. 1998) via dithiocarbamate route. The authors reported that these polymers possess bandgap in the range of 1.7 to 1.8 eV and good thermal stability up to 400 °C. As per the report, the solubility of the polymer can be improved by attaching the alkyl side chains into the phenyl group on 3,4-diphenylthiophene ring of the polymer backbone.



In pioneering studies, Shin et al. (2007) developed the synthetic method for a new low bandgap D-A type conjugated polymer (**S-26**) based on 3,4-disubstituted thiophene. In this molecule alkoxy thiophene acts as a donor and benzothiazole acts as an acceptor. Due to the high electron releasing capacity of thiophene and withdrawing nature of benzothiazole, polymers showed the HOMO and LUMO energy levels at -4.82, -3.7 eV, respectively. The optical bandgap of the polymer was determined to be 1.5 eV and it was used in bulk hetero junction solar cell.



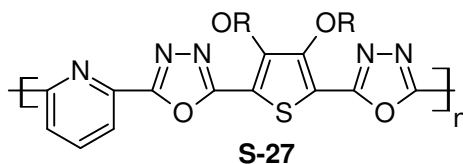
Thus, literature survey on the thiophene based conjugated polymers reveals that introduction of thiophene ring in the polymer main chain or side chain enhances the stability, charge carrying nature, linear/nonlinear optical behavior, and optoelectronic properties and reduces the bandgap. Keeping this in view, in the present work it has been planned to design new thiophene based donor-acceptor type conjugated polymers carrying 3,4-dialkoxythiophene units as electron rich segments along with the other electron deficient moieties with the hope that the resulting polymers would show improved properties like solubility, charge carrying potential, linear optical and nonlinear optical responses.

2.2.2. Conjugated polymers containing 1,3,4-oxadiazoles

1,3,4-Oxadiazole is one of the main electron transport systems and it has good electron withdrawing capacity. Incorporation of 1,3,4-oxadiazole moiety in the

polymer main chain or side chain enhances the stability and charge transport property. Besides these properties, 1,3,4-oxadiazole ring has high electron affinity, which makes the polymer useful, when it is copolymerized with electron rich segments like alkoxythiophene. Balanced electron-hole injection and transport can be achieved in donor acceptor polymer containing 1,3,4-oxadiazole as a potent acceptor moiety with different electron donating spacers (Ojha et al. 2003). Further, introduction of this rigid 1,3,4-oxadiazole heterocycle along the polymer backbone strengthens the enhancement in the D-A nature of the polymer and, also it enhances the nonlinear behavior (Udayakumar et al. 2006).

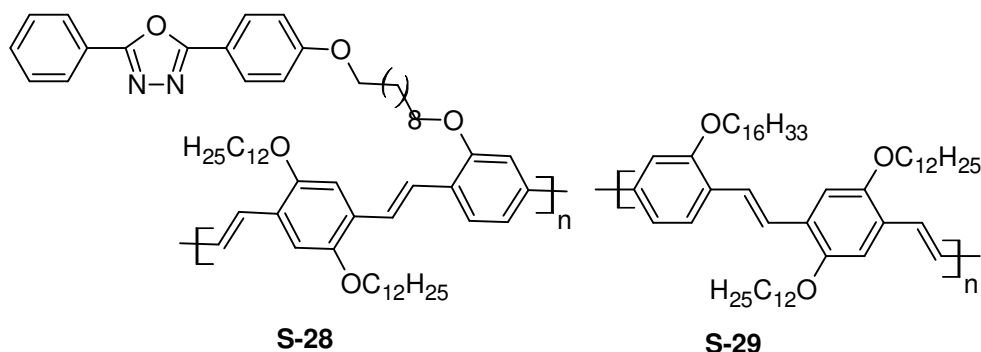
A new series of NLO active conjugated polymers (**S-27**) consisting of alternate 3,4-dialkoxythiophene and (1,3,4-oxadiazolyl)pyridine moieties were synthesized by Hegde et al. (2009). These polymers showed good thermal stability up to 300 °C and their electrochemical bandgap was found to be in the range of 2.3 - 2.55 eV. The polymers were shown to possess good optical limiting behavior with enhanced nonlinear susceptibility of the order of 10^{-12} esu, which is dependent on alkoxy chain length.



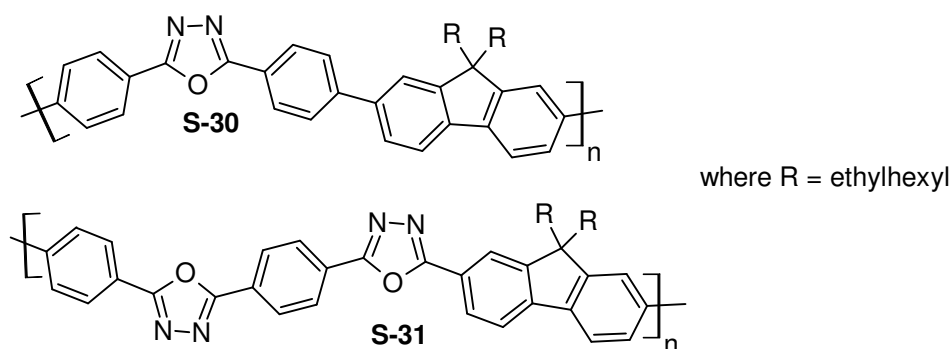
where R = C₃H₇, C₅H₁₁, C₇H₁₅

In an interesting study, Kim (2008) designed and synthesized two new conjugated polymers (**S-28** and **S-29**) with phenylene vinylene linkages. In addition they studied the effect of 1,3,4-oxadiazole moiety on the optical properties of the resulting polymers. They introduced 1,3,4-oxadiazole containing pendants in one of the studied polymers in order to investigate the effect of side chain on the behavior of polymer. The bandgaps of the polymers were found to be almost identical. But the external quantum efficiency of the device fabricated using the polymer containing oxadiazole pendant was higher than that of other polymer without 1,3,4-oxadiazole. The energy levels figured out from optical and electrochemical data strongly support that the oxadiazole pendants have hole blocking properties. Single layer structured EL

device obtained from oxadiazole carrying polymer showed the emission at the reverse bias with an efficiency of 0.043 cd/A.

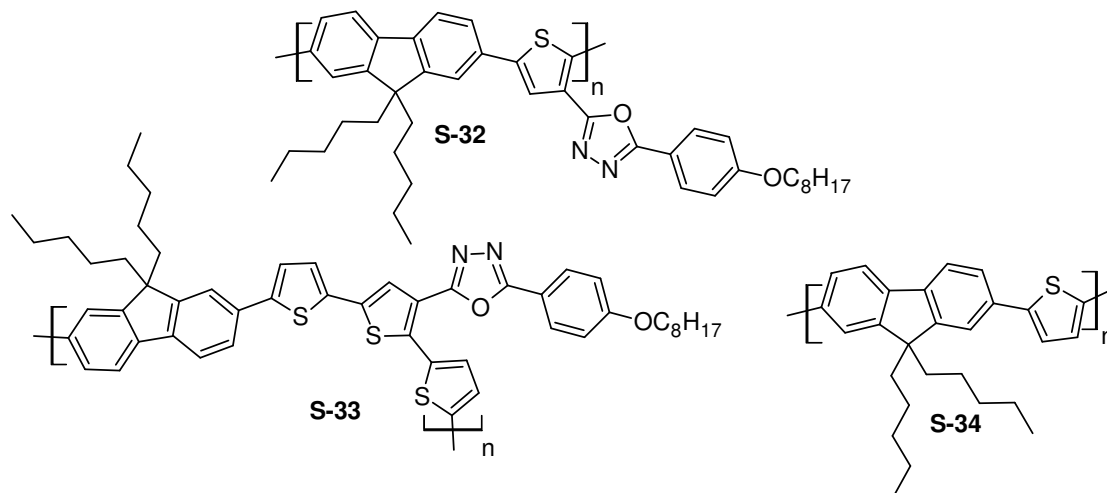


Zhan et al. (2002) developed synthesis of new conjugated polymers (**S-30** and **S-31**) containing 1,3,4-oxadiazole in the main chain by palladium-catalyzed Suzuki coupling reaction. According to authors, the polymers possessed excellent thermal stability with glass transition temperatures of 114-208 °C and onset decomposition temperatures of 387-415 °C. Cyclic voltammetric studies showed that these polymers possess LUMO energy levels ranging from -3.01 to -3.37 eV and HOMO energy levels ranging from -6.13 to -6.38 eV. Thus, the polymers were shown to possess very good electron-transporting or hole-blocking property. Interestingly, they also exhibited strong blue luminescence in the range of 414-476 nm with narrow bandwidth upon photo-excitation.

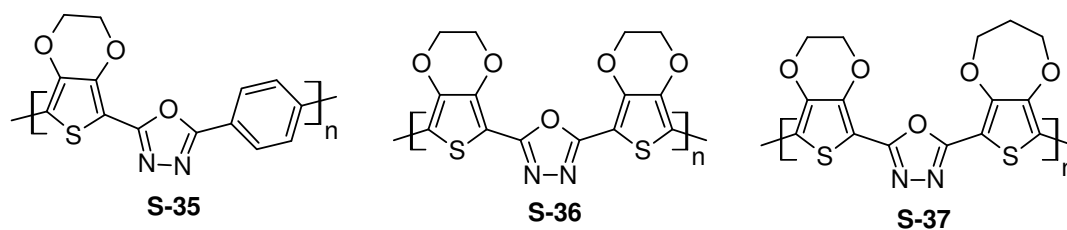


In an important study, Zhao et al. (2009) developed new series of conjugated polymers (**S-32-S-34**) comprising of 9,9-dihexylfluorene and thiophene derivatives with/without 1,3,4-oxadiazole side chains through palladium catalyzed Suzuki cross coupling reaction. They studied the effect of 1,3,4-oxadiazole side chains on their thermal, optical, electrochemical and photovoltaic properties. They observed that introduction of rigid 1,3,4-oxadiazole side chain improved the thermal stability of the

polymer; further it enhanced the electron-injection and charge transporting properties. Photovoltaic study showed a maximum power conversion efficiency of 1.49 %.

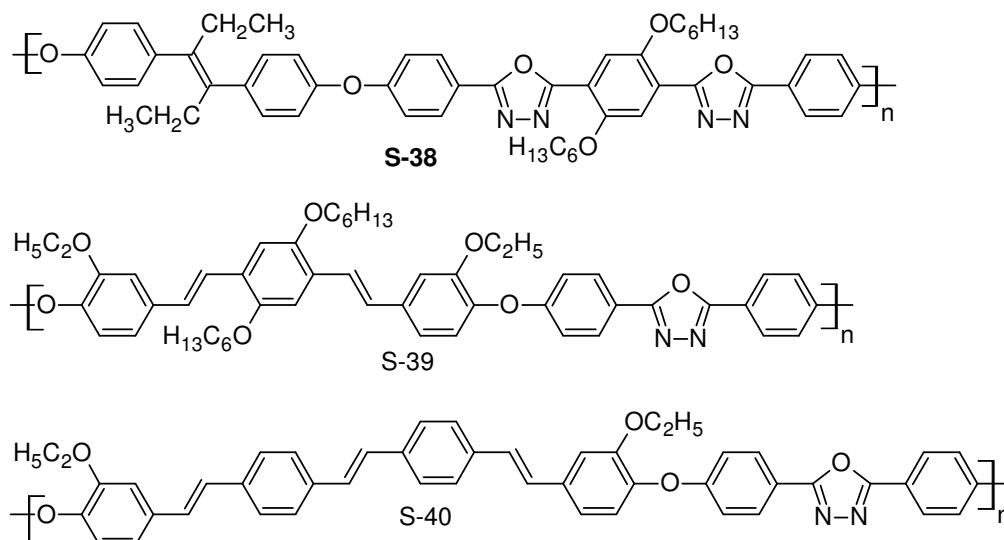


Three new conjugated polymers (**S-35** - **S-37**) containing 1,3,4-oxadiazoles and 3,4 dialkanedioxythiophenes were synthesized by Ojha et al. (2003) using precursor polyhydrazide route. The polymers displayed good solubility and exhibited high thermal stability with onset decomposition temperature around 330 °C. Their optical and electrochemical studies substantiated their applications in light emitting diodes.

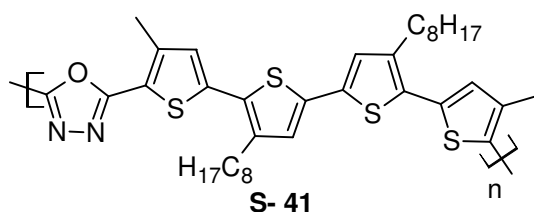


Poly(ether)s (**S-38** - **S-40**) consisting of alternate stilbene, distyrylbenzene, and 1,3,4-oxadiazole chromophores were prepared by Chen et al. (2002) for LED applications. As reported, the polymers are amorphous materials with decomposition temperature greater than 250 °C and their solubility enhanced with the incorporation of hexyloxy side chain. Further, their fluorescence study showed emission maxima at 442, 540 and 528 nm, respectively. Based on the results, authors concluded that presence of oxadiazole chromophores in polymer backbone enhanced the electron affinity, whereas pendant hexyloxy group reduced the ionization potential. The

fabricated PLED showed maximum threshold voltage and luminance of ITO/Polymer (S-39) (100 nm)/Al single layer device are 17V and 950 cd/m².



Levi and his associates (Levi et al. 2006) described synthesis of a new macro-monomer (S-41) containing oligo(alkyloxy thiophene) and 1,3,4-oxadiazole sub units. Further it was polymerized using electro-polymerization technique. Results of the electrochemical study suggest that the incorporation of π -conjugated electron accepting units (1,3,4-oxadiazole) into the poly(thiophene) backbone leads to significant improvement in the n-doping and redox stability of the resulting polymer.



With relevance to the literature reports, it can be concluded that the incorporation of the electron accepting 1,3,4-oxadiazole units with any electron releasing system in a polymer backbone would enhance the D-A nature with reduction in the bandgap. From the literature, it is clear that the polymers containing 1,3,4-oxadiazole moiety possess good thermal stability, electron carrying property, light emitting property and optical nonlinearity. Owing to the importance of the 1,3,4-oxadiazole moiety, in the present work it has been planned to design new D-A type of

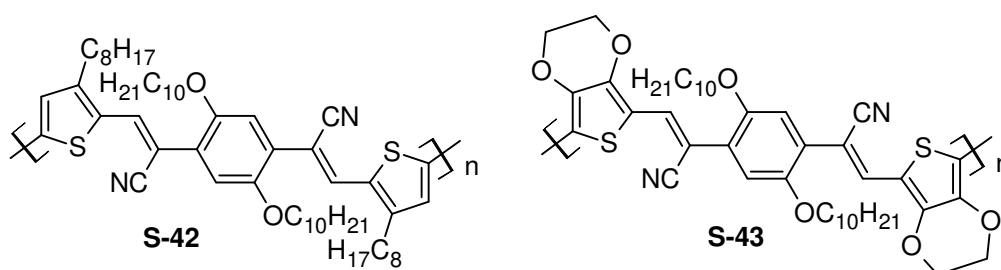
conjugated polymers bearing 1,3,4-oxadiazole as powerful electron accepting group, with the expectation of enhanced optical and electrochemical properties.

2.2.3. Cyanovinylene based conjugated polymers

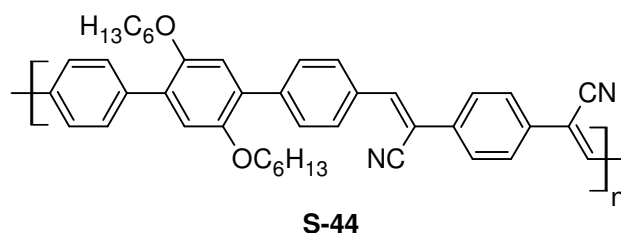
Cyanovinylene based conjugated polymers possess very good electroluminescence properties and hence they are most suitable as hole-injecting and electron transporting materials (Bradley et al. 1993). To set an adequate balance in the injection flows coming from each side of the LED device, it is necessary to use electron transporting layer of CNPPV. Such derivatives are generally synthesized via Knoevenagel condensation between aromatic diacetonitrile and corresponding aromatic dialdehydes.

Conjugated polymers based on cyanovinylene groups are known for their low bandgap. Since cyano group is a good electron-accepting unit, its presence along with electron donor system in a polymer chain makes it strongly p-type. Such polymers offer various attractive features for use in a variety of device architectures like thin-film transistor (TFT), light emitting diodes (LED), nonlinear optical devices (NLO), photovoltaic cells etc. Some of the selected literature reports on D-A type polymer containing cyanovinylene units as a strong electron acceptor are given below.

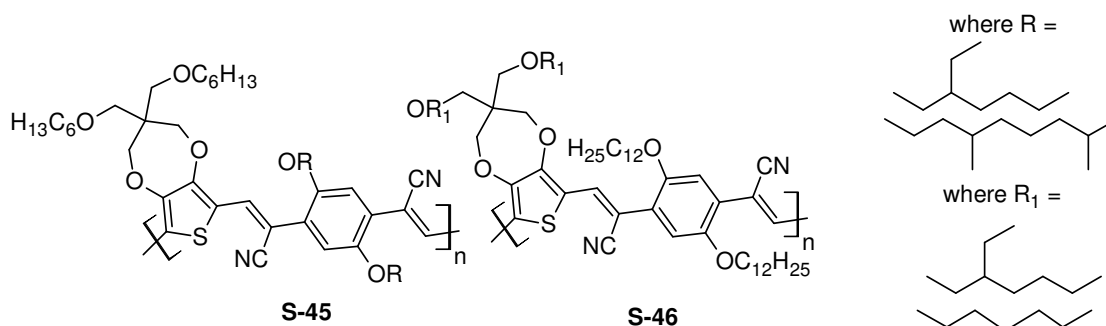
Colladet et al. (2007) synthesized a series of new D-A type conjugated polymers (**S-42** and **S-43**) carrying bis(1-cyano-2-thienylvinylene)phenylene in the main chain, via oxidative polymerization using FeCl_3 as oxidizing agent. They reported that the polymers are highly soluble in common organic solvents because of the presence of alkyl and alkyloxy side chains. Absorption maxima of these polymers were found to be 720 and 780 nm, respectively. Optical and electrical properties showed that their bandgaps are 1.72 and 1.59 eV, respectively. These low bandgap polymers blended with PCBM showed efficient charge transfer property, which was confirmed by photo luminescence studies.



A new electroluminescent conjugated polymer (CN-P3PV) (**S-44**) containing electron withdrawing cyano group was synthesized (Wu et al. 2001) and studied for its optoelectronic properties. It showed high thermal stability ($T_d \approx 360$ °C, $T_g \approx 151$ °C), high electron affinity, and good film forming ability. Electrical characterization of a double-layer organic LED on the structure of ITO/CuPc/CN-P3PV/Ca/Ag displayed high electron transporting ability and good electroluminescence performance with the emission of bright orange light.

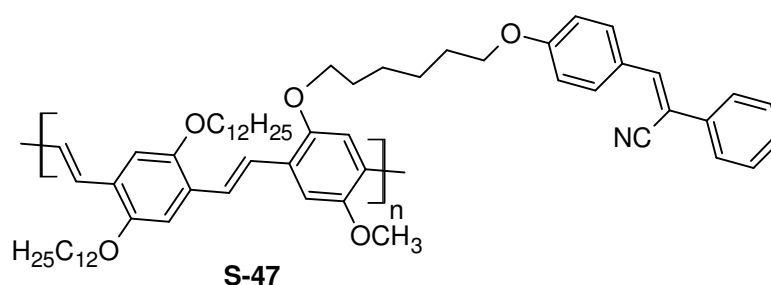


An interesting class of low bandgap cyanovinylene based polymers (**S-45** and **S-46**) were designed and synthesized by Galand and his co-workers using Knoevenagel condensation method (Galand et al. 2006). The authors introduced linear and branched alkoxy chains in the backbone in order to increase the solubility and film forming nature of the polymer. A blue shift in absorption spectra was observed when linear alkoxy chain was replaced by a branched chain in the polymer side chain. Their optical bandgap was found to be in the range of 1.70-1.75 eV. They showed significant photovoltaic performance as electron donors when combined with an electron acceptor such as (6, 6)-phenyl C61-butyric acid methyl ester (PCBM) in bulk heterojunction photovoltaic devices with an efficiency of 0.4 - 0.5 %.

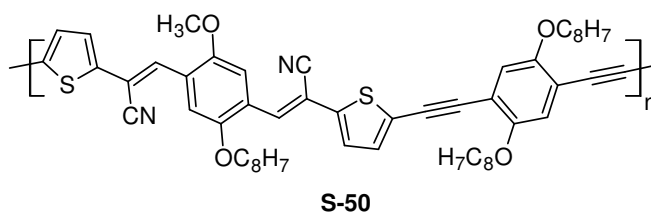
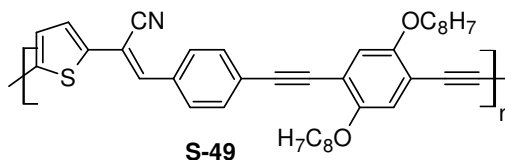
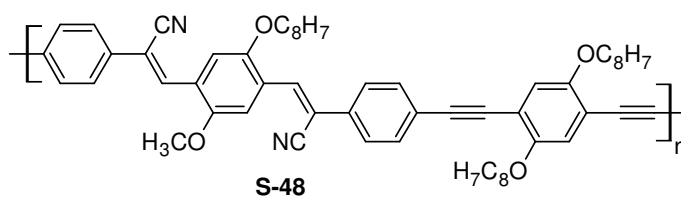


Kim and Lee (2003) reported the synthesis and optoelectronic properties of a new poly(*p*-phenylenevinylene) derivative (**S-47**) carrying pendent 1,2-diphenyl-2-cyanoethene unit via Heck coupling reaction. In this polymer, electron withdrawing

pendant (1,2-diphenyl-2-cyanoethene) unit is linked to main chain through linear 1,6-hexamethylenedioxy chain. Its bandgap figured out from the UV-vis spectrum was 2.10 eV and photoluminescence (PL) maximum appeared at 582 nm. Their HOMO and LUMO energy levels were estimated to be -4.99 and -2.89 eV. A single layer EL device based on this polymer has an efficiency of 0.114 cd/A. These results indicate that the pendant 1, 2-diphenyl-2-cyanoethene (CNST) unit is a good electron transporting material.



Zou et al. (2009) designed three new D-A type conjugated polymers (**S-48 - S-50**) containing cyanovinylene group and a triple bond in the main chain for their applications in photovoltaics. The new design resulted in increase in their reduction potentials. Their absorption maxima were found to be 453, 431 and 512 nm, and the observed bandgaps are 2.03, 2.02, and 1.7 eV respectively. Because of their high absorption range and good electron acceptor nature, they are most suited for solar cell applications.

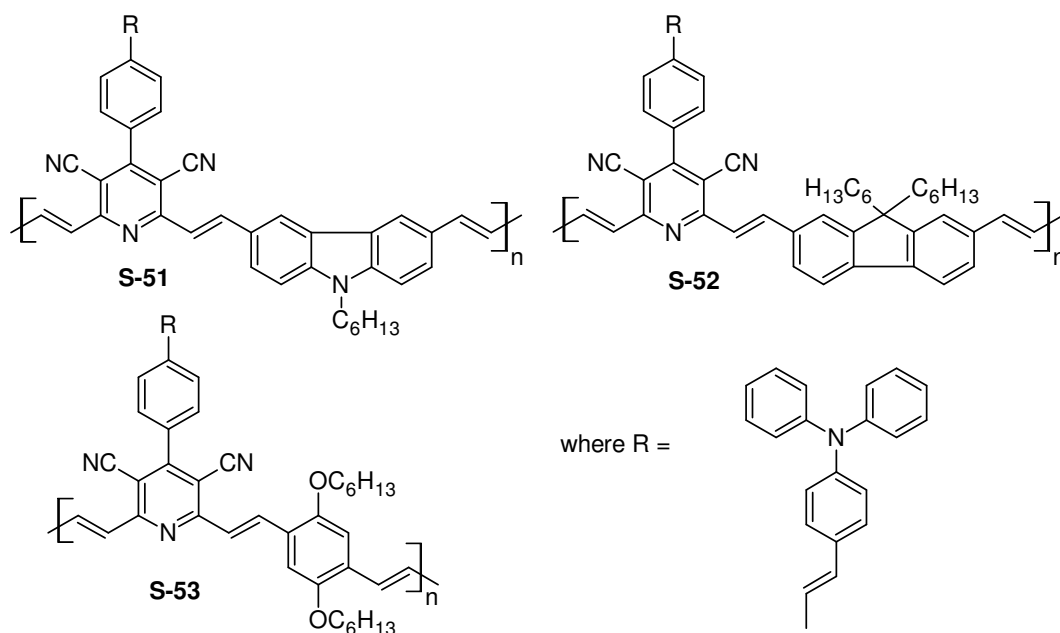


From the foregoing account, it is clear that the polymers containing cyanovinylene unit in the main chain possess high UV-vis. absorption maxima and low bandgap. Thus, introduction of this moiety along the main chain would enhance the optoelectronic property of the resulting polymer. Keeping this in view, it has been contemplated to design the new conjugated polymers with cyanovinylene as potent electron accepting unit in the main chain.

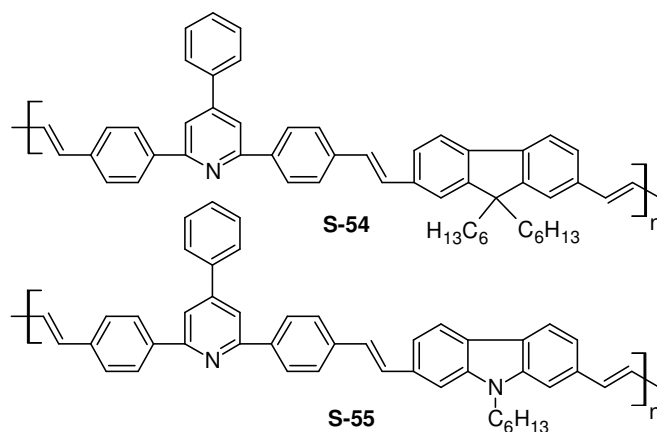
2.2.4. Pyridine based conjugated polymers

Different types of nitrogen heterocycles are incorporated into various conjugated polymer backbones in order to tune their optoelectronic and photonic properties. Amongst a variety of hetero-cycles, pyridine plays an important role as it is a strong electron accepting system. Some of the most extensively studied structures carrying the pyridine moiety include poly(2,5-pyridine), poly(3,5pyridine), poly(p-pyridylene vinylene)s and poly(phenylene vinylene pyridylene vinylene)s (Akcelrud et al. 2001). Also, pyridine containing conjugated polymers showed enhanced donor-acceptor nature with good optical limiting threshold (Wang et al. 2006). A brief account on some of the selected literature available on pyridine based conjugated polymers are presented below.

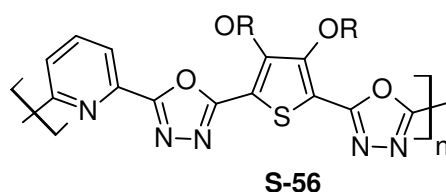
In an interesting study, Wang et al. (2006) synthesized three new donor acceptor conjugated polymers (**S-51** - **S-53**) derived from 3,5-dicyano-2,4,6-tristyrylpyridine through the Knoevenagel reaction. The polymers showed good solubility in common organic solvents and high molecular weight. Their UV-vis. absorption maxima were found to be 417, 443 and 448 nm, respectively and photoluminescence was observed at 596, 564 and 570 nm, respectively. From the results of their optical power limiting study, the authors concluded that fluorene containing conjugated polymer emerged as good optical power limiter with the power limiting value 728 m J/cm^2 .



Recently, an interesting class of new 2,4,6-triphenylpyridine based conjugated polymers (**S-54** and **S-55**) containing fluorene or carbazole moiety were synthesized by Mikroyannidis et al. in the year 2009 via Heck coupling. The polymers showed good thermal stability with the degradation temperature around 300 °C. Presence of kinked 2,4,6-triphenylpyridine units along the polymer backbone caused a partial interruption of the π -conjugation. The polymers emitted blue-green light with emission maxima at 446 and 464 nm and quantum yields of 0.52 and 0.28, respectively in THF solution. Their electroluminescence spectra showed a strong red shift to its emission maxima, which is mainly attributed to the direct cross recombination transition between electrons and holes trapped on carbazole or triphenylpyridine subunits. They displayed good efficiency in electroluminescence devices with luminescence of 647 and 615 cd/m^2 .

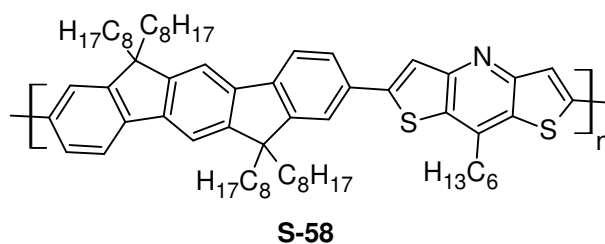
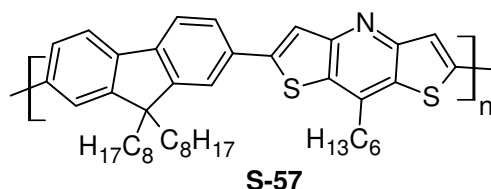


In another study, three new donor acceptor type conjugated polymers (**S-56**) bearing 3,4-dialkoxythiophene and (1,3,4-oxadiazolyl)pyridine moieties were designed and synthesized by Hegde et al., through poly-condensation method (Hegde et al. 2009). The authors reported that polymers possess good thermal stability with the onset decomposition temperature up to 300 °C. The absorption maxima of the polymers were found to be in the range of 342-360 nm. Further, they were shown to display bluish-green fluorescence in solution state and their bandgaps were determined to be about 2.55 eV. They were found to be good NLO materials with χ^3 values 0.881×10^{-12} , 0.901×10^{-12} , 1.03×10^{-12} esu, respectively.



where R = C₃H₇, C₅H₁₁, C₇H₁₅

Sonar et al. (2004) reported two new pyridine based conducting polymers with fluorene and indofluorene units in the main chain (**S-57** and **S-58**). The polymers displayed reduction potentials about 0.5 V lower than that of the corresponding fluorene and indenofluorene homo polymers, indicating much improved electron-accepting properties. Light emitting diodes, fabricated using these polymers as the emitting layers produced blue-green emission with low turn-on voltages with aluminum electrodes confirming their improved electron affinity. While, the indenofluorene polymer showed an irreversible red shift in emission at high voltages, which is attributed to oxidation of the indenofluorene units.



Choon et al. (2001) evaluated the optical and electrochemical properties of a novel polymer (**S-59**), i.e. poly(2,5-dialkoxy-1,4-phenylene-*alt*-2,5-pyridine) functionalized with alternating donor/acceptor repeat units. This was synthesized by Suzuki-coupling reaction. Study of optical properties of the polymer revealed that the absorption maximum and bandgap of it are 383 nm and 3 eV, respectively. Further, it was found that the polymer is facile in n-doping and is a good electron transporting material due to the presence of electron-withdrawing pyridine unit. The polymer displayed bathochromic shift when protonated with trifluoro acetic acid in chloroform solutions.



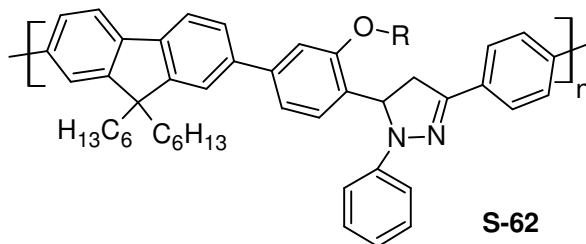
On the basis of literature reports on pyridine based polymers, it can be concluded that introduction of electron withdrawing pyridine nucleus in the polymer backbone enhances the thermal stability and solubility of the resulting polymer. Also, presence of pyridine hetero-cycle in the polymer chain influences the optical and electrochemical property. Further, cyanopyridine being a fluorescent chromophore with electron withdrawing property enhances the fluorescence emission maxima of the polymer if it is connected adjacent to the highly electron releasing systems.

Keeping the above facts in view, it has been planned to introduce the cyanopyridine moiety as one of the main electron withdrawing units next to electron releasing aromatics in the design of new polymers, with the hope that the resulting D-A type polymers would possess good fluorescent emission and good nonlinear response.

2.2.5. Pyrazole based conjugated polymers

According to literature, pyrazole containing conjugated polymers are good electron transport materials with high charge carrying nature (Tameev et al. 2004). Generally, the molecular weights of such polymers are high (Chung et al. 1997) and these polymers are good electroluminescent materials. Also, they show good quantum efficiency in the polymer light emitting diodes (Danel et al. 1999). However, in the

-5.71 to -5.81 eV. Newly synthesized polymers showed green fluorescence emission with photoluminescence (PL) quantum yields of 45-59 %. The external quantum efficiency of the PLED designed from these polymers was found to be 0.6 and 2.53 %, respectively.



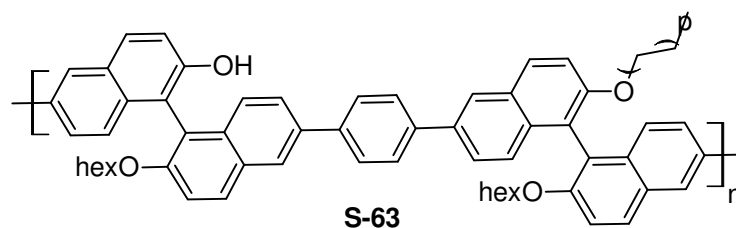
where R = (CH₂)₅ CH₃, (CH₂)₁₁ CH₃

From the literature survey on the polymers derived from pyrazole, it is clear that the introduction of pyrazole moiety along the polymer backbone would enhance its charge carrying property and fluorescence behavior. Keeping this in view, it has been planned to introduce pyrazole as one of the potent electron donor groups in the polymer chain in order to study the effect of it on the optical properties of the resulting polymers.

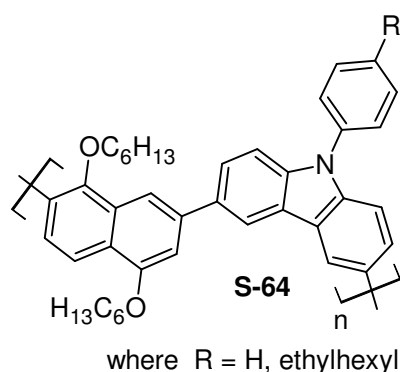
2.2.6. Naphthalene based conjugated polymers

In the field of organic semiconductor research, naphthalene plays an important role. Naphthalene based organic materials are often showing intense fluorescence emission, which is due to the π -electronic interaction of the molecular stacks. Generally, such materials are thermally stable and hence they find applications in the field of optoelectronics. However, there is less number of reports available on D-A type conjugated polymers with high electron releasing thiophene segments along with naphthalene units, in the literature. Some of the relevant reports on the naphthalene based conjugated polymers are outlined in the following section.

Koeckelberghs et al. (2003) developed the synthesis of a new helical poly(binaphthalene)s (**S-63**) as a potential nonlinear material, via Mitsunobu reaction. Thin films fabricated using the polymer were measured for their second-harmonic generation effect; they showed non resonant nonlinear susceptibilities up to 10.6 pm/V. Also, they displayed good third order NLO properties.



Mori and Kijima (2009) designed and synthesized naphthalene based carbazole containing conjugated polymers (**S-64**) by Ni-mediated Yamamoto coupling and Pd-catalyzed Suzuki coupling reactions. These thermally stable polymers exhibited blue photoluminescence in the film state and high fluorescence quantum efficiencies in solution state. Polymer light emitting diodes fabricated from these polymers showed good electroluminescence with a maximum brightness of 8370 cd/m² at 13 V and a maximum efficiency of 2.16 cd/A at 7 V.



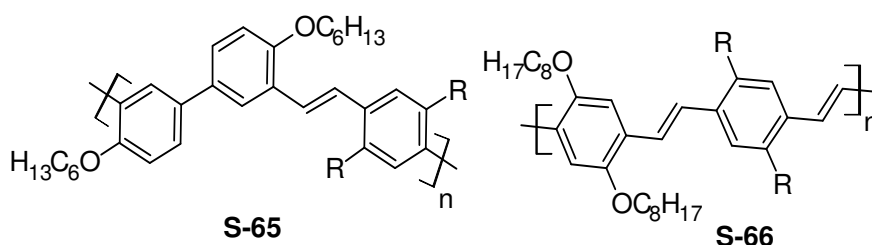
Owing to the importance and established properties of the reported naphthalene based polymers, it has been contemplated to synthesize new D-A type polymers carrying a rigid naphthalene unit along with electron releasing 3,4-dialkoxythiophenes and electron accepting 1,3,4-oxadiazole rings. It has been hoped that new polymers would exhibit better thermal and optoelectronic properties.

2.2.7. p-(Phenylenevinylene) based conjugated polymers

Poly-(p-phenylenevinylene) (PPV) is an interesting material for electro-optical applications. This was the first reported electro luminescent polymer that showed green yellow emission. This polymer possesses good thermal stability with high photoluminescence efficiency. However, it is insoluble and infusible making it difficult to fabricate into thin films. Interestingly, incorporation of alkyloxy or alkyl as side chains into these PPV derivatives makes them soluble in common organic solvents and it enhances the optical and electrochemical properties of the polymers

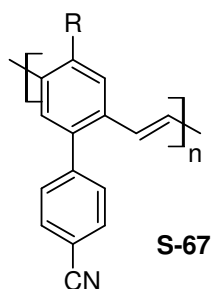
significantly (Akcelrud et al. 2001). Also, these polymers show excellent nonlinear optical response in their film state (Samoc et al. 1998).

Junjian et al. (2008), in an approach to develop new materials for LEDs, synthesized two new conjugated polymers (**S-65** and **S-66**) containing triphenyl amine-substituted poly(*p*-phenylenevinylene) derivatives through Wittig-Hornor reaction. UV-vis absorption spectra of these polymers showed absorption maxima at 348 and 478 nm, respectively in their film state. The optical bandgaps of these polymers were found to be 2.8 and 2.25 eV respectively. Polymer light-emitting diodes fabricated by these polymers showed the maximum luminance of 3003 cd/m² at 10 V.



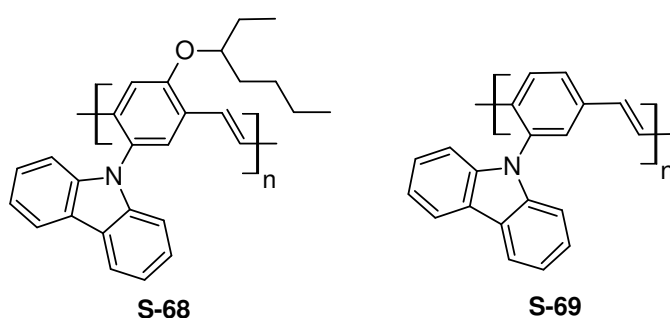
where R = triphenyl amine

Novel poly(*p*-phenylenevinylene) derivatives (**S-67**) containing an electron-withdrawing cyano-phenyl group on the polymer backbone, synthesized by Seung et al. via the Gilch polymerization (Seung et al. 2002) were shown to be good electroluminescent materials. The polymers displayed thermal resistance up to 400 °C and showed high glass transition temperature (T_g above 180 °C), rendering electroluminescence (EL) devices constructed from these polymers are thermally stable. Here, presence of electron-withdrawing cyano-phenyl group lowered the HOMO and LUMO energy levels to those of simple PPV derivatives reported in the literature. PLED device constructed from these polymers exhibited good electroluminescence at 546 and 516 nm, respectively.

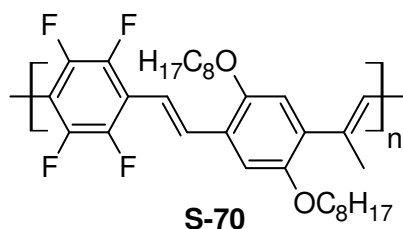


where R = ethylhexyloxy, dimethyl octylsilyl

Kim et al. (2001) demonstrated that the newly synthesized poly(p-phenylenevinylene) derivatives (**S-68** and **S-69**) carrying hole transport carbazole as pendent through Gilch polymerization, are very good donor materials in PLED. Electroluminescence spectra of these polymers revealed that the polymer containing alkoxy side chain is yellow-green light emitter (**S-68**) (530 nm) and the other polymer (**S-69**) is green light emitter (490 nm) in the device; maximum luminance of alkoxy substituted polymer was found to be 30390 cd m² at an electric field 1.50 MV cm⁻¹.

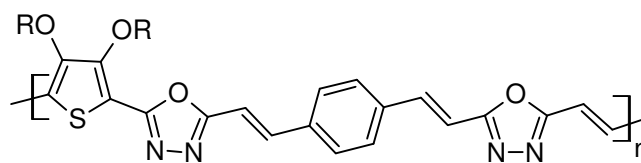


Babudri and co-workers (Babudri et al. 2003) synthesized a polymer carrying tetrafluoro and dialkoxy-substituted poly(p-phenylenevinylene) (PPV) with a high percentage of fluorinated units, via Stille cross-coupling reaction. The polymer showed good third order nonlinear optical activity with enhanced susceptibility values. The introduction of electron-deficient aromatic rings gave a high $\chi^{(3)}$ coefficient of 6.2×10^{-10} esu. This susceptibility value was found to be more than one order of magnitude larger than that of its homo-polymeric counterpart in the absence of fluorinated units.



A series of D-A type conjugated polymers (**S-71**) carrying oxadiazole and phenylenevinylene units in the backbone, synthesized by Udayakumar et al. (2006) was shown to possess high NLO response. The authors explored the third order nonlinear property of the polymers using Z-scan and four-wave mixing techniques

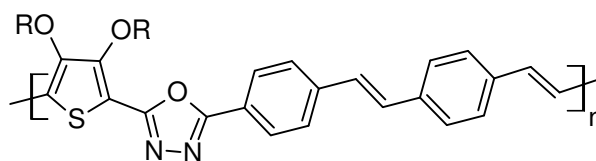
(DFWM). Z-scan measurement results showed a negative nonlinear refractive index (n_2) whose magnitude is of the order of 10^{-10} esu with enhanced optical limiting property. These results suggested that such donor acceptor polymers are useful in photonic switching and optical limiting devices.



S-71

where R = C₆H₁₃, C₈H₁₇, C₁₀H₂₁

Manjunatha et al. (2009) synthesized a series of new conjugated polymers (S72) carrying 3,4-dialkoxythiophene as electron donor and 1,3,4-oxadiazole ring as an electron acceptor by Wittig condensation method. The optical bandgaps of these polymers were observed in the range of 2.47 to 2.55 eV. Electrochemical study revealed that these polymers possess good charge carrying property.



S-72

where R = C₃H₇, C₅H₁₁, C₇H₁₅

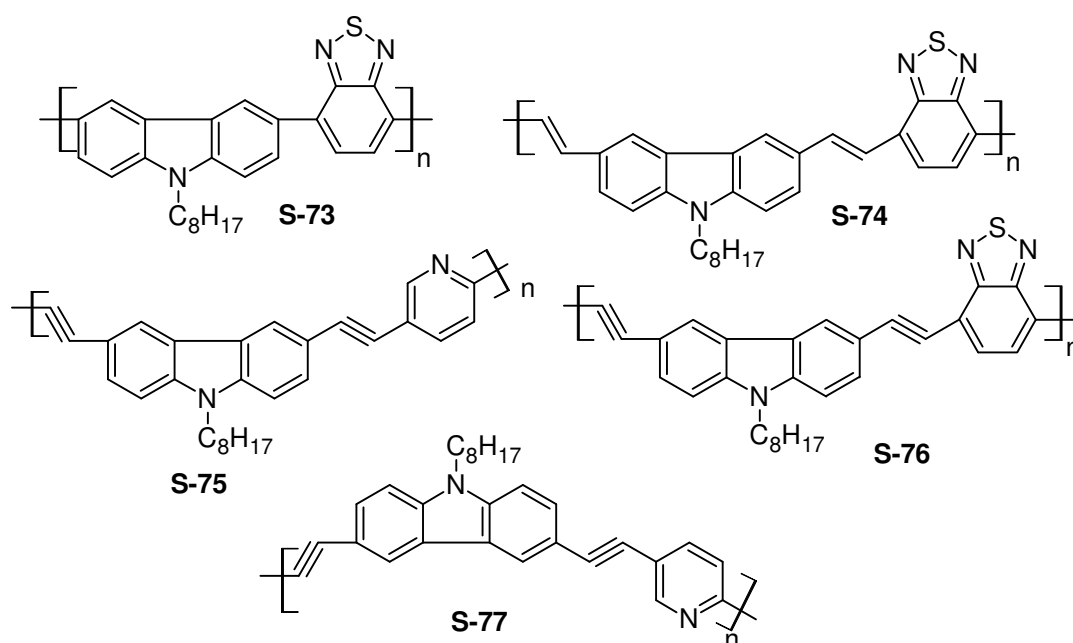
From the above mentioned reports, it is clear that the introduction of phenylenevinylene linkage along the polymer main chain increases the conjugation path length leading to enhancement in the absorption maxima and hence decreases the bandgap. Keeping this in view, it has been planned to design new D-A type conjugated polymers containing phenylenevinylene moiety in the backbone, with the hope that new design would show improved optical response.

2.2.8. Carbazole containing conjugated polymers

Since carbazole is one of the most important electron donating materials, its incorporation into a polymeric backbone enhances its photo-conducting and electron-donating properties (Mircea et al. 2005). Further, introduction of 3,6-disubstituted carbazole induces a bent conformation for the resulting macromolecular chain, which

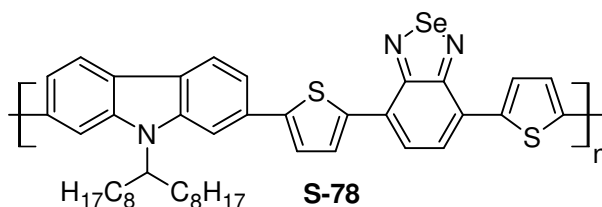
in-turn brings about enhanced thermal stability, solubility, extended glassy nature and moderately high oxidation potential of the resulting polymer (Grazulevicius et al. 2003). Also introduction of this moiety along the main chain or side chain enhances their optical nonlinearity considerably (Yoon et al. 2007).

In an interesting report, Michinobu et al. (2008) synthesized carbazole-containing donor-acceptor type conjugated polymers (**S-73** - **S-77**) by Sonogashira cross-coupling reactions of 3,6-diethynyl-9-hexadecylcarbazole with arylene dibromides. The polymerization with 4,7-dibromo-2,1,3-benzothiadiazole furnished an orange-colored polymer with a charge-transfer band at 440 nm in dichloromethane, indicating the efficient intra molecular donor-acceptor interactions. They observed good solvatochromic behavior in polymers carrying 2,5-substituted pyridine derivative. Further, they introduced various conjugated spacers in the main chain in order to study the effect of bridges on the properties of the polymer. The authors concluded that the ethynylene bridge serves as a more efficient π -spacer than vinylene units.

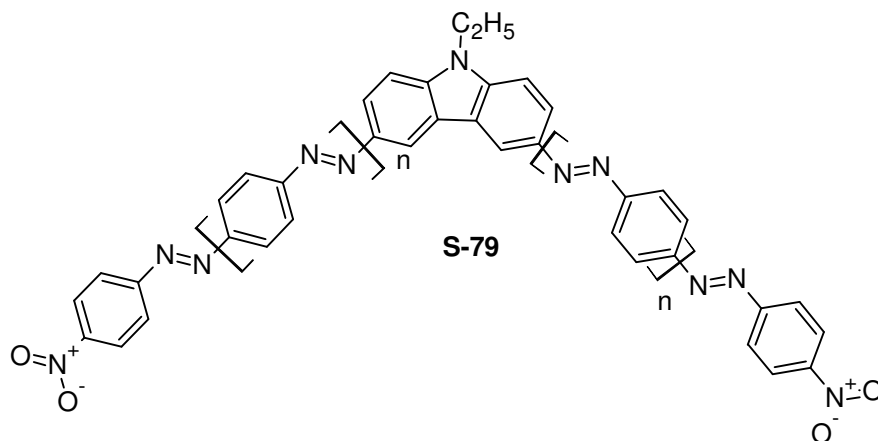


Recently, a novel conjugated alternating polymer (**S-78**) comprising of carbazole, thiophene and benzoselenadiazole was synthesized through Suzuki polycondensation reaction by Zhao et al. (2010). The polymer showed an excellent thermal stability with the decomposition temperature 390 °C and absorption peaks at 412 and 626 nm. The bandgap of the polymer was found to be 1.73 eV. Photovoltaic

cell fabricated using this polymer exhibited very good power conversion efficiency (PCE) of 2.58 %. The authors suggested that presence of N-substituted carbazole is mainly responsible for the low bandgap of the polymer.

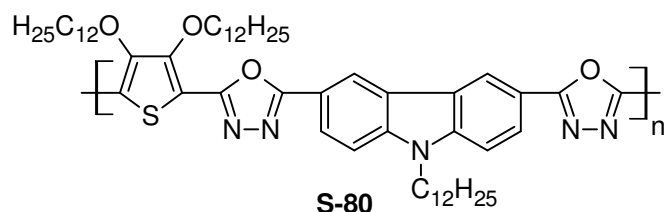


Qian et al. (2006) designed and synthesized a new conjugated polymer (**S-79**) having carbazole units along with diazo functionality. Further, they investigated its third order nonlinear optical activity using Z-scan technique. The NLO studies revealed that larger second-order hyperpolarizabilities (γ) can be readily achieved in such carbazole chromophores because of increased strength of electron withdrawing group and enhanced the molecular conjugation length with two aromatic bridges in the conjugated system. Based on the results, they concluded that the enhancement in the second-order hyperpolarizabilities arises from the conjugation path of the delocalized electrons which leads to large third-order nonlinear optical effects.



Manjunatha et al. (2009) described the synthesis of an interesting carbazole based conjugated polymer (**S-80**) with electron accepting 1,3,4-oxadiazole and electron donating substituted thiophene moieties, as a potent NLO material. The polymer was found to be electro-active both in oxidation and reduction cycle. It exhibited good thermal stability and solubility. In its solid state, the polymer showed green light emission with the electrochemical bandgap of 2.15 eV and the third order

NLO studies showed a strong three photon absorption process with high β values. The optical and electrochemical studies revealed that the new polymer is a promising material for development of efficient photonic devices.

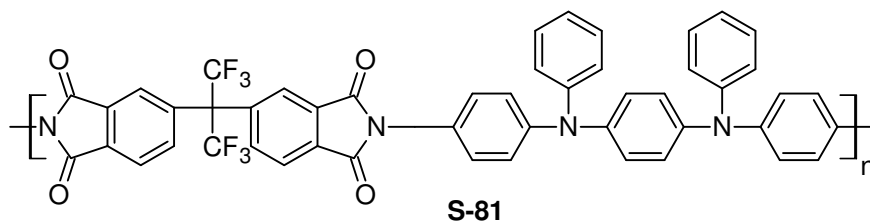


With this background which gives a vivid picture on importance of polymer carrying carbazole rings, it has been contemplated to incorporate carbazole unit as one of the electron releasing moieties in the design of new D-A type conjugated polymers with the expectation that the new molecules would show enhanced linear and nonlinear properties.

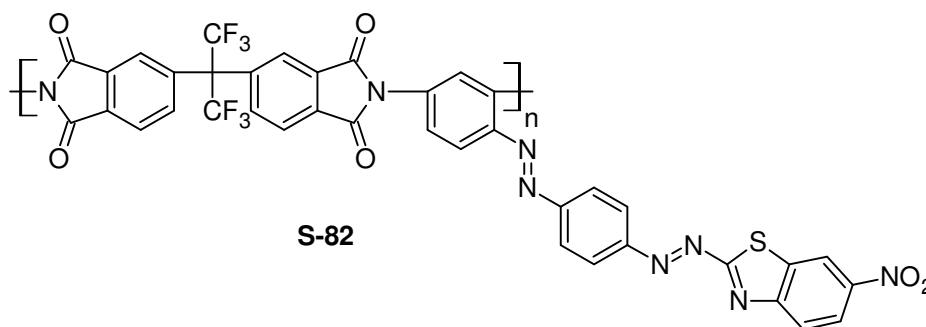
2.2.9. Conjugated cyclic polyimides

As an interesting class of polymeric materials, polyimides have attracted much attention because of their high T_g , which can be utilized to stabilize the dipole alignment of the NLO chromophore, particularly at high temperatures. High thermal stability of such polymers (Jung et al. 2006) leads to display good electro-optic properties at high temperatures also. The presence of cyclicimide functionality along the polymer back bone enhances the molecular hyperpolarizability and hence it results in the enhancement in the optical nonlinearity of the resulting polymers (Chen et al. 1995).

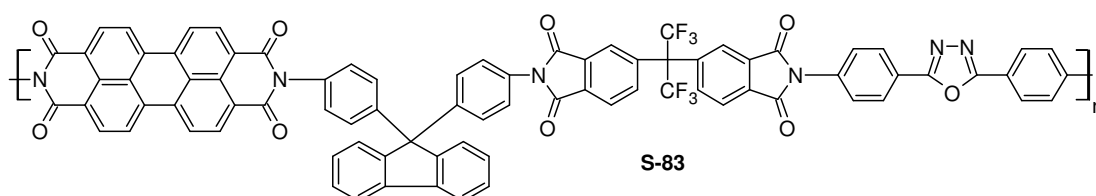
A new polyimide (**S-81**) containing triphenylamine unit, synthesized by Jung and coworkers (Jung et al. 2006) was shown to possess good electroluminescence property. It was prepared from the reaction of diamine monomer with 4,4-(hexafluoropropylidene)-diphthalic anhydride, which involved ring-opening polymerization followed by cyclo-dehydration process. The highest occupied molecular orbital (HOMO) level of the polymer was measured to be 5.5 eV and the optical bandgap of the polymer was estimated to be 3.1 eV. The polymer light-emitting diode fabricated by this polymer was shown to possess good efficiency and stability.



A thermally stable polyimide (**S-82**) with high molecular weight was synthesized by Leng et al. in the year 2001 through ring opening polymerization of dianhydride with two aromatic diamine containing benzothiazole moieties, as NLO active chromophore. It exhibited good second order NLO activity with electro optical coefficient 22 pm/V at the wavelength 830 nm.

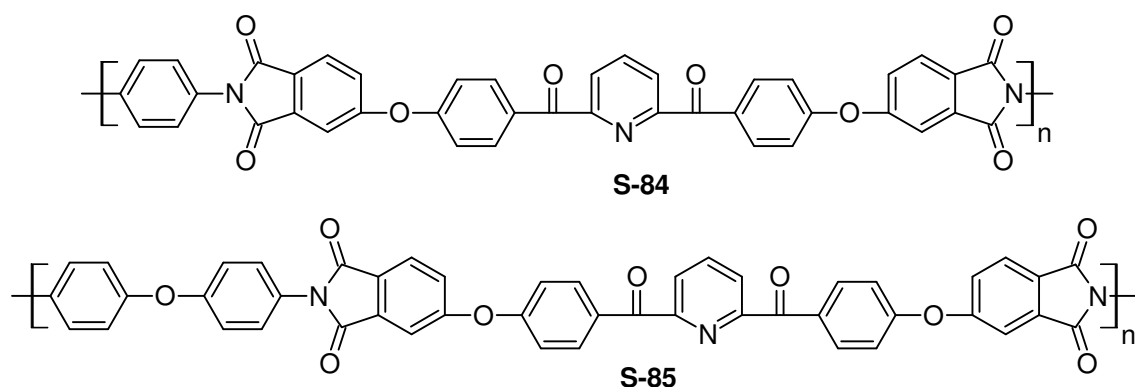


Xu et al. (2005) designed and synthesized an interesting polyimide (**S-83**) containing perylene, fluorene and oxadiazole units in the polymer backbone, through one-step polycondensation at high temperature. The polymer was soluble in common organic solvents and it exhibited high thermal stability with onset decomposition temperature around 494 °C in nitrogen atmosphere. Polymer exhibited reddish orange fluorescence with high quantum yield. The authors suggested that it can be used as thermally stable light-emitting and electron transporting material.

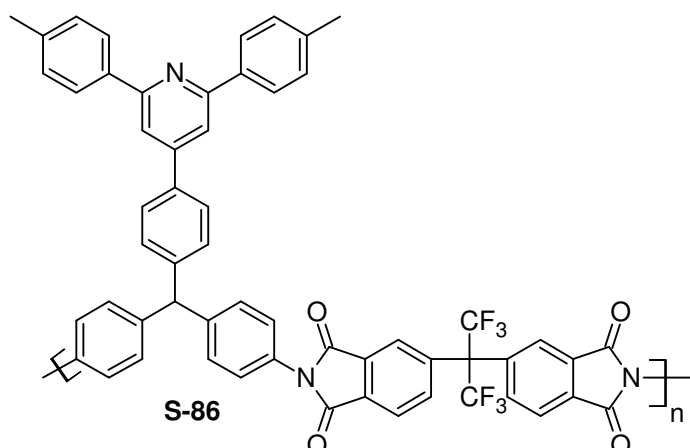


Interesting two new polymers carrying pyridine moiety (**S-84** and **S-85**) were prepared from the dianhydride monomer with aromatic diamines via conventional two-stage process, i.e. ring-opening polycondensation forming the poly(amicacid)s and further thermal or chemical imidization forming polyimides (Wang et al. 2006). The polymers were found to be soluble in aprotic amide solvents and cresols, such as

N,N-dimethylacetamide, N-methyl-2-pyrrolidone, and m-cresol, etc. Further, these materials were shown to possess good thermal stability with the glass transition temperatures of 221-278 °C, high degradation stability up to 512-540 °C, and low dielectric constants. According to authors, the polymers are potential candidates for photonic devices.



A series of novel polyimides containing heterocyclic pyridine and triphenylamine groups were synthesized (Wang et al. 2008) via polycondensation from various aromatic tetracarboxylic dianhydrides in N-methyl-2-pyrrolidinone medium. Amongst studied polymers, poly(imide) (**S-86**) derived from 4,4-hexafluoroisopropylidenedipthalic anhydride showed enhanced T_g (313 °C), mechanical, and thermal properties. This polymer exhibited the UV-vis absorption bands in the region of 240-500 nm and it displayed strong orange fluorescence (around 600 nm) in its protonated form.



Based on literature reports available on imide containing polymers, it is seen that the presence of imide functionality in the conjugated polymeric backbone

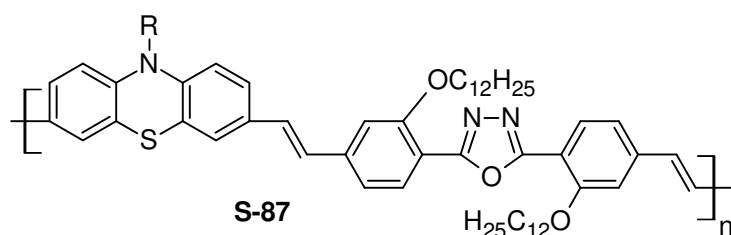
enhances the rigidity and thermal stability. Also, introduction of this moiety leads to an increase in the molecular hyperpolarizability of the resulting material which in-turn enhances its NLO property. Keeping this in view it has been planned to incorporate different cyclic anhydride moiety as conjugated spacers in the design of new D-A type conjugated polymers with the hope that the resulting polymers would show better optical response.

2.2.10. Phenothiazine and diphenylamine based conjugated polymers

Phenothiazine is a stable two membered heterocyclic system with electron donating character. The phenothiazine nucleus is often employed in photorefractive materials because of its unique property, i.e. charge carrier generation under light irradiation. Therefore, incorporation of phenothiazine in conjugated polymers as electron releasing group normally results in increase in absorption maxima and decrease in bandgap. Further, as it shows bent form arising from the dihedral angle in C-N-C (140.0°) and C-S-C (141.9°), its incorporation brings about reduction in electrostatic interaction between the chromophores in the polymer chain. Thus, the presence of phenothiazine chromophores improves the macroscopic nonlinearity.

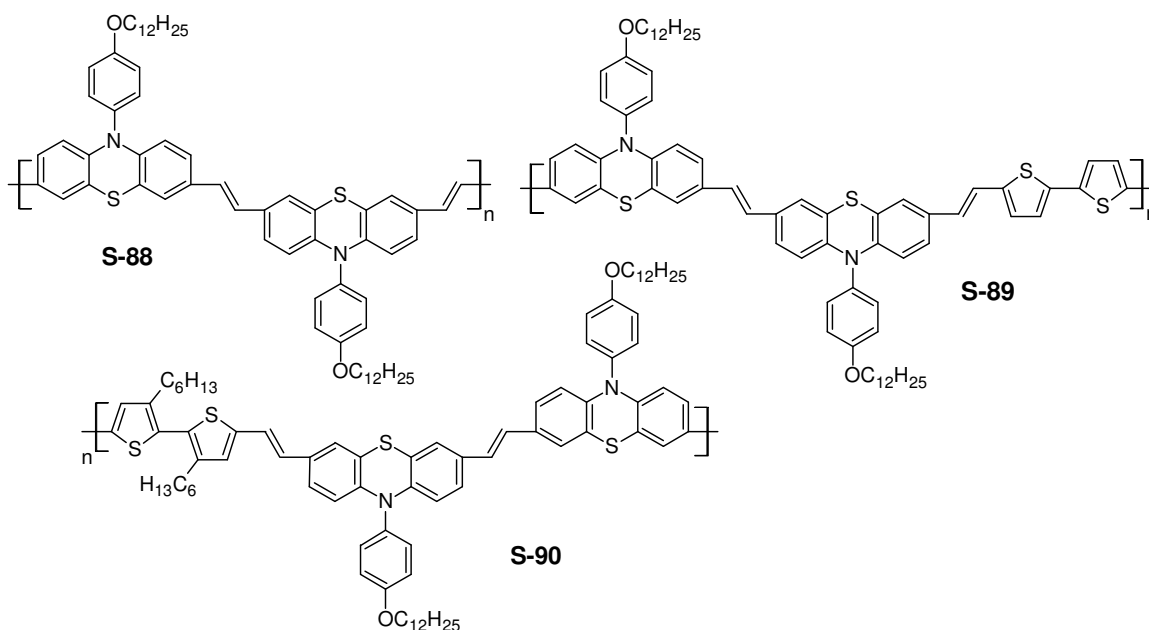
Similarly, presence of electron donating diphenylamine/triphenylamine moieties in a polymer chain enhances its fluorescence emission, electrochemical and optical properties. Also, diphenylamine/triphenylamine contributes significantly in enhancing the NLO response of the polymer (Hu et al. 2004 and Qian et al. 2009). Some of the important literature reports on conjugated polymers derived from phenothiazine and diphenylamine moieties are given below.

In an interesting study, a novel conjugated polymer (**S-87**) containing phenothiazine and oxadiazole moiety was synthesized by Yin et al. in the year 2003 via Wittig condensation method. The polymer was found to be highly soluble in common organic solvents because of the presence of 2-ethylhexyl group as substituent in its side chain. Single layer LED based on this polymer was fabricated successfully by them. In the PLED, a bright yellow light emission was observed at 566 nm and it showed a brightness of 2000 cd/m^2 over 102 mm^2 displayed area at 40 mA current.

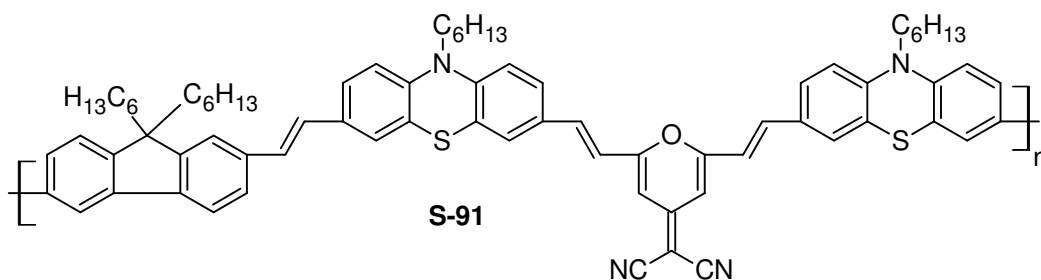


where R = 2-ethylhexyl

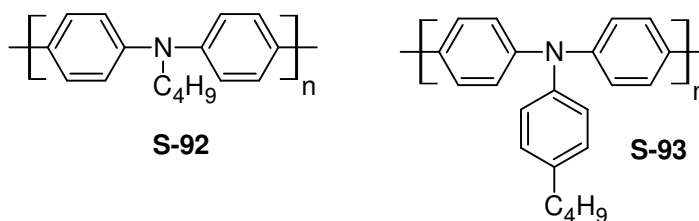
A series of new phenothiazylene vinylene and thiophene based polymers (**S-88** -**S-90**) were synthesized via Yamamoto and Stille coupling reaction (Kim et al. 2011) in order to study the effect of phenothiazine unit on their optical property. The UV-visible absorption spectra of the polymers showed two strong absorption bands in the ranges 306-325 nm and 430-480 nm. These observed bands were mainly attributed to the presence of phenothiazine segments and the conjugated main chains, respectively. Solution-processed field-effect transistors (FETs) fabricated with these polymers exhibit characteristic features of p-type organic thin film transistors. The field-effect mobilities polymers were measured to be 1.8×10^{-4} , 5.7×10^{-4} , and 2.5×10^{-7} $\text{cm}^2 \text{V}^{-1} \text{s}^{-1}$, respectively, with the corresponding on/off ratios of 5×10^2 , 1×10^4 , and 5×10^2 , respectively. The authors concluded that introduction of phenothiazine unit along the backbone enhanced the optical as well as electrochemical properties of the new polymers.



An interesting conjugated polymer (**S-91**) consisting of electron accepting 2-pyran-4-ylidenemalononitrile and electron donating fluorene connected through different electron-donating conjugated moieties in the main chain were synthesized by Li and coworkers through Suzuki coupling polymerization (Li et al. 2010). They studied the effect of donor strength on the bandgap of the polymers as well as power conversion efficiency. Amongst the studied polymer, polymer containing phenothiazine showed low bandgap of 1.92 eV. Further, bulk heterojunction photovoltaic devices were fabricated by using the polymers as donors and (6, 6)-phenyl C-61-butyric acid methyl ester (PCBM) as acceptor. The polymer having phenothiazine in its backbone showed maximum power conversion efficiency of 0.52 % under simulated AM 1.5 solar irradiation of 100 mW/cm², and the highest V_{oc} reached was 0.82 V.

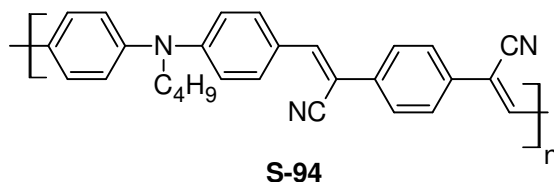


Sim et al. (2008) designed and synthesized two conjugated polymers (**S-92** - **S-93**) containing N, N- diphenylamine and N-(4-butyl phenyl)-N,N-diphenylamine through oxidation polymerization using iron chloride as oxidizing agent. The polymers exhibited good fluorescence with blue light emission. Electrochemical characterization indicated that these polymers are good hole transporting materials for electroluminescent devices.



Kim et al. (1996) synthesized an interesting diphenylamine based conjugated polymer (**S-94**) bearing cyanovinylene spacer for electroluminescent application. The polymer exhibited high thermal degradation stability up to 450 °C. The absorption maximum of the polymer was found to be 480 nm with the emission maxima of 560

nm. The polymer showed good light emitting efficiency, low threshold voltage when compared with a block copolymer having similar conjugated units. The synthetic strategy for the polymer with nitrogen atom linkage instead of a non-conjugated segment provided a relatively simple technique for the design of new series of polymers, with low threshold voltages, exhibiting a range of emission spectra.



Encouraged by the above reports on the phenothiazine and diphenylamine based conjugated polymers, it has been planned to introduce good hole transporting as well as UV-active phenothiazine and diphenylamine units into the polymer chain in order to enhance the optical and electrochemical properties of the newly designed polymers. It has been hoped that incorporation of these units along the polymer chain would influence the hole-carrying and optical properties favorably.

2.3. SCOPE AND OBJECTIVES OF PRESENT WORK

Conjugated polymers, being organic semiconductors are important class of materials for extensive applications mainly in PLEDs, PVs, TFTs, NLO and various types of sensors. These conjugated polymers exhibit characteristic properties of inorganic semiconductors; because of this they are promising materials in organic electronics. The main advantage of these conjugated polymers over their inorganic counterparts is their processability in the fabrication of electronic devices. Also, the parameters such as their solubility, thermal stability, film-forming ability, electron-transport, light-emitting, electronic and photovoltaic properties made them highly useful in several applications. The goal, with organic polymer-based devices is not necessarily to attain or exceed the level of performance of inorganic semiconductor technologies (silicon is still the best at the many things that it does) but to benefit from a unique set of characteristics combining the electrical properties of (semi)conductors with the properties of typical plastics, i.e. low cost, versatility of chemical synthesis, ease of processing, and flexibility.

During past several years various types of conjugated polymers have been synthesized and their electrical, electrochemical and optoelectronic properties have

been evaluated in detail. But, at the earlier stages the electronic devices fabricated using conjugated polymers showed very low efficiency due to the imbalanced charge carrying property, lack of environmental stability, and poor film forming ability etc.

Recently, polymer researchers concentrated their efforts to overcome these drawbacks by developing a new strategy called donor acceptor approach for the design of new conjugated polymers with desired properties. In this approach, new polymers are designed by arranging donor and acceptor moieties alternatively so as to impart good charge carrying properties for the molecules. By the introduction of suitable donor-acceptor moieties along the polymer chain, it is possible to achieve alteration in HOMO and LUMO energy levels of the polymer molecule. In the literature, several donor-acceptor types of polymers were reported with the possible applications in optoelectronic and photonic devices. However, these polymers did not achieve all the above said requirements. So, quest for new D-A type conjugated polymers is going on intensively. Still, there is adequate scope to investigate and develop new donor-acceptor type polymers with novel characteristics such as stability, processability, optical, electrochemical and photonic properties.

Keeping this in view, it has been contemplated to design some of the new donor acceptor type of conjugated polymers bearing 3,4-dialkoxythiophene heterocycle along with the other interesting electron donor and acceptor moieties. It has been hoped that the new polymers would be showing better optoelectronic properties and hence they would be promising materials for photonic and optoelectronic device applications.

Based on the above facts and the detailed literature survey, the following main objectives have been intended in the present research work.

- 1) Design and synthesis of new monomers and D-A type conjugated polymers containing substituted 3,4-dialkoxythiophene, naphthalene carbazole, phenylenevinylene, diphenylamine, imine and pyrazole systems as electron donors and 1,3,4-oxadiazole, cyanopyridine, cyanovinylene, cyclic-imide moieties as electron acceptors by precursor polyhydrazide route, polycondensation, Wittig condensation, Knoevenagel condensation methods.
- 2) Characterization of newly synthesized molecules:

- a) Monomers by ^1H NMR, FTIR and mass spectroscopy followed by elemental analysis
 - b) Polymers by GPC (Gel permeation chromatography), ^1H NMR, FTIR spectroscopy
- 3) Evaluation of linear optical properties by means of UV absorption spectroscopy, fluorescence emission spectroscopy and determination of solvatochromic behavior of selected polymers in various polar organic solvents
 - 4) Determination of electrochemical properties, charge carrying properties and bandgaps using cyclic voltammetric studies
 - 5) Investigation of nonlinear optical and optical limiting properties of newly synthesized conjugated polymers in their solution phase
 - 6) Study of effect of polymer structures on their electrochemical, linear and nonlinear optical properties

Conclusively, the present research investigation aimed at design, synthesis, and characterization of new donor-acceptor (D-A) type conjugated polymers containing thiophene, 1,3,4-oxadiazole, pyridine, naphthalene, phenylenevinylene, cyanovinylene, diphenylamine, cyclic-imides, imine and pyrazole, with required electrical and optoelectronic properties, which will have possible applications in PLED, NLO and photovoltaic devices. Further, there is an ample of scope for modification of polymeric structure through functionalization of monomers, which may lead to achieve desired properties in the resulting polymers. The newly developed polymers may find applications in certain fascinating areas like super capacitors, florescent sensors and thin film transistors. Also, the new reaction intermediates may be useful in other interesting fields.

2.4. DESIGN OF NEW POLYMERS

A detailed literature survey reveals that thiophene based conjugated polymers are currently under intense research investigation. These polymers are promising materials for optical and optoelectronic applications, due to their easy processability, chemical stability, readiness of functionalities, good film forming characteristics,

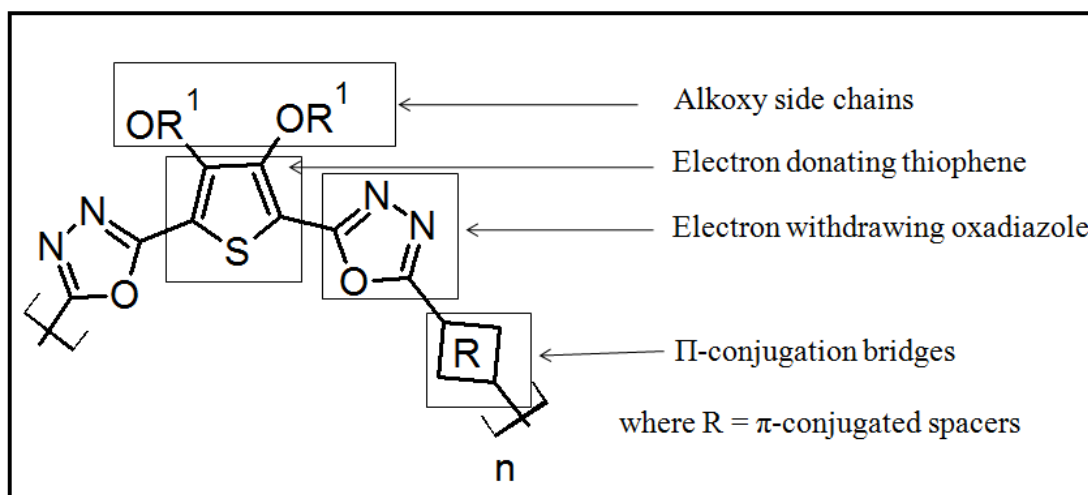
optical transparency, adequate mechanical strength and solubility in organic solvents. According to the recent reports, optical and electrochemical properties can be synthetically tuned in poly(thiophene)s through donor-acceptor approach by incorporating electron donating and electron withdrawing segments in the polymer chain. This would increase the delocalization in the molecule and hence bring about enhancement of the required electronic and optoelectronic properties. Against this background, our new designs have been centered on substituted thiophene derivatives.

Poly(3,4-ditetradecyloxythiophene)s carrying thiophene, naphthalene, isophthalyl, vinyl and pyrazole π -conjugated spacers (Series 1, P1-P5)

As reported in the literature, the introduction of aliphatic side chain into the thiophene ring of thiophene based conjugated polymer backbone generally enhances the solubility and film forming nature of it (Udayakumar et al. 2006). Therefore, the new polymers have been designed with alkoxy side chains substituted at positions 3, 4 of thiophene ring in order to enhance the solubility.

Further, the desired optical properties can be achieved when new conjugated systems are composed of donor-acceptor (D-A) segments with different heterocyclic systems which allow the fine tuning of important physical and/or photo-physical properties. Such aromatic D-A type molecules with push-pull mechanism are quite stable and they exhibit reasonably good β values (Cassano et al. 2002) in their NLO behaviour. Keeping this in view, new polymers consisting of different π -conjugated donor and acceptor moieties have been designed.

In the new design (**Design-1**), electron donating 3,4-ditetradecyloxythiophene and electron withdrawing 1,3,4-oxadiazole units have been incorporated along the D-A-D backbone. In addition, un-substituted thiophene, naphthalene, isophthalyl, vinylene and pyrazole moieties have been introduced as electron donating spacers for polymers **P1**, **P2**, **P3**, **P4** and **P5**, respectively. While designing, the above mentioned conjugated spacers have been selected in the decreasing order of their electron donating ability. Due to the difference in the electron donating ability as well as conjugation path length it is expected that these polymers show variable optical and electrochemical properties. Also, it is predicted that the new design would facilitate the enhancement in the optical limiting behavior of new polymers.



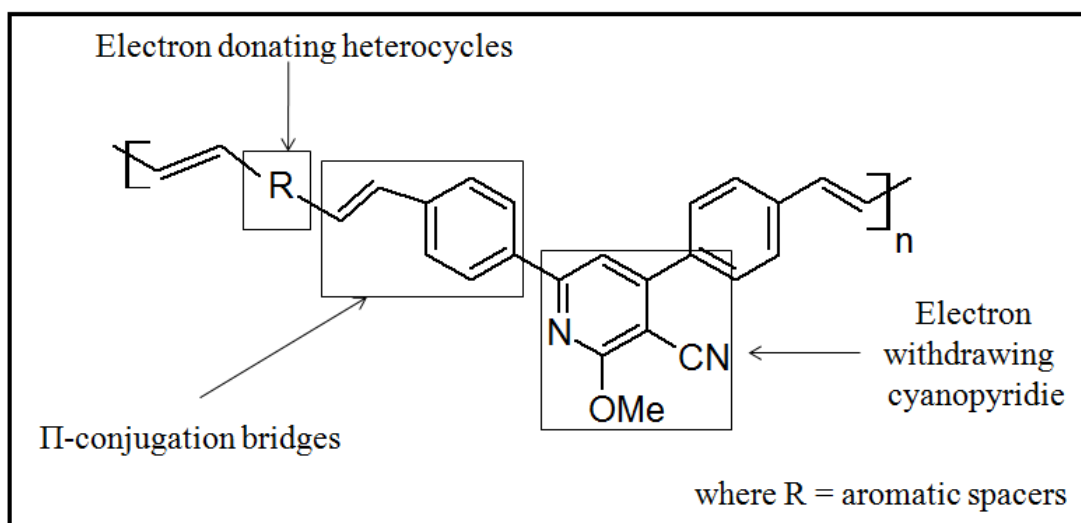
Design-1: 3,4-Dialkoxythiophene based conjugated polymers **Series 1 (P1-P5)**

Poly(cyanopyridines) containing phenyl, carbazole, alkoxythiophene, phenothiazine and dipenyl amine as electron donating bridges (Series 2, P6-P10)

Pyridine has attracted much attention of many researchers, particularly for designing new conjugated polymers (Liu et al. 2007 and Wang et al. 2008) because of its thermal stability and variable optical and optoelectronic properties. In addition, as pyridine ring is a highly electron withdrawing moiety, when it is introduced into the polymer main chain, it brings about enhanced electron-transporting ability and optical properties. Additionally, presence of the nitrile (CN) substituent on the pyridine ring further promotes its electron-transporting nature and hence incorporation of cyanopyridine ring into polymer chain would lead to enhancement of charge carrying tendency of the resulting polymer (Michelle et al. 2002). Also, the literature study reveals that conjugated polymers carrying cyanopyridine possess very good optical limiting property (Hongli et al. 2006).

Similarly the introduction of carbazole and phenothiazine moieties into the polymeric backbone enhances its photo-conducting and electron-donating properties. Further, incorporation of 3,6-disubstituted carbazole induces a bent conformation for the resulting macromolecular chain, which in-turn enhances thermal stability, solubility, extended glassy nature and oxidation potential of polymers (Grazulevicius et al. 2003). Furthermore, it has been well established that many conjugated polymeric systems carrying five membered aromatic heterocyclic rings like

thiophene, pyrrole, pyrazole, etc exhibit an increased hyperpolarizability when compared to those carrying benzenoid systems (Jumin et al. 2008, Batista et al. 2007 and Rosa et al. 2007). Also, thiophene based polymers were shown to possess better electron relay properties and hence they are very good nonlinear optical materials. Besides the electron transmission efficiency, they possess inherent stability (Franz et al. 1995). An extensive literature survey reveals that 3,4-dialkoxythiophene based conjugated polymers show facile dopability and low bandgap ascribe to the electron donating nature of the alkoxy substituent. Keeping this in view, highly electron withdrawing cyanopyridine moiety has been incorporated along D-A type architecture with various electron releasing moieties such as phenyl, carbazole, 3,4-dialkoxythiophene, phenothiazine and diphenylamine in new polymers **P6**, **P7**, **P8**, **P9** and **P10**, respectively. Schematic representation of **Design-2** is given below.



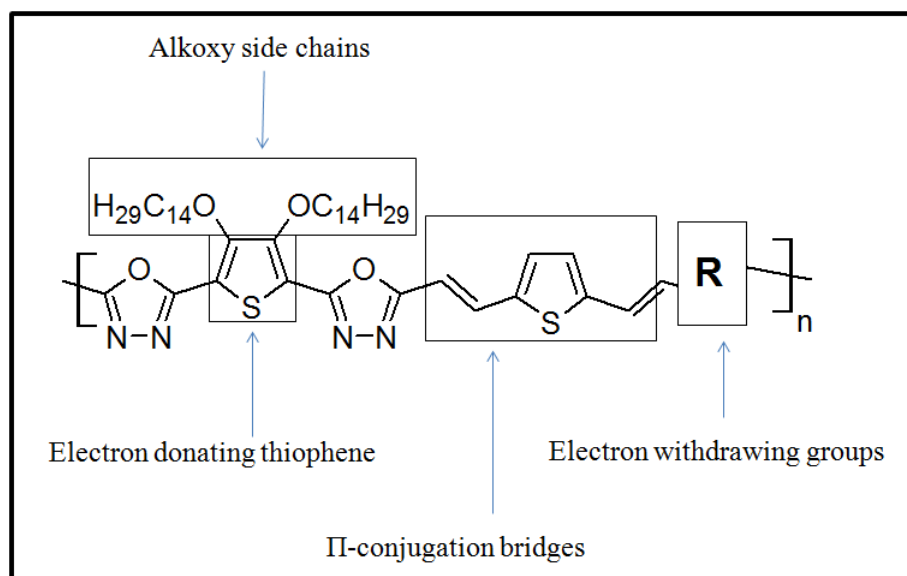
Design-2: Cyanopyridine based conjugated polymers **Series 2 (P6-P10)**

Poly(3,4-ditetradecyloxythiophene)s involving various extended π -conjugated spacers (Series 3, P11-P14)

As supported by the literature, vinylene units can be inserted into the polymer backbone to enhance its conjugation path length. It was reported that introduction of the vinylic linkage into the polymer chain increases the planarity of the molecule and shifts its absorption maxima towards higher wavelength region by decreasing the bandgap (Epstein et al. 1996). Further, presence of this unit enhances the light emitting and optoelectronic properties of the resulting polymers. Furthermore,

enhanced molecular hyperpolarizability can be achieved by the insertion of vinylene units along the polymer backbone which leads to enhancement in third order optical nonlinearity (Udayakumar et al. 2006).

Generally, incorporation of electron accepting nitrogen-containing heterocycles into the conjugated polymer backbone imparts good stability to the polymer as well as electroluminescent behavior. Also, introduction of electron withdrawing 1,3,4-oxadiazole into the conjugated polymer chain would increase the planarity of the molecule. Further, its existence in the polymer main/side chain normally enhances the light emitting property (Zhao et al. (2009), electron injection behavior and optical nonlinearity (Hegde et al. 2009). Furthermore, incorporation of oxadiazole units along the backbone enhances the optical nonlinearity of the polymer (Carella et al. 2002). Based on these facts, new polymers (**P11-P14**) carrying electron withdrawing 1,3,4-oxadiazole, cyanopyridine, and cyanovinylene and electron donating 3,4-dialkoxythiophene have been designed, as outlined in **Design-3**.

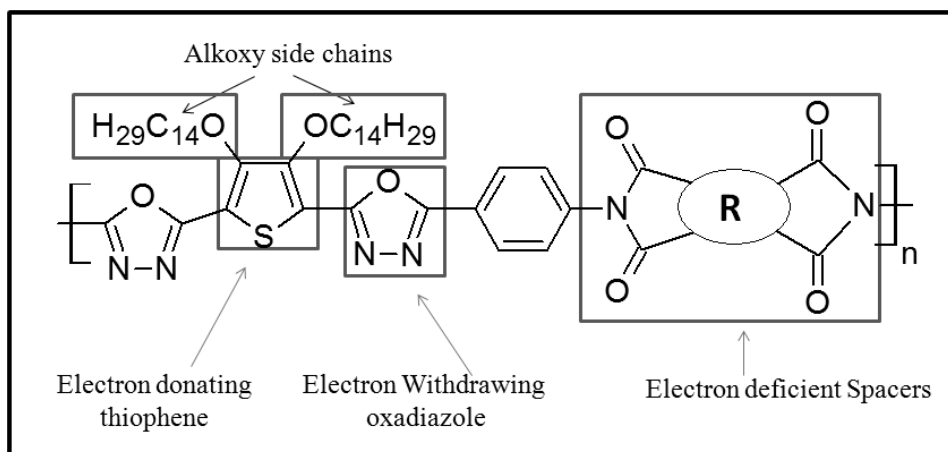


Design-3: Vinylic linkage containing polymers **Series 3 (P11-P14)**

Poly(3,4-ditetradecyloxythiophene)s carrying different conjugated cyclicimides (Series 4, P15-P16)

As an interesting type of polymeric materials, polyimides have attracted much attention because of their high T_g . This is an important property to stabilize the dipole alignment of the NLO chromophore at high temperatures. Another advantage of polyimides is their high thermal stability (Jung et al. 2006), due to which they exhibit

good electro-optic properties even at high temperatures. Literature study reveals that various polyimide-based NLO materials were designed, synthesized, and studied for their optical limiting properties (Becker et al. 1994, Chen et al. 1995, saadeh et al. 1997, Tsutsumi et al. 1998 and Qiu et al. 2006.). Reports also highlight that there are three types of NLO polyimides, which have been used as polymer hosts for composite materials, as polymer backbones and as backbones for side-chain NLO chromophores. However, most of the aromatic polyimides are insoluble in organic solvents and exhibit high softening temperatures, causing serious processing difficulties. In order to overcome these problems, several approaches are generally used. In fact, the approach involving use of monomers containing alkoxy groups is of particular interest, because this method brings about improvement in solubility and processability of the resulting polyimides. Owing to the importance of imide functionality, in our present work, new series of conjugated polymers have been designed by incorporating various cyclic imide as conjugated spacers in the new D-A-D architecture containing 3,4-dialkoxythiophene and 1,3,4-oxadiazole systems. The schematic representation of **Design-4** is given below.

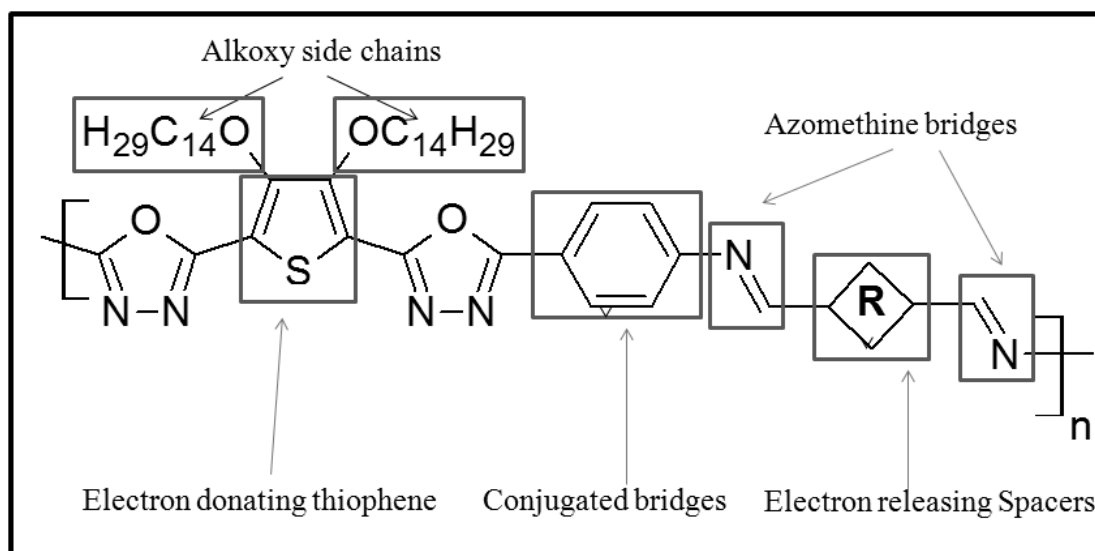


Design-4: Polymers with imide functionality **Series 4 (P15-P16)**

Poly(3,4-ditetradecyloxythiophene)s with imine functionalized electron donors as π -conjugated bridges (Series 5, P17-P20)

Incorporation of imine functional groups (-C=N-) into the conjugated system is another approach to form classes of materials with equally interesting electronic and optical properties (Grigoras and Antonoaia, 2005). Recently, conducting polymers containing imine functionality have been shown to possess a wide range of

practical applications in several areas such as light emitting diodes, thin film transistors, electrochromic devices and photovoltaic cells. Further, NLO chromophores containing imine spacers coupled with varying donor and acceptor conjugated systems were reported in the literature. However organic NLO compounds containing -C=N- linkers have received relatively little attention when compared to systems containing azo and ethylidene linkers. It has been observed that, the presence of imine spacers in conjugated system results in a lowering of the hyperpolarisability of polymer chain. Also, the introduction of strong acceptor units along the conjugated polymer backbone with imine functionality leads to achieve acceptable figures of merits in its NLO behavior (Bhuiyan et al. 2010). Against this background, imine functionality have been incorporated as conjugated spacer along with donor acceptor groups in our new **Design 5**. Further, donor strength of the polymer has been varied by incorporating 1,4-phenyl, 1,3-phenyl, diphenylamine and 3,4-dilkoxythiophene spacers in the main chain. The schematic representation of **Design 5** is given below.



Design-5: Polymers with imine functionality **Series 5 (P17-P20)**

From the forgoing account it is clear that introduction of certain structural units with specific properties in the polymer chain would bring about drastic changes in their basic characteristics. Accordingly, interesting moieties/groups were selected for incorporation so that they induce desired properties in the resulting polymers. Therefore it has been contemplated to synthesize following newly designed five series of D-A type conjugated polymers, comprising twenty polymers and to investigate the

influence of the incorporated moieties on the electrochemical, linear and nonlinear optical properties.

- (i) Poly(3,4-ditetradecyloxythiophene)s carrying thiophene, naphthalene, isophthalyl, vinyl and pyrazole moieties as π -conjugated spacers (**Series 1, P1-P5**)
- (ii) Poly(cyanopyridines) containing phenyl, carbazole, alkoxythiophene phenothiazine and diphenylamine based electron donating bridges (**Series 2, P6-P10**)
- (iii) Poly(3,4-ditetradecyloxythiophene)s involving vinylene π -conjugated spacers (**Series 3, P11-P14**)
- (iv) Poly(3,4-ditetradecyloxythiophene)s carrying aromatic conjugated cyclic imides (**Series 4, P15 and P16**)
- (v) Poly(3,4-ditetradecyloxythiophene)s with imine functionalized electron donors as π -conjugated bridges (**Series 5, P17-P20**)

The newly designed polymers **P1-P20** have been synthesized by means of various synthetic techniques as per **Schemes 4.1, 4.2, 4.3, 4.4, 4.5** and **4.6**, summarized in **Chapter 4**. Their preparation methods and experimental conditions have been established. The required monomers have been prepared according to the **Schemes 3.1, 3.2, 3.3, 3.4, 3.5, 3.6** and **3.7** as described in **Chapter 3**. Structures of newly synthesized intermediates and monomers have been confirmed by FTIR, ^1H NMR, mass spectral studies followed by elemental analysis. Further, the newly synthesized polymers have been characterized by FTIR spectroscopy, NMR studies, elemental analysis, gel permeation chromatography (GPC) and thermogravimetric analysis (TGA). Their redox properties have been investigated by cyclic voltammetric studies. Also, they have been evaluated for UV-visible absorption and fluorescence emission spectral studies. Finally, their third order nonlinear optical properties have been explored using Z-scan technique. A detailed account of synthetic protocols of various intermediates and monomers along with their structural characterization data has been discussed in **Chapters 3** and **4**. Further, the details of electrochemical and linear as well as nonlinear optical studies are given in **Chapters 5** and **6**, respectively.

Abstract

This chapter deals with experimental part of the present work involving design and synthesis of different conjugated monomers required for the preparation of new target designed polymers P1-P20. It also involves the structural characterization of new monomers with detailed discussion.

3.1. INTRODUCTION

In order to obtain newly designed polymers **P1-P20**, different types of monomers with various conjugated functionalities were designed and synthesized starting from simple organic molecules. **Scheme 3.1** describes the synthesis of required 3,4-dialkoxythiophene-2,5-dicarbohydrazides (**6a-b**), starting from thiodiglycolic acid through multistep reactions. These monomers were utilized in the synthesis of polymers **P1-P5** and **P11-P20**. Further, **Scheme 3.2** depicts the synthetic protocol of Wittig salt **10** which is a major monomer in the synthesis of polymers **P11** and **P12**. Similarly, extended conjugated dicarbaldehyde monomer **13** (**Scheme 3.3**) was synthesized and it was employed in the synthesis of polymers **P12** and **P14**. Furthermore, 3,4-didodecyloxythiophene dialdehyde monomer **15** was synthesized from simple two-step reaction involving reduction of ester followed by the oxidation of dialcohol to corresponding dialdehyde (**Scheme 3.4**). Similarly, cyano pyridine containing Wittig salt **19** (**Scheme 3.5**) was prepared via series of reactions. This is an important electron withdrawing monomer used in the synthesis of polymers **P6-P10** and **P14**. **Scheme 3.6** depicts the synthesis of N-tetradecyl carbazole-3,6-dicarbaldehyde, N-tetradecyldiphenylaminedicarbaldehyde and N-tetradecyl phenothiazine-3,7-dicarbaldehyde via Vilsmeier-Haak reaction. The conjugated diamine monomer **27** (**Scheme 3.7**) was prepared from corresponding dinitro compound through catalyst free reduction process using hydrazine hydrate. A detailed description of experimental protocols followed for the synthesis and characterization of all the monomers and their intermediates is given in the following sections.

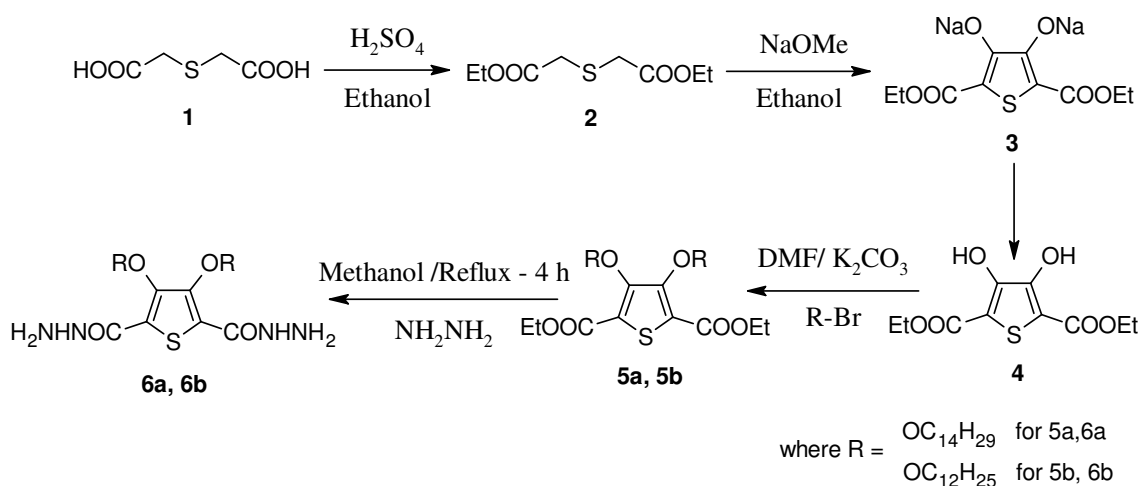
3.2. MATERIALS AND INSTRUMENTATION

Dimethylformamide (DMF) and acetonitrile were dried by distillation over calcium hydride. Sodium hydride and n-bromo alkanes were purchased from Lancaster (UK) and were used as received. Lithium aluminium hydride (LiAlH₄) and

2,3-dichloro-5,6-dicyano benzoquinone (DDQ) were purchased from Sigma Aldrich. All other solvents and reagents used were of analytical grade. They were purchased commercially and used without further purification. Progress of the reaction was monitored by thin layer chromatography (TLC), performed on open Silica gel 60 F₂₄ coated aluminium sheet. Melting points were determined on open capillaries using Stuart SMP3 (BIBBY STERLIN Ltd. UK) apparatus and they were uncorrected. Infrared spectra of all intermediate compounds and polymers were recorded on a Nicolet Avatar 5700 FTIR (Thermo Electron Corporation). ¹H NMR spectra were obtained with Bruker-400 MHz FT-NMR spectrometer using TMS/solvent signal as internal reference. Elemental analyses were performed on a Flash EA1112 CHNS analyzer (Thermo Electron Corporation). Mass spectra were recorded on a Jeol SX-102 (FAB) Mass Spectrometer.

3.3. SYNTHESIS OF 3,4-DIALKOXYTHIOPHENE-2,5-CARBOXY DIHYDRAZIDES (6a,b)

The monomers 3,4-dialkoxythiophene-2,5-carboxyhydrazides (**6a-b**) required for the synthesis of **Series 1, 3, 4** and **5** polymers were prepared as per **Scheme 3.1**.



Scheme 3.1: Synthesis of dihydrazide monomers (**6a,b**)

3.3.1. Chemistry

The starting material, thiodiglycolic acid (**1**) was esterified with ethanol using conc. sulfuric acid as catalyst. Further, this diester **2** was condensed with diethyl oxalate in presence of sodium ethoxide to give cyclized product **3**. The product was obtained as

sodium salt of diethyl 3,4-dihydroxythiophene-2,5-dicarboxylate **3** which was further hydrolyzed to get corresponding 3,4-dihydroxythiophene-2,5-dicarboxylate **4**. Then alkylation of compound **4** was done with different alkyl bromides. The resulting diethyl 3,4-dialkoxythiophene-2,5-dicarboxylates (**5a,b**) were converted to corresponding 3,4-dialkoxythiophene-2,5-carboxyhydrazides (**6a,b**) by the action of hydrazine hydrate in presence of methanol/ethanol according to the reported procedures (Udayakumar et al. 2006).

3.3.2. Synthesis and characterization

The compounds **5a,b** were synthesized according to the methods described by Zhang et al. (1998) and the spectral data of compounds **2-5a,b** were in good agreement with earlier reports. Synthetic procedure followed for the preparation of 3,4-dialkoxythiophene-2,5-carboxyhydrazides (**6a, b**) are given in the following section.

Synthesis of 3,4-dialkoxythiophene-2,5-carboxyhydrazides (6a, b)

Diethyl 3,4-dialkoxythiophene-2,5-dicarboxylate (**5a**, 0.5 g) was added to a solution of 5 mL hydrazine monohydrate in 40 mL of ethanol. The reaction mixture was refluxed for 3 h. Upon cooling the solution to room temperature, a white precipitate was obtained. The precipitate was filtered, washed with petroleum ether, dried under vacuum and finally re-crystallized from ethanol to get crystalline white solid. Similar procedure was followed for compound **6b** and characterization data of **6a, b** are as follows.

6a: Yield: 92 %. FTIR (cm^{-1}): 3412 (-NH₂), 3341 (-NH-), 2915, 2848, 1650 (>C=O), 1501, 1302, 1043, 956,720. ¹H NMR (400 MHz, CDCl₃), δ (ppm): 8.32 (s, 2H, >C=O NH), 4.16-4.12 (t, 4H, -OCH₂-, J = 6.4 Hz), 4.07 (s, 4H, -NH₂), 1.82-1.29 (m, 48 H, aliphatic), 0.88-0.86 (t, 6H, -CH₂-CH₃, J = 8 Hz). Element. Anal. Calcd. (%) for C₃₄H₆₄N₄O₄S: C, 65.34; H, 10.32, N, 8.96, S, 5.13. Found: C, 65.31; H, 10.35; N, 8.95; S, 5.15.

6b: Yield: 86 %. FTIR (cm^{-1}): 3414 (-NH₂), 3345 (-NH-), 2914, 2854, 1656 (>C=O), 1510, 1312, 1042, 959,720. ¹H NMR (400 MHz, CDCl₃), δ (ppm): 8.31 (s, 2H, >C=O NH), 4.16-4.13 (t, 4H, -OCH₂-, J = 6.4 Hz), 4.08 (s, 4H, -NH₂), 1.80-1.30 (m, 40 H, aliphatic), 0.89-0.86 (t, 6H, -CH₂-CH₃, J = 8 Hz). Element. Anal. Calcd. (%)

for $C_{30}H_{56}N_4O_4S$: C, 63.34; H, 9.92; N, 9.85; S, 5.64. Found: C, 63.36; H, 9.95; N, 9.84, S, 5.64.

FTIR and 1H NMR spectra of dihydrazide monomer **6a** were represented in **Figure 3.1** and **Figure 3.2**.

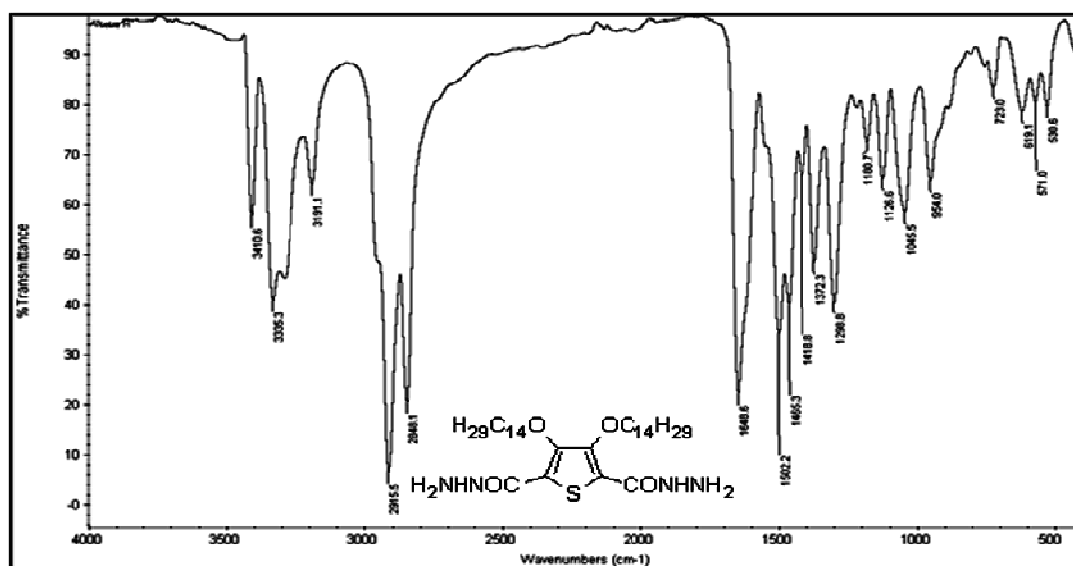


Figure 3.1: FTIR spectrum of dihydrazide **6a**

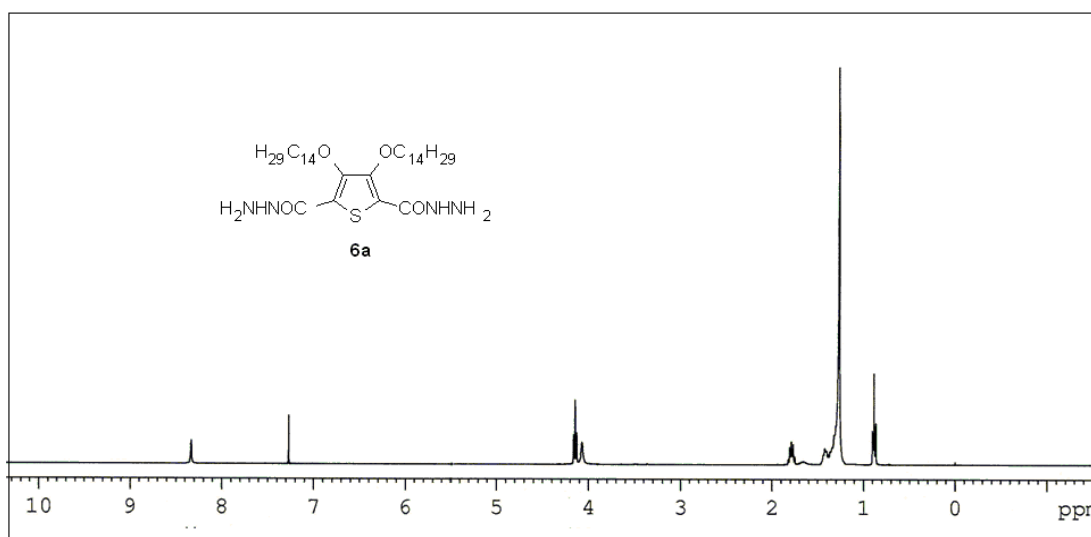


Figure 3.2: 1H NMR spectrum of dihydrazide **6a**

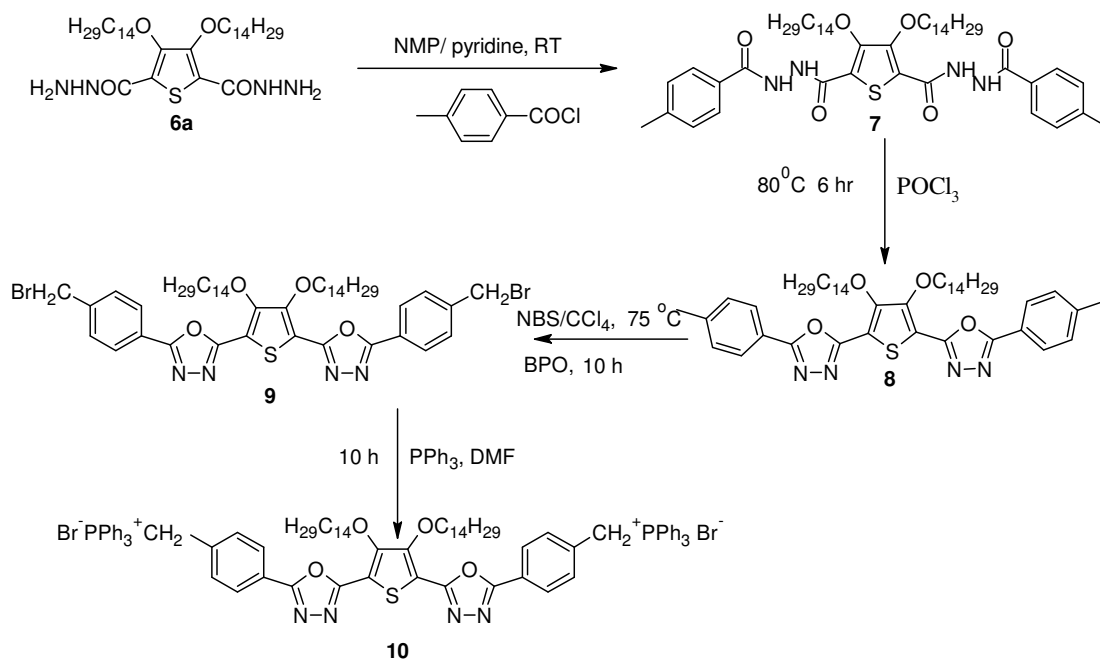
3.3.3. Results and discussion

The structure of newly synthesized carboxydihydrazides (**6a**, **b**) was confirmed by FTIR, 1H NMR spectral data followed by elemental analysis. FTIR spectrum of compound **6a** showed sharp peaks at 3412, 3341 and 1650 cm^{-1} (**Figure**

3.1) indicating the presence of -NHNH_2 and >C=O groups, respectively. Further, its ^1H NMR spectrum (**Figure 3.2**) displayed peaks at δ 8.34 and 4.98 ppm for >CONH and -NH_2 protons, respectively.

3.4. SYNTHESIS OF THIOPHENYLTRIPHENYLPHOSPHENE (10)

The multistep synthesis of monomer, viz. thiophenyl triphenylphosphene (**10**) starting from dihydrazide **6a** is summarized in **Scheme 3.2**.



Scheme 3.2: Synthesis of thiophenyl triphenylphosphene (**10**)

3.4.1. Chemistry

As given in **Scheme 3.2**, the 3,4-ditetradecyloxythiophene-2,5-carboxy dihydrazide (**6a**) was tolylated using tosyl chloride to yield 3,4-bis(tetradecyloxy)-N'2,N'5-bis(4-methylbenzoyl)thiophene-2,5-dicarbohydrazide (**7**), which on treatment with phosphorus oxychloride gave corresponding 5,5'-(3,4-bis(tetradecyloxy)thiophene-2,5-diyl)bis(2-p-tolyl-1,3,4-oxadiazole) (**8**) in good yield. This bis-oxadiazole compound **8** was then Wohl-Ziegler brominated using N-bromo succinimide (NBS) in carbon tetrachloride (CCl_4) and the resulting 5,5'-(3,4-bis(tetradecyloxy)thiophene-2,5-diyl)bis(2-(4-(bromomethyl)phenyl)-1,3,4-oxadiazole) (**9**) was further converted into 5,5'-(3,4-bis(tetradecyloxy)thiophene-2,5-diyl)bis(2-(4-triphenylphosphoniummethyl)phenyl) 1,3,4-oxadiazole (**10**) on treatment with

triphenylphosphine in presence of DMF. Details of their synthetic procedures and structural characterization data are as follows.

3.4.2. Synthesis and characterization

The thiophenyl triphenylphosphene derivative (**10**) was synthesized starting from dihydrazide **6a** by following standard methods. Details are given in the following section.

Synthesis of N2,N5-di-(4-methylbenzoyl)-3,4-ditetradecyloxy thiophene-2,5-dicarbohydrazide (7)

To a clear solution of dihydrazide **6a** (5 g, 8.79 mmol) and 2 mL of pyridine in 50 mL of N-methylpyrrolidinone (NMP), 2 equivalents of 4-methylbenzoyl chloride (2.71 g, 17.58 mmol) was added slowly at room temperature while stirring. The stirring was continued at room temperature for 1 h. The resulting solution was stirred at 80 °C for 5 h. After cooling to room temperature, the reaction mixture was poured into excess of cold water to get a precipitate. The precipitate obtained was collected by filtration, washed with excess of water, dried in oven and re-crystallized from ethanol/chloroform mixture to get desired product. Yield: 82 %. M.P: 144-146 °C. FTIR (cm⁻¹): 3245 (-CO-NH-), 2917, 2849 (Aromatic), 1666, 1621, 1447, 1274, 1046, 835, 732. ¹H NMR (400 MHz, CDCl₃), δ (ppm): 10.22 (s, 2H, -NH-), 9.71 (s, 2H, -NH-), 7.75 (d, 4H, Ar-H, J = 8.4 Hz), 7.15 (d, 4H, Ar-H, J = 8.0 Hz), 4.24 (t, 4H, -OCH₂-, J = 7.0 Hz), 2.38 (s, 6H, Ar-CH₃), 1.12-1.84 (m, 48H, -(CH₂)₁₂-) 0.80 (t, 6H, -CH₂-CH₃, J = 7.4 Hz). Element. Anal. Calcd. (%) for C₅₀H₇₆N₄O₆S: C, 69.73; H, 8.89; N, 6.51; S, 3.72. Found: C, 69.72; H, 8.84; N, 6.53; S, 3.71.

Synthesis of 2,2'-(3,4-ditetradecyloxythiophene-2,5-diyl)bis(5-(4-methyl phenyl)-1,3,4-oxadiazole) (8)

A mixture of dicarbohydrazide **7** (5 g, 6.2 mmol) and 50 mL of phosphorous oxychloride was stirred at 80 °C for 6 h. The reaction mixture was then cooled to room temperature and poured into an excess of ice-cold water. The resulting precipitate was collected by filtration, washed with water and dried in oven. Further purification was done by re-crystallization of the obtained solid from ethanol/chloroform mixture. Yield: 85 %. M. P: 98-100 °C. FTIR (cm⁻¹): 2915, 2848,

1587 (-C=N-), 1556, 1481, 1465, 1279, 1054, 823, 726. ^1H NMR (400 MHz, CDCl_3) δ (ppm): 7.94 (d, 4H, Ar-H, $J = 8.4$ Hz), 7.29 (d, 4H, Ar-H, $J = 8.0$ Hz), 4.25 (t, 4H, -O-CH₂-, $J = 6.6$ Hz), 2.38 (s, 6H, Ar-CH₃), 1.13-1.83 (m, 48H, -(CH₂)₁₂-), 0.82 (t, 6H, -CH₃, $J = 6.8$ Hz). Element. Anal. Calcd. (%) for C₅₀H₇₂N₄O₄S: C, 72.77; H, 8.79; N, 6.79; S, 3.89. Found: C, 72.72; H, 8.72; N, 6.81; S, 3.9.

Synthesis of 2,20-(3,4-ditetradecyloxythiophene-2,5-diyl) bis(5-(4-bromo methylphenyl) - 1,3,4-oxadiazole) (9)

A mixture of dimethyl bisoxadiazole **8** (3 g, 3.9 mmol), N-bromosuccinimide (1.38 g, 7.8 mmol) and 5 mg of benzoyl peroxide in 30 mL of benzene was refluxed for 5 h. After the solvent was removed, 20 mL of water was added with stirring for 1 h. The resulting crude product was filtered and the residue was re-crystallized from methyl acetate/chloroform mixture. Yield: 65 %). FTIR (cm⁻¹): 2915, 2849, 1557 (-C=N-), 1482, 1465, 1279, 1054, 952, 822, 726. ^1H NMR (400 MHz, CDCl_3) δ (ppm): 7.92 (d, 4H, Ar-H, $J = 8.4$ Hz), 7.27 (d, 4H, Ar-H, $J = 8.0$ Hz), 4.5 (s, 4H, Ar-CH₂-Br), 4.24 (t, 4H, -O-CH₂-, $J = 6.6$ Hz), 1.13-1.83 (m, 48H, -(CH₂)₁₂-), 0.80 (t, 6H, -CH₂-CH₃, $J = 7.0$ Hz). Element. Anal. Calcd. (%) for C₅₀H₇₀Br₂N₄O₄S: C, 61.09; H, 7.18; N, 5.70; S, 3.26. Found: C, 61.05; H, 7.15; N, 5.71; S, 3.28.

Synthesis of 2,20-(3,4-ditetradecyloxythiophene-2,5-diyl)bis(5-((4-triphenyl phosphonium methyl) phenyl)-1,3,4-oxadiazole)dibromide (10)

A mixture of dibromide compound **9** (1 g, 1.07 mmol) and triphenylphosphine (0.565 g, 2.157 mmol) in 5 mL of DMF was refluxed with stirring for 10 h. The reaction mixture was cooled to room temperature and poured into 50 mL of ethyl acetate. The resulting precipitate was filtered off, washed with excess of ethyl acetate and dried at 40 °C for 10 h. (**10**) Yield: 72 %. M. P: Above 300 °C. FTIR (cm⁻¹): 2922, 2855, 1583, 1459, 1352, 1048, 956, 727. ^1H NMR (400 MHz, CDCl_3) δ (ppm): 7.21-7.90 (m, 38H, Ar-H), 5.95 (s, 4H, Ar-CH₂-P-), 4.25 (t, 4H, -OCH₂-, $J = 6.9$ Hz), 1.12-1.83 (m, 48H, -(CH₂)₁₂-), 0.79 (t, 6H, -CH₂-CH₃, $J = 7.0$ Hz). Element. Anal. Calcd. (%) for C₈₆H₁₀₀Br₂N₄O₄P₂S: C, 68.52; H, 6.69; N, 3.72; S, 2.13. Found: C, 68.58; H, 6.66; N, 3.38; S, 2.23.

FTIR and ^1H NMR spectra of biscarbohydrazide **7** and bisoxadiazole **8** were represented in **Figures 3.3 – 3.6**.

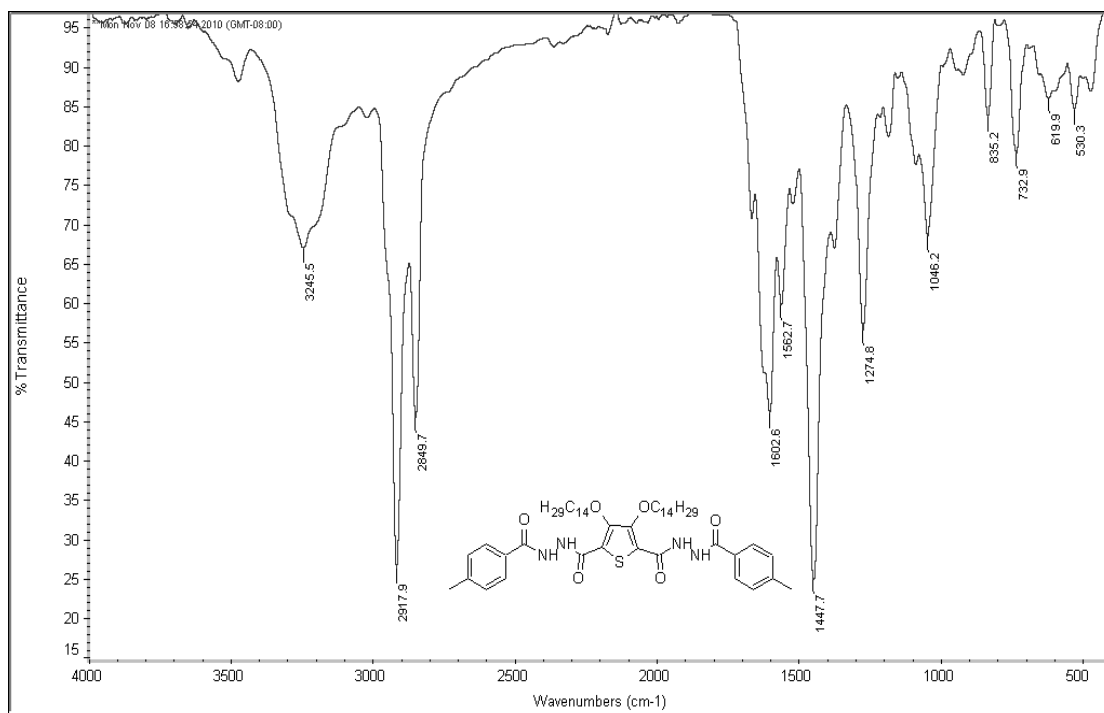


Figure 3.3: FTIR spectrum of bis-carbohydrazone 7

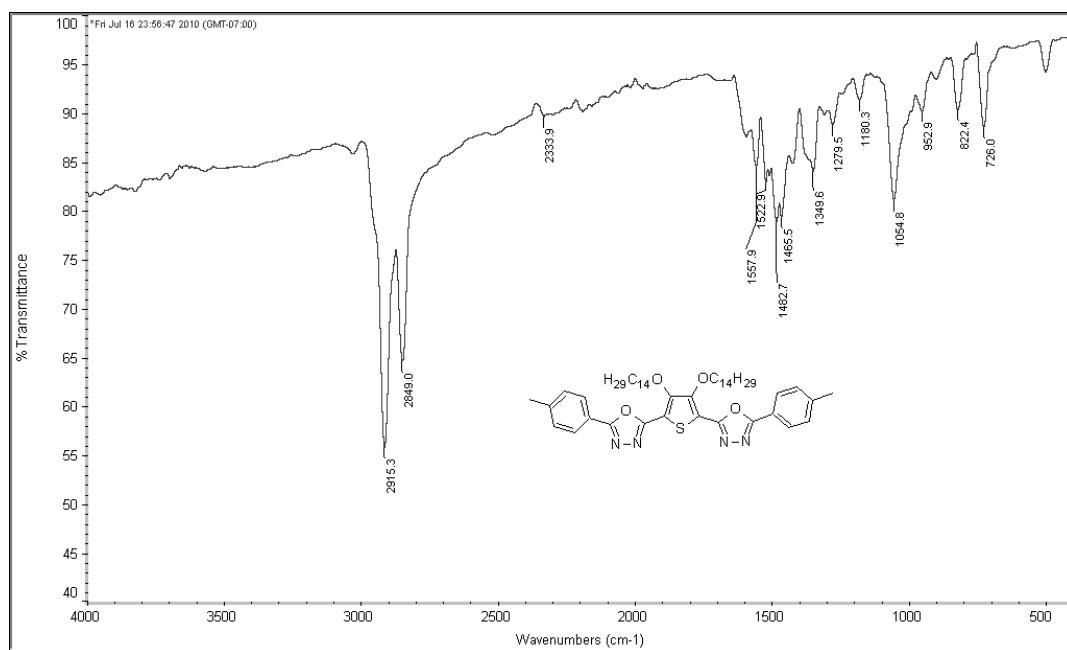


Figure 3.4: FTIR spectrum of bis-oxadiazole 8

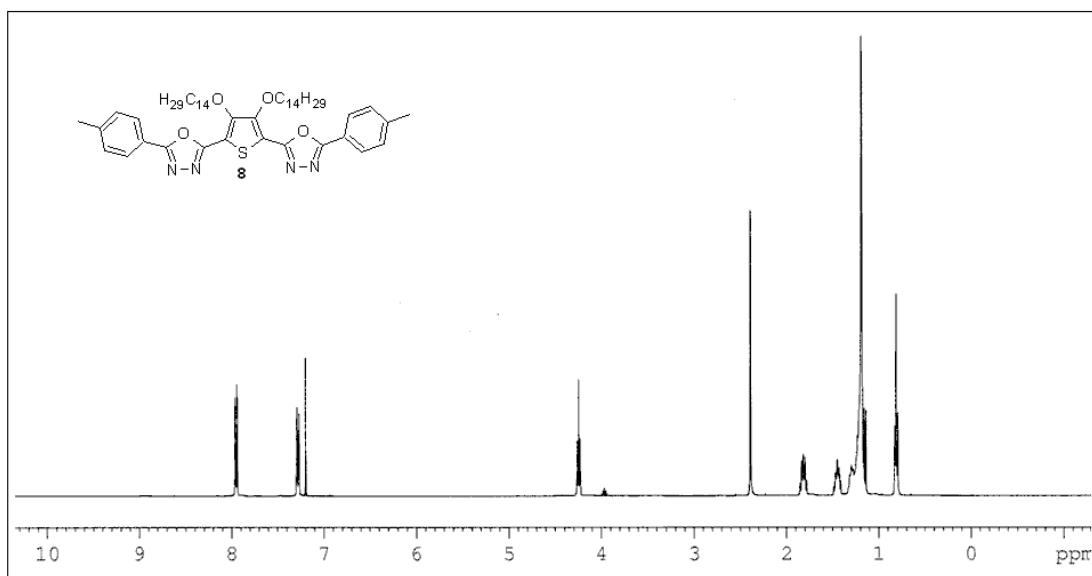


Figure 3.5: ¹H NMR spectrum of bisoxadiazole **8**

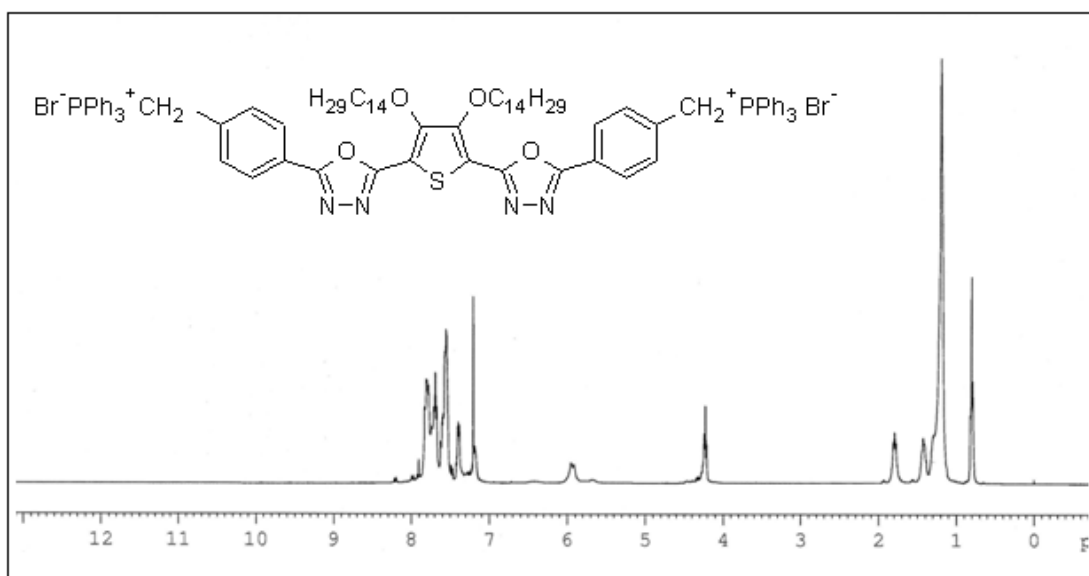


Figure 3.6: ¹H NMR spectrum of triphenylphosphene salt **9**

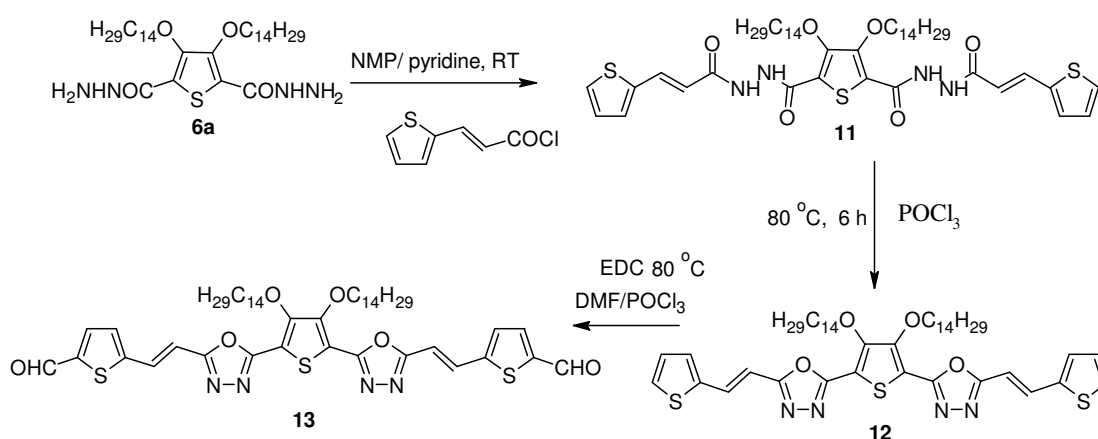
3.4.3. Results and discussion

The structures of intermediates and monomer were confirmed by elemental analysis and spectroscopic techniques. The conversion of bishydrazide **6a** to biscarbohydrazide **7** was confirmed by its FTIR spectral and elemental analysis studies. It exhibited sharp peaks at 3245 and 1666 cm⁻¹, indicating the presence of -NH- and >C=O groups, respectively as shown in **Figure 3.3**. Further, its ¹H NMR

spectrum showed peaks at δ 2.38, 10.22 and 9.71 ppm indicating the presence of the tolyl methyl protons and amidic protons, respectively. Formation of bisoxadiazole **8** from biscarbohydrazide **7** was established by FTIR, ^1H NMR and mass spectral analyses. The disappearance of bands in the region 3245 and 1666 cm^{-1} and appearance of new band at 1587 cm^{-1} (**Figure 3.4**) indicate the formation of oxadiazole ring in the molecule. Further, the conversion was confirmed by ^1H NMR spectrum, wherein bisoxadiazole **8** showed disappearance of peak due to amidic protons (**Figure 3.5**) ($>\text{CO-NH-}$). Also, the aromatic protons were de-shielded. Conversion of compound **8** to its dibromo derivative **9** was confirmed by ^1H NMR spectral studies and elemental analysis. In its ^1H NMR spectrum the disappearance of tolyl methyl protons and appearance of a new peak at δ 4.5 ppm indicate the bromination of methyl groups attached to aromatic rings. Further, formation of Wittig salt **10** was confirmed by its ^1H NMR (**Figure 3.6**) and mass spectral analyses. It showed a peak at δ 5.95 ppm indicating the presence of $-\text{CH}_2-$ groups attached to aromatic ring with phosphonium groups on either side.

3.5. SYNTHESIS OF DITHIOPHENE DICARBALDEHYDE (**13**)

The synthesis strategy for the preparation of monomer, dithiophene-2-carbaldehyde **13** starting from dihydrazides **6a** is summarized in **Scheme 3.3**.



Scheme 3.3: Synthesis of dithiophene-2-carbaldehyde **13**

3.5.1. Chemistry

The monomer dithiophene-2-carbaldehyde (**13**) was prepared by a series of reactions as given in **Scheme 3.3**. To begin with, 3-(thiophen-2-yl)acryloyl chloride was made to react with 3,4-bis (tetradecyloxy) thiophene-2,5-dicarbohydrazide (**6a**) in presence of pyridine to get 3,4-bis(tetradecyloxy)-N'2,N'5-bis(-3-(thiophen-2-yl)acryloyl)thiophene-2,5-dicarbohydrazide (**11**) which was then cyclized using phosphorus oxychloride to yield 5,5'-(3,4-bis(tetradecyloxy)thiophene-2,5-diyl)bis(2-(2-(thiophen-2-yl)vinyl)-1,3,4-oxadiazole) (**12**). In the penultimate step, this compound was converted into the required monomer, viz. (5,5'-(3,4-bis (tetradecyloxy) thiophene-2,5-diyl) bis(1,3,4-oxadiazole-5,2-diyl)) bis(ethene-2,1-diyl) dithiophene-2-carbaldehyde (**13**) by Vilsmeier Haack reaction using phosphorus oxychloride and DMF.

3.5.2. Synthesis and characterization

The dithiophene-2-carbaldehyde **13** was synthesized starting from dihydrazide **6a** by following standard methods. Details are given in the following section.

Synthesis of 3,4-bis(tetradecyloxy)-N'2,N'5-bis-3-(thiophen-2-yl)acryloyl thiophene - 2,5- dicarbohydrazide (11)

To a mixture of compound **6a** (5 g, 8 mmol) and 2 mL of pyridine in 50 mL of NMP, 3-(thiophen-2-yl)acryloyl chloride (2.76 g, 16 mmol) was added slowly at room temperature while stirring. The stirring was continued at room temperature for 8 h. The reaction mixture was poured into excess of water to get a precipitate. The precipitate obtained was collected by filtration, washed with excess of water, dried in an oven and re-crystallized from ethanol/chloroform mixture. Yield: 82 %, M. P: 210-212 °C. FTIR (cm⁻¹): 3310, 3214, 2918, 2852, 1685, 1648, 1495, 1303, 1051, 931, 723. ¹H NMR (400 MHz, CDCl₃) δ (ppm): 9.98(s, 2H, -CONH-), 9.21(s, 2H, -CONH-), 7.74 (d, 2H, -CH=CH-, J = 16 Hz), 7.42 (d, 2H, Ar-H, J = 4.8 Hz), 7.29 (d, 2H, Ar-H, J=3.6), 7.10 (m, 2H, Ar-H), 6.9 (d, 2H, -CH=CH-, J = 16 Hz), 4.31 (t, 4H, -O-CH₂-, J = 7 Hz), 1.24-1.83 (m, 48H, -(CH₂)₁₂-), 0.89 (t, 6H, Ar-CH₃, J = 6.8 Hz). Element. Anal. Calcd. (%) for: C₄₈H₇₂N₄O₆S₃: C, 64.25; H, 8.09; N, 6.24; S, 10.72. Found: C, 64.34; H, 8.23; N, 6.29; S, 10.86.

Synthesis of 5,5'-(3,4-bis(tetradecyloxy)thiophene-2,5-diyl)bis(2-(2-(thiophen-2-yl)vinyl)-1,3,4-oxadiazole) (12)

A mixture of dicarbohydrazide **11** (3 g, 3.4 mmol) and 50 mL of phosphorous oxychloride was heated at 80 °C for 6 h. The reaction mixture was then cooled to room temperature and poured into crushed ice. The resulting precipitate was collected by filtration, washed with water and dried in oven. Further purification was done by column chromatography using silica gel with PE/EA as eluent. Yield 56 %, M. P: 189-190 °C. FTIR (cm⁻¹): 2916, 2849, 1585(-C=N-), 1458, 1274, 1044, 955, 712. ¹H NMR (400 MHz, CDCl₃) δ (ppm): 7.74 (d, 2H, -CH=CH-, J = 16 Hz), 7.42(d, 2H, Ar-H, J = 4.8 Hz), 7.29 (d 2H, Ar-H, J = 3.6), 7.10(m, 2H, Ar-H), 6.9(d, 2H, -CH=CH-, J = 16 Hz), 4.31 (t, 4H, -O-CH₂-, J = 7 Hz), 1.24-1.83 (m, 48H, -(CH₂)₁₂-), 0.89 (t, 6H, Ar-CH₃, J = 6.8 Hz). Element. Anal. Calcd. (%) for C₄₈H₆₈N₄O₄S₃: C, 66.94; H, 7.96; N, 6.51; S, 11.17. Found: C, 67.04; H, 7.99; N, 6.65; S, 11.24.

Synthesis of 2,2'-(5,5'-(3,4-bis(tetradecyloxy)thiophene-2,5-diyl)bis(1,3,4-oxadiazole-5,2-diyl)) bis(ethene-2,1-diyl)dithiophene-2-carbaldehyde (13)

Dialdehyde **13** was synthesized by using the Vilsmeier-Haack reaction for which the following procedure was followed.

N,N-Dimethylformamide (0.954 g, 13 mol) cooled to 0 °C was treated dropwise with phosphorus oxychloride (1.989 g, 13 mol). The resulting orange solution was stirred at 0 °C for 1 h and at 25 °C for 1 h, and then compound **8a** (2 g, 2.18 mmol) in 20 mL of 1,2-dichloroethane was added slowly. The mixture was heated at 90 °C for 24 h, cooled, and poured onto 200 g of crushed ice. Brown oil separated, which was taken up in dichloromethane. The extract was washed with saturated aqueous bicarbonate and then with water containing a little ammonium chloride and the organic layer was dried over anhydrous Na₂SO₄. The solvent was removed under reduced pressure, and the crude viscous product was separated on a silica gel column, using hexane:ethyl acetate (1:1) as eluent. The yield of the dialdehyde **13** was 37 %. FTIR (cm⁻¹): 2918, 2849, 1662 (-HC=O), 1590, 1458, 1354, 10044, 809, 720. ¹H NMR (400 MHz, CDCl₃) δ(ppm): 9.94 (s, 2H, Ar-CHO), 7.74 (m, 4H, -CH=CH-), 7.37 (d, 2H, Ar-H, J = 4.8 Hz), 7.11(m, 2H, Ar-H), 4.31 (t, 4H, -O-CH₂-, J = 7 Hz), 1.85-1.24 (m, 48H, - (CH₂)₁₂-), 0.87 (t, 6H, Ar-CH₃, J = 6.8 Hz). Element. Anal.

Calcd. (%) for: $C_{50}H_{68}N_4O_6S_3$: C, 65.47; H, 7.47; N, 6.11; S, 10.49. Found: C 65.55; H, 7.58; N, 6.23; S, 10.51.

FTIR and 1H NMR spectra of bisoxadiazole **12** and dialdehyde **13** were represented in the **Figures 3.7 –3.10**.

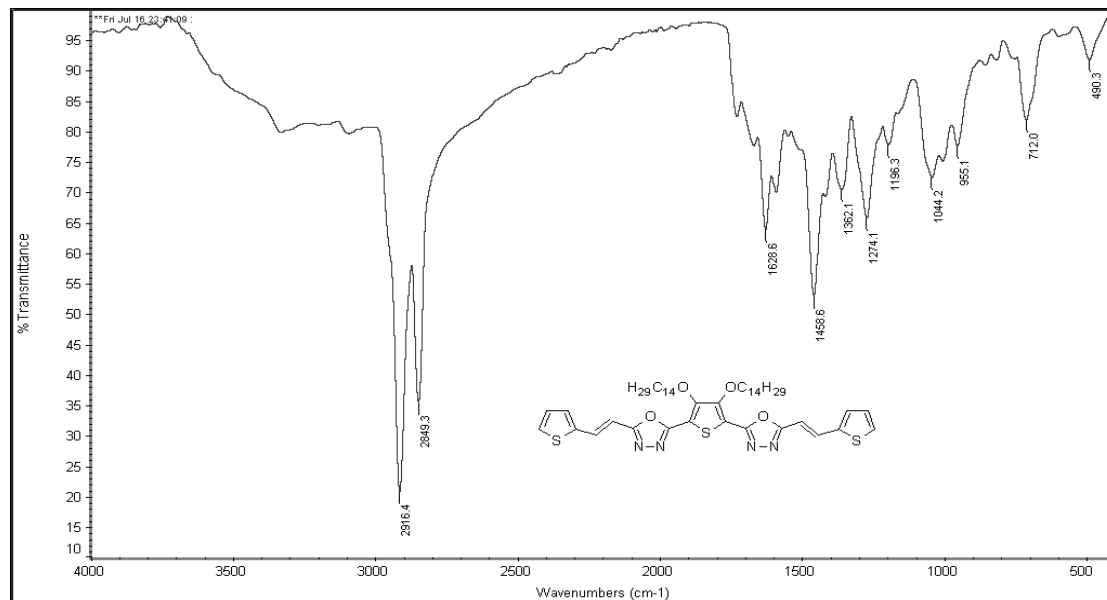


Figure 3.7: FTIR spectrum of bisoxadiazole **12**

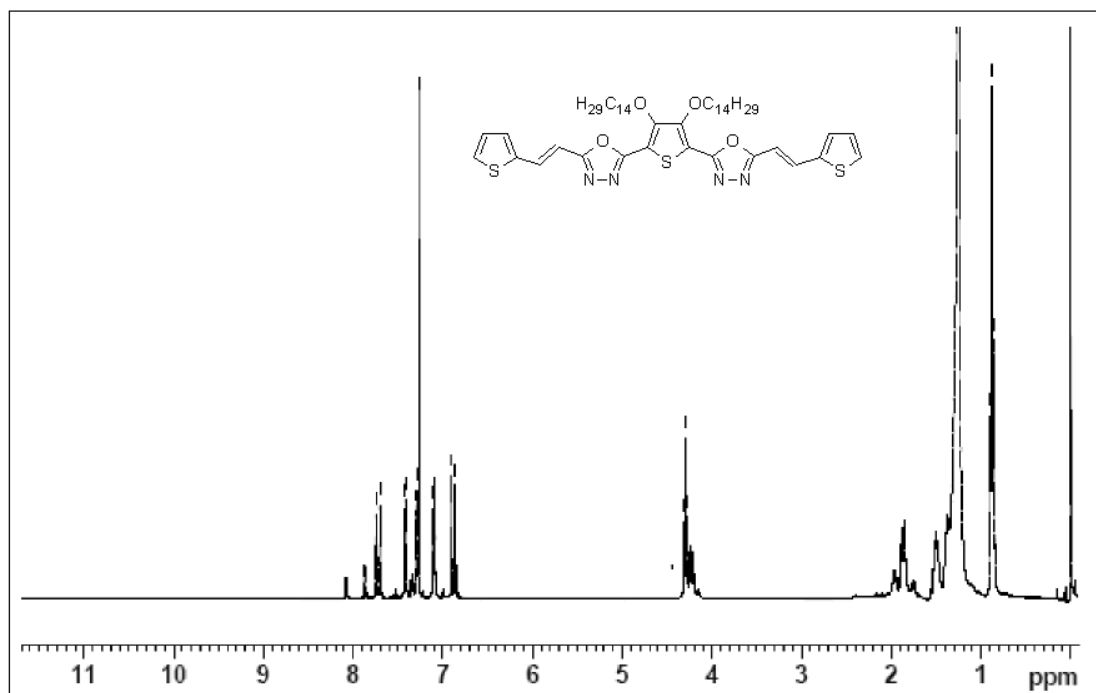


Figure 3.8: 1H NMR spectrum of bisoxadiazole **12**

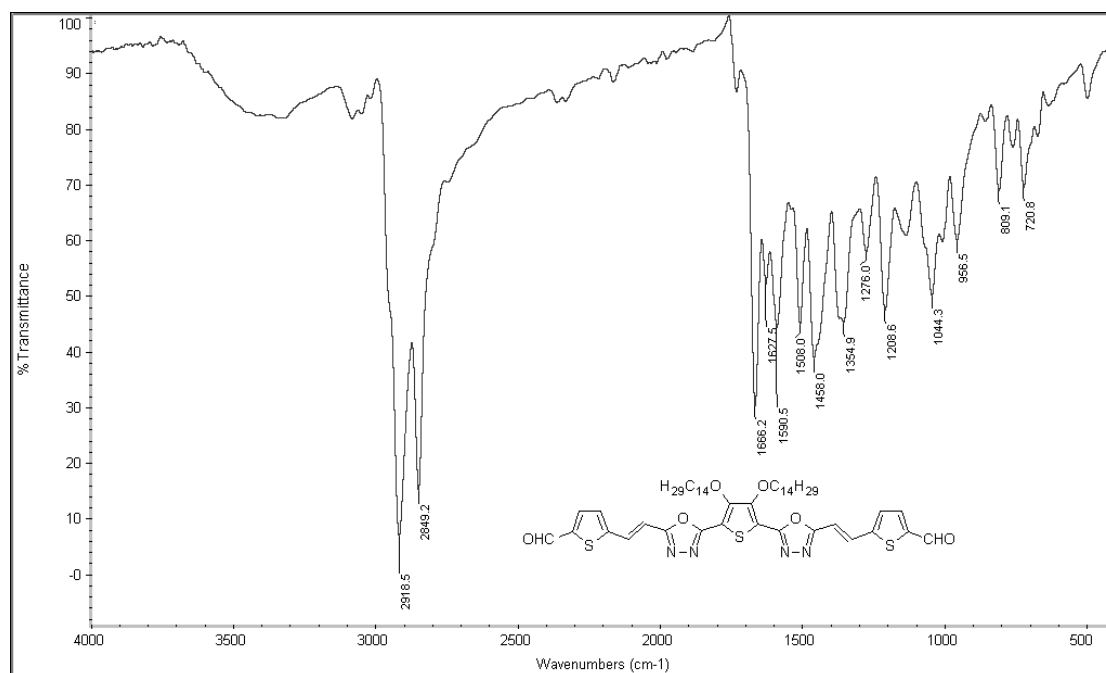


Figure 3.9: FTIR spectrum of dicarbaldehyde compound 13

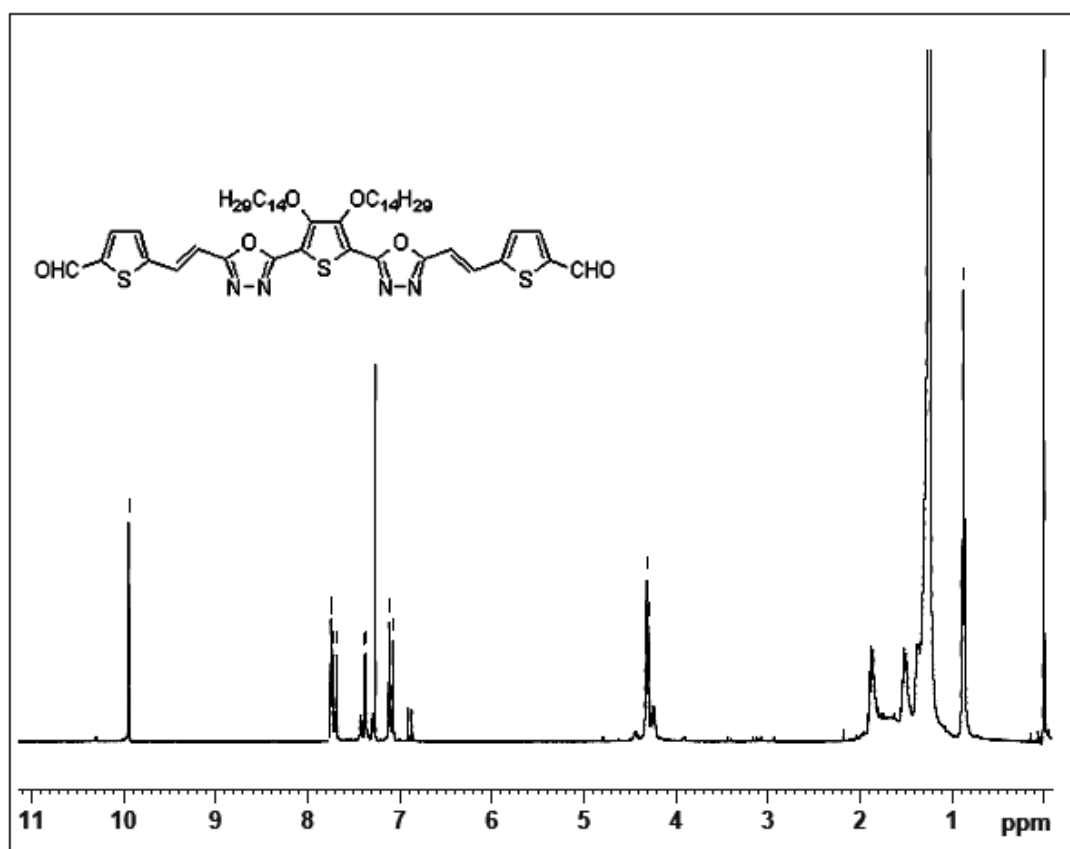


Figure 3.10: ¹H NMR spectrum of dicarbaldehyde compound 13

the dialcohol **14** was conveniently oxidized to dialdehyde **15** using DDQ in presence of diethyl ether.

3.6.2. Synthesis and characterization

Details of synthesis of 3,4-didodecyloxythiophene 2,5-dicarbaldehyde (**15**) starting from diester **5a** are given in the following section.

*Synthesis of (3,4-didodecyloxythiophene-2,5-diyl)dimethanol (**14**)*

To a clear solution of 0.5 g (0.0008 mol) of diethyl 3, 4-didodecyloxy thiophene-2,5-dicarboxylate (**5**) in 10 mL of dry diethyl ether, 0.13 g (0.004 mol) of anhydrous lithium aluminium hydride was added portion-wise, while stirring. Stirring was continued for 4 h at room temperature. The reaction mixture was then poured into cold dilute sulfuric acid to decompose the excess lithium aluminium hydride. The organic layer was separated and washed with saturated sodium bicarbonate solution. After the evaporation of the solvent, the obtained solid was filtered and re-crystallized from hexane. Yield: 0.35 g (81 %). M. P: 46-48 °C. FTIR (cm⁻¹): 3345(-OH), 2917(Ar-H), 2851(Aliphatic -C-H). ¹H NMR (400 MHz, CDCl₃), δ (ppm): 7.11 (broad singlet, 2H, -OH), 4.68 (s, 4H, -OCH₂-), 4.01 (t, 4H, -OCH₂-), 1.74-1.27 (m, 40H, -(CH₂)₁₀-), 0.89 (t, 6H, -CH₃, J = 6.8 Hz). FABHRMS: m/z, 513 (Calculated: 512.82). Element. Anal. Calcd (%) for C₃₀H₅₆O₄S: C, 70.26; H, 11.01; S, 6.25. Found: C, 70.08; H, 10.88; S, 6.37.

*Synthesis of 3,4-didoecyloxythiophene-2,5-dicarbaldehyde (**15**)*

A mixture of 0.5 g (0.001 mol) of 3,4-didodecyloxythiophene-2,5-diyl)dimethanol (**6**), 0.88 g (0.004 mol) of dicyanodichloroquinine (DDQ) and 15 mL of dry diethyl ether was stirred for 98 h at room temperature under nitrogen atmosphere. After completion of the reaction, the mixture was filtered. The filtrate was evaporated to get a solid which was re-crystallized from ethanol. Yield: 0.41 g (80 %). M. P: 36-37 °C. FTIR (cm⁻¹): 1690(>C=O). ¹H NMR (400 MHz, CDCl₃), δ (ppm): 10.12 (s, 2H, -CHO), 4.27 (t, 4H, -OCH₂-), 1.84-1.31 (m, 40H, -(CH₂)₁₀-), 0.89 (t, 6H, -CH₃, J = 6.8Hz). FABHRMS: m/z, 509 (Calculated: 508.79). Element. Anal. Calcd. (%) for C₃₀H₅₂O₄S: C, 70.82; H, 10.30; S, 6.30. Found: C, 70.99; H, 10.52; S, 6.17.

¹H NMR spectra of dimethanol **14** and dialdehyde **15** were represented in **Figures 3.11** and **3.12**.

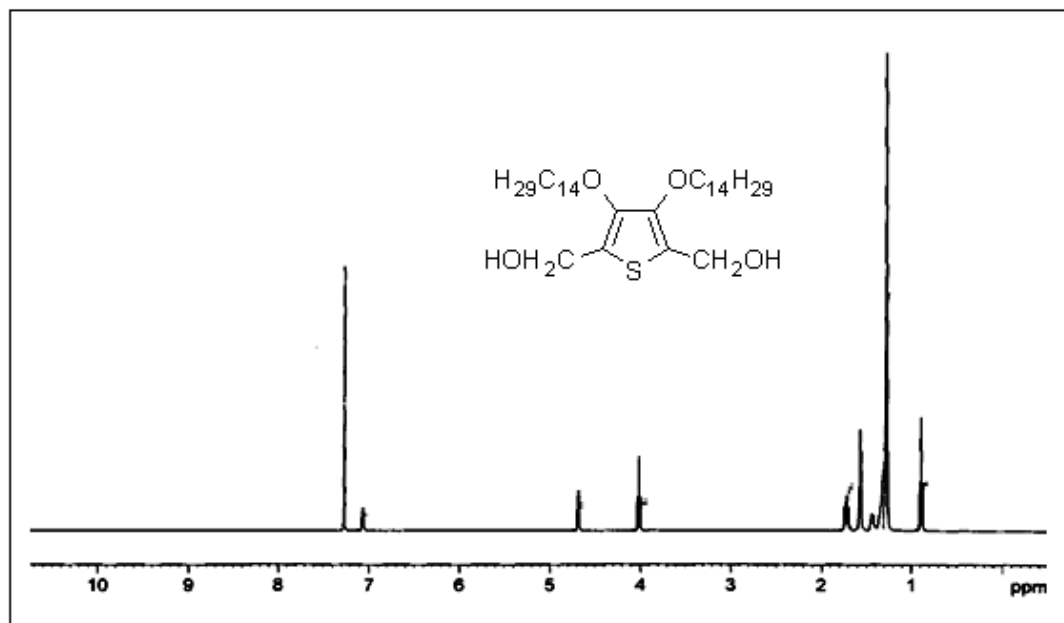


Figure 3.11: ¹H NMR spectrum of dimethanol **14**

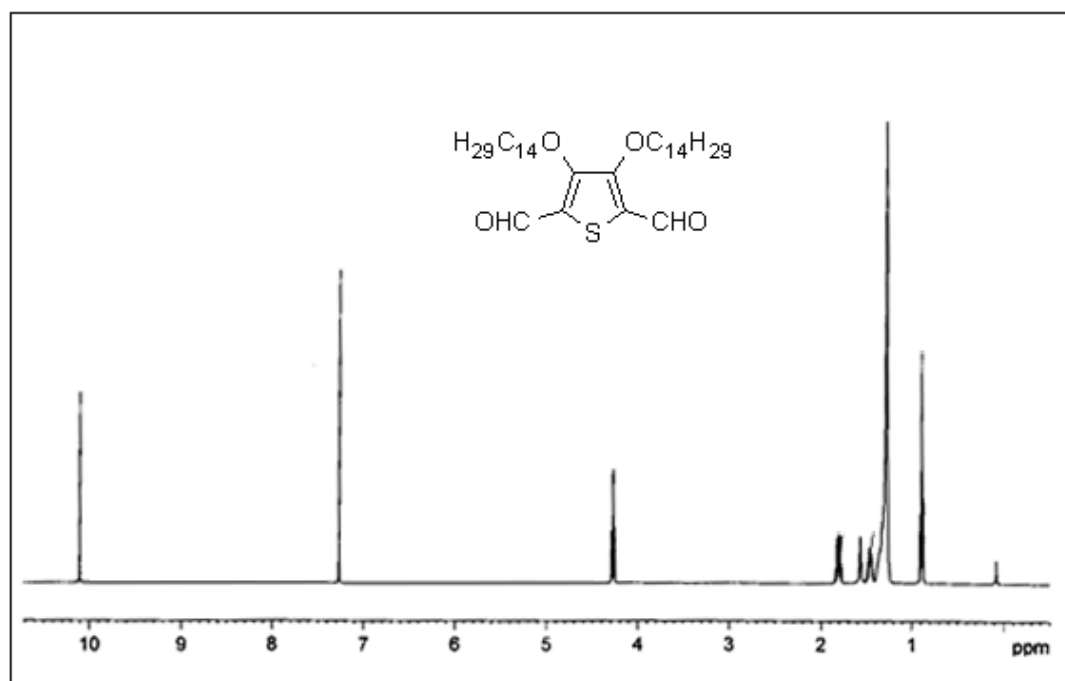


Figure 3.12: ¹H NMR spectrum of dicarbaldehyde **15**

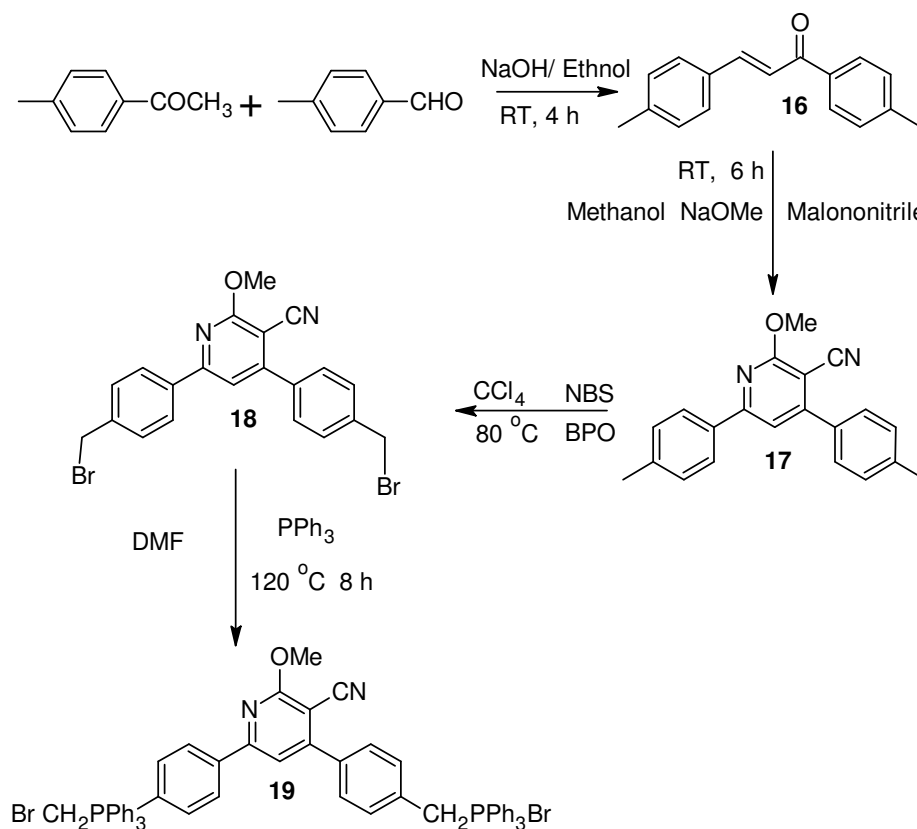
3.6.3. Results and discussion

Structures of dimethanol **14** and dialdehyde **15** were confirmed by FTIR, ¹H NMR spectral and elemental analyses. The ¹H NMR spectrum of dimethanol **14** (**Figure 3.11**) showed a peak at δ 4.68 ppm and its FTIR spectrum displayed a broad

peak at 3345 cm^{-1} confirming the presence of alcoholic $-\text{OH}$ groups in the molecule. Further, dialdehyde **15** showed a peak at δ 10. 12 ppm due to an aldehydic proton in its ^1H NMR spectrum (**Figure 3.12**) and it displayed a sharp peak at 1690 cm^{-1} in its FTIR spectrum indicating the presence of formyl group ($-\text{CHO}$).

3.7. SYNTHESIS OF CYANOPYRIDINE TRIPHENYLPHOSPHINE SALT (19)

The monomer cyanopyridine triphenylphosphonium bromide salt **19** was prepared starting from acetophenone as given in **Scheme 3.5**.



Scheme 3.5: Synthesis of cyanopyridine triphenylphosphine salt **19**

3.7.1. Chemistry

The required chalcone **16** was prepared from toluadehyde and 4-methyl acetophenone through Claisen-Schmidth reaction. It was then cyclized to cyanopyridine **17** by reacting it with malononitrile in presence of sodium methoxide. Further, dimethyl cyanopyridine **17** was brominated via Wholzigler method using

NBS and BPO to get dibromo derivative **18**. Compound **18** was conveniently converted into its phosphonium salt **19** through Wittig reaction.

3.7.2. Synthesis and characterization

Details of synthesis of cyanopyridine triphenylphosphine salt (**19**) from 4-methyl acetophenone are given below.

Synthesis of 1,3-bis(4-methylphenyl)prop-2-en-1-one (16)

A mixture of tolualdehyde (5 g, 41.6 mmol) and 4-methylacetophenone (5.5 g, 41.6 mmol) was dissolved in 50 mL of ethanol and stirred in presence of potassium hydroxide solution (2.3 g in 5 mL water) at room temperature. After 10 h, obtained solid was filtered and re-crystallized from chloroform-methanol system to get yellow needle shaped solid. Yield 8.9 g (90 %). FTIR (cm⁻¹): 1644, 1591, 1169, 987, 805, 726, Element. Anal. Calcd (%) for C₁₇H₁₆O: C, 86.40; H, 6.82; Found C 86.41; H, 6.84.

Synthesis of 2-methoxy-4,6-bis(4-methylphenyl)pyridine-3-carbonitrile (17)

Chalcone **16** (5 g, 21.1mmol) was added slowly to a freshly prepared sodium methoxide solution (223.3 mmol of sodium in 100 mL of methanol) during stirring. Malononitrile (1.39 g, 21.1 mmol) was then added with continuous stirring at room temperature until the precipitate separates out. The separated solid was collected by filtration and re-crystallized from hot ethanol-chloroform. Yield: 4.5 g (67 %). M. P: 142-144 °C.). FTIR (cm⁻¹): 2993, 2219, 1580, 1546, 1451, 1359, 1139, 821. ¹H NMR (400 MHz, CDCl₃) δ (ppm): 8.00 (m, 2H, Ar-H), 7.55(m, 2H, Ar-H), 7.44 (s, 1H, Ar-H (pyridine)), 7.34-7.28 (m, 4H, Ar-H), 4.19 (s, 3H,-O-CH₃), 2.43 (s, 6H, Ar-CH₃)Element. Anal. Calcd. (%) for C₂₁H₁₈N₂O: C, 80.23; H, 5.77; N, 8.91; Found: C, 80.25; H, 5.75; N, 8.93.

Synthesis of 4,6-bis(4-(bromomethyl)phenyl)-2-methoxypyridine-3-carbonitrile (18)

A mixture of dimethylcyanopyridine **17** (3 g, 9.5 mmol), N-bromosuccinimide (1.38 g, 19.1 mmol), 5 mg of benzoyl peroxide in 30 mL of carbon tetrachloride was refluxed for 8 h. After the solvent was removed, 20 mL of water was added with stirring for 1 h. The resulting crude product was re-crystallized from ethyl acetate-chloroform mixture to get pure white colored solid. Yield: 3.5 g (77 %). M. P: 202-

205 °C. FTIR (cm^{-1}): 2993, 2219, 1580, 1546, 1359, 1139, 1007, 821,600. ^1H NMR (400 MHz, CDCl_3) δ (ppm): 8.00 (m, 2H, Ar-H), 7.99-7.55(m, 4H, Ar-H), 7.5-7.3(m, 2H, Ar-H), 7.29 (s, 1H, Ar-H (pyridine)), 4.81 (s, 4H, Ar- CH_2 -Br), 4.13 (3H, -O- CH_3), Element. Anal. Calcd. (%) for $\text{C}_{21}\text{H}_{16}\text{Br}_2\text{N}_2\text{O}$: C, 53.42; H, 3.42; N, 5.93. Found: C, 53.46; H, 3.45; N, 5.94.

Synthesis of (4,6-bis(44-triphenyl phosphonium methyl) phenyl)-2-methoxy, 3-cyano pyridine)dibromide (19)

A solution of dibromide **18** (1 g, 6.3 mmol) and triphenylphosphine (3.34 g, 12.7 mmol) in 5 mL of DMF was refluxed with stirring for 8 h. The reaction mixture was cooled to room temperature and poured into 50 mL of ethyl acetate. The resulting mixture was sonicated for 30 min to get precipitate. The obtained white amorphous solid was filtered off, washed with excess of ethyl acetate and dried at 40 °C for 10 h. Yield: 82 %. M. P: above 300 °C. FTIR (cm^{-1}): 3365, 3051, 2853, 2211, 1658, 1430, 1103, 728, 682, 495. ^1H NMR (400 MHz, $\text{DMSO-}d_6$) δ (ppm): 8.14-8.12 (m, 2H, Ar-H), 7.99 -7.50 (m, 33H, Ar-H), 7.16-7.12(m, 4H, Ar-H), 5.26 (s, 4H, Ar- CH_2), 4.13 (s, 3H, -O- CH_3). Element. Anal. Calcd. (%) for $\text{C}_{57}\text{H}_{46}\text{Br}_2\text{N}_2\text{OP}_2$: C, 68.68; H, 4.65; N, 2.81. Found: C, 68.66; H, 4.68; N, 2.84.

FTIR and ^1H NMR spectra of cyanopyridine based compounds 17, 18 and 19 were represented in **Figures 3.13 – 3.17**.

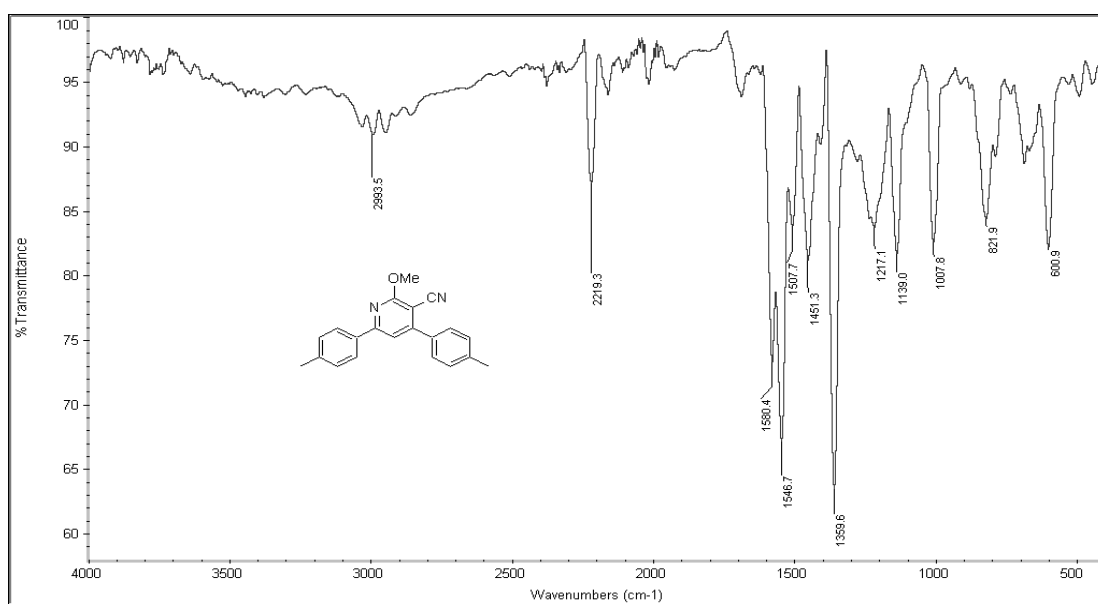


Figure 3.13: FTIR spectrum of cyanopyridine **17**

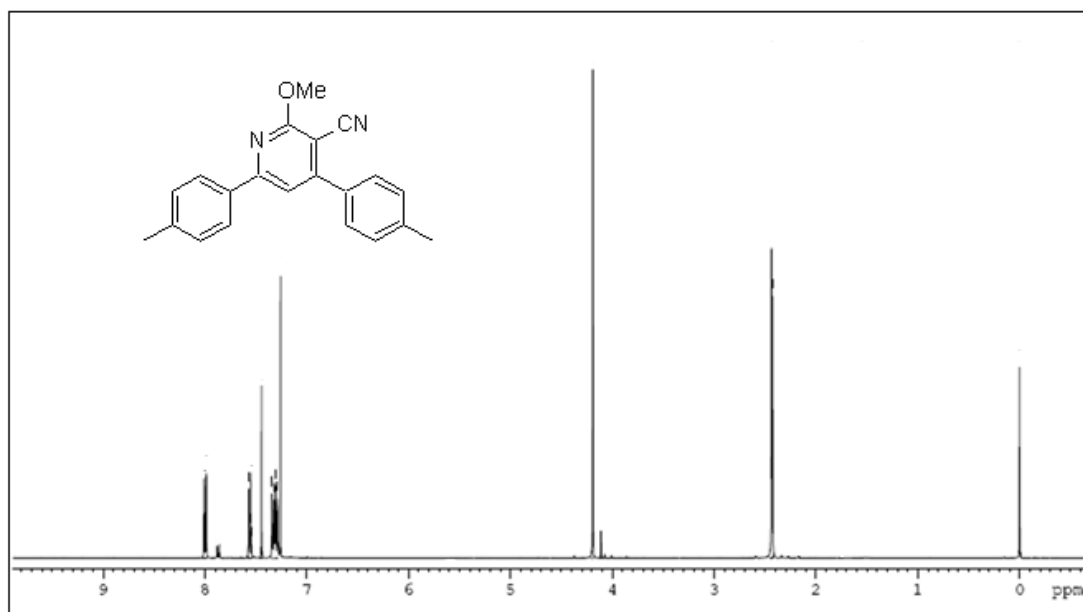


Figure 3.14: ¹H NMR spectrum of cyanopyridine 17

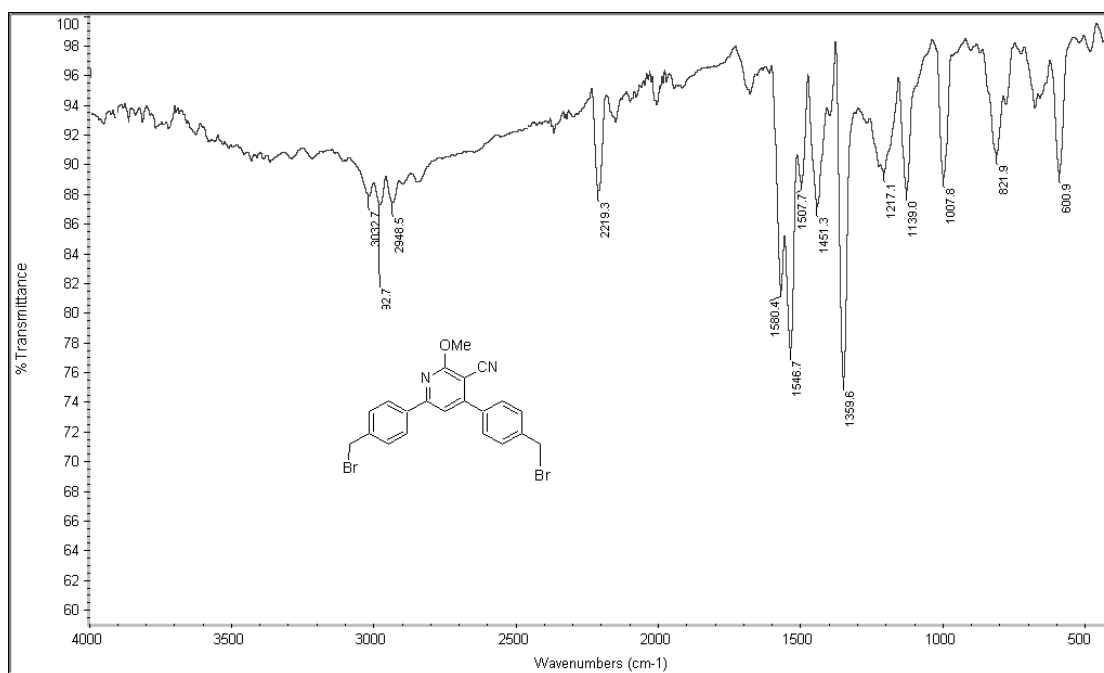


Figure 3.15: FTIR spectrum of dibromomethylcyanopyridine 18

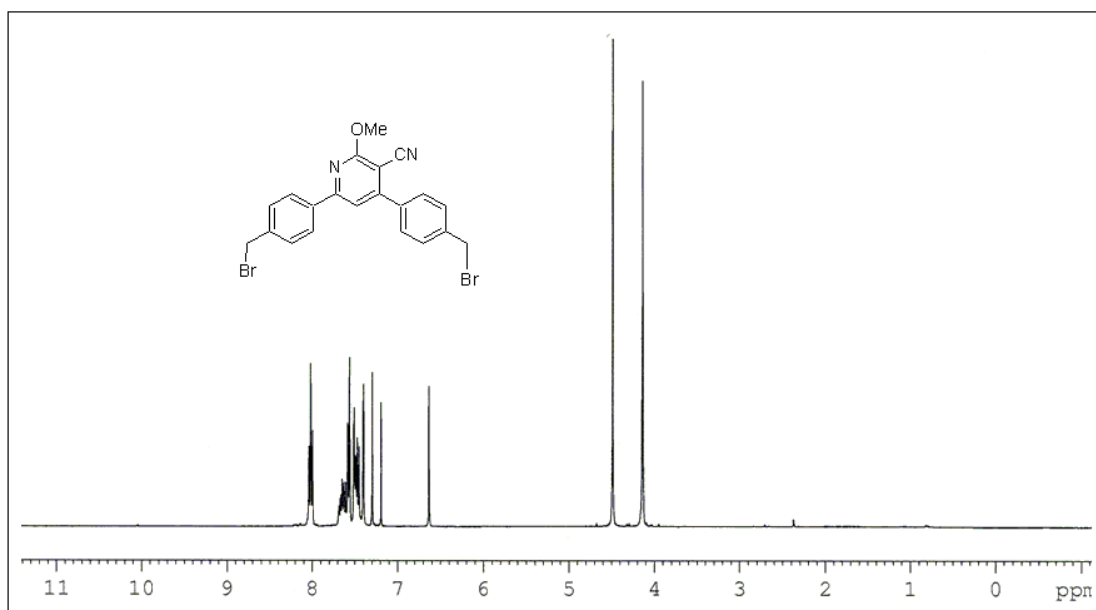


Figure 3.16: ¹H NMR spectrum of dibromomethylcyanopyridine **18**

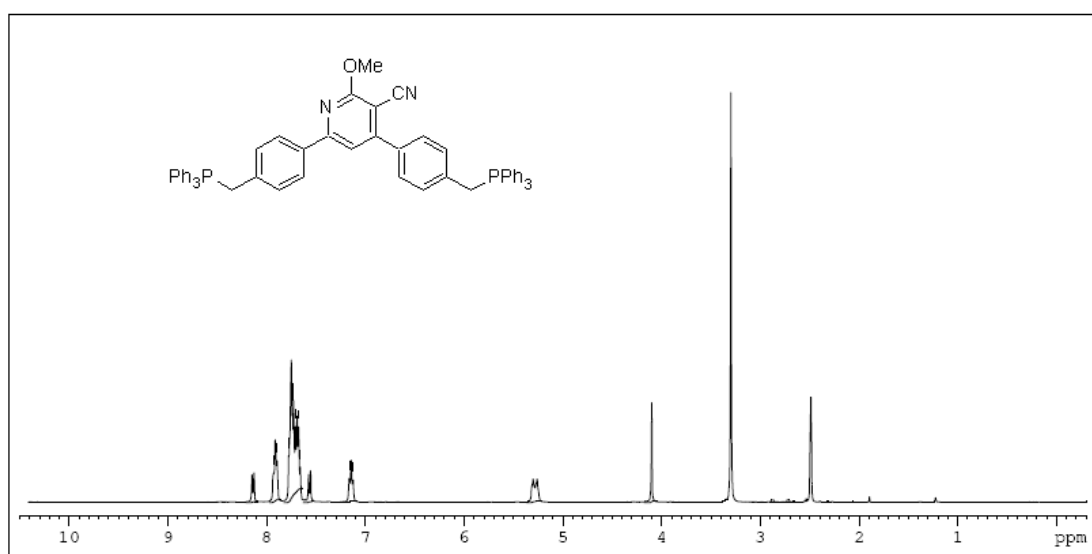


Figure 3.17: ¹H NMR spectrum of cyanopyridine wittig salt **19**

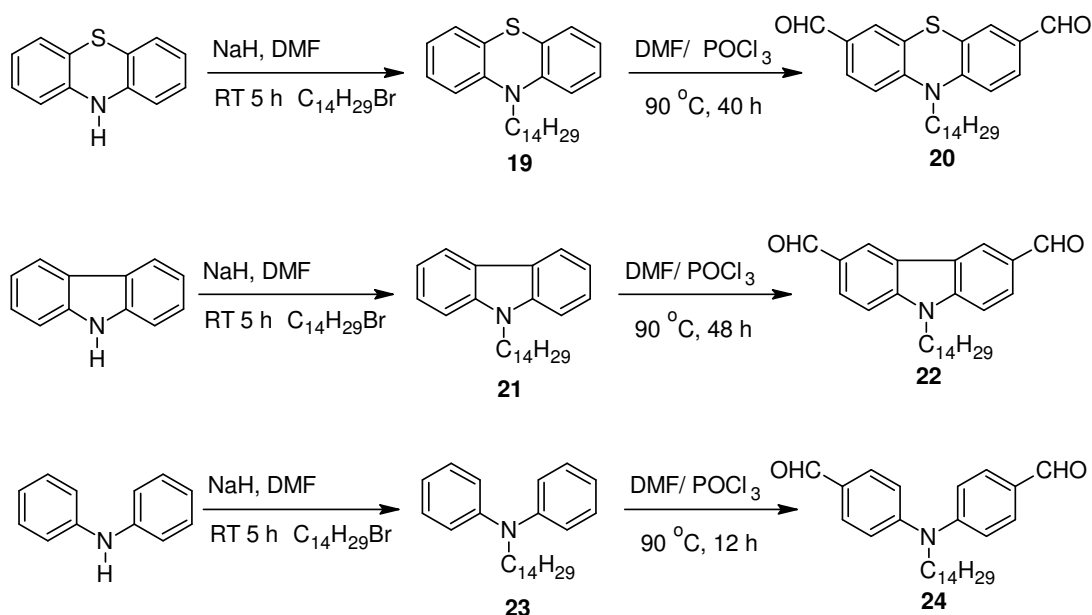
3.7.3. Results and discussion

Structures of the intermediates as well as monomers were established by elemental analysis and spectroscopic techniques. The spectral characteristics of chalcone **16** matched with the reported data. Cyclization of chalcone to cyanopyridine **17** was confirmed by its ¹H NMR spectrum (**Figure 3.14**) wherein it showed a signal at δ 4.19 ppm which corresponds to -OCH₃ protons of the pyridine ring. In its FTIR spectrum (**Figure 3.13**), it displayed a sharp peak at 2217 cm⁻¹ indicating the presence

of cyano group. Formation of dibromomethyl cyanopyridine **18** was confirmed by its ^1H NMR spectrum (Figure 3.16), wherein it showed a signal at δ 4.81 ppm that corresponds to methylene protons, which is de-shielded to a greater extent when compared to compound **17**. Further, the structure of monomer **19** was evidenced by its ^1H NMR spectral data (Figure 3.17). In its spectrum, methyl protons of phosphonium salt resonated at δ 5.26 ppm, being largely de-shielded when compared to that of compound **18**.

3.8. SYNTHESIS OF N-TETRADECYLSUBSTITUTED PHENOTHIAZINE-/CARBAZOLE-/DIPHENYLAMINE DICARBALDEHYDES (**20**, **22**, **24**)

Scheme 3.6 illustrates the synthetic route for the preparation of N-tetradecyl substituted-phenothiazine/carbazole/diphenylamine dicarbaldhyde monomers.



Scheme 3.6: Synthesis of dicarbaldhydes of phenothiazine, carbazole, and diphenylamine (**20**, **22**, **24**)

3.8.1. Chemistry

In the first step, phenothiazine, carbazole and diphenylamine were alkylated with n-bromotetradecane in DMF solvent media using sodium hydride. Further, these alkylated products were subjected to Vilsmeier-Haak formylation to obtain required dialdehyde monomers, viz. N-tetradecylsubstituted phenothiazine-/ carbazole-/ diphenylamine dicarbaldhydes (**20**, **22** and **24**). Their synthetic procedures and characterization data are given in the following section.

3.8.2. Synthesis and characterization

This section explains the synthesis of various aromatic dicarbaldehydes through two step reactions involving alkylation followed by Villsmayer-Haack formylation reaction.

Synthesis of alkylated phenothiazine, carbazole, diphenylamine (19, 21, 23)

Sodium hydride (0.62 g, 25.5 mmol) was added to a solution of phenothiazine (5 g, 25.1 mmol, dissolved in 50 mL of DMF) and the resulting mixture was stirred for about 30 min. Then 1-bromo tetradecane (8.29 g, 29.9 mmol) was added slowly into the reaction mixture and stirred for 5 h at room temperature. After the completion of reaction, the resulting crude mixture was poured into cold water. The organic layer was extracted with ethyl acetate and then dried over Na₂SO₄. The solvent was evaporated under reduced pressure. The resulting semi-solid was purified by column chromatography by using hexane and ethyl acetate as eluent. Similar synthetic procedures were followed for compounds dicarbaldehydes **21** and **23** and their characterization data are summarized as follows.

10-tetradecyl-10H-phenothiazine (19): Yield: 8.5 g (85 %). FTIR (cm⁻¹): 2920, 2859, 1616, 1592, 1470, 1345, 1252, 1134, 894, 729. ¹H NMR (400 MHz, CDCl₃), δ (ppm): 8.11 (d, 2H), 7.45 (m, 4H), 7.21 (t, 2H), 4.29 (t, 2H, J = 8 Hz), 1.86 (m, 2H), 1.31 (m, 22H), 0.85 (t, 3H, J = 7.2 Hz). Element. Anal. Calcd (%) for C₂₆H₃₇NS: C, 78.93; H, 9.43; N, 3.54; S, 8.10. Found: C, 78.93; H, 9.42; N, 3.51; S, 8.14.

9-tetradecyl-9H-carbazole (21): Yield: 8.4 g (77 %). FTIR (cm⁻¹): 2922, 2857, 2802, 1610, 1591, 1470, 1348, 1254, 1150, 1128, 898, 804, 760, 729. ¹H NMR (400 MHz, CDCl₃), δ (ppm): d 8.15 (d, 2H), 7.41 (m, 4H), 7.25 (t, 2H), 4.23 (t, 2H, -OCH₂-, J = 8 Hz), 1.80 (m, 2H), 1.35 (m, 22H), 0.85 (t, 3H, -CH₃, J = 7 Hz). Element. Anal. Calcd. (%) for C₂₆H₃₇N: C, 85.89; H, 10.26; N, 3.85. Found: C, 85.85; H, 10.29; N, 3.86.

N-tetradecyl diphenylamine (23): Yield: 8.8 g (82 %). FTIR (cm⁻¹): 2920, 2852, 1590, 1494, 1309, 891, 743. ¹H NMR (400 MHz, CDCl₃), δ (ppm): 7.36-7.04 (m, 10H, Ar-H), 3.83 (t, 2H, -NCH₂-, J = 8 Hz), 1.74 (m, 2H, -NCH₂CH₂-), 1.34-1.24 (m, 22H, -CH₂CH₂), 0.87 (t, 3H, CH₃, J = 7 Hz). Element. Anal. Calcd. (%) for C₂₆H₃₉N: C, 85.42; H, 10.75; N, 3.83. Found; C, 85.39; H, 10.78; N, 3.84.

Synthesis of N-tetradecyl-phenothiazine / carbazole / diphenylamine dicarbaldehydes (20, 22, 24)

General method

Freshly distilled phosphorus oxychloride (11.4 mL, 75.8 mmol) was added drop-wise to 5.5 mL of anhydrous DMF at 0 °C over a period of 30 min. Later on N-tetradecyl phenothiazine (5 g, 12.6 mmol in 20 mL of 1,2 dichloroethane) was slowly added to the reaction mixture and heated to 90 °C for 40 h. After the completion of reaction, solution was cooled to room temperature, poured into ice-cold water, and neutralized to pH 6-7 by drop-wise addition of saturated sodium hydroxide solution. The product was extracted with ethyl acetate. The organic layer was dried with anhydrous Na₂SO₄ and then concentrated under reduced pressure. The crude product was purified by column chromatography using hexane/ethyl acetate as eluent. A light orange low melting solid was obtained. Similar synthetic protocol was used in the preparation of carbazole dicarbaldehyde **22** and diphenylamine dicarbaldehyde **24**.

10-Tetradecyl-10H-phenothiazine-3,7-dicarbaldehyde (20): Yield: 3.52 g (61 %). FTIR (cm⁻¹): 2919, 2845, 1680, 1578, 1504, 1345, 1160, 820, 720. ¹H NMR (400 MHz, CDCl₃), δ (ppm): 9.80 (s, 2H, -aldehydic), 7.74-7.69 (m, 2H), 7.57 (d, 2H), 7.25 (d, 2H), 4.00 (t, 2H, -N-CH₂-, J = 8 Hz), 1.68 (m, 2H), 1.17-1.37 (m, 22 H), 0.83 (t, 3H, J = 7.2 Hz). Element. Anal. Calcd. (%) for C₂₈H₃₇NO₂S: C, 74.46; H, 8.26; N, 3.10; S, 7.10. Found: C, 74.47; H, 8.24; N, 3.14; S, 7.12.

9-Tetradecyl-9H-carbazole-3,6-dicarbaldehyde (22): Yield: 4.1 g (71 %). FTIR (cm⁻¹) 2922, 2858, 1688, 1606, 1591, 1473, 1345, 1251, 1134, 893, 725. ¹H NMR (400 MHz, CDCl₃), δ (ppm): 10.04 (s, 2H, -aldehydic), 8.83 (s, 2H), 8.01 (d, 2H), 7.80 (d, 2H), 4.16 (t, 2H, J = 7.8 Hz), 1.69 (m, 2H), 1.16 (m, 22 H), 0.73 (t, 3H, J = 7 Hz). Element. Anal. Calcd (%) for C₂₈H₃₇NO₂: C, 80.15; H, 8.89; N, 3.34. Found: C, 80.18; H, 8.85; N, 3.31.

N-tetradecyl diphenylamine 4,4'-dicarbaldehyde (24): Yield: 4.1 g (71 %). FTIR (cm⁻¹): 2915, 2848, 1685, 1578, 1502, 1359, 1157, 820, 719. ¹H NMR (400 MHz, CDCl₃), δ (ppm): 9.88 (s, 2H, -aldehydic), 7.81(d, 4H, Ar-H), 7.14 (d, 4H, Ar-H), 3.83 (t, 2H, -NCH₂-, J = 8 Hz), 1.74 (m, 2H, -NCH₂CH₂-), 1.34-1.24 (m, 22H, -

CH₂CH₂), 0.87 (t, 3H, CH₃, J = 7.2 Hz). Element. Anal. Calcd. (%) for C₂₈H₃₉NO₂: C, 79.76; H, 9.32; N, 3.32. Found: C, 76.79; H, 9.28; N, 3.35.

FTIR and ¹H NMR spectra of dicarbaldehyde **24** were represented in **Figures 3.18** and **3.19**.

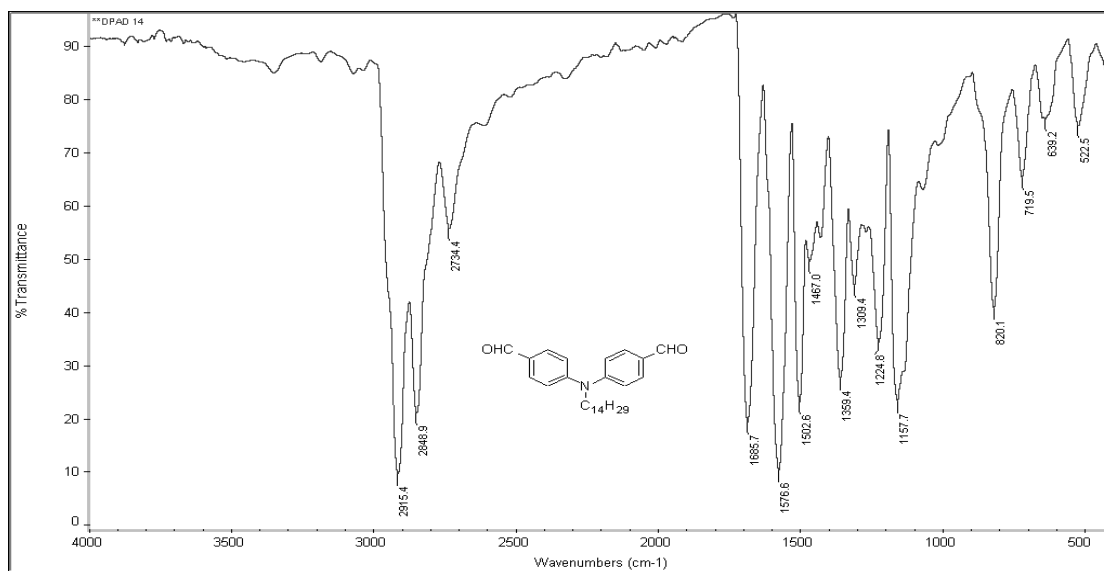


Figure 3.18: FTIR spectrum of N-tetradecyldiphenylamine-3,6-dicarbaldehyde **24**

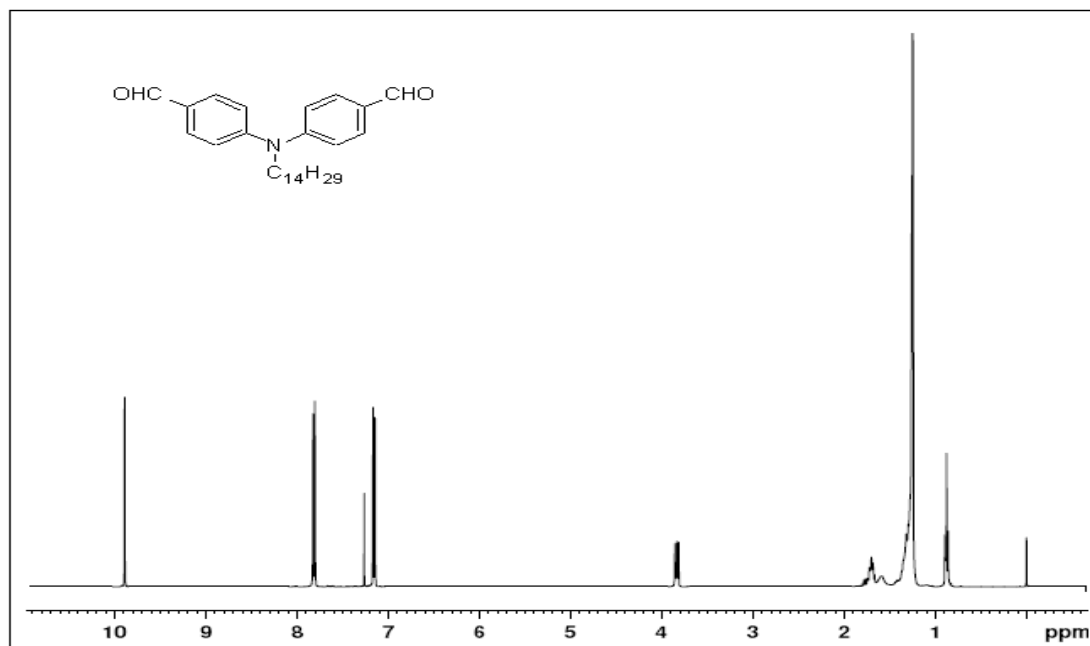


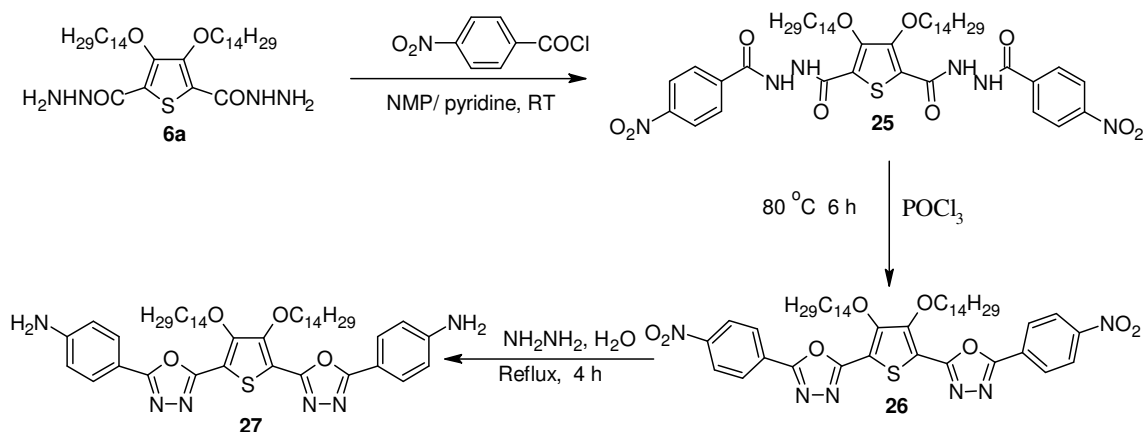
Figure 3.19: ¹H NMR spectrum of N-tetradecyldiphenylamine-3,6-dicarbaldehyde **24**

3.8.3. Results and discussion

Structures of the intermediates and dialdehyde monomers **20**, **22** and **24** were confirmed by FTIR, ^1H NMR spectral and elemental analyses. The structures of N-alkylated phenothiazine (**19**), carbazole (**21**) and diphenylamine (**23**) (**Figure 3.19**) were confirmed by their FTIR spectra, wherein they showed a strong absorption band around 2850 cm^{-1} corresponds to the lengthy alkyl chains. Similarly their ^1H NMR spectra displayed characteristic peaks due aliphatic chains. Further, ^1H NMR spectra of phenothiazine dicarbaldehyde (**20**), carbazole dicarbaldehyde (**22**) and diphenylamine dicarbaldehyde (**24**) (**Figure 3.19**) confirmed the presence of aldehydic group; also their FTIR spectra (**Figure 3.18**) showed the aldehydic carbonyl stretching frequency at around 1650 cm^{-1} establishing the structure.

3.9. SYNTHESIS OF DIAMINE MONOMER CARRYING THIOPHENE AND OXADIAZOLE RINGS (**27**)

The monomer 4,4'-(5,5'-(3,4-bis(tetradecyloxy)thiophene-2,5-diyl)bis(1,3,4-oxadiazole-5,2-diyl))dianiline was synthesized from dihydrazide **6a** as outlined in the **Scheme 3.7**.



Scheme 3.7: Synthesis of diamine monomer **27**

3.9.1. Chemistry

In the reaction sequence, the dihydrazide **6a** was made to react with nitrobenzoyl chloride to get dicarbohydrazide **25**, which was on treatment with phosphorousoxychloride as cyclizing agent underwent smooth cyclization to yield its dinitro derivative **26**. The resulting dinitro compound was reduced to diamine

monomer **27** using hydrazine hydrate in ethanolic media without any metal catalyst. This is a unique single-step reduction reaction giving an excellent yield, which completes in a very short span of time. It is interesting to note that presence of highly electron withdrawing oxadiazole ring at 4th position of the nitrophenyl unit facilitated almost quantitative reduction of nitro groups without any side product. The possible mechanism is outlined in **Figure 3.20**.

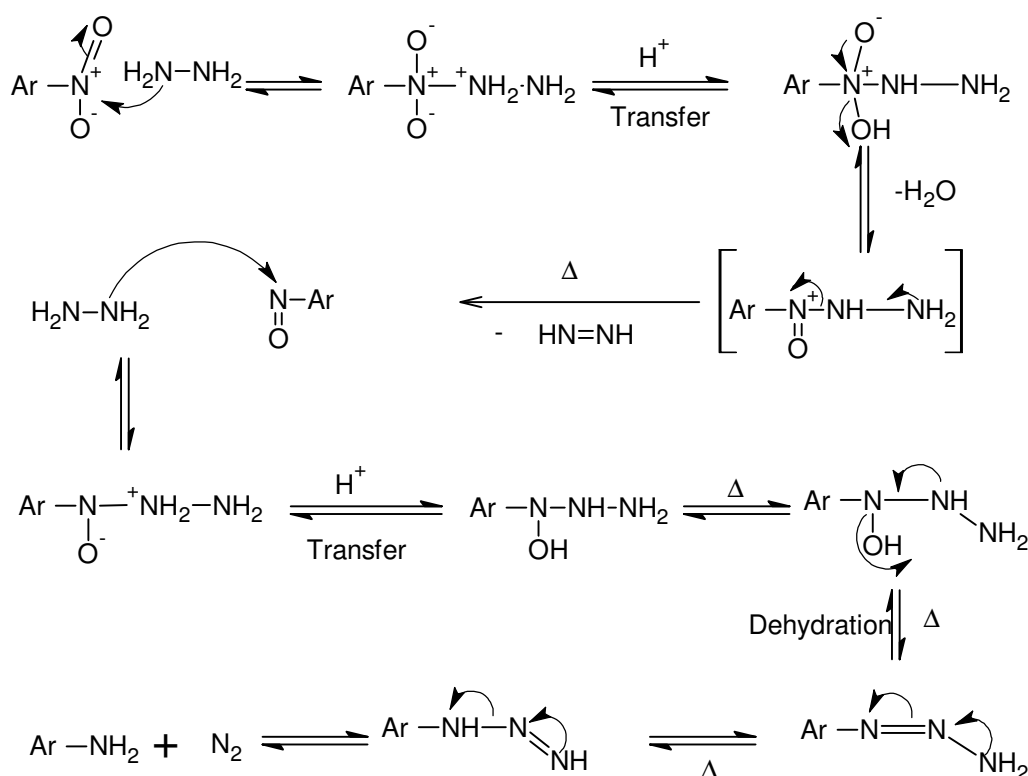


Figure 3.20: Reaction mechanism of reduction of dinitro derivative **26**

3.9.2. Synthesis and characterization

The experimental procedures used for the synthesis of diamine monomer **27** and its intermediates along with their characterization data are given as follows.

Synthesis of N,N'-5-bis(4-nitrobenzoyl)-3,4-bis(tetradecyloxy) thiophene-2,5-dicarbohydrazide (25).

To a mixture of dihydrazide **6a** (5 g, 8.01 mmol) and 2 mL of pyridine in 50 mL of NMP, 2 equivalents of 4-nitrobenzoyl chloride (2.97 g, 16.02 mmol) was added slowly at room temperature while stirring. The stirring was continued at room temperature for 1 h. The resulting solution was stirred at 80 °C for 5 h. After cooling

to room temperature, the reaction mixture was poured into excess of cold water to get a precipitate. The precipitate obtained was collected by filtration, washed with excess of water, dried in oven and re-crystallized from ethanol/chloroform mixture to get desired product. Yield: 89 %. FTIR (cm^{-1}): 3454, 3290, 2915, 2648, 1634, 1595, 1518, 1455, 1286, 1032, 852, 706. ^1H NMR (400 MHz, CDCl_3), δ (ppm): 10.52 (s, 2H, -NH-), 9.74 (s, 2H, -NH-), 8.25 (d, 4H, Ar-H, $J = 8.4$ Hz), 7.45 (d, 4H, Ar-H, $J = 8.0$ Hz), 4.35 (t, 4H, $-\text{OCH}_2-$, $J = 8.0$ Hz), 1.12-1.84 (m, 48H, $-(\text{CH}_2)_{12}-$) 0.80 (t, 6H, $-\text{CH}_2-\text{CH}_3$, $J = 7.4$ Hz). Element. Anal. Calcd. (%) for $\text{C}_{48}\text{H}_{70}\text{N}_6\text{O}_{10}\text{S}$: C, 62.45; H, 7.64; N, 9.10; S, 3.47. Found: C, 62.41; H, 7.55; N, 9.14; S, 3.51.

5,5'-(3,4-Bis(tetradecyloxy) thiophene-2,5-diyl) bis(2-(4-nitrophenyl)-1,3,4-oxadiazole) (26)

A mixture of dicarbohydrazide **25** (5 g, 5.4 mmol) and 50 mL of phosphorous oxychloride was stirred at 80 °C for 6 h. The reaction mixture was then cooled to room temperature and poured into an excess of ice-cold water. The resulting precipitate was collected by filtration, washed with water and dried in an oven. Further, it was purified by re-crystallization from ethanol-chloroform mixture. Yield: 80 %. M. P: 158 °C. FTIR (cm^{-1}): 2917, 2649, 1583, 1518, 1466, 1338, 1042, 853, 713. ^1H NMR (400 MHz, CDCl_3) δ (ppm): 8.42 (d, 4H, Ar-H, $J = 8$ Hz), 8.30 (d, 4H, Ar-H, $J = 8$ Hz), 4.35 (t, 4H, $-\text{OCH}_2-$, $J = 8.0$ Hz), 1.9-1.29 (m, 48 H), 0.87 (t, 6H, $-\text{CH}_2-\text{CH}_3$, $J = 8$ Hz). Element. Anal. Calcd. (%) for $\text{C}_{48}\text{H}_{66}\text{N}_6\text{O}_8\text{S}$: C, 64.99; H, 7.50; N, 9.47; S, 3.61. Found: C, 64.89; H, 7.54; N, 9.45; S, 3.63.

4,4'-(5,5'-(3,4-bis(tetradecyloxy)thiophene-2,5-diyl)bis(1,3,4-oxadiazole-5,2-diyl))dianiline (27)

To a stirred solution of dinitro derivative **26** (5 g, 5.6 mmol) in ethanol at 60 °C, hydrazine hydrate (5 mL, excess) was added drop-wise over a period of 5 min. Then the reaction mixture was refluxed for about 4 h. After completion of the reaction, ethanol was removed by vacuum distillation under reduced pressure. The resulting reaction mixture was poured into water and the precipitated product was collected by vacuum filtration. The crude compound was further re-crystallized by chloroform-ethanol mixture to obtain dimine monomer **27**. Yield: 94 %. M. P: 178 °C. FTIR (cm^{-1}): 3341, 3217, 2917, 2649, 1604, 1487, 1371, 1304, 1174, 1045, 830, 728.

^1H NMR (400 MHz, CDCl_3) δ (ppm): 8.04 (d, 4H, Ar-H, $J = 8$ Hz), 6.75 (d, 4H, Ar-H, $J = 8$ Hz), 4.34 (t, 4H, $-\text{OCH}_2-$, $J = 8$ Hz), 4.09 (s, 4H, $-\text{NH}_2$), 1.9-1.2 (m, 48H, $-\text{OCH}_2-$), 0.86 (t, 6H, $-\text{CH}_2-\text{CH}_3$, $J = 8$ Hz). Element. Anal. Calcd. (%) for $\text{C}_{48}\text{H}_{70}\text{N}_6\text{O}_4\text{S}$: C, 69.70; H, 8.53; N, 10.16; S, 3.88. Found: C, 69.71; H, 8.55; N, 10.26; S, 3.81.

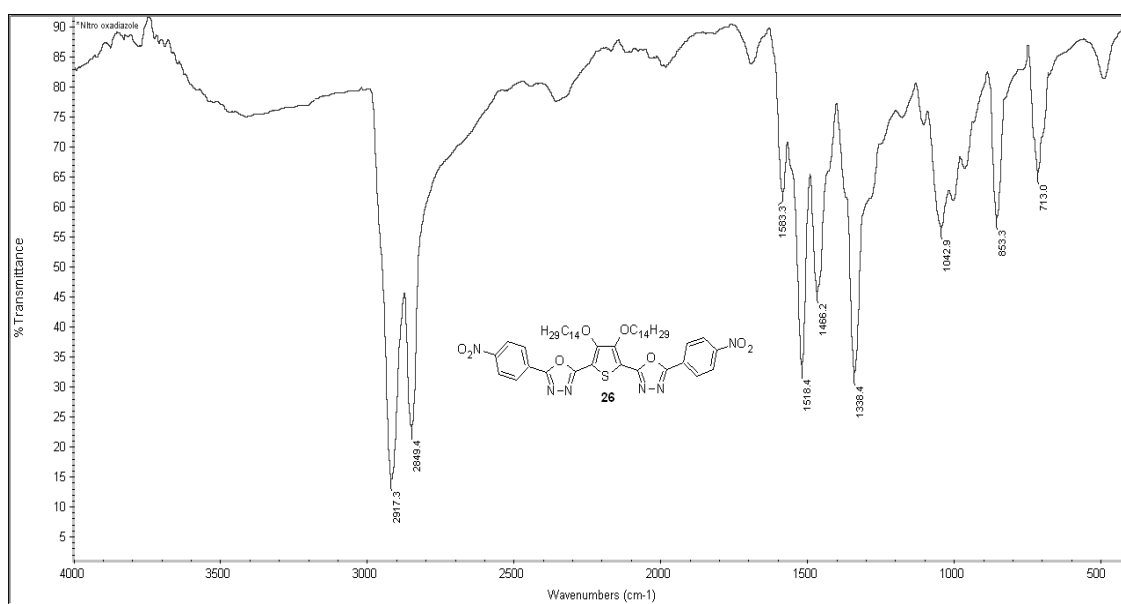


Figure 3.21: FTIR spectrum of dinitro compound 26

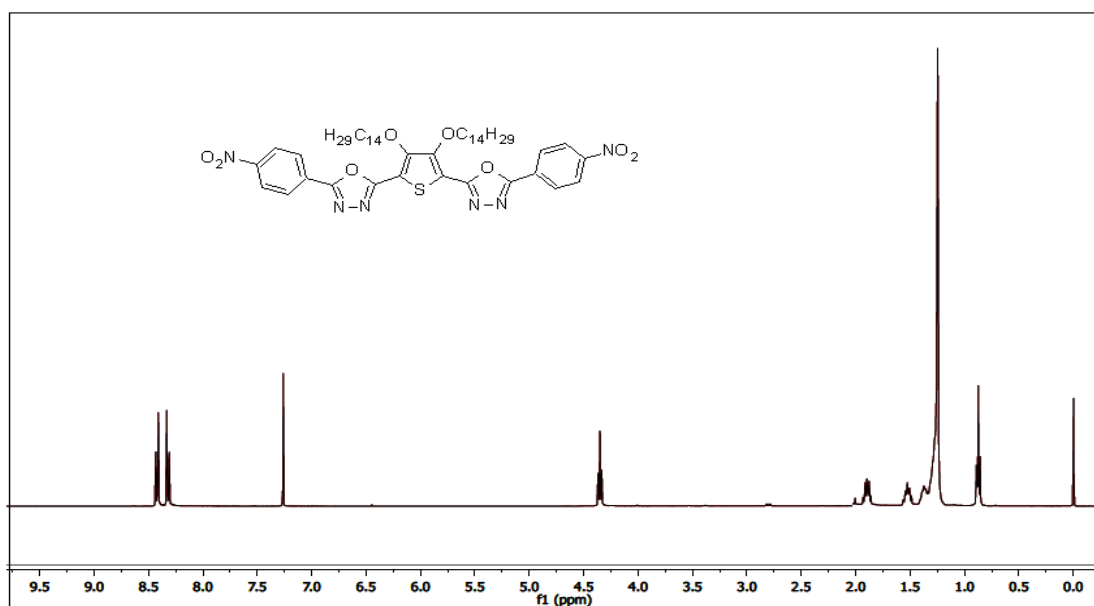


Figure 3.22: ^1H NMR spectrum of dinitro compound 26

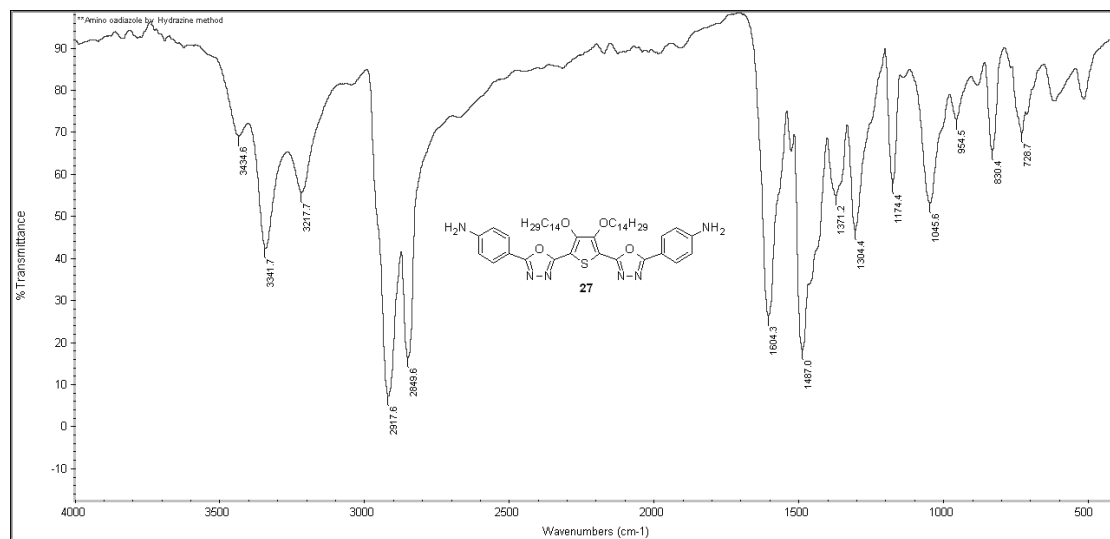


Figure 3.23: FTIR spectrum of diamine **27**

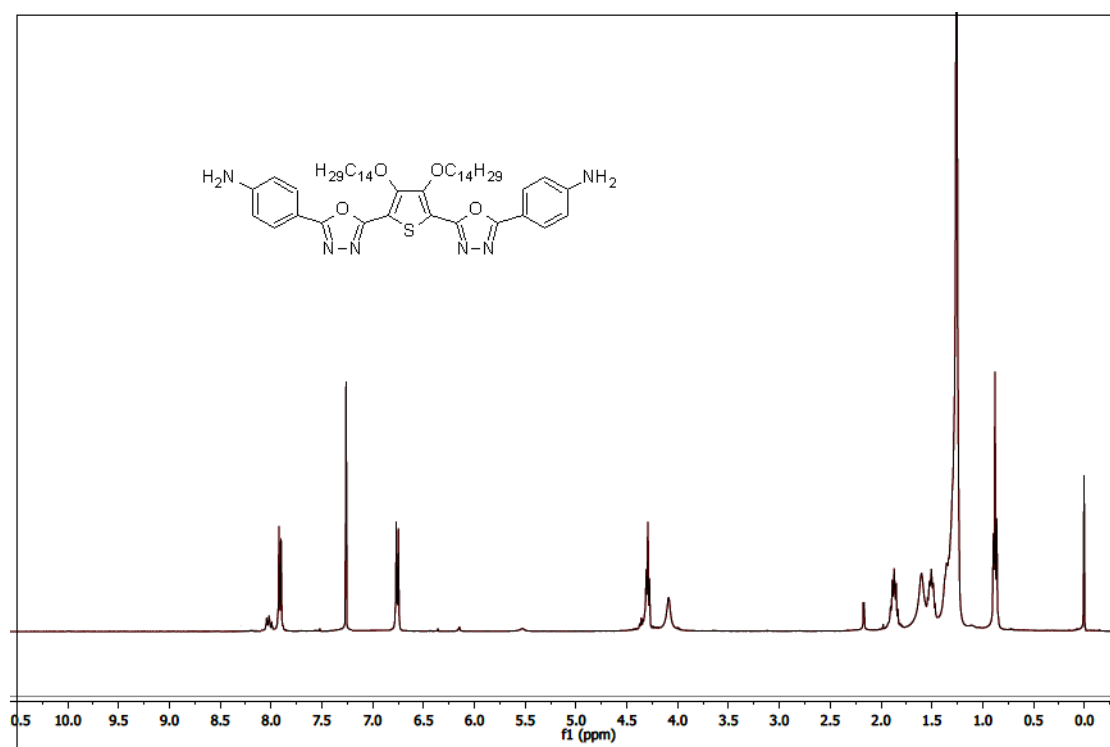


Figure 3.24: ^1H NMR spectrum of diamine **27**

3.9.3. Results and discussion

^1H NMR spectrum of dinitro derivative **26** (**Figure 3.22**) showed no peaks due to amidic protons, but showed de-shielding effect of aromatic protons clearly indicating formation of oxadiazole ring. Further, in its FTIR spectrum (**Figure 3.21**) it showed the absence of amidic carbonyl absorption bands and appearance of $-\text{C}=\text{N}-$

stretching absorption peaks indicating the cyclization. Similarly, formation of conjugated diamine **27** was confirmed by its FTIR spectrum (**Figure 3.23**) wherein it showed strong absorption bands that correspond to the primary amine (3341, 3217 cm^{-1}). Also its ^1H NMR (**Figure 3.24**) displayed the appearance of a broad singlet at δ 4.09 ppm which confirms the presence of primary amine. Furthermore, the aromatic protons of the benzene ring attached to the amine functionality shielded to a great extent and hence they resonated at δ 6.75 ppm confirming the conversion.

3.10. CONCLUSIONS

In conclusion, seven new series of monomers required for the synthesis of target polymers were successfully synthesized through multistep reactions. Synthetic methods used for the preparations of intermediates and monomers **6a**, **10**, **13**, **15**, **19**, **20**, **22**, **24**, and **27** were established. Chemical structures of all the intermediates and monomers were evidenced by their FTIR, ^1H NMR, mass spectral and elemental analyses. Upcoming chapter (**Chapter 4**) includes the experimental part leading to synthesis and characterization of new conjugated polymers **P1-P20** using these monomers.

Abstract

This chapter includes the experimental part leading to synthesis of five new series of D-A type conjugated polymers (P1-P20) from their respective monomers. Further, it describes the characterization of new polymers by spectral, thermo gravimetric, and gel permeation chromatographic analyses.

4.1. INTRODUCTION

In the previous chapter, synthesis and characterization of new monomers required for target polymers have been described. These monomers have been utilized in the synthesis of newly designed twenty conjugated D-A type polymers via various polymerization techniques. The first series of polymers, viz. **P1-P5** have been obtained through poly-condensation reactions from dihydrazide monomers **6a**, via polyhydrazide route. Further, the cyanopyridine based polymers **P6-P10**, belonging to 2nd series have been prepared from Wittig condensation technique from various dicarboxaldehydes. On the similar lines, polymers of **Series 3** have been synthesized from their respective monomers. The conjugated dialdehyde monomer **13** has been condensed with phenyl diacetonitrile through Knoevengel condensation reaction to obtain **P13** of the same series. Furthermore, cyclic-imide polymers **P15** and **P16** have been prepared by condensing conjugated diamine **27** with corresponding dianhydrides. Finally, polymers **P17-P20** have been synthesized through poly-condensation of dialdehydes with conjugated dimine **27**. Details of experimental protocols followed for the synthesis of new polymers **P1-P20** and their characterization data are discussed in the following sections.

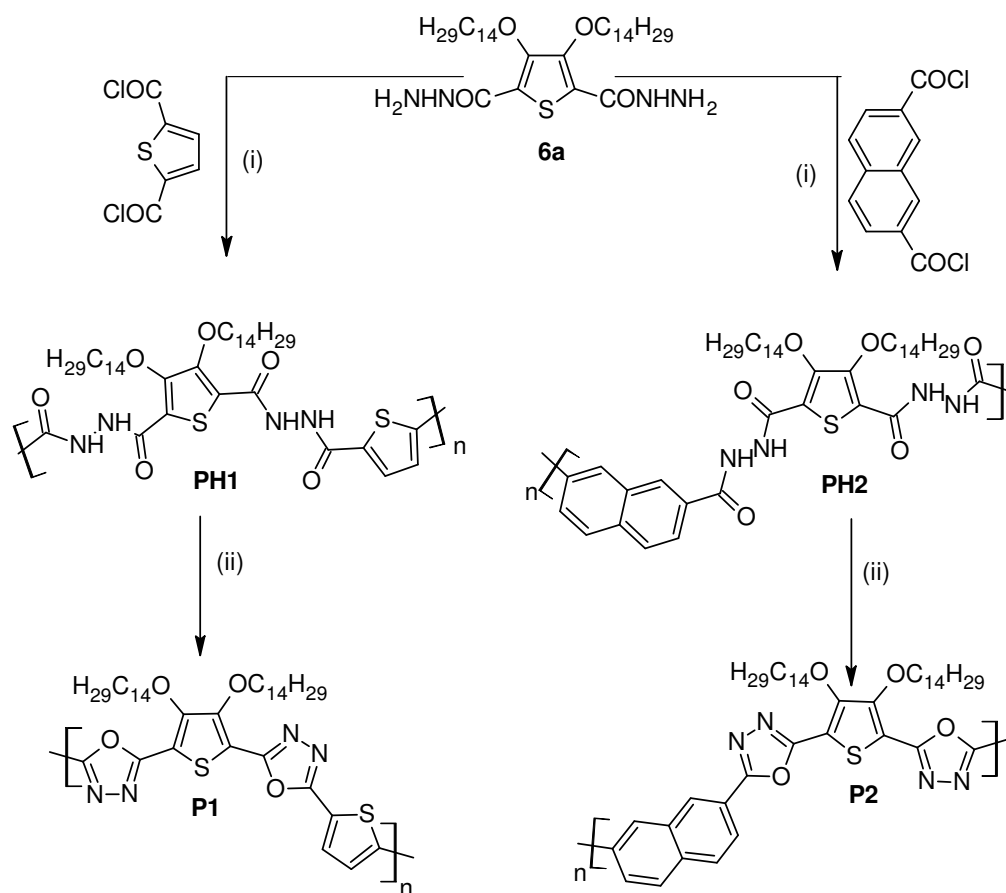
4.2. MATERIALS AND INSTRUMENTATION

The required starting materials were purchased from Aldrich chemicals. The reagents (analytical grade) were purchased commercially and used without further purification. The specifications of FTIR and ¹H NMR spectrometers and CHNS analyzer have been mentioned in **Chapter 3**. Molecular weights of the polymers were determined on Waters make Gel Permeation Chromatography (GPC) using polystyrene standards in THF solvent. Thermo Gravimetric Analyzer (TGA), SII-EXSTAR6000/TG/DTA6300 was used for their thermal characterization. The TG

analysis was carried at the rate of 3 °C /min over the temperature range of 30-800 °C under nitrogen atmosphere.

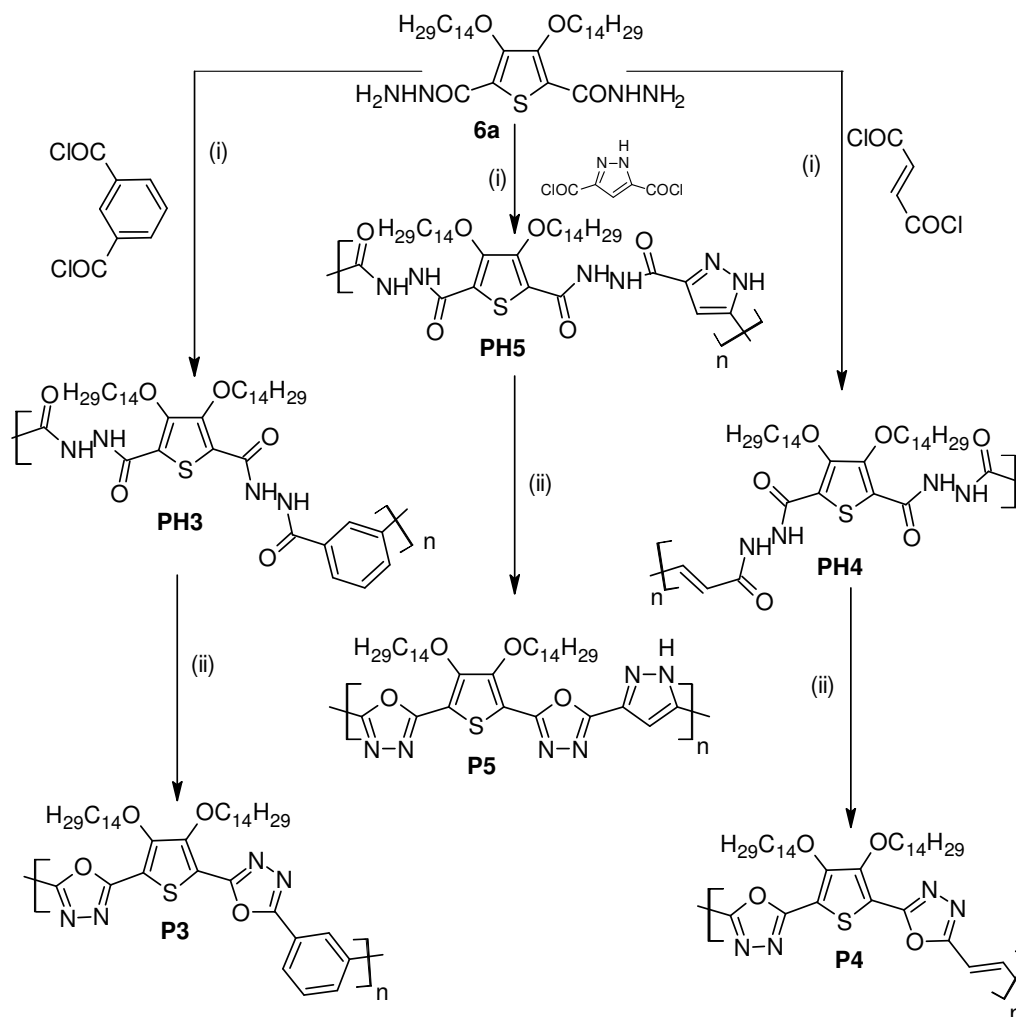
4.3. SYNTHESIS OF DIALKOXYTHIOPHENE BASED POLYMERS (SERIES 1, P1-P5)

According to **Schemes 4.1** and **4.2**, the first series of D-A type conjugated polymers comprising **P1-P5** with electron donating conjugated bridges were synthesized and their synthetic procedures are given in the following section along with their characterization data.



where (i) NMP, Pyridine, LiCl, 80 °C, 12 h, (ii) POCl_3 , 80 °C, 20 h

Scheme 4.1: Synthesis of polymers **P1-P2**



where (i) NMP, Pyridine, LiCl, 80 °C, 12 h (ii) $POCl_3$, 80 °C, 20 h

Scheme 4.2: Synthesis of polymers **P3-P5**

4.3.1. Chemistry

As outlined in **Scheme 4.1** and **4.2**, the precursor polyhydrazides, viz. **PH1-PH5** were prepared by condensing dicarbohydrazide monomer **6a** with diacid chlorides derived from thiophene, naphthyl, isophthalyl, fumaryl and pyrazole, respectively. Further, they were converted to their corresponding polymers **P1-P5** through oxidative cyclization using phosphorus oxychloride as cyclizing agent.

4.3.2. Synthesis and characterization

New polymers **P1-P5** and their corresponding precursors **PH1-PH5** were synthesized as per the following procedures.

General procedure for the synthesis of polyhydrazides PH1-PH5

To a stirred solution of one equivalent of dihydrazide **6a** (0.5 mmol) in 20 mL of (NMP), LiCl (0.2 g, 2 mmol), 2 drops of (catalytic amount) of pyridine, 2,5-thiophenediacid chloride was added slowly under constant stirring. The reaction temperature was slowly raised to 80 °C and stirred at same temperature for 12 h. After the completion of polymerization, the reaction mixture was cooled to room temperature, and poured into excess methanol to obtain crude polymer. Further, the crude product was washed with water, followed by ethanol and finally purified by re-precipitation technique using chloroform-methanol system to obtain pure polymer of a polyhydrazide **PH1**. Similarly, remaining polymers were prepared and their characterization data are as follows.

PH1. Yield: 91 %. FTIR (cm^{-1}): 3299(-NHCO-), 2919, 2851, 1633 (>C=O), 1457, 1289, 1041, 715. ^1H NMR (400 MHz, CDCl_3), δ (ppm): 10.99 (s, 1H, -CONH-), 9.89 (s, 1H, -CONH), 7.9-7.7 (m 2H, Ar-H), 4.3-4.25 (t, 4H, -OCH₂-), 1.9-1.2 (m, -CH₂-, 48H), 0.840 (s, 6H-CH₂-CH₃).

PH2: Yield 94 %. FTIR (cm^{-1}): 3266, 2920, 2852, 1633, 1460, 1037. ^1H NMR (400 MHz, CDCl_3) δ (ppm): 10.9 (d, 1H, -CONH-), 9.8 (s, 1H, -CONH-), 7.90-7.45 (m, 6H, Ar-H), 4.21 (s, 4H, -OCH₂-), 1.23-1.89 (m, 48H, -CH₂-), 0.85 (t, 6H, -CH₂-CH₃).

PH3: Yield 88 %. FTIR (cm^{-1}): 3230, 2920, 2851, 1634, 1605, 1457, 1301, 1041, 727. ^1H NMR (400 MHz, CDCl_3), δ (ppm): 10.87 (d, 1H, -CONH-), 9.70 (s, 1H, -CONH), 7.45-6.5 (m 4H, Ar-H), 4.32-4.23 (m, 4H, -OCH₂-), 1.90-1.01 (m, -CH₂-, 48H), 0.845(s, 6H, -CH₂-CH₃).

PH4: Yield 85 %. FTIR (cm^{-1}): 3230, 2920, 2851, 1634, 1605, 1457, 1301, 1041, 727. ^1H NMR (400 MHz, CDCl_3), δ (ppm): 11.17-11.03(d, 1H, -CONH-), 10.00-9.96(s, 1H, -CONH), 7.09-6.62 (m 2H, Ar-H), 4.3-4.25 (m, 4H, -OCH₂-), 1.91-1.06 (m, -CH₂-, 48H), 0.843 (s, 6H, -CH₂-CH₃).

PH5: Yield 93 %. FTIR (cm^{-1}): 3244, 2919, 2851, 1635, 1460, 1308, 1039, 727. ^1H NMR (400 MHz, CDCl_3) δ (ppm): 11.10-11.02 (d, 1H, -CONH-), 10.07-9.94

(s, 1H, -CONH), 7.69-7.41 (m 2H, Ar-H), 4.33-4.26 (m, 4H, -OCH₂-), 1.90-1.06 (m, -CH₂-, 48H), 0.845 (s, 6H, -CH₂-CH₃).

General procedure for the synthesis of polymers P1-P5

The precursor polyhydrazide **PH1**, (0.2 g) was dispersed in 20 mL of POCl₃ at room temperature. Then the mixture was refluxed for 20 h with constant stirring. After completion of the reaction, the reaction product was cooled to room temperature. Further, the reaction mass was poured into crushed ice under vigorous stirring. The precipitate was collected by filtration and was washed with water, ethanol, followed by ether and finally dried under vacuum at room temperature. The polymer was further purified by the re-precipitation method using chloroform-methanol system. On the similar lines, polymers **P2-P5** were prepared and their characterization data given below

P1: Yield 81 %. FTIR (cm⁻¹): 2921, 2853, 1575, 1461, 1368, 1283, 1030, 818, 725. ¹H NMR, (400 MHz, CDCl₃), δ (ppm): 8.15-8.11 (m 2H, Ar-H), 4.34-4.28 (m, 4H, -OCH₂-), 1.95-1.25 (m, -CH₂-, 48H), 0.890 (s, 6H, -CH₂-CH₃). Element. Anal. Calcd. (%) for C₄₀H₆₀N₄O₄S₂: C, 66.26; H, 8.34; N, 7.73; S, 8.84. Found: C, 66.21; H, 8.25; N, 7.65; S, 8.75. Weight average molecular weight (\bar{M}_w) is 13800 with poly dispersity 2.24.

P2: Yield 85 %. FTIR, (cm⁻¹): 2919, 2851, 1582, 1524, 1459, 1368, 1038. ¹H NMR, (400 MHz, CDCl₃), δ (ppm): 7.96-7.50 (m, 6H, Ar-H), 4.4-4.2 (s, 4H, -OCH₂O), 1.92-1.21 (m, 48H), 0.86 (t, 6H). Element. Anal. Calcd. (%) for C₄₆H₆₄N₄O₄S: C, 71.84; H, 8.39; N, 7.28; S, 4.17. Found: C, 71.68; H, 8.24; N, 7.21; S, 4.08. Weight average molecular weight (\bar{M}_w) is 8300 with poly dispersity 2.35.

P3: Yield 86 %. FTIR, (cm⁻¹): 2919-2851 (-C-H), 1582-1524 (>C=N-), 1459, 1368, 1038 (-C-O-C-). ¹H NMR, (400 MHz, CDCl₃), δ (ppm): 8.54-7.55 (m, 4H, Ar-H), 4.5-4.2 (m, 4H, -OCH₂O-), 1.93-1.25 (m, 48H), 0.86 (t, 6H). Element. Anal. Calcd. (%) for C₄₂H₆₂N₄O₄S: C, 70.16; H, 8.69; N, 7.79; S, 4.46. Found: C, 70.02; H, 8.59; N, 7.62; S, 4.41. Weight average molecular weight (\bar{M}_w) is 8300 with poly dispersity 2.35.

P4: Yield 88 %. FTIR (cm^{-1}): 2919, 2851, 1576, 1460, 1371, 1290, 1007. ^1H NMR, (400 MHz, CDCl_3), δ (ppm): 7.15-7.58(m 2H, vinylic), 4.345 (m, 4H, $-\text{OCH}_2-$), 1.89-1.24 (m, $-\text{CH}_2-$, 48H), 0.849 (s, 6H, $-\text{CH}_2-\text{CH}_3$). Element. Anal. Calcd. (%) for $\text{C}_{38}\text{H}_{62}\text{N}_4\text{O}_4\text{S}$: C, 68.02; H, 9.31; N, 8.35; S, 4.78. Found: C, 67.85; H, 9.22; N, 8.26; S, 4.71. Weight average molecular weight (\overline{M}_w) is 15300 with poly dispersity 2.04.

P5: Yield 80 %. FTIR (cm^{-1}): 3334, 2918, 2850, 1585, 1459, 1254, 10038, 724. ^1H NMR, (400 MHz, CDCl_3), δ (ppm): 6.89-6.56(m, 1, Ar-H), 4.68-4.32 (m, 4H, $-\text{OCH}_2-$), 1.78-1.26 (m, 48H, aliphatic), 0.85 (t, 6H, $-\text{CH}_3$). Element. Anal. Calcd. (%) for $\text{C}_{39}\text{H}_{60}\text{N}_6\text{O}_4\text{S}$: C, 66.07; H, 8.53; N, 11.85; S, 4.52. Found: C, 65.87; H, 8.41; N, 11.81; S, 4.43.

FTIR and ^1H NMR spectra of polymers **PH1** and **P1** are represented in **Figures 4.1- 4.4**.

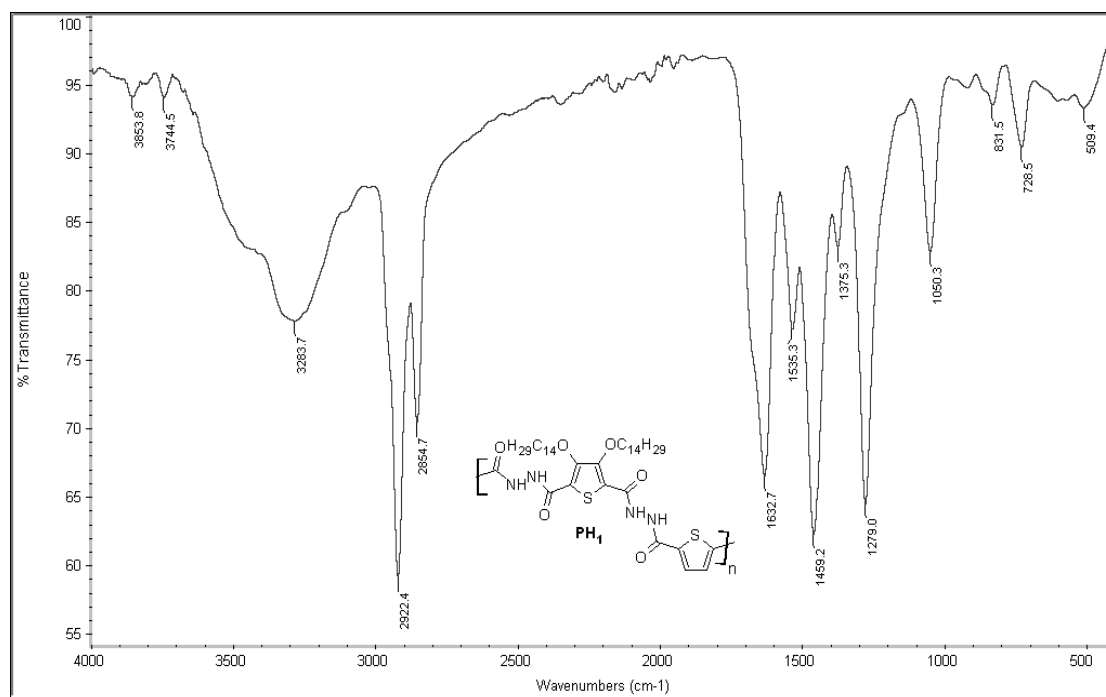


Figure 4.1: FTIR spectrum of polymer **PH1**

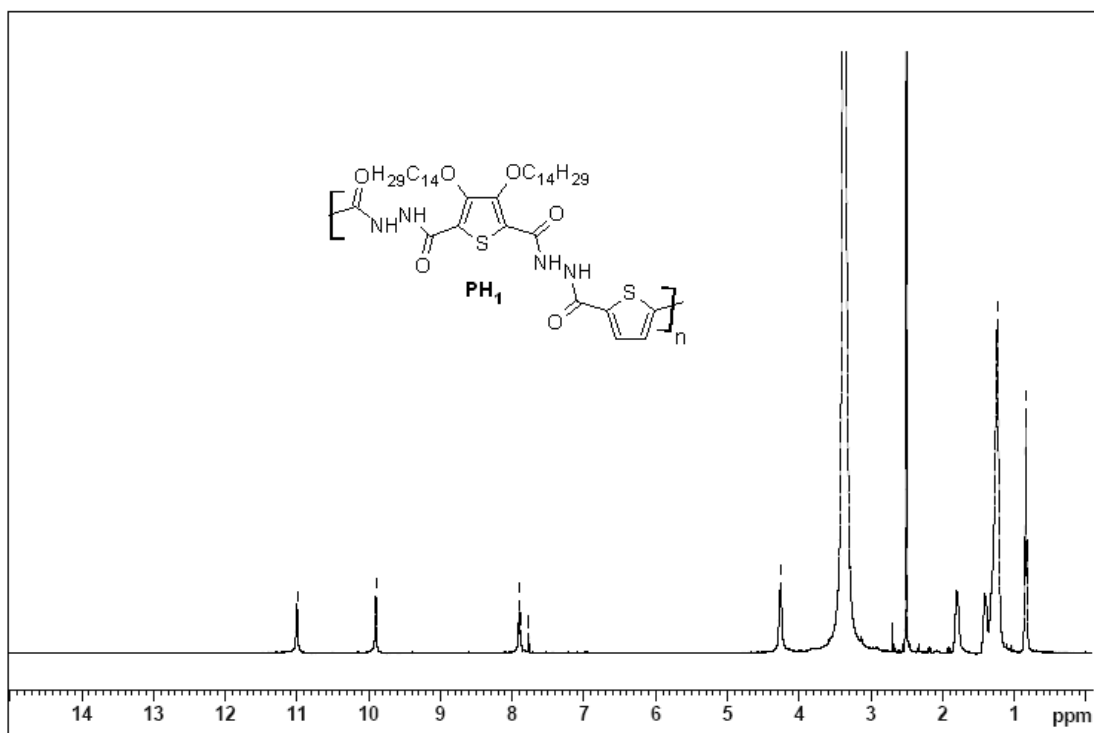


Figure 4.2: ^1H NMR spectrum of polymer PH1

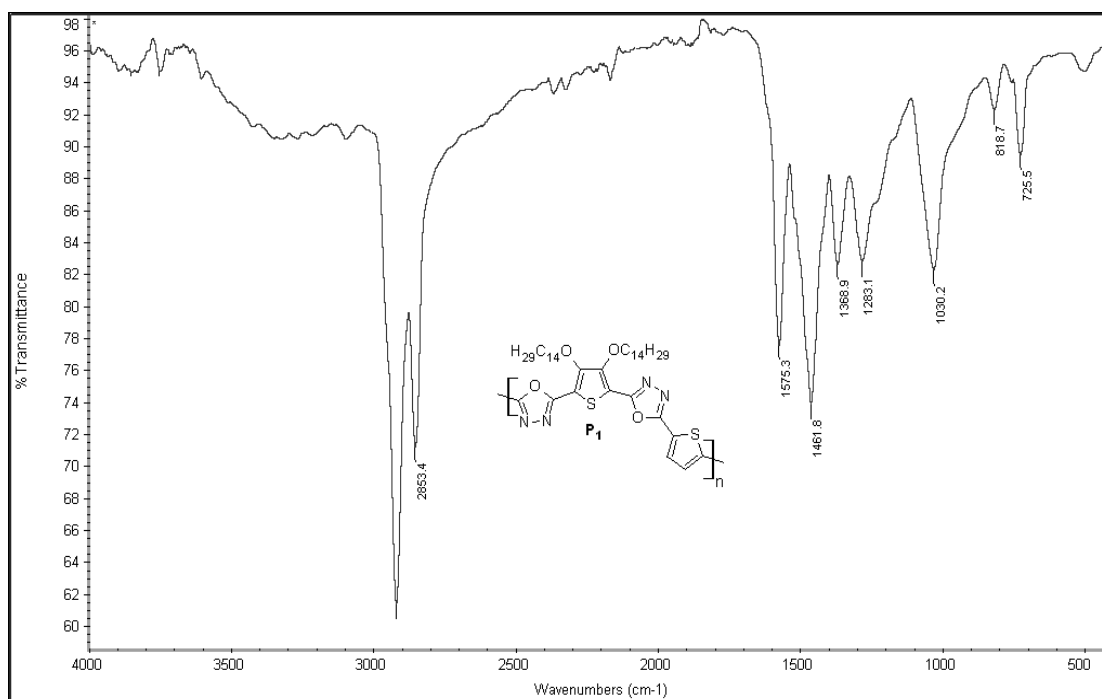


Figure 4.3: FTIR spectrum of polymer P1

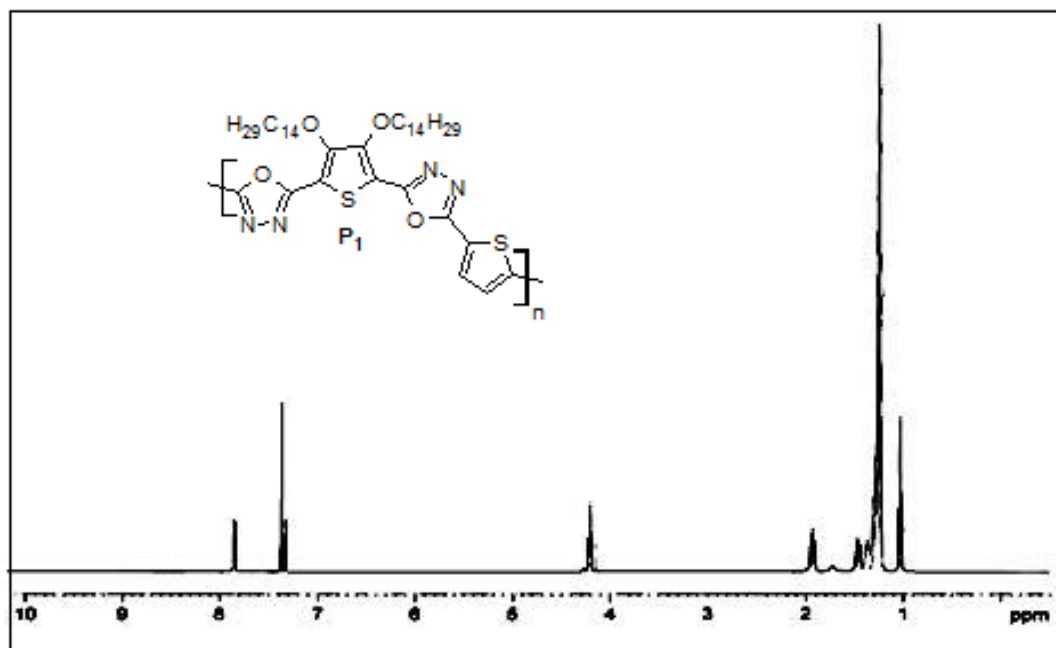


Figure 4.4: ^1H NMR spectrum of polymer **P1**

4.3.3. Results and discussion

The structures of polymers **P1-P5** and their corresponding polyhydrazides (**PH1-PH5**) were established by their FTIR and ^1H NMR spectral data. The polyhydrazide **PH1** showed strong absorption bands at 3283 and 1650 cm^{-1} in its FTIR spectrum (**Figure 4.1**) indicating the presence of amide functionality. The presence of two major peaks in the range of δ 11 ppm in its ^1H NMR spectrum (**Figure 4.2**) also confirms the presence of amide ($>\text{CO-NH-}$). Further, disappearance of peak at 3283 cm^{-1} in the FTIR spectrum (**Figure 4.3**) of polymer **P1** confirms the cyclization. Also, in its ^1H NMR spectrum, (**Figure 4.4**) the absence of peak at δ 11 ppm indicates the formation of poly(oxadiazole). Similarly, remaining polymers in the series displayed characteristic peaks in their FTIR and ^1H NMR spectra.

The newly synthesized polymers (**P1-P5**) are soluble in polar organic solvents such as chloroform, chlorobenzene, dichloromethane, tetrahydrofuran and dimethylsulfoxide. The study of thermogravimetric analysis (TGA) revealed that these polymers are quite stable up to $260\text{ }^\circ\text{C}$. The onset degradation temperatures of these polymers were found to be 300 , 304 , 285 , 321 and $310\text{ }^\circ\text{C}$ for **P1**, **P2**, **P3**, **P4** and **P5**, respectively. The gradual weight loss around $300\text{ }^\circ\text{C}$ may be attributed to the

degradation of the attached alkoxy chains on the 3rd and 4th positions of thiophene ring. Similar behavior was observed for substituted polythiophenes in earlier reports also. The weight loss that took place in the temperature range of 300-900 °C corresponds to the degradation of polymer backbone leaving behind a residue content of less than 25%. Further, there may be occurrence of cross-linking in polymer across longer side chain or degradation of bulky side chains (Hu and Xu, 2000, Swager et al. 1995, Marcos et al. 2011) at high temperatures, as seen in their TGA traces. The thermograms of polymers **P1-P5** are given in the **Figure 4.5**. Their weight average molecular masses (\overline{M}_w) were found to be in the range of 8300-16000 Da with polydispersity range 1.5-2.2.

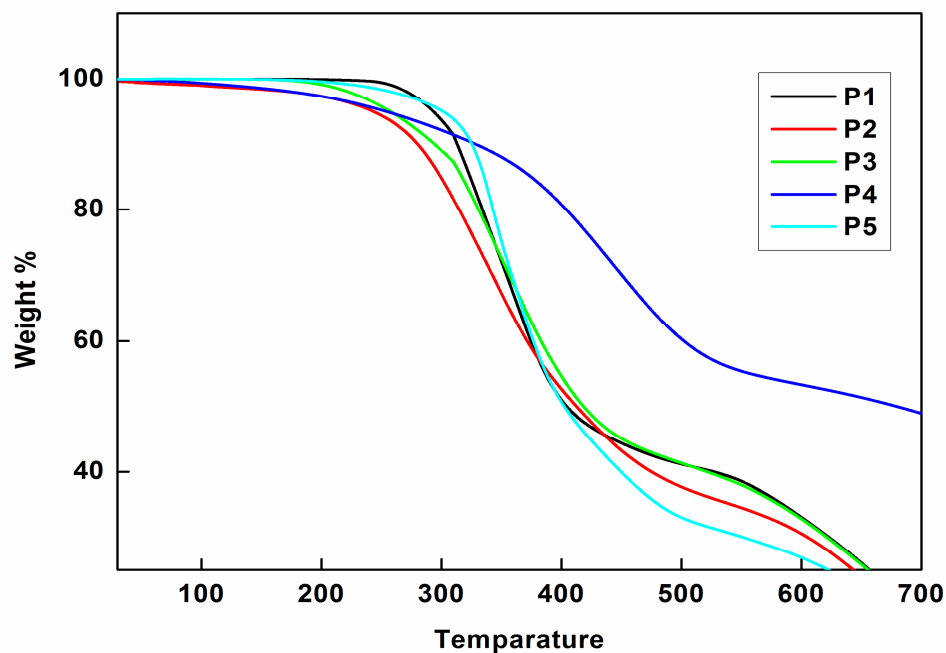
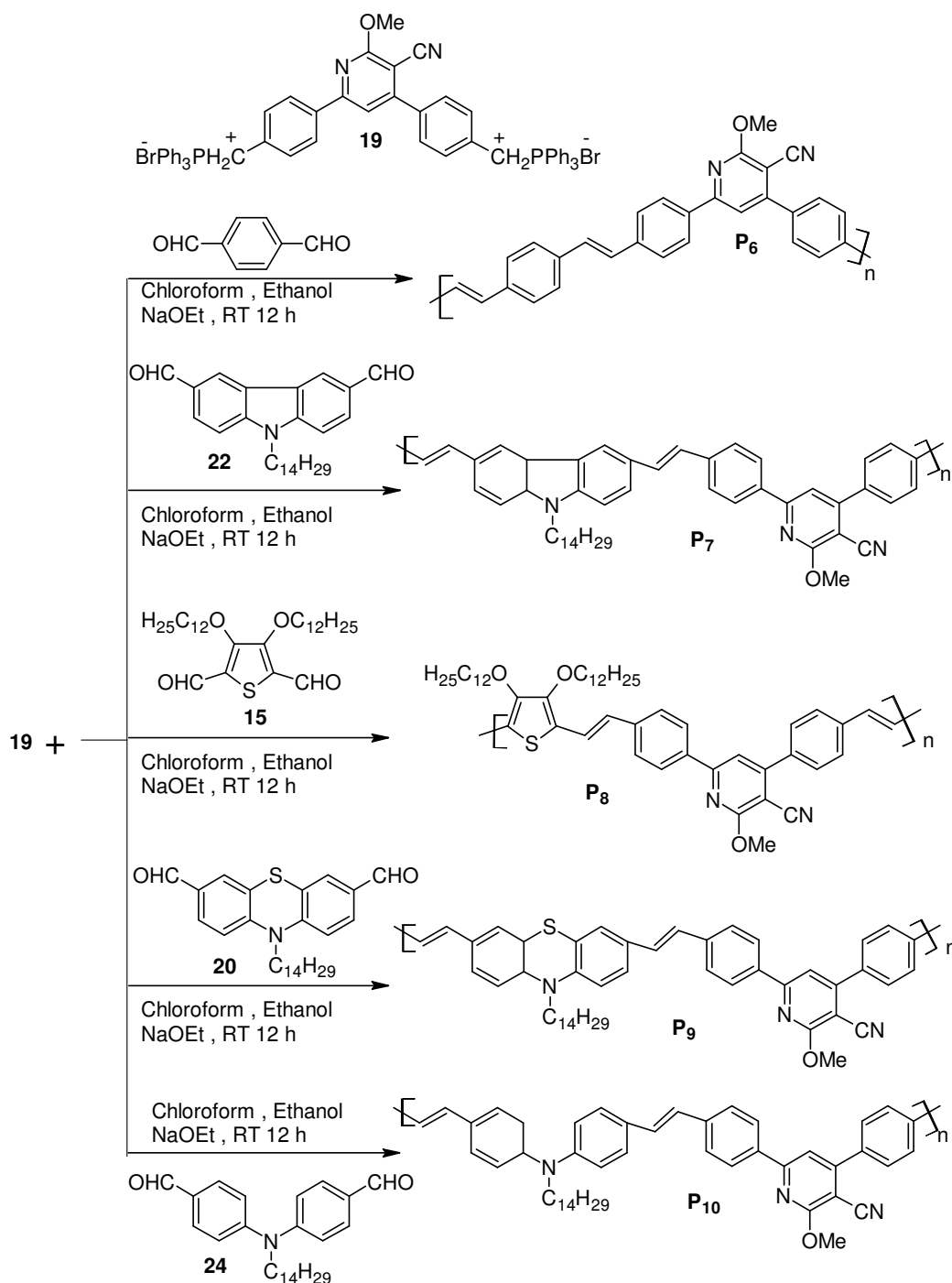


Figure 4.5: Thermogravimetric traces of polymers **P1-P5**

4.4. SYNTHESIS OF CYANOPYRIDINE BASED POLYMERS (SERIES 2, P6-P10)

As described in **Schemes 4.3**, the second series of cyanopyridine based D-A type conjugated polymers (**P6-P10**) carrying powerful electron donating phenyl, carbazole, 3,4-dialkoxythiophene phenothiazine and diphenylamine units were synthesized. The detailed procedures followed for their synthesis along with characterization data are given in the following section.



Scheme 4.3: Synthetic schemes for polymers **P6-P10**

4.4.1. Chemistry

New polymers **P6-P10** were synthesized from cyanopyridine Wittig salt monomer **19** by condensing it with terphthalaldehyde, carbazoledicarboxaldehyde, 3,4-didodecyloxythiophenedicarboxaldehyde, phenothiazine dicarboxaldehyde and diphenylamine dicarboxaldehyde, respectively through Wittig condensation method.

The reaction was carried out in alcoholic media using strong sodium ethoxide. Here chloroform-ethanol system was used as solvent because it facilitates homogenization of the reaction mixture leading to easy polymerization. Also, salt generated, i.e. triphenylphosphineoxide readily dissolves in chloroform causing effective polymer chain growth without any hindrance.

4.4.2. Synthesis and characterization

Experimental protocol for the synthesis of **P6-P10** and their spectral, thermal and molecular weight measurement data are given in the following paragraphs.

General procedure for synthesis of polymers P6-P10

A mixture of Wittig salt **19** (0.5 g, 0.5 mmol) and terphthalaldehyde (0.067 g, 0.5 mmol) was dissolved in a combination of 5 mL of chloroform and 15 mL of ethanol. Sodium ethoxide (0.020 g, 1 mmol in 10 mL of ethanol) was added to the reaction mass at room temperature under nitrogen atmosphere. Then, reaction mixture turned into yellow color. It was stirred for 12 h at room temperature. After completion of the reaction, solvent was removed under reduced pressure. The crude product **P6** was poured into excess of methanol and stirred for about 30 min. The precipitated polymer was filtered and then washed thoroughly with acetone, re-dissolved in chloroform and poured into excess of methanol to remove impurities like oligomers. The resulting precipitate was filtered off and dried at 40 °C under vacuum for 24 h to give fluorescent deep greenish yellow colored powder. On the similar lines, remaining polymers were prepared. The characterization data of **P6-P10** are given below.

P6: Yield 61 %. FTIR (cm⁻¹): 2220, 1573, 1540, 1445, 1356, 1009, 832. ¹H NMR, (400 MHz, CDCl₃), δ (ppm): 7.90-7.18 (m, 13H, Ar-H), 6.78-6.74 (m, 2H, -CH=CH-), 4.21 (s, 3H, -O-CH₃). Element. Anal. Calcd. (%) for C₂₉H₂₀N₂O: C, 84.44; H, 4.89; N, 6.79. Found: C, 84.34; H, 4.82; N, 6.62. Weight average molecular weight (\overline{M}_w): 12900 with poly dispersity 2.01.

P7: Yield 70 %. FTIR (cm⁻¹): 2919, 2853, 2215, 1576, 1540, 1478, 1448, 1353, 1135, 1010, 807. ¹H NMR, (400 MHz, CDCl₃), δ (ppm): 8.32-6.91(m, 15H, Ar-H), 6.65-6.00 (m, 2H, -CH=CH-), 4.28-4.15 (m, 5H, -O-CH₃ and -NCH₂-), 2.41-1.25

(m, 24H, aliphatic), 0.85 (t, 3H, -CH₃). Element. Anal. Calcd. (%) for C₄₉H₅₃N₃O: C, 84.08; H, 7.63; N, 6.00. Found: C, 83.59; H, 7.65; N, 5.84. Weight average molecular weight (\overline{M}_w): 6400 with poly dispersity 1.56.

P8: Yield 55 %. FTIR (cm⁻¹): 2918, 2849, 2218, 1579, 1539, 1452, 1359, 1260, 1014, 850, 811. ¹H NMR, (400 MHz, CDCl₃), δ (ppm): 8.13-6.56 (m, 9H, Ar-H), 6.8-6.68 (m, 2H, -CH=CH-), 4.68-4.32 (m, 7H, -O-CH₃ and -OCH₂-), 1.78-1.26 (m, 48H, aliphatic), 0.85 (t, 6H, -CH₃). Element. Anal. Calcd. (%) for C₅₁H₆₆N₂O₃S: C, 77.82; H, 8.45; N, 3.56; S, 4.07. Found: C, 77.72; H, 8.35; N, 3.45; S, 4.01. Weight average molecular weight (\overline{M}_w): 9500 with poly dispersity 1.98.

P9: Yield 68 %. FTIR (cm⁻¹): 2917, 2848, 2217, 1574, 1540, 1506, 1462, 1403, 1355, 1244, 1010, 812. ¹H NMR, (400 MHz, CDCl₃), δ (ppm): 8.08-6.70 (m, 15H, Ar-H), 6.55-6.53 (m, 2H, -CH=CH-), 4.25-4.10 (m, 5H, -O-CH₃ and -NCH₂-), 2.44-1.24 (m, 24H, aliphatic), 0.875 (t, 3H, -CH₃). Element. Anal. Calcd. (%) for C₄₉H₅₁N₃OS: C, 80.62; H, 7.04; N, 5.76; S, 4.39. Found: C, 80.42; H, 7.59; N, 5.55; S, 4.18. Weight average molecular weight (\overline{M}_w): with poly dispersity 2.03.

P10: Yield 81 %. FTIR (cm⁻¹): 2919, 2849, 2217, 1579, 1503, 1356, 1237, 1009, 818. ¹H NMR, (400 MHz, CDCl₃), δ (ppm): 8.2-7.0 (m, 16H, Ar-H), 7.0-6.8 (m, 2H, -CH=CH-), 4.20 (m, 4H, -O-CH₃), 3.72-3.69 (m, 2H, -NCH₂-), 2.2-1.1 (m, 24H, aliphatic), 0.87 (t, 3H, -CH₃). Element. Anal. Calcd. (%) for C₄₉H₅₅N₃O: C, 83.84; H, 7.90; N, 5.99. Found: C, 83.74; H, 7.81; N, 5.81. Weight average molecular weight (\overline{M}_w): 8400 with poly dispersity 1.90.

4.4.3. Results and discussion

The structures of polymers **P6-P10** were established by FTIR and ¹H NMR spectroscopic techniques. The polymer **P8** showed a peak at 2218 cm⁻¹, in its FTIR spectrum which confirms the presence of cyano group in the polymer backbone. Also, its ¹H NMR showed a peak at δ 4.2 ppm confirming the presence of methoxy group of **P8**. In addition, the -NCH₂ protons of polymer **P10** resonated at δ 3.7 ppm in its ¹H NMR confirming the presence of diphenylamine unit along the polymer backbone. Similarly, remaining polymers showed characteristic FTIR and ¹H NMR spectral data

confirming their structures. **Figures 4.6** and **4.8** depict FTIR spectra of polymers **P8** and **P10** respectively, while **Figures 4.7** and **4.9** show ^1H NMR spectra of polymers **P8** and **P10**, respectively.

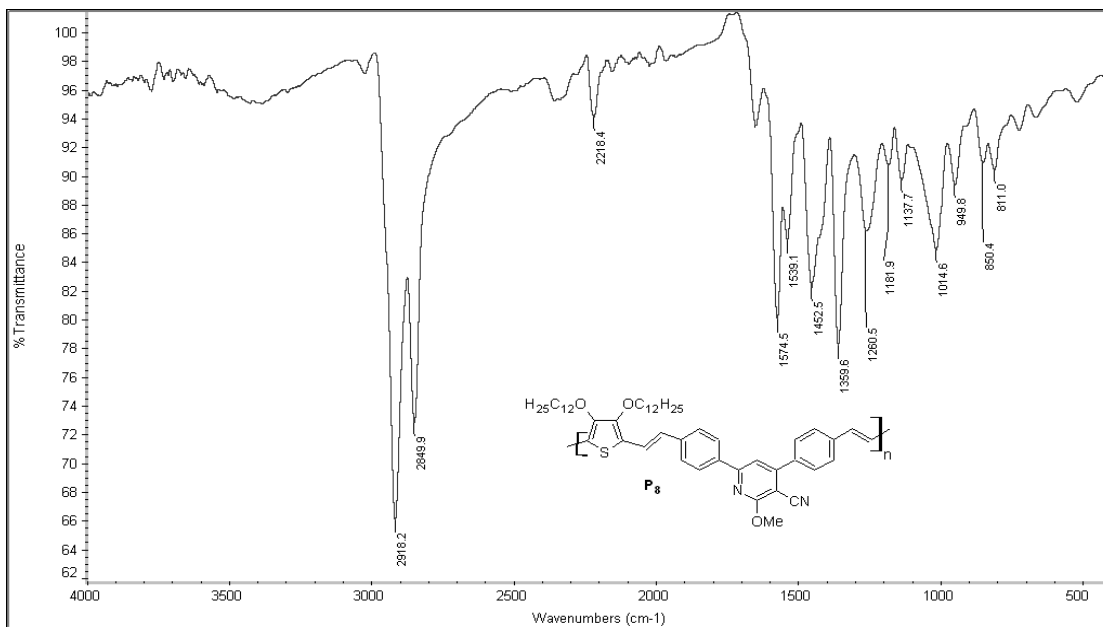


Figure 4.6: FTIR spectrum of polymer **P8**

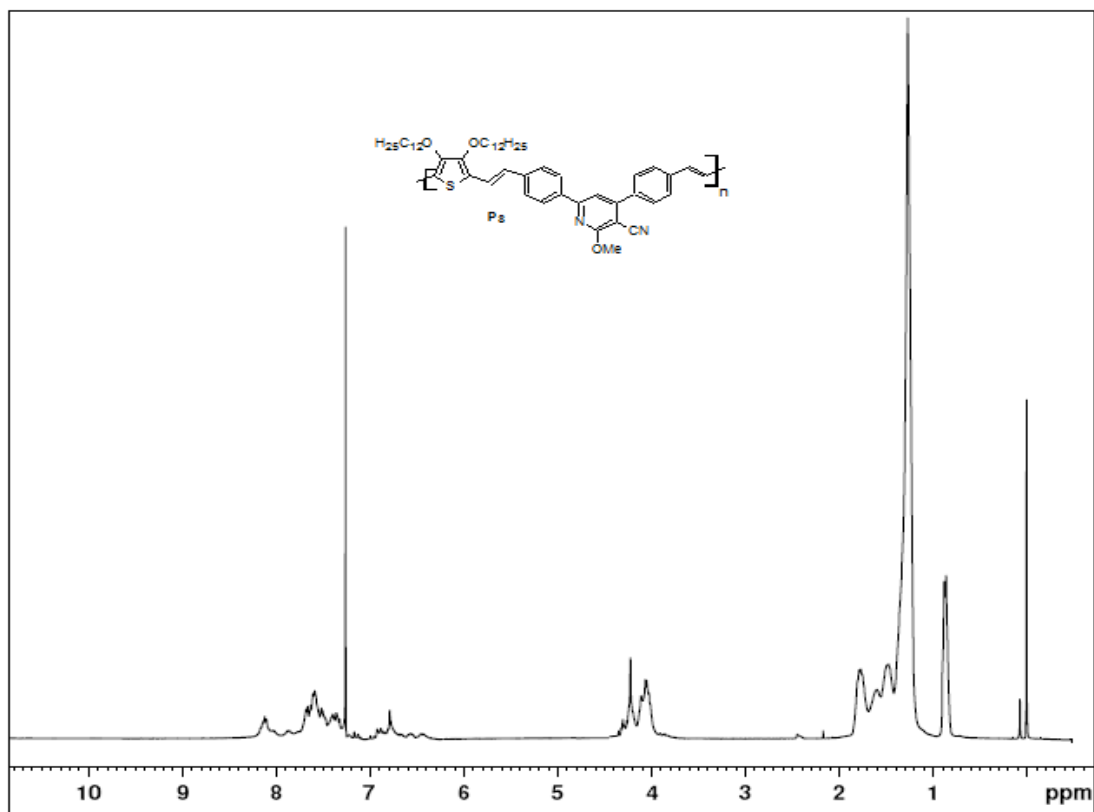


Figure 4.7: ^1H NMR spectrum of polymer **P8**

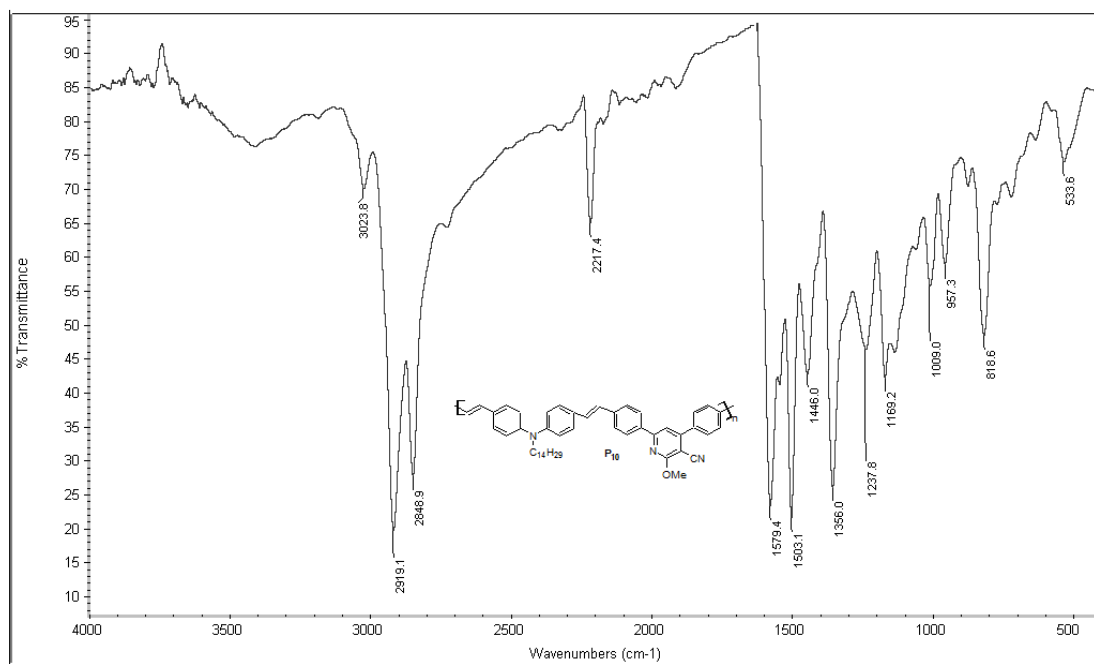


Figure 4.8: FTIR spectrum of polymer P10

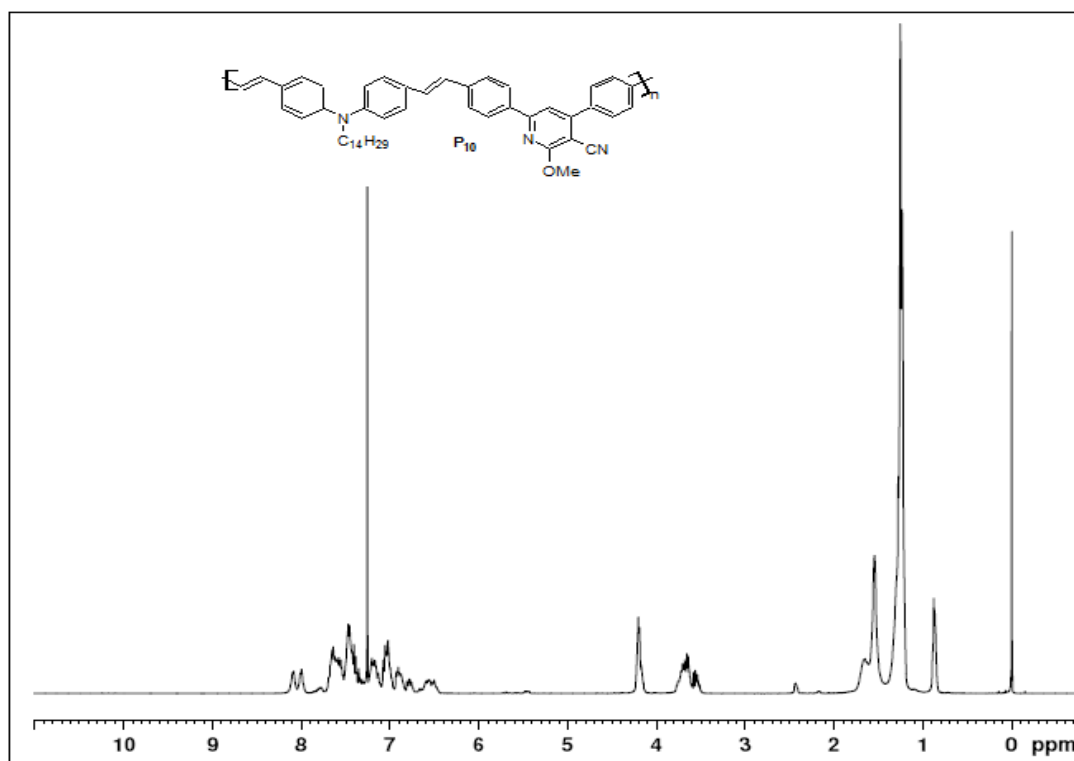


Figure 4.9: ¹H NMR spectrum of polymer P10

The synthesized polymers **P6-P10** are soluble in common organic solvents such as chloroform, dichloromethane, and dimethylsulfoxide. Thermogravimetric analysis (TGA) revealed that they are thermally stable up to 300 °C. The onset degradation temperatures of the polymers were found to be 340, 320, 325, 320 and 330 °C for polymers **P6**, **P7**, **P8**, **P9** and **P10**, respectively. The observed weight loss beyond 300 °C may be attributed to the degradation of the attached bulky alkoxy side chains. Similar behavior was observed in many of the alkoxy side chain containing polymers reported in the literature (Hu and Xu, 2000, Swager et al. 1995, Marcos et al. 2011). Among these polymers, **P6** showed the highest onset decomposition temperature. This is because of the fact that its strand does not contain any alkyl/alkoxy side chain. The observed weight average molecular weights (\overline{M}_w) of these polymers **P6-P10** are in the range of 6000-19000 da with poly dispersity range 1.5-2. Thermogravimetric traces of polymers **P6-P10** are depicted in **Figure 4.10**.

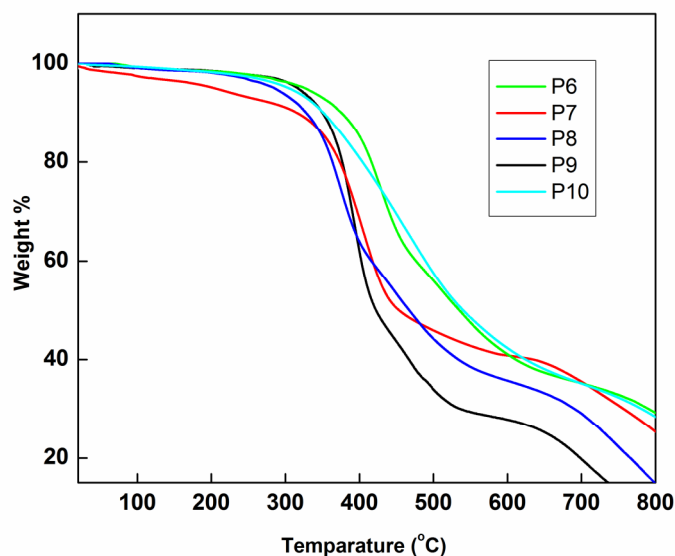
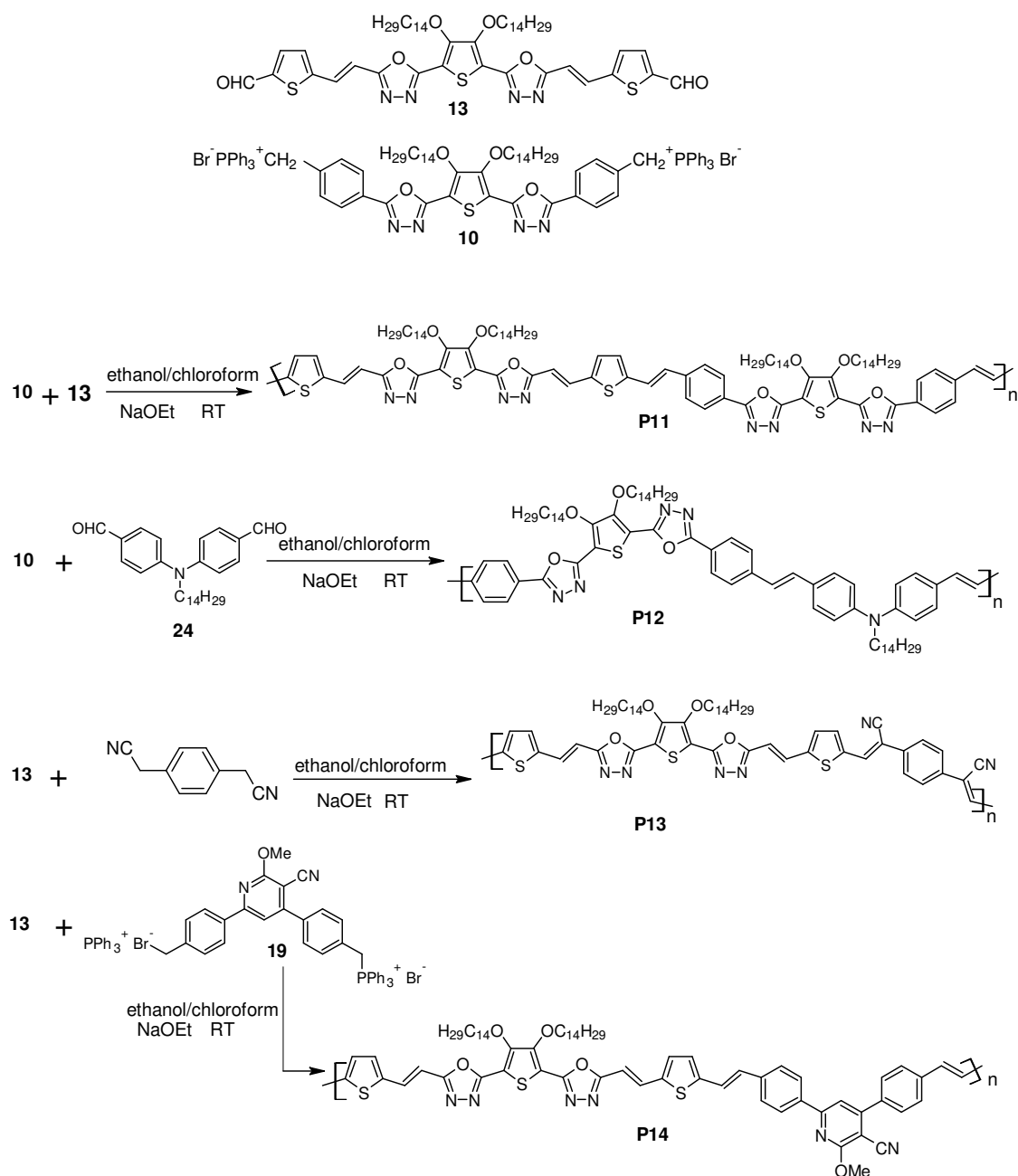


Figure 4.10: Thermogravimetric traces of polymers **P6-P10**

4.5. SYNTHESIS OF OXADIAZOLE BASED POLYMERS (SERIES 3, P11-P14)

The third series of polymers, viz. **P11-P14** comprised of electron donating 3,4-ditetrdecyloxythiophene and electron withdrawing 1,3,4 oxadiazole with extended conjugated spacers were synthesized from their monomers as explained in **Scheme 4.4**. Their synthetic methods and their analysis data are given in the following part.

Scheme 4.4: Synthesis of polymers **P11-P14**

4.5.1. Chemistry

New polymer **P11** was obtained by reacting Wittig salt monomer **10** with extended conjugated dialdehyde monomer **13** through Wittig condensation method under basic condition. Similarly Wittig salt monomer **10** when treated with diphenylamine dialdehyde monomer **24** yielded polymer **P12**. On the similar lines, polymer **P14** was synthesized by condensing dialdehyde monomer **13** with

cyanopyridine Wittig salt **19**, in good yield. Further, the dialdehyde monomer **13** when condensed with phenyl diacetonitrile under basic medium underwent Knoevenagel reaction to yield polymer **P13**.

4.5.2. Synthesis and characterization

Detailed experimental protocols and characterization data of polymers **P11-P14** are presented below.

General procedure for the synthesis of polymers P11-P14

Wittig salt monomer **10** (0.5 mmol) and dithiophene-2-carbaldehyde **13** (0.5 mmol) were dissolved in a mixture of 5 mL of chloroform and 15 mL of ethanol. Sodium ethoxide (0.030 g, 1 mmol in 10 mL of ethanol) was added to the reaction mass at room temperature under nitrogen atmosphere. The resulting yellow colored solution was stirred for 12 h at room temperature. After the completion of reaction, solvent was removed under reduced pressure. The crude product **P11** was poured into excess of methanol and stirred for about 30 min. The obtained polymer was filtered, washed thoroughly with acetone, re-dissolved in chloroform and poured into excess of methanol to remove impurities like oligomers. The resulting precipitate was filtered off and dried at 40 °C under vacuum for 24 h to give fluorescent deep yellowish orange colored powder. On the similar lines, polymers **P12-P14** were prepared. The characterization data of **P11-P14** are as follows.

P11: Yield 55 %. FTIR (cm⁻¹): 2918, 2850, 1585, 1457, 1055, 949, 723. ¹H NMR (400 MHz, CDCl₃) δ (ppm): 8.1 (d, 2H, Ar-H, J=8 Hz), 8.0 (d 2H, Ar-H, J=8 Hz), 6.9-7.6 (m, 6H, aromatic and vinylic), 4.35 (m, 4H, -OCH₂-), 2.0-1.31 (m, 48H, -(CH₂)₁₂-), 0.92 (t, 12H, -CH₃, J = 6.8 Hz). Element. Anal. Calcd. (%) for C₁₀₀H₁₃₆N₈O₈S₄: C, 70.38; H, 8.03; N, 6.57; S, 7.52. Found: C, 70.18; H, 7.89; N, 6.28; S, 7.41. Weight-average molecular weight (\overline{M}_w): 8250 poly dispersity 2.5.

P12: Yield 75 %. FTIR (cm⁻¹): 2919, 2850, 1585, 1499, 1366, 1175, 827, 726. ¹H NMR, (400 MHz, CDCl₃), δ (ppm): 8.1-7.1 (m, 12H, Ar-H), 7.1-6.9 (m, 2H, -CH=CH-), 4.31 (m, 4H, -O-CH₂-), 3.73-3.71 (m, 2H, -NCH₂-), 2.2-1.1 (m, 72H, aliphatic), 0.87 (t, 9H, -CH₂CH₃). Element. Anal. Calcd. (%) for C₇₈H₁₀₇N₅O₄S: C,

77.37; H, 8.91; N, 5.78; S, 2.65. Found: C, 77.17; H, 8.78; N, 5.62; S, 2.49. Weight-average molecular weight (\overline{M}_w): 12,900 with polydispersity of 1.8.

P13: Yield 45 %. FTIR (cm^{-1}): 2919, 2850, 2220 (CN), 1625, 1582, 1455, 1364, 1073, 947. ^1H NMR, (400 MHz, CDCl_3), δ (ppm): 7.75-7.26 (m, 14 H, Ar-H, vinylic), 4.42-4.25(m, 4H), 1.85-1.23 (m, $-\text{CH}_2-$), 0.86 (s, $-\text{CH}_2-\text{CH}_3$). Element. Anal. Calcd. (%) for $\text{C}_{60}\text{H}_{72}\text{N}_6\text{O}_4\text{S}_3$: C, 69.46; H, 7.00; N, 8.10; S, 9.27. Found: C, 69.26; H, 7.10; N, 7.98; S, 9.04. Weight average molecular weight (\overline{M}_w):27800 with poly dispersity 4.

P14: Yield 68 %. FTIR (cm^{-1}): 2919, 2849, 2218 ($-\text{CN}$), 1576, 1449, 1358, 1257, 1013, 947, 806. ^1H NMR, (400 MHz, CDCl_3), δ (ppm): 8.21-6.73 (m, 19 H, Ar-H, vinylic), 4.30-4.21(m, 7H), 2.17-1.24 (m, $-\text{CH}_2-$), 0.86 (s, $-\text{CH}_2-\text{CH}_3$). Element. Anal. Calcd. (%) for $\text{C}_{71}\text{H}_{82}\text{N}_6\text{O}_5\text{S}_3$: C, 71.32; H, 6.91; N, 7.03; S, 8.05. Found: C, 71.19; H, 6.82; N, 6.89; S, 7.88. Weight average molecular weight (\overline{M}_w) is 18200 with poly dispersity. 2.5. FTIR and ^1H NMR of polymers **P12** (Figure 4.11 and Figure 4.12) and **P14** (Figure 4.13 and Figure 4.14) are represented below.

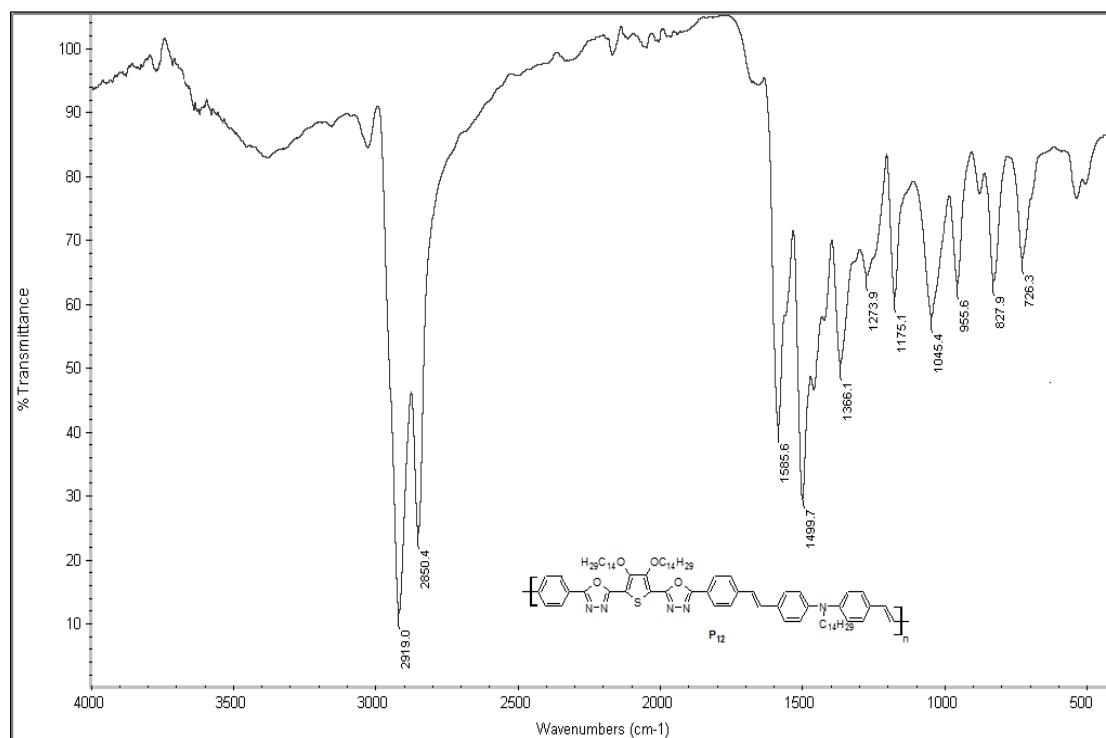


Figure 4.11: FTIR spectrum of polymer **P12**

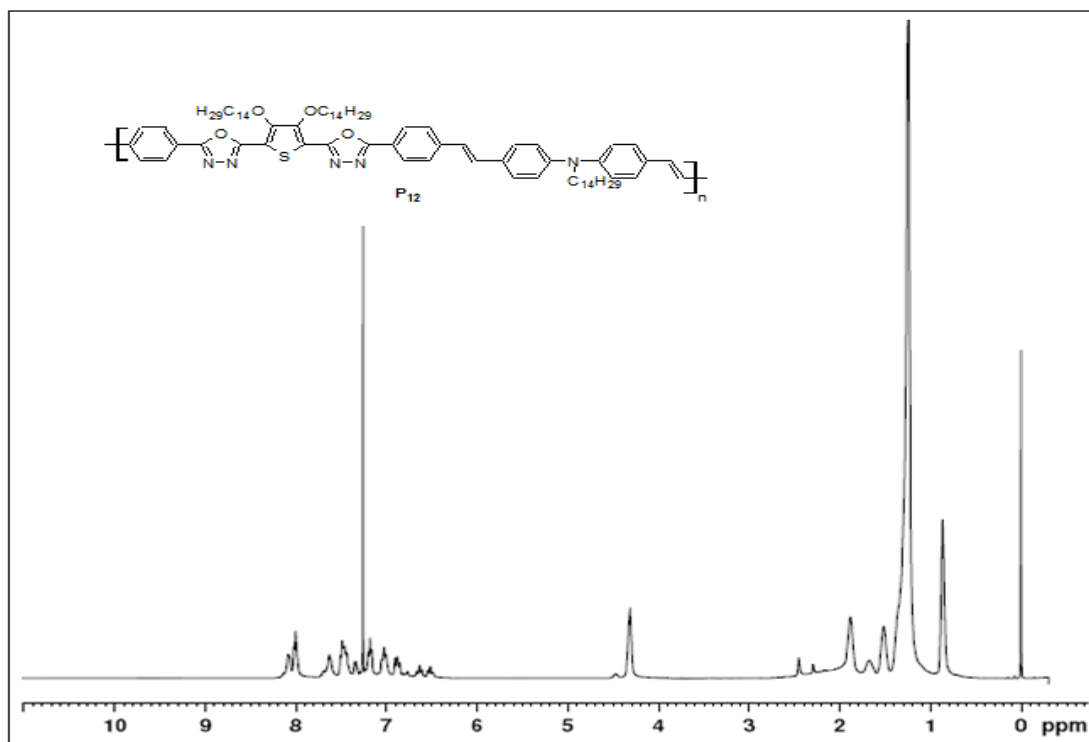
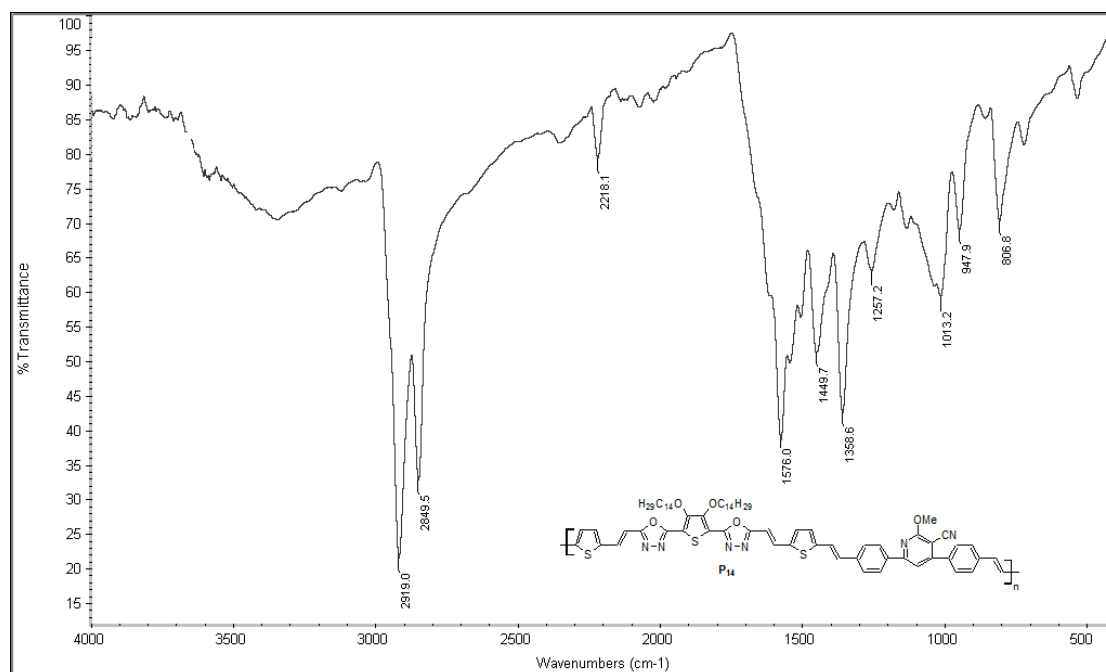
Figure 4.12: ^1H NMR spectrum of polymer P12

Figure 4.13: FTIR spectrum of polymer P14

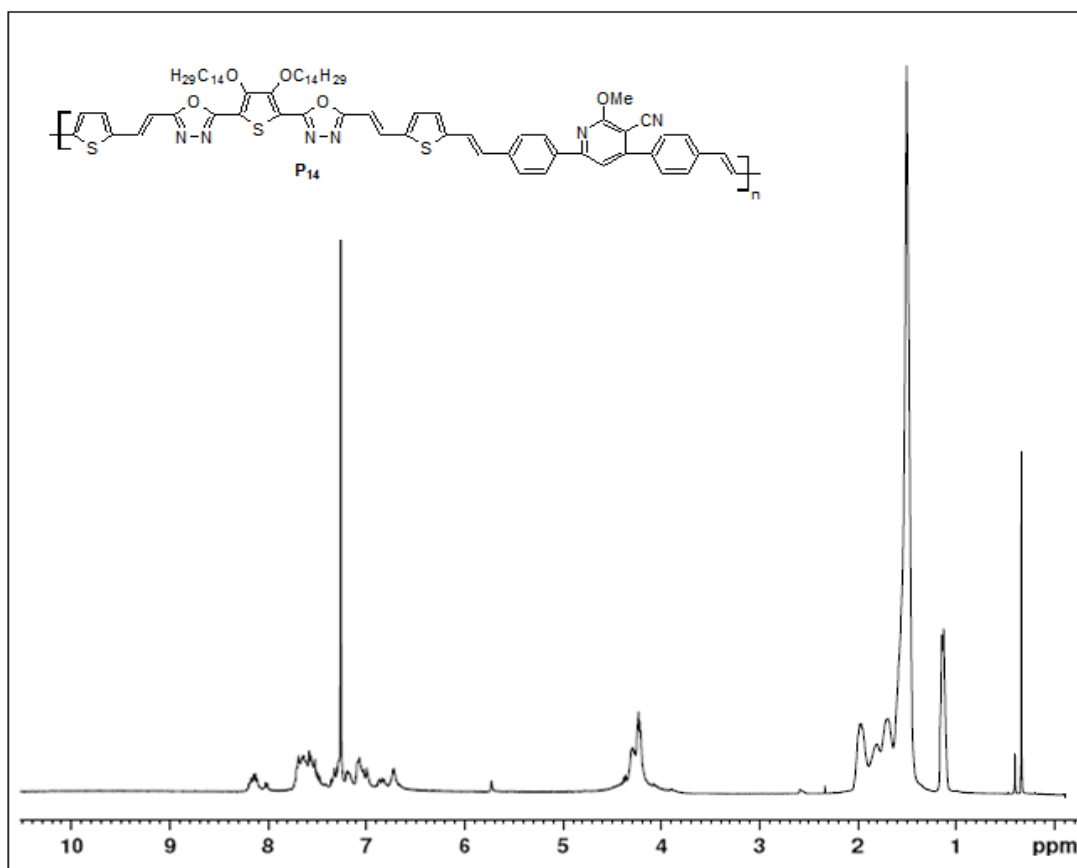


Figure 4.14: ¹H NMR spectrum of polymer **P14**

4.5.3. Results and discussion

From the results of TGA traces (**Figure 4.15**) it can be concluded that the polymers exhibit a high thermal stability up to 300 °C and their weight loss below 300 °C is negligible. Polymers of this series showed similar trend in their thermograms because of the presence of similar backbone with bulky alkoxy side chains. The weight loss beyond 300 °C may be due to the degradation of the polymer backbone. Further, all the polymers are soluble in common organic solvents such as chloroform, chlorobenzene, dichloromethane, tetrahydrofuran and dimethylsulfoxide. They possess good film-forming ability and hence good processability. The molecular weights of these polymers were found to be in the range of 8200-18500 Da with the poly-dispersity range of 1.8-4. Their thermogravimetric traces are depicted in **Figure 4.15**.

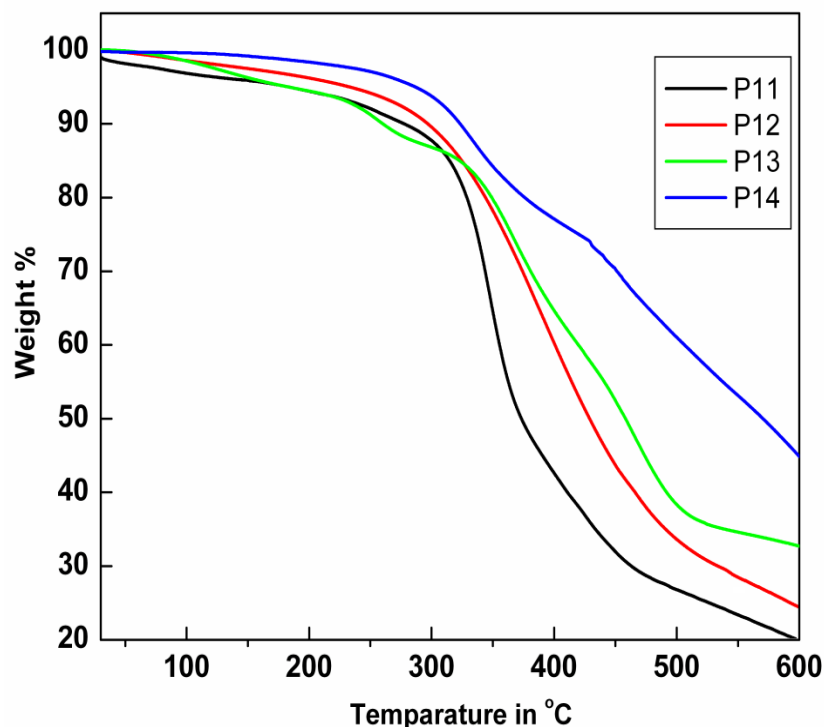


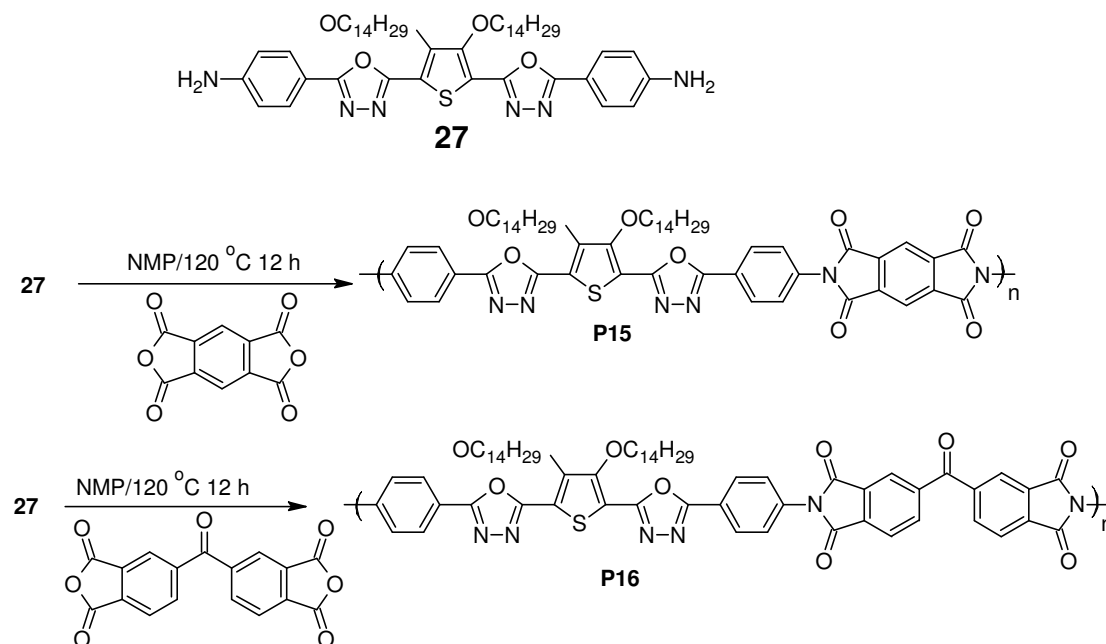
Figure 4.15: Thermogravimetric traces of polymers P11-P14

4.6. SYNTHESIS OF CYCLIC IMIDE POLYMERS (SERIES 4, P15 AND P16)

The fourth series of polymers, viz. **P15-P16** carrying electron donating 3,4-ditetrdecyloxythiophene and electron withdrawing 1,3,4-oxadiazole rings with thermally stable cyclic imide functionality in the backbone were synthesized from their monomers as explained in **Scheme 4.5**. Their experimental procedures and their analytical data are given in the following section.

4.6.1. Chemistry

As outlined in **Scheme 4.5**, polymers **P15** and **P16** were synthesized by condensing conjugated diamine monomer **27** with cyclic dianhydrides. Here the polymerization was carried out using two-step reaction involving amidation followed by oxidative cycloaddition. Since cyclic anhydrides are rigid in their structure, they undergo polymerization reaction slowly. Therefore, the reaction was carried out at high temperature, i.e. 120 °C in an inert solvent.

Scheme 4.5: Synthesis of polymers **P15** and **P16**

4.6.2. Synthesis and characterization

Synthetic procedures for two new poly(imide)s **P15** and **P16** have been described as follows.

General procedure for the synthesis of polymers P15-P16

A stoichiometric amount of diamine monomer **27** (0.5 g, 0.60 mmol) was added to a solution of pyromellitic anhydride (0.13 g, 0.60 mmol) in NMP solution at 0 °C under inert atmosphere. After the addition, the reaction mass was slowly stirred at room temperature for about 2 h. Then the reaction was maintained at 120 °C with constant stirring for about 12 h. After completion of polymerization, the crude polymer was cooled to room temperature and poured into cold water and stirred for 30 min, the resulting solid was filtered and dried. The crude polymer was washed with acetone and further it was purified by re-precipitation method using chloroform-methanol system to get target polymer **P15**. On the similar lines, polymer **P16** was prepared and purified. Their experimental data are as follows:

P15: Yield 54 %. FTIR (cm⁻¹): 2916, 2851, 1675, 1461, 1372, 1288, 1049. ¹H NMR (400 MHz, CDCl₃) δ (ppm): 8.55-7.91(m, Aromatic), 6.81-6.75 (m, aromatic), 4.37-4.27 (t, 4H, -OCH₂-, J= 8 Hz), 2.1-1.24 (m, 48H, -CH₂-), 0.86 (t, 6H, -CH₂CH₃, J= 8 Hz). Elemental analysis calcd. (%) for C₅₈H₆₈N₆O₈S: C, 69.02; H, 6.79; N, 8.33;

S, 3.18. Found: C, 68.79; H, 6.71; N, 8.23; S, 3.06. Weight average molecular weight (\bar{M}_w) is 16500 with polydispersity (PD) of 2.5.

P16: Yield 66 %. FTIR (cm^{-1}): 2920, 2847, 1675, 1640, 1486, 1372, 1305. ^1H NMR (400 MHz, CDCl_3) δ (ppm): 8.52-7.90 (m, Aromatic), 6.82-6.74 (m, aromatic), 4.37-4.26 (t, 4H, $-\text{OCH}_2-$, $J = 8$ Hz), 11.89-1.24 (m, 48H, $-\text{CH}_2-$), 0.86 (t, 6H, $-\text{CH}_2\text{CH}_3$, $J = 8$ Hz). Element. Anal. Calcd. (%) for $\text{C}_{65}\text{H}_{72}\text{N}_6\text{O}_9\text{S}$: C, 70.12; H, 6.52; N, 7.55; S, 2.88. Found: C, 70.02; H, 6.32; N, 7.49; S, 2.71. Weight average molecular weight (\bar{M}_w) is 12500 with polydispersity (PD) of 2.1.

Representative FTIR and ^1H NMR spectra of polymer **P15** have been given in **Figures 4.16** and **4.17**, respectively.

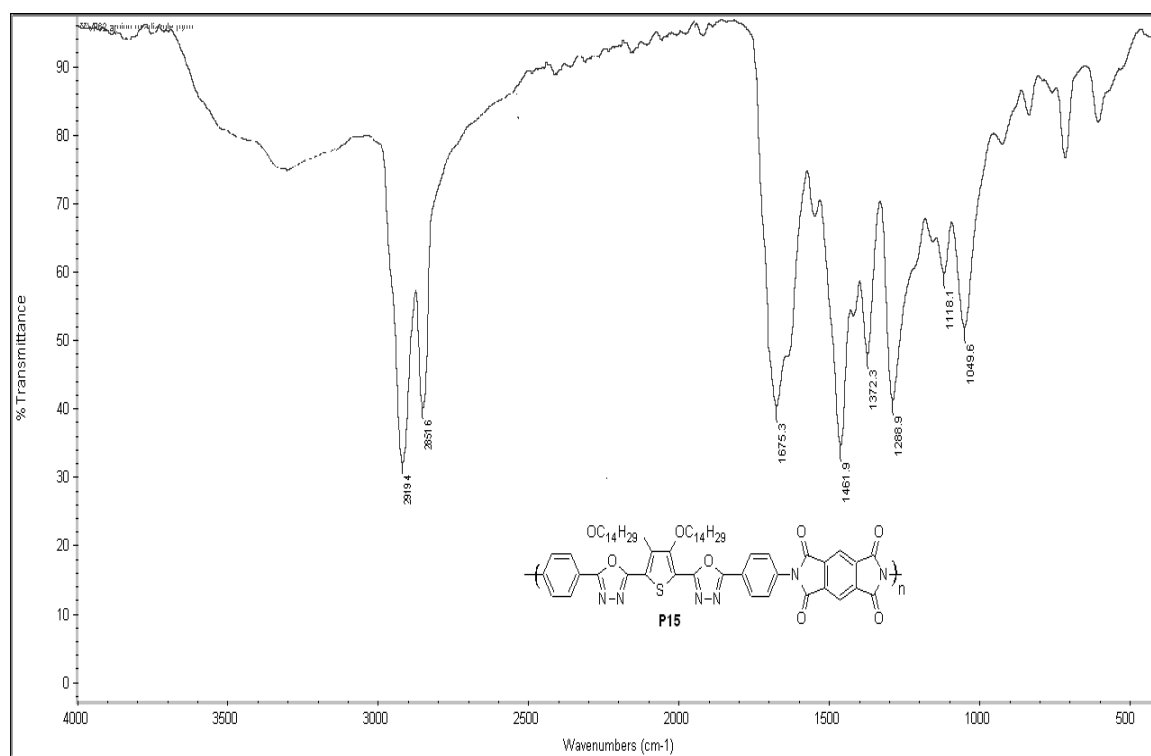


Figure 4.16: FTIR spectrum of polymer **P15**

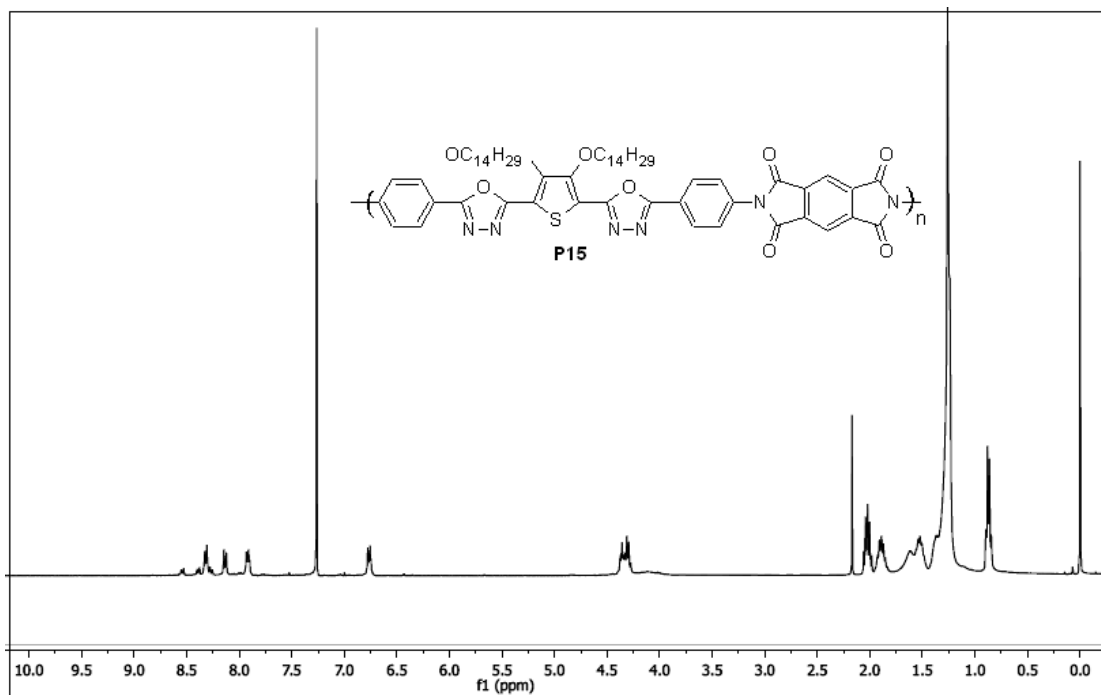


Figure 4.17: ¹H NMR spectrum of polymer P15

4.6.3. Results and discussion

Structures of polymers P15 and P16 were established using FTIR and ¹H NMR spectral data. In FTIR spectrum of polymer P15, (Figure 4.16) absorption band was observed at 1650 cm⁻¹ due to two cyclicamidic carbonyl groups. Further its ¹H NMR spectrum (Figure 4.17) showed no peaks due to primary amine confirming the formation of polymer. Similar observations were made in the spectrum of polymer P16 also.

The cyclic imide containing conjugated polymers showed good thermal stability up to 310 °C. The enhanced thermal stability is due to incorporation of imide units in the polymer backbone. The observed degradation after 310 °C is attributed to the decomposition of polymeric backbone. These results indicate that polymers can be used in the high temperature applications also. Weight average molecular weight (\overline{M}_w) polymer P15 and P16 were found to be 16500 and 18000 with poly dispersity of 2.5 and 1.6, respectively. Their thermogravimetric traces are depicted in Figure 4.18.

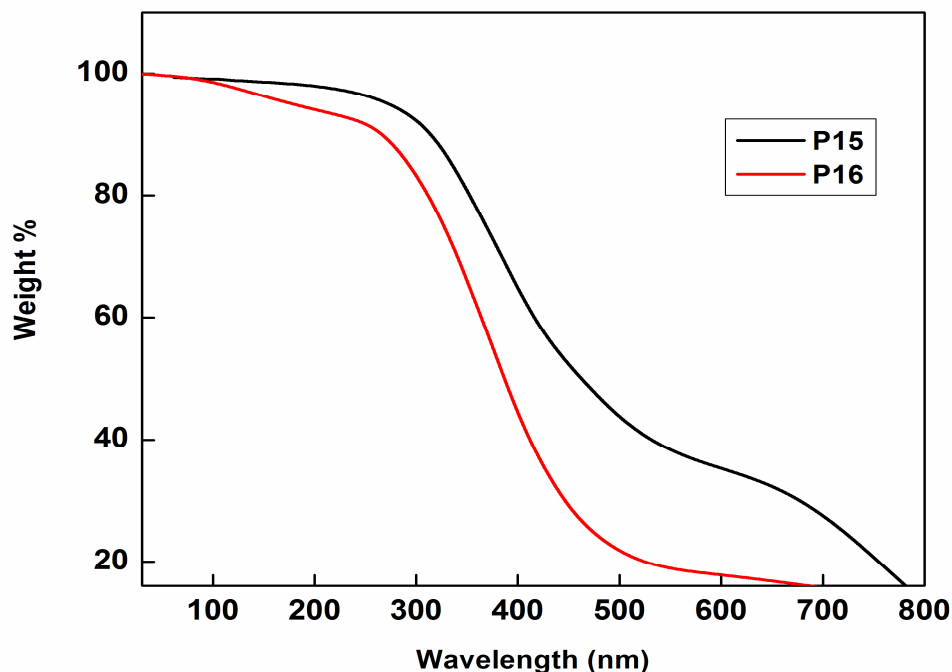


Figure 4.18: Thermogravimetric traces of polymers **P15** and **P16**

4.7. SYNTHESIS OF IMINE CONTAINING POLYMERS (SERIES 5, P17-P20)

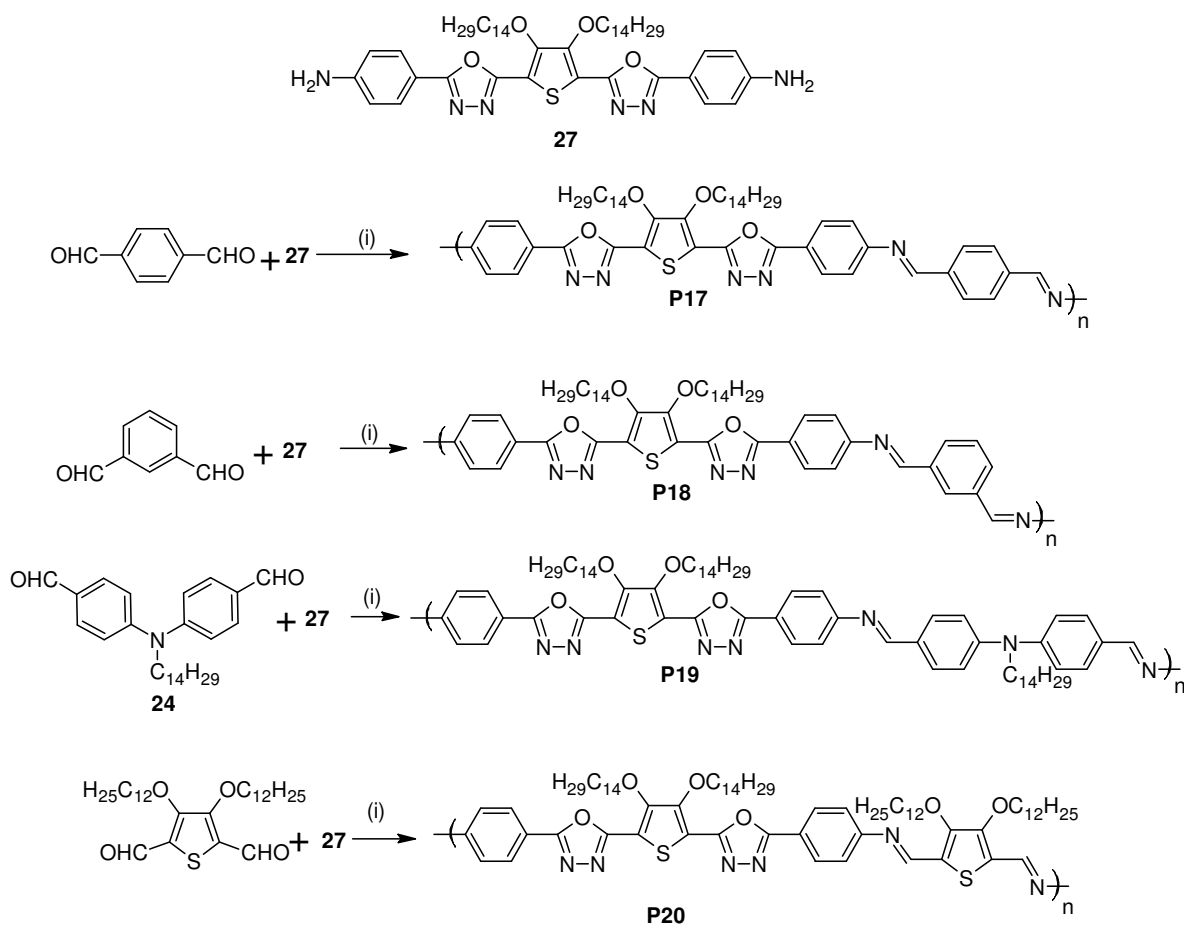
The final series of new conjugated polymers **P17-P20** carrying electron donating phthalyl, isophthalyl, diphenylamine and 3,4-dialkoxythiophene groups were synthesized as shown in **Scheme 4.6**. Their preparation methods and their analysis details are given in the following section.

4.7.1. Chemistry

New polymers **P17-P20** with imine ($-C=N-$) functionality in their main chain were obtained by condensing conjugated diamine monomer **27** with terphthalaldehyde, isophthalaldehyde, diphenylamine dialdehyde and 3,4-didodecyloxythiophene dialdehyde, respectively. Catalytic amount of acetic acid was used for the synthesis of imine based polymers.

4.7.2. Synthesis and characterization

Experimental methods used for the synthesis of polymers **P17-P20** with their characterization details are given below. Synthetic scheme for the preparation of polymers **P17-P20** is represented in **Scheme 6**.



where (i) Chloroform/ethanol, 3 drops of acetic acid reflux for 8 h

Scheme 6: Synthesis of polymers **P17-P20** where (i) Chloroform/ethanol, 3 drops of acetic acid reflux for 8 h

General procedure for the synthesis of polymers **P17-P20**

To a stirred solution of diamine monomer **27** (0.5 g, 0.60 mmol) in 2:1 chloroform-methanol, terephthalaldehyde (0.081 g, 0.60 mmol in chloroform) was added drop-wise with constant stirring under inert atmosphere. Catalytic amount (3 drops) of glacial acetic acid was added to the reaction mass under vigorous stirring. Then reaction mixture was refluxed for about 6 h. The reaction mass was quenched into cold water and stirring was continued for about 30 min at room temperature. The resulting solid was filtered, washed with acetone and purified by re-precipitation method using chloroform-methanol system. Similar procedures were followed for other polymers in this series and their characterization data are given below.

Characterization of **P17**: Yield 68 %. FTIR (cm^{-1}): 2918, 2649, 1593, 1484, 1365, 1169, 1042, 840. ^1H NMR (400 MHz, CDCl_3) δ (ppm): 8.59-8.04 (m, 8H, Ar-H), 6.79-6.76 (m, 4H, Ar-H), 4.30-4.15 (m, 4H, -O-CH₂-), 2.32-1.24 (m, 48, -CH₂-), 0.88 (t, 6H, -CH₂-CH₃, J= 8 Hz). Element. Anal. Calcd. (%) for C₅₆H₇₂N₆O₄S: C, 72.69; H, 7.84; N, 9.08; S, 3.47. Found: C, 72.49; H, 7.75; N, 8.88; S, 3.25. Weight average molecular weight (\overline{M}_w) is 14600 with polydispersity (PD) of 1.7.

Characterization of **P18**: Yield 60 %. FTIR (cm^{-1}): 2917, 2649, 1595, 1481, 1360, 1169, 1046, 849. ^1H NMR (400 MHz, CDCl_3) δ (ppm): 8.59-7.90 (m, 8H, Aromatic), 6.78-6.75 (m, 4H, Ar-H), 4.37-4.27 (m, 4H, -O-CH₂-), 2.39-1.24 (m, 48, -CH₂-), 0.88 (t, 6H, -CH₂-CH₃, J= 8 Hz). Element. Anal. Calcd. (%) for C₅₆H₇₂N₆O₄S: C, 72.69; H, 7.84; N, 9.08; S, 3.47. Found: C, 72.45; H, 7.69; N, 9.01; S, 3.26. Weight average molecular weight (\overline{M}_w) is 13400 with polydispersity (PD) of 1.8.

Characterization of **P19**: Yield 50 %. FTIR (cm^{-1}): 2918, 2649, 1577, 1495, 1450, 1349, 1173, 1038, 832, 726. ^1H NMR (400 MHz, CDCl_3) δ (ppm): 8.55-8.14 (m, 8H, Ar-H), 6.78-6.73 (m, 4H, Ar-H), 4.30-4.15 (m, 4H, -O-CH₂-), 3.8-3.6 (m, 2H, -N-CH₂-), 2.32-1.24 (m, 48, -CH₂-), 0.88 (t, 6H, -CH₂-CH₃, J= 8 Hz), Element. Anal. Calcd. (%) for C₇₆H₁₀₅N₇O₄S: C, 75.27; H, 8.73; N, 8.08; S, 2.64. Found; C, 75.05; H, 8.63; N, 7.91; S, 2.44. Weight average molecular weight (\overline{M}_w) is 15500 with polydispersity (PD) of 1.48.

Characterization of **P20**: Yield 55 %. FTIR (cm^{-1}): 2918, 2851, 1571, 1472, 1270, 1042, 831, 720. ^1H NMR (400 MHz, CDCl_3) δ (ppm): 8.69-7.9 (m, 5H, Aromatic), 6.8-6.75 (m, 4H, aromatic), 4.36-4.20 (m, 8H, -O-CH₂-), 1.93-1.20 (m, 88H, -CH₂-), 0.88 (t, 6H, -CH₂-CH₃, J= 8 Hz). Element. Anal. Calcd. (%) for C₇₈H₁₁₈N₆O₆S₂: C, 72.07; H, 9.15; N, 6.46; S, 4.93. Found: C, 71.87; H, 9.02; N, 6.29; S, 4.69. Weight average molecular weight (\overline{M}_w) is 27000 with polydispersity (PD) of 3.9.

FTIR and ^1H NMR spectra of polymer **P20** are represented in **Figures 4.19** and **4.20**.

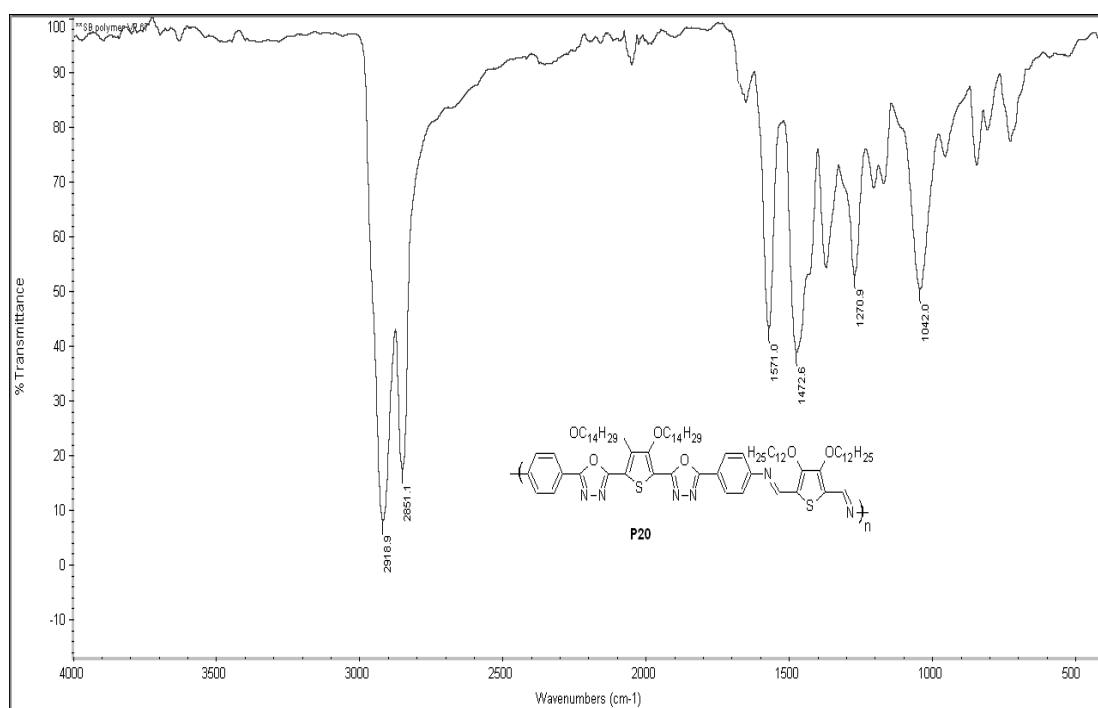


Figure 4.19: FTIR spectrum of polymer 20

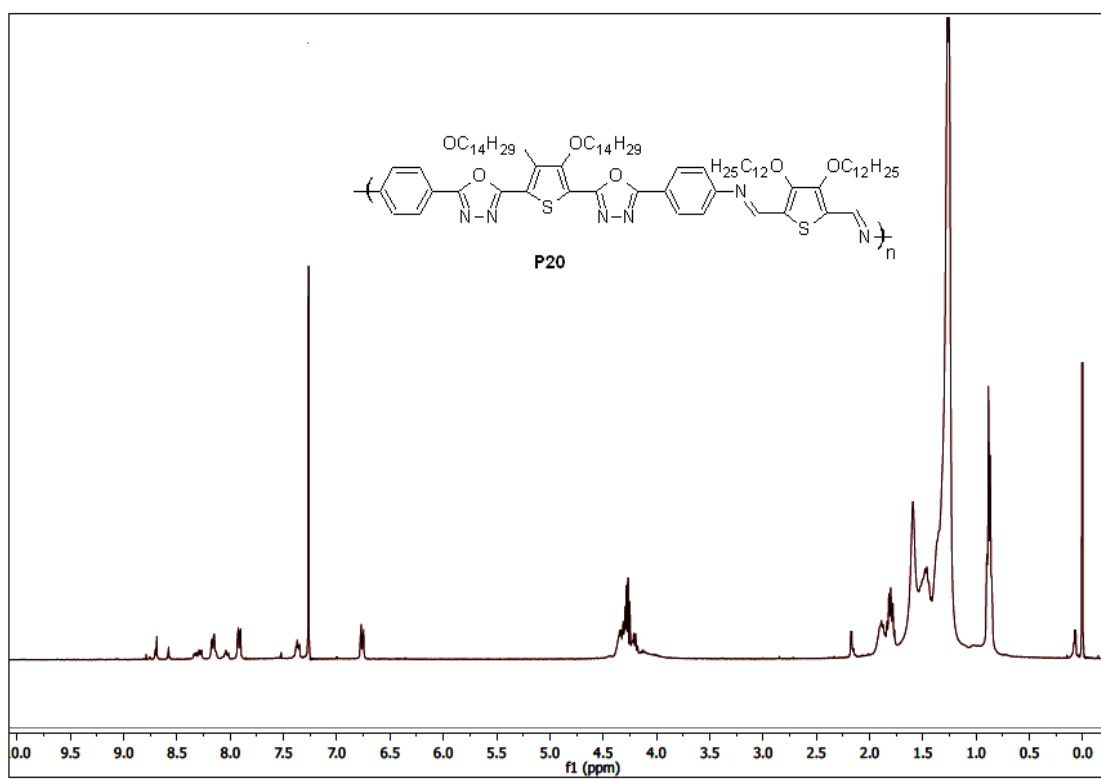


Figure 4.20: ¹H NMR spectrum of polymer 20

4.7.2. Results and discussion

Newly synthesized polymers **P17-P20** were characterized by FTIR and ^1H NMR spectral data. FTIR spectrum of polymer **P17** displayed two strong absorption bands in the region of $2900\text{-}2600\text{ cm}^{-1}$, which confirmed the presence of aromatic and aliphatic groups. Further the appearance of absorption bands at 1590 cm^{-1} confirms the presence of imine functionality in the backbone. Also, in its ^1H NMR spectrum disappearance of peaks due to aldehydic group and appearance of a sharp peak at δ 8 ppm corresponding to imine functionality clearly indicates the formation of Schiff's base. Similar observations were made in the spectra of polymers **P18-P20** also.

Thermogravimetric analysis of these polymers revealed that they are quite stable up to $300\text{ }^\circ\text{C}$. The onset decomposition temperatures were found to be 335, 310, 289 and $295\text{ }^\circ\text{C}$ for polymers **P17-P20**, respectively. Among the polymers, **P17** showed the highest onset decomposition temperature because it contains phenyl conjugated spacer without alkoxy pendants. On the other hand, polymers **P19** and **P20** showed less thermal stability due to the presence of bulky alkoxy side chains attached to conjugated spacers. Further, the polymers are readily soluble in common organic solvents and particularly polymers **P19** and **P20** showed very good film forming ability. The weight average molecular weights of the polymers were found to be in the range of $14500\text{-}27000\text{ da}$ with the polydispersity ranging from $1.4\text{-}3.9$. The thermogravimetric traces of polymers **P17-P20** are summarized in **Figure 4.21**.

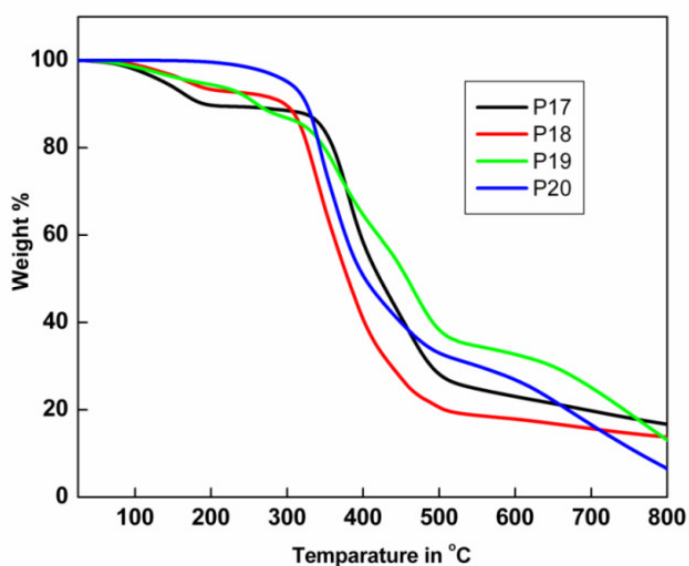


Figure 4.21: Thermo-gravimetric traces of conjugated polymers **P17-P20**

4.8. CONCLUSIONS

In conclusion, five new series of D-A type conjugated polymers **P1-P20** were successfully synthesized and their synthetic methods were established. Polymers **P1-P5** was obtained through poly-condensation technique followed by oxidative cyclization process, while polymers **P6-P12** and **P14** were prepared through Wittig condensation method. Similarly **P13** was synthesized via Knoevengel condensation. Further, polymers **P15** and **P16** were prepared by the poly-condensation followed by cyloimidation reaction. At the end Schiff's base type polymers **P17-P20** were synthesized through poly-condensation reactions. The structures of the newly synthesized polymers **P1-P20** were evidenced by different spectral methods. Further, the polymers were characterized by GPC and TGA analyses. Their thermogravimetric study revealed that they are thermally stable up to 300 °C. Also, it has been observed that introduction of alkoxy/alkyl side chains enhanced solubility of the polymer. Furthermore, incorporation of cyclic imide functionality along the polymer chain enhanced their thermal stability. In the next chapter the electrochemical study of the new polymers has been discussed in detail.

Abstract

This chapter deals with electrochemical characterization of new polymers P1-P20 using cyclic voltammetry. Further, it describes determination of redox potentials, calculation of HOMO-LUMO energy levels, barrier energies and bandgap of the polymers. Also, their structure - property relations have been discussed.

5.1. INTRODUCTION

Electrochemical study of the conjugated polymers plays an important role in understanding their basic electronic structures. It describes their redox properties, which are highly useful in the determination of HOMO-LUMO energy levels, bandgap and charge carrying properties. Also, it provides a method for preparing them in the convenient form of thin films on electrode (metal, glassy carbon, any semiconductor) surfaces for their future applications. Generally, cyclic voltammetry (CV) is employed for electrochemical studies.

5.2. CYCLIC VOLTAMMETRY

Cyclic voltammetry (CV) was introduced by Hickling for electrochemical studies of materials in the year late 50s (Hickling 1942). Further, Janietz et al. (1997) used this technique for measuring ionization potentials of conjugated polymers and also their bandgaps. Cyclic voltammetric setup constitutes an electrochemical cell working in a three-electrode configuration and a potentiostat. These three electrodes (working, counter, and reference) are connected to a potentiostat, whose function is to supply a current, which is regulated in the particular voltage range (-2.5 to +2.5 V). The electrodes are immersed in an electrolyte, which provides the ionic conductivity. Generally glassy carbon button electrode is used as working electrode; on which a polymer film is coated. In the case of p-doping, which corresponds to oxidation of the polymer, electrons are transferred from polymer to metal and the reverse for n-doping, which corresponds to a reduction. The resulting transfer of charges during the doping process gives rise to the current flowing through the working electrode. The corresponding potential of the working electrode indicates the absolute potential (versus the reference electrode) at which the conjugated polymer is doped. Importantly, the separation between the potentials of the p-type doping and the n-type doping processes indicates the value of electrochemical bandgap. The onset potentials

for p-doping and n-doping are calculated as the intersection of the baseline with the tangent of the current curve at the half maximum of the current curve. The electrochemical reactions on electrode surface are represented in **Figure 5.1**.

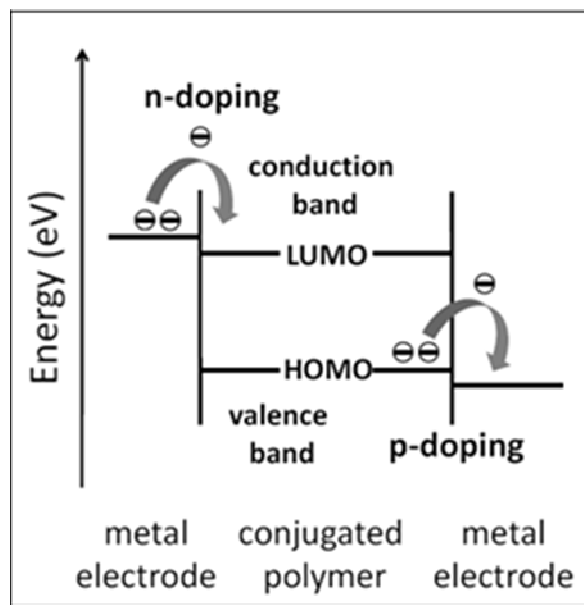


Figure 5.1: Electrochemical reactions on electrode surface

5.3. EXPERIMENTAL PROTOCOLS FOR ELECTROCHEMICAL STUDIES

The electrochemical studies were carried out using AUTOLAB PGSTAT 30 electrochemical analyzer. Cyclic voltammograms were recorded using a three-electrode cell system, with a glassy carbon button as working electrode, a platinum (Pt) wire as the counter electrode and an Ag/AgCl electrode as the reference electrode.

In the CV experiments, polymer to be analyzed was coated on a glassy carbon button electrode by evaporating their CHCl_3 or DMF solutions. The CV was run in 0.1 M tetrabutylammoniumperchlorate (TBAPC) solution in dry acetonitrile at a scan rate 25 mV/s. As the setup is sensitive to the presence of air in the cell, the entire cell was flushed with nitrogen prior to running the experiments. The electrochemical reduction behavior of the polymers was studied in the potential range 0 to -2.5 V, whereas the oxidation cyclic voltammograms were recorded by sweeping the potential in the range 0 to +2.5 V. Experiments were conducted at laboratory temperature.

The onset oxidation and reduction potentials were used to estimate the highest occupied molecular orbital (HOMO) and the lowest unoccupied molecular orbital

(LUMO) energy levels of the polymers. Their HOMO and LUMO energy levels are calculated from the following equations (**Eq. 5.1** and **Eq. 5.2**).

$$E_{\text{HOMO}} = - (E_{\text{onset}}^{\text{oxd}} + 4.4\text{eV}) \dots \dots \dots (\text{Eq. 5.1})$$

$$E_{\text{LUMO}} = - (E_{\text{onset}}^{\text{red}} - 4.4\text{eV}) \dots \dots \dots (\text{Eq. 5.2})$$

where $E_{\text{onset}}^{\text{oxd}}$ and $E_{\text{onset}}^{\text{red}}$ are the onset potentials versus standard calomel electrode (SCE) for the oxidation and reduction of the material referred, were used for the calculation. Further, their electrochemical bandgaps were determined by the difference between HOMO and LUMO energy levels.

$$E_g = E_{\text{HOMO}} - E_{\text{LUMO}} \dots \dots \dots (\text{Eq. 5.3})$$

where E_g is electrochemical bandgap.

All electrochemical measurements reported in the thesis are reference versus Fc/Fc^+ and the conversion to the HOMO and LUMO energies was accomplished by addition of 4.4 eV to the onsets of oxidation and reduction of the polymer, respectively (Fc/Fc^+ is at 4.4 eV below the vacuum level). The electrochemical characterization data of polymers **P1-P20** are summarized in **Table 5.1**.

5.4. RESULTS AND DISCUSSION

From electrochemical results important data such as HOMO/LUMO energy levels, barrier potentials and bandgaps of polymers **P1-P20** were calculated as their characterization parameters (**Table 5.1**). Further, their series-wise discussion on structure-property relationship has been given in the following section.

Polymers **P1-P5** (Series 1)

The cathodic scan of polymers **P1**, **P2**, **P3**, **P4** and **P5** showed reduction peaks at -1.1, -1.25, -1.31, -1.7 and -1.11 V, respectively with onset reduction potentials at -0.68, -0.85, -0.78, -1.14 and -0.64 V, respectively (**Figure 5.3**). The observed reduction potentials are lower than that of 2-(4-biphenyl)-5-(4-*tert*-butylphenyl)-1,3,4-oxadiazole (PBD) (Strukelj, et al. 1995; Janietz, et al. 1997), one of the most widely used electron transporting materials, and are comparable with those of some good electron-transporting materials reported in the literature (Emilie et al. 2006). These n-doping potentials are comparable to other oxadiazole-containing light-emitting polymers (Strukelj et al. 1995), reported earlier.

While sweeping anodically, **P1-P5** displayed oxidation peaks at 1.77, 2.01, 1.30, 1.31 and 2.14 V, respectively (**Figure 5.3**) with onset oxidation potentials at 1.22, 1.22, 1.15, 0.94 and 1.64 V, respectively. These values are almost similar to those of some reported donor-acceptor poly(oxadiazole)s in the literature (de Leeuw et al. 1997). These polymers exhibit irreversible oxidation and reduction potentials. Their electrochemical bandgaps were found to be 1.90, 2.07, 1.93, 2.08 and 2.28 eV, for **P1-P5**, respectively. The structures of these polymers are given in **Figure 5.2**.

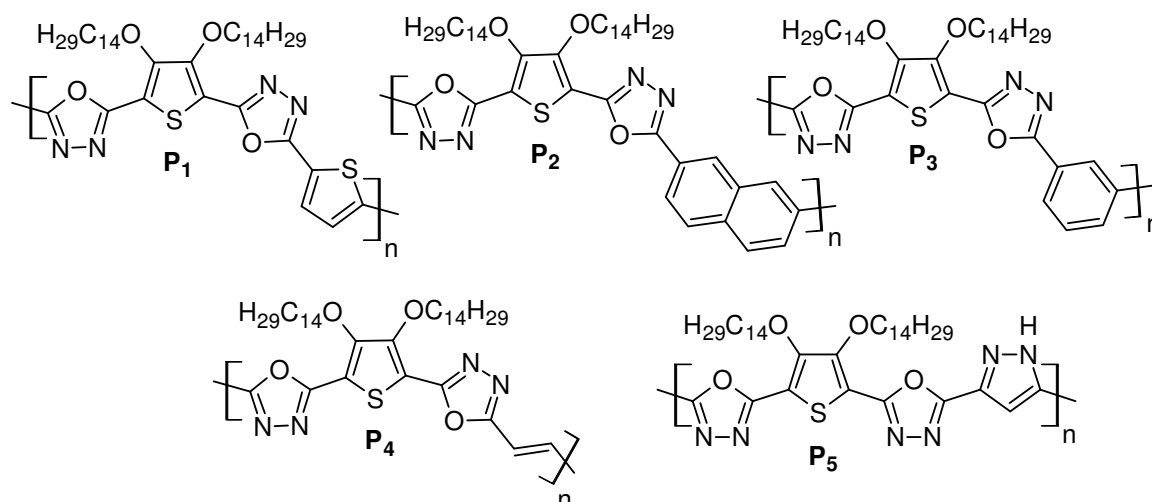


Figure 5.2: Structures of the polymers **P1-P5**

The observed electrochemical behavior in **P1-P5** can be well explained on the basis of their structures. In general, when electron-withdrawing substituents (oxadiazoles) are attached to the conjugated molecules, the electron density in the π -system of the conjugated molecule decreases (Zhao et al. 2009). Consequently, the molecule will be stabilized and its oxidation potential will be increased. Also, in our polymers **P1-P5**, presence of thiophene, naphthalene, isophthalyl, vinylene and pyrazole units has influenced significantly the HOMO energy level due to their high electron donating ability and accordingly they showed high-lying HOMO energy levels. Usually, the bandgap of any conjugated polymer is influenced by conjugation length (Izumi et al. 2003), solid-state intermolecular ordering and the presence of electron-withdrawing or donating moieties. Similar observations were made in our polymers **P1-P5**. Also, among five polymers in the series, **P1** showed lowest bandgap of 1.9 eV. The cyclic voltametric traces of polymers **P1-P5** are depicted in **Figure 5.3**. This may be due to the high electron donating nature of the un-substituted thiophene ring, present in between two highly electron withdrawing 1,3,4-oxadiazole

moieties in D-A-D type polymeric backbone. In addition, the effective conjugation length, which is dependent upon the torsion angle between the repeating units along the polymer chain, has been controlled by introduction of sterically hindered bulky 3,4-ditetradecyloxy side chains, thereby twisting the units out of plane (Andersson et al. 1999 and Perzon et al. 2006).

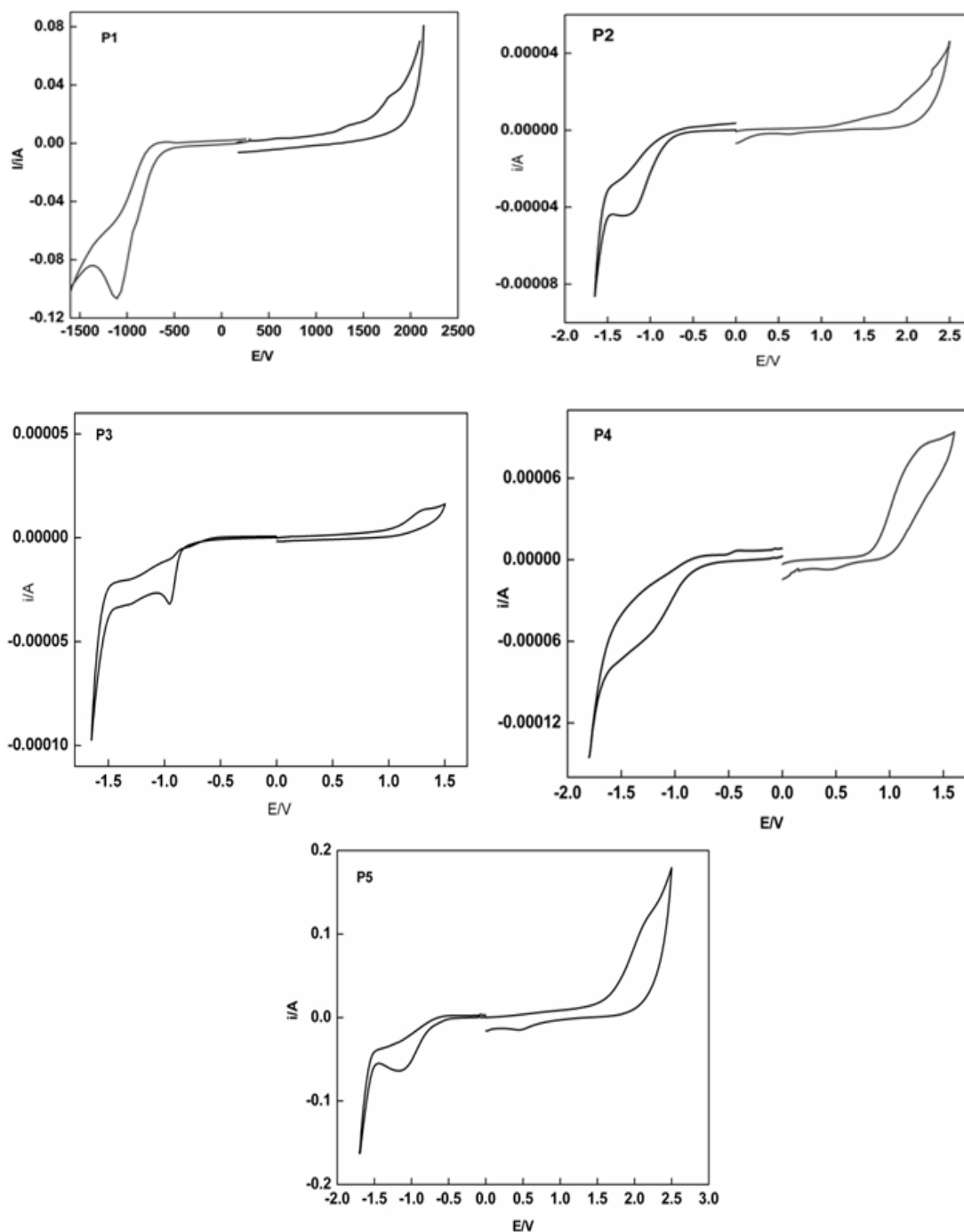


Figure 5.3: Cyclic voltammograms of polymers **P1-P5**

Polymers P6-P10 (Series 2)

From the CV traces (**Figure 5.5**) onset oxidation potentials of polymers of **Series 2** were estimated to be 1.050, 1.069, 0.98, 1.022 and 1.41 V for **P6, P7, P8 P9, and P10**, respectively. These p-doping potentials are comparable to other oxadiazole-containing light-emitting polymers reported in the literature. For the *n*-doping (reduction) process, the onset potentials for the polymers were determined to be -0.905, -0.821, - 0.791, - 0.650 and -0.67 V for **P6, P7, P8 P9, and P10**, respectively. These onset reduction values are even lower than that of 2-(4-biphenyl)-5-(4-*tert*-butylphenyl)-1,3,4-oxadiazole (PBD). In these polymers, reversibility of the *p*-doping process is not as good as that of its *n*-doping.

The HOMO energy levels of **P8, P9** and **P10** are almost same as that of poly(cyanoterphthalylidene) (CN-PPV), indicating that the polymers have similar hole-injection ability as CN-PPV when they are used in PLEDs. However, all these values are higher than those of PPV and other p-type conjugated polymers; this could be due to the introduction of cyanopyridine units along the polymer backbone (Michelle et al. 2002).

The LUMO energy levels of polymers are lower than those of PPV and other conjugated poly(thiophene)s. Further, the values are lower than those of CN-PPV, and some poly(oxadiazole)s (Udayakumar et al. 2006) indicating that, these polymers have better electron-injection ability in PLED applications. The electrochemical bandgaps of these polymers **P6-P10** were found to be 1.95, 1.89, 1.77, 1.67 and 2.00 eV, respectively. Structures of polymers **P6-P10** are given in **Figure 5.4**.

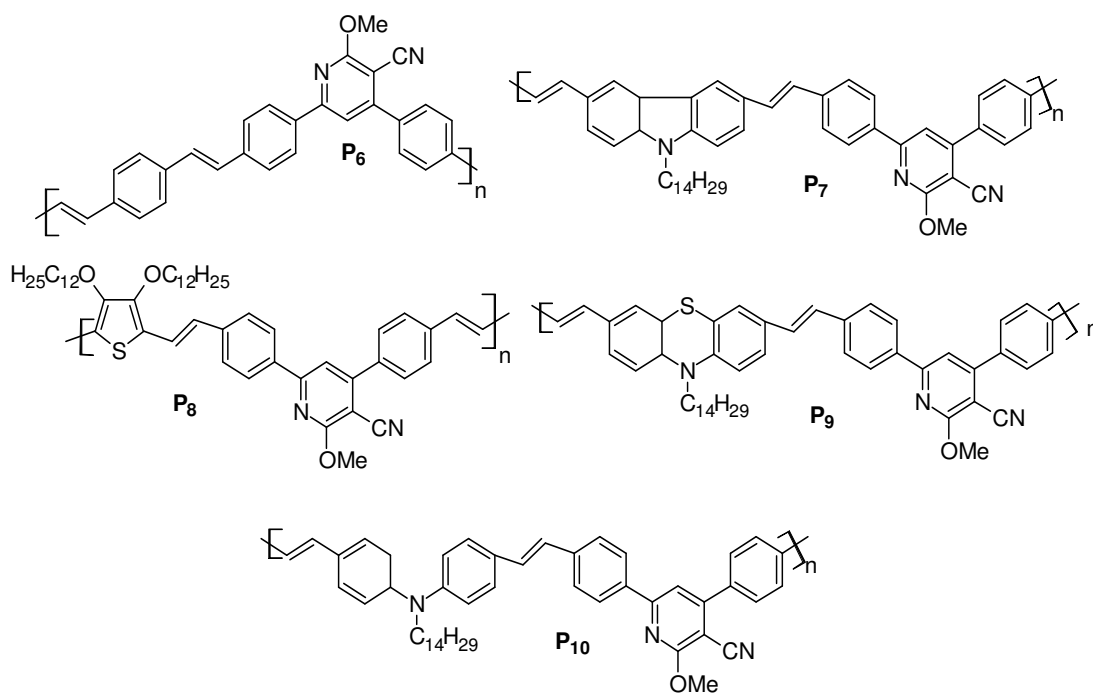


Figure 5.4: Structures of the polymers **P6-P10**

In general, when electron-withdrawing substituent is attached to the conjugated molecules, the electron density in the π -system of the conjugated molecule will be decreased. As a result, there will be a shift of the HOMO energy level to lower energy. So, introduction of highly electron withdrawing cyanopyridine in **P6-P10** has reduced the HOMO energy level decreasing their bandgap (Michelle et al. 2002). Polymers **P7-P10** showed enhancement of oxidation potentials, which is attributed to the presence of sterically hindered bulky alkoxy side chains. Introduction of electron-donating 3,4-didodecyloxythiophene group in polymer **P8** has produced an increase of the HOMO level, accompanied by a reduction in the bandgap. Thus, the inductive effect of simple alkyl groups has decreased the oxidation potential of the thiophene ring. On the other hand, linear alkyl chains of sufficient length indirectly contribute to reduce the energy gap by enhancing the long-range order in the polymer, through lipophilic interactions between the alkyl chains. Because of this reason **P8** and **P9** showed low bandgaps (Roncali et al. 1987). Also, insertion of phenothiazine chromophores is much more effective in lowering the ionization potential and hence bandgap of the polymer. Similarly, presence of electron rich carbazole and phenothiazine units also influences the HOMO energy level (Grazulevicius et al. 2003). In this series, polymer **P6** does not possess any alkyl side chain and hence it

has showed low electron donating ability that resulted in the high bandgap. Similarly, **P10** also showed high band-gap when compared to other polymers in the series due to the presence of non aromatic nitrogen bridge.

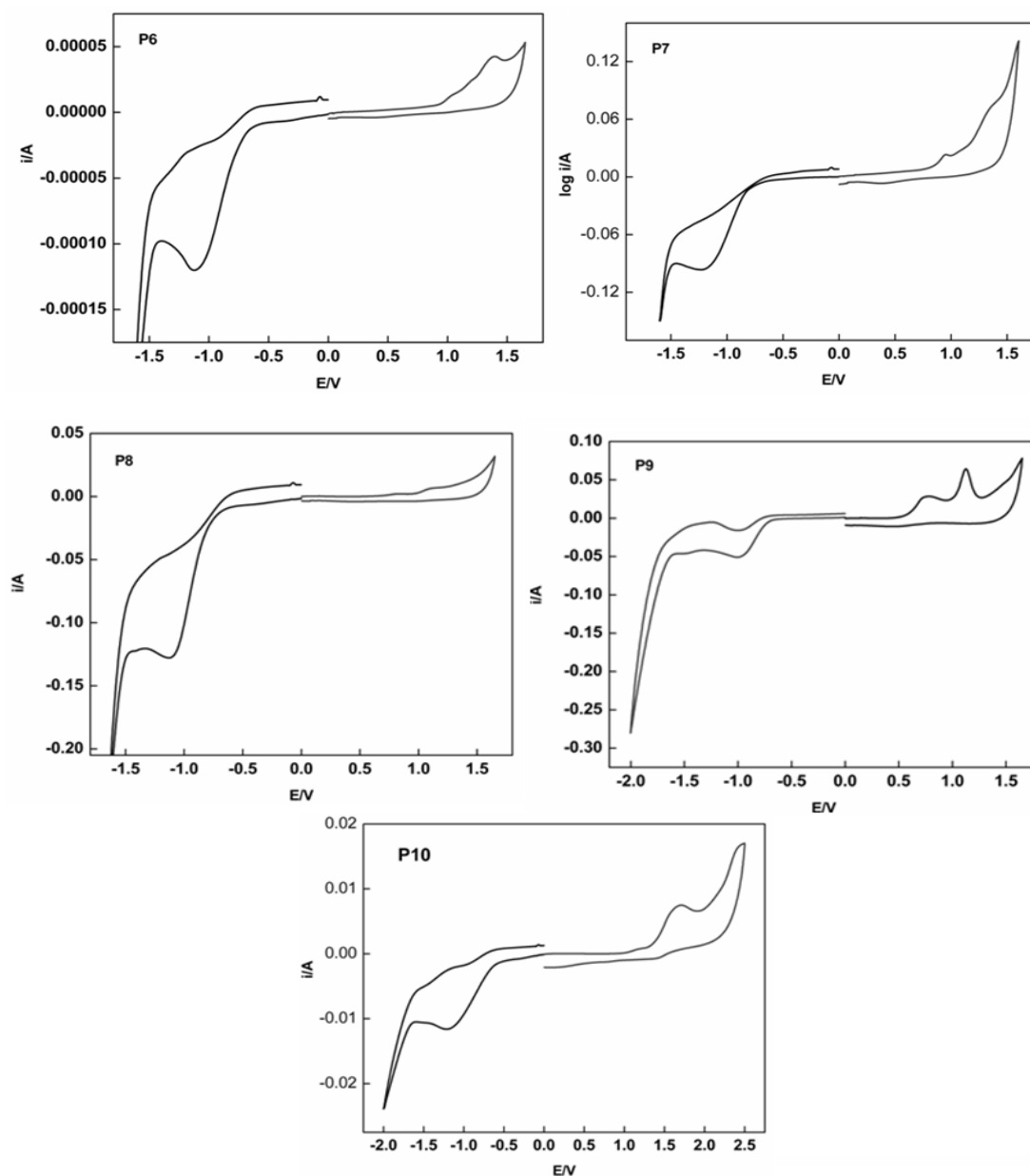


Figure 5.5: Cyclic voltammograms of polymers **P8-P10**

Polymers P11-P14 (Series 3)

The estimated onset oxidation potentials of polymers of **Series 3** (p-doping) (**Figure 5.7**) were found to be 1.51, 1.09, 1.04 and 0.99 V for **P11**, **P12**, **P13** and **P14**, respectively. For the *n*-doping (reduction) process, the onset reduction potentials

appeared at -0.65, -0.93, -0.68 and -0.76 V for **P11**, **P12**, **P13** and **P14**, respectively. The observed values were almost matching with that of other oxadiazole based light emitting conjugated polymers. The HOMO energy levels of **P11**, **P12**, **P13** and **P14** were estimated to be -5.91, -5.57, -5.44 and 5.39 eV, respectively. The LUMO energy levels of **P11**, **P12**, **P13** and **P14** were estimated to be -3.70, -3.47, 3.72 and 3.67 eV, respectively. These results have close resemblance to that of poly(cyanoterphthalylidene) (CNPPV), indicating that the polymers have similar hole-injection ability with CNPPV when they are used in PLED devices. Further, the electrochemical bandgaps of the polymers were determined to be 2.21, 2.10, 1.72 and 1.75 eV, for **P11**, **P12**, **P13** and **P14**, respectively. Structures of polymers **P11-P14** is depicted in **Figure 5.6**.

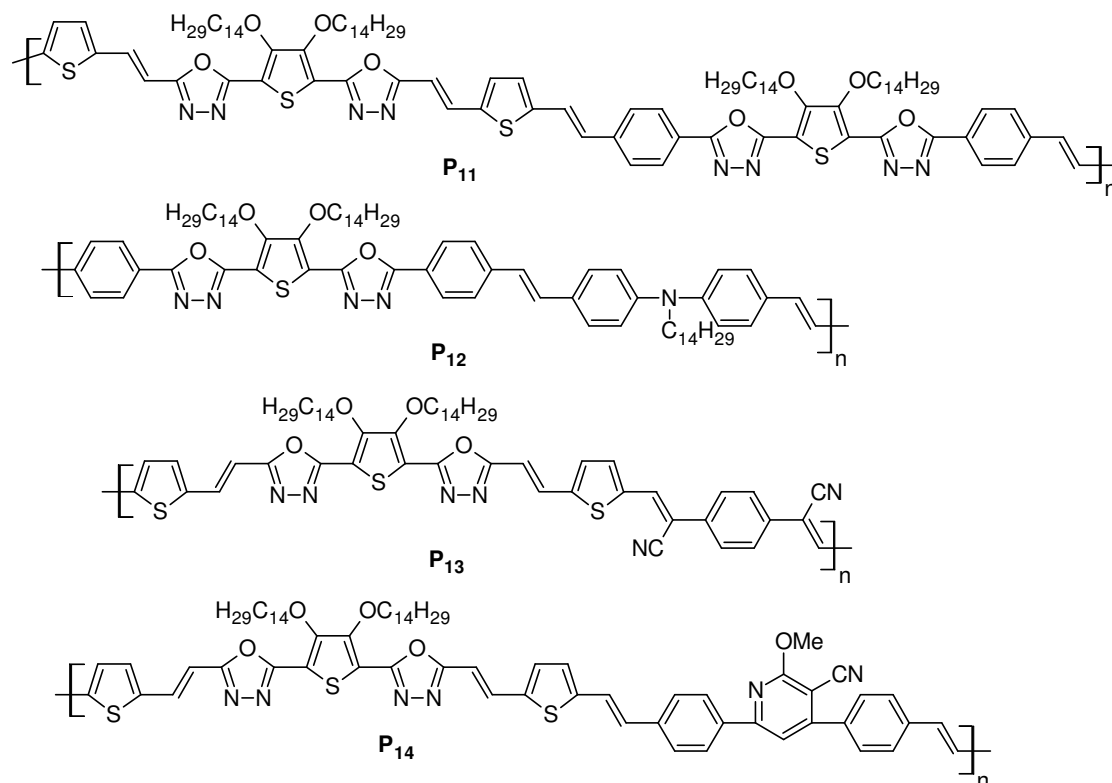


Figure 5.6: Structures of the polymers **P11-P14**

In polymers **P11**, **P13** and **P14** incorporation of the vinylene units into the D-A type conjugated polymer main chain decreased the bandgap of the polymer by altering the HOMO and LUMO energy levels. This is because the introduction of π -excessive thiophene ring increases the effective conjugation length, planarity and lowers the bandgap of the resulting polymer. Similarly, presence of 3,4-

ditetradecyloxythiophene in these polymers has influenced the HOMO energy level due to their high electron donating ability. In these polymers, ethylenic linkages have eliminated the torsion angle due to steric interactions between adjacent phenyl/thiophene rings, allowing the conjugated system to adopt a planar structure.

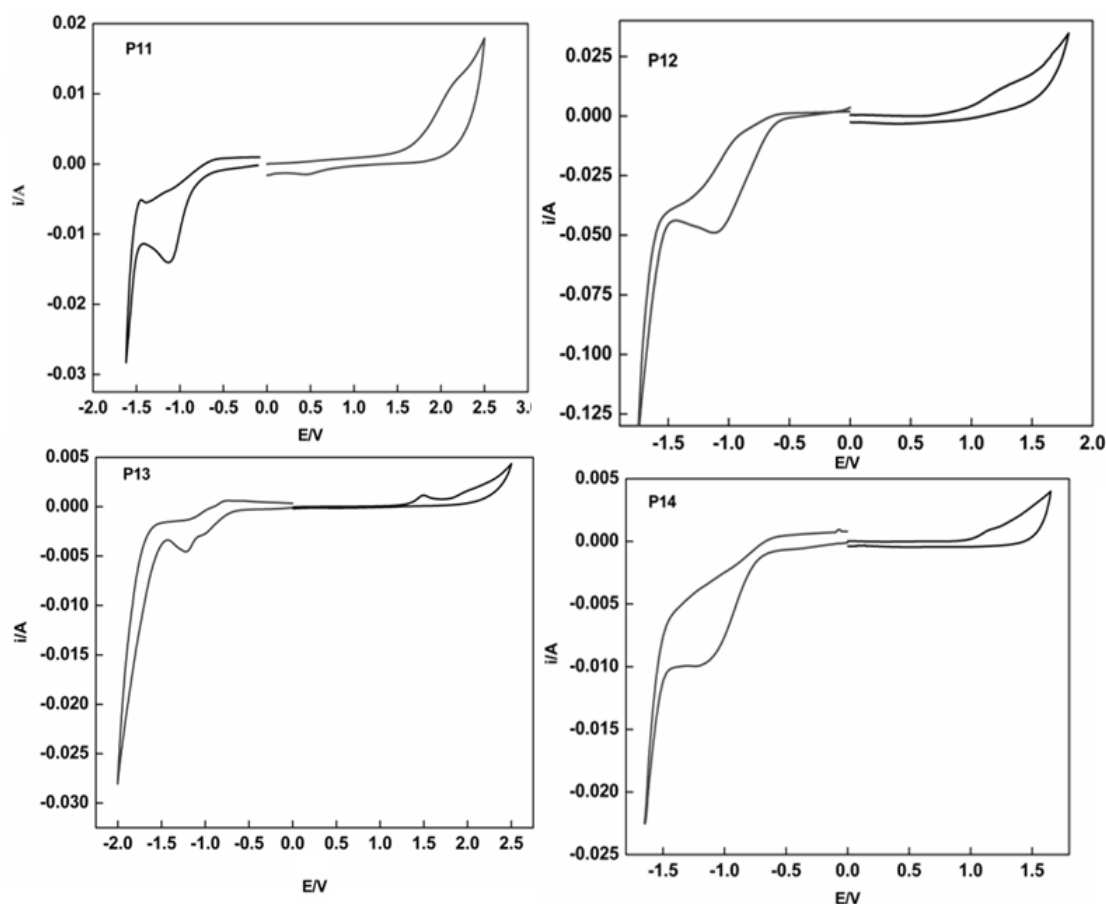


Figure 5.7: Cyclic voltammograms of polymers **P11-P14**

Another important effect is that the insertion of double bonds has led to a decrease in the overall aromaticity of the polymeric system and hence it has caused a reduction in the bandgap (Jen et al. 1987). In addition, incorporation of a cyanopyridine moiety along the polymer **P14** has decreased the bandgap due to its high electron-withdrawing property. Similarly, **P13** showed the lowest bandgap in the series, which is mainly attributed to the presence of highly electron-withdrawing cyanovinylene units along the polymer backbone. Furthermore, incorporation of the electron-

withdrawing cyano groups has decreased the HOMO energy level which in turn resulted in stabilization of the neutral state of the system.

Polymers P15-P16 (Series 4)

The polymers **P15** and **P16** showed strong donor-acceptor character with reversible reduction and irreversible oxidation processes. The oxidation potentials of them were found to be 1.80 and 1.86 V with onset oxidation potentials of 1.41 and 1.64 V, respectively (**Figure 5.9**). Also, the reduction potentials of these polymers were estimated to be -0.90 and -0.85 V with onset reduction potentials -0.72 and -0.58 V, respectively. These values are analogous to that of other D-A type conjugated polymers reported in the literature, indicating that these materials are suitable candidates for their applications in PLED devices. The estimated HOMO energy levels of the **P15** and **P16** were found to be -5.81 and -6.04 eV with LUMO energy levels of -3.68 and -3.82 eV, respectively. The electrochemical bandgaps of **P15** and **P16** were found to be 2.13 and 2.22 eV, respectively. **Figure 5.8** shows the structures of **P15-P16**.

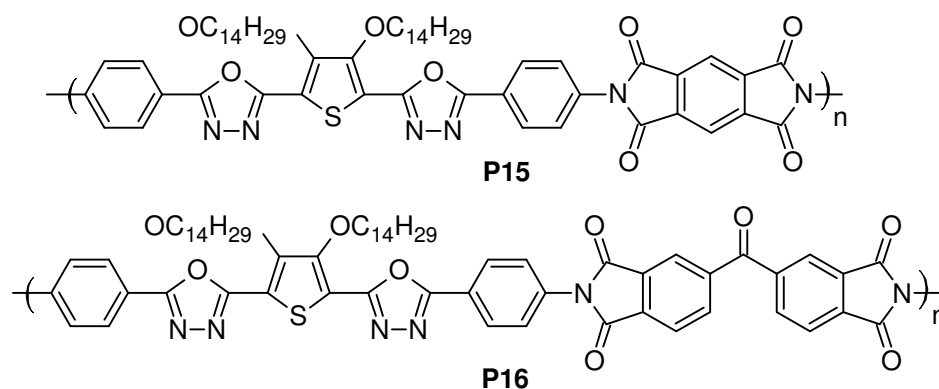


Figure 5.8: Structures of the polymers **P15** and **P16**

The determined electrochemical data of polymers **P15** and **P16** show good resemblance to the imide containing polymers, reported in the literature (Viehbecke al. 1990). This observation indicates that the imide's carbonyl group in the polymers acts as an electro-active site. Further, appearance of reversible reduction peak indicates that the carbonyl group is responsible for reversible redox reaction in the polymers. The reduction potential of **P16** appeared at a more negative potential than

that of **P15**, indicating that the reduction potential relates to the electron affinity of the additional carbonyl group present in **P16**. The observed bandgaps of the polymers are quite low compared to the polyamides reported in literature. This may be attributed to the enhancement of conjugation path-length and D-A type arrangement in the polymer backbone. Also, introduction of cyclic imides in the polymeric backbone has resulted in the reduction of steric interaction of bulky alkoxy pendants, which leads to decrease in the band-gap of the resulting polymer.

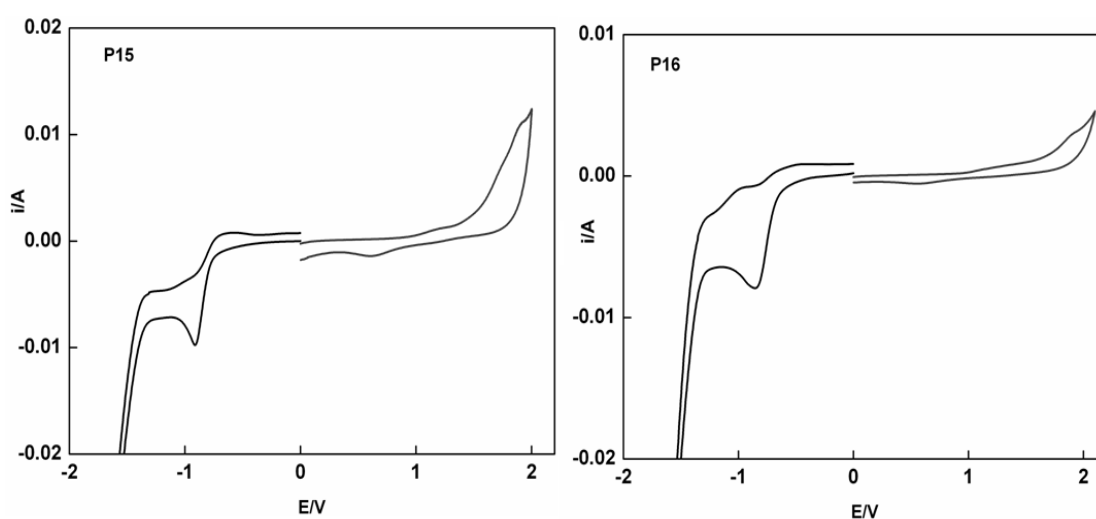


Figure 5.9: Cyclic voltammograms of polymers **P15** and **P16**

Polymers **P17-P20** (Series 5)

The onset oxidation potentials of the polymers **P17**, **P18**, **P19** and **P20** were found to be 1.89, 1.37, 1.28 and 1.33 V (**Figure 5.11**) with onset oxidation potentials of 1.55, 1.20, 1.17, 1.14 V, respectively and their reduction potentials were determined to be -0.64, -0.64, -0.78, and -0.80 V with onset reduction potentials of -0.87, -0.85, -0.94 and -1.20 V, respectively. Their calculated HOMO energy levels are -5.95, -5.65, -5.57 and -5.54 eV, respectively. The LUMO energy levels are found to be -3.76, -3.76, -3.62 and -3.60 eV, respectively. These values are higher than that of PPV (-2.5 eV) and comparable with some of the poly(oxadiazole)s (-2.8 to -3.0 eV) reported in the literature. Electrochemical band gap the polymers were found to be 2.19, 1.84, 1.95, and 1.94 eV for **P17**, **P18**, **P19** and **P20**, respectively. The structures of polymer are given in **Figure 5.11**.

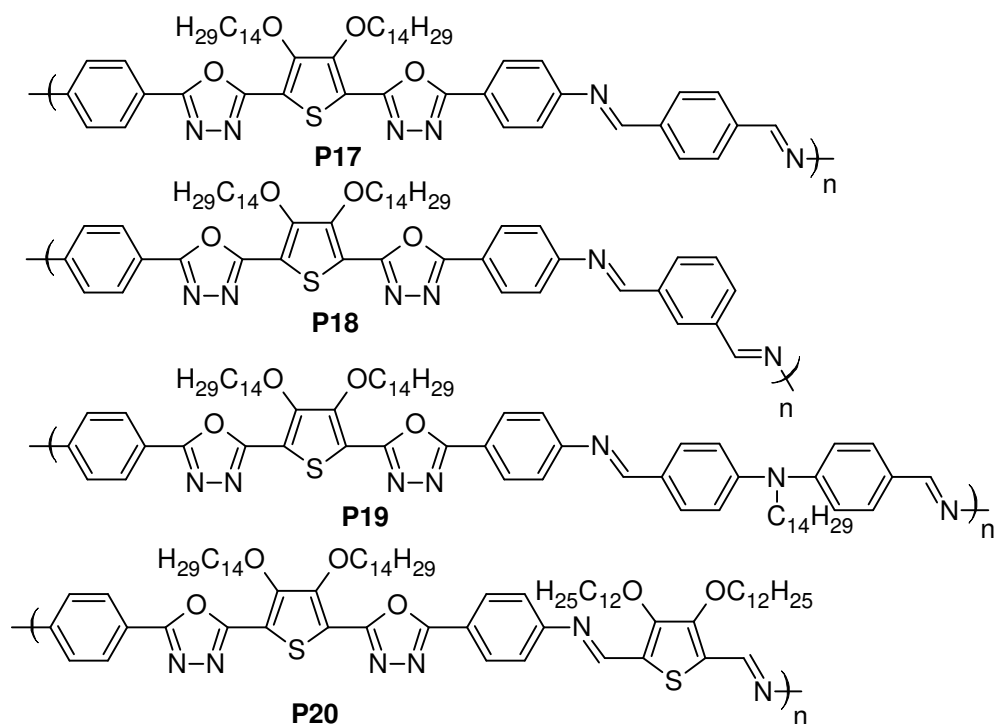


Figure 5.10: Structures of the polymers **P17-P20**

In the polymers, presence of 3,4-ditetradecyloxythiophene units along the main chain influences the HOMO energy level due to their high electron donating ability. Usually, the bandgap of any conjugated polymer can be influenced by its conjugation length and presence of electron-withdrawing or donating moieties. Consequently, polymers **P19** and **P20** showed low bandgap when compared to the other polymers in the series. Presence of additional alkyl/alkoxy side-chains of thiophene and diphenylamine units has enhanced the electron releasing ability and hence decreased their bandgap. Normally, incorporation of π -excessive thiophene units into the D-A type conjugated polymer main chain decreases its bandgap because of increase in effective conjugation length. As a result of this, polymer **P20** showed the lowest bandgap of 1.94 eV, which is attributed to the presence of high electron rich 3,4-didodecyloxythiophene unit as electron donor. In polymers **P17** and **P18** conjugation path length has enhanced due to presence of electron donating terphthalyl and isophthalyl moieties.

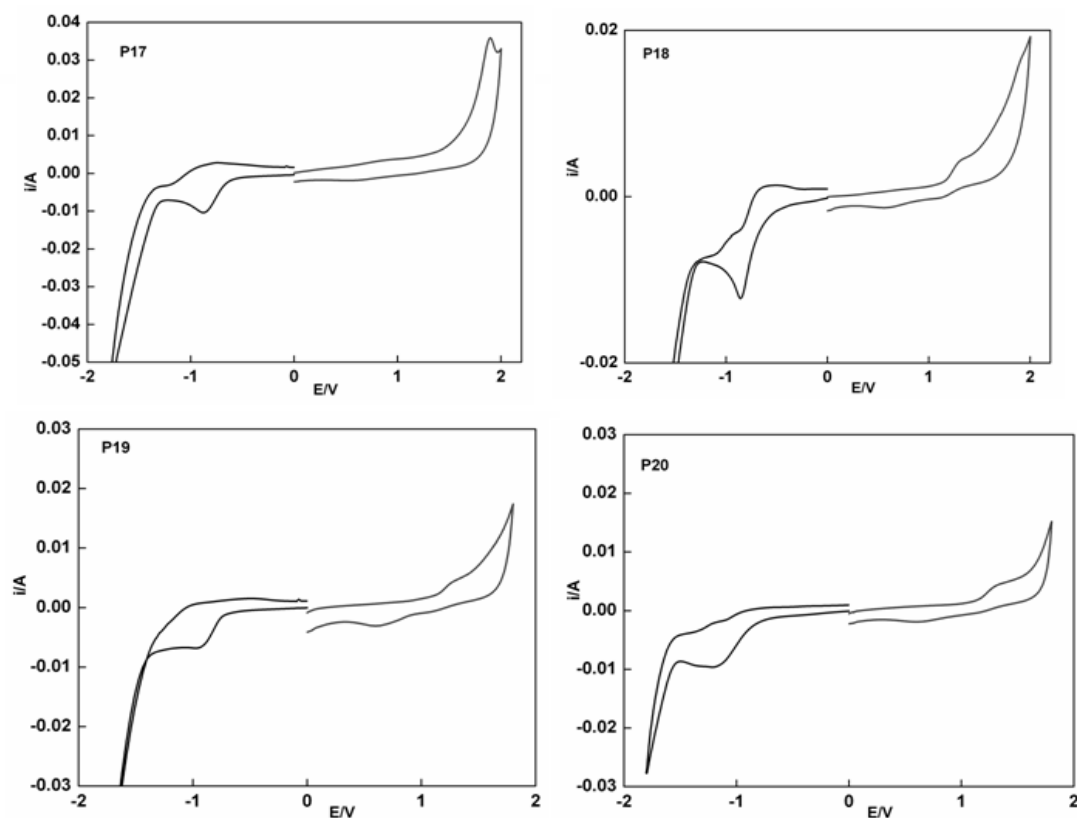


Figure 5.11: Cyclic voltammograms of polymers **P7-P20**

Electrochemical characterization data of polymers **P1-P20** are summarized in **Table 5.1** and **Table 5.2**.

Table 5.1: Electrochemical characterization data of polymers **P1-P10**

Polymer	E_{oxd} (V)	E_{red} (V)	E_{oxd} (onset)	E_{red} (onset)	E_{HOMO} (eV)	E_{LUMO} (eV)	E_g (eV)
P1	1.77	-1.11	1.22	-0.68	-5.62	-3.72	1.90
P2	2.01	-1.25	1.22	-0.85	-5.62	-3.55	2.07
P3	1.30	-1.31	1.15	-0.78	-5.55	-3.62	1.93
P4	1.31	-1.70	0.94	-1.14	-5.34	-3.26	2.08
P5	2.14	-1.11	1.64	-0.64	-6.04	-3.76	2.28
P6	1.38	-1.36	1.05	-0.90	-5.45	-3.49	1.95
P7	1.34	-1.21	1.06	-0.82	-5.46	-3.57	1.89
P8	1.10	-1.11	0.98	-0.79	-5.38	-3.60	1.77
P9	1.12	-0.96	1.02	-0.65	-5.42	-3.75	1.67
P10	1.69	-1.20	1.41	-0.67	-5.81	-3.73	2.00

Table 5.2: Electrochemical characterization data of polymers **P11-P20**

Polymer	E_{oxd} (V)	E_{red} (V)	E_{oxd} (onset)	E_{red} (onset)	E_{HOMO} (eV)	E_{LUMO} (eV)	E_{g} (eV)
P11	2.14	-1.12	1.51	-0.65	-5.91	-3.70	2.21
P12	1.17	-1.46	1.09	-0.93	-5.57	-3.47	2.10
P13	1.64	-0.90	1.04	-0.68	-5.44	-3.72	1.72
P14	1.14	-1.18	0.99	-0.76	-5.39	-3.67	1.75
P15	1.80	-0.90	1.41	-0.72	-5.81	-3.68	2.13
P16	1.86	-0.85	1.64	-0.58	-6.04	-3.82	2.22
P17	1.89	-0.87	1.55	-0.64	-5.95	-3.76	2.19
P18	1.37	-0.85	1.20	-0.64	-5.65	-3.76	1.84
P19	1.28	-0.94	1.17	-0.78	-5.57	-3.62	1.95
P20	1.33	-1.20	1.14	-0.80	-5.54	-3.60	1.94

5.5. CHARGE CARRYING PROPERTIES

The barrier energies of conjugated polymers **P1-P20** were determined and their values are tabulated in **Table 5.3**. The hole-injection barrier potential (ΔE_{h}) was calculated using the equation, $\Delta E_{\text{h}} = (E_{\text{HOMO}} - 4.8)$ eV, where 4.8 is the work function of **ITO** anode and the electron-injection barrier potential (ΔE_{e}) was obtained by using the relation, $\Delta E_{\text{e}} = (4.3 - E_{\text{LUMO}})$ eV, where 4.3 is the work function of aluminium cathode. The difference between the electron- and hole-injection barriers ($\Delta E_{\text{e}} - \Delta E_{\text{h}}$, barrier energy) is a useful parameter for evaluating the balance in electron and hole injection rates. Generally, a lower ($\Delta E_{\text{e}} - \Delta E_{\text{h}}$) value indicates improved injection balance of electrons and holes from the cathode and anode, respectively. In fact, the work function plays an important role in the fabrication of PLED devices. The band diagrams obtained from HOMO and LUMO energies of polymers are given in **Figures 5.12, 5.13, 5.14, 5.15** and **5.16** along with work functions of ITO anode and aluminium cathode.

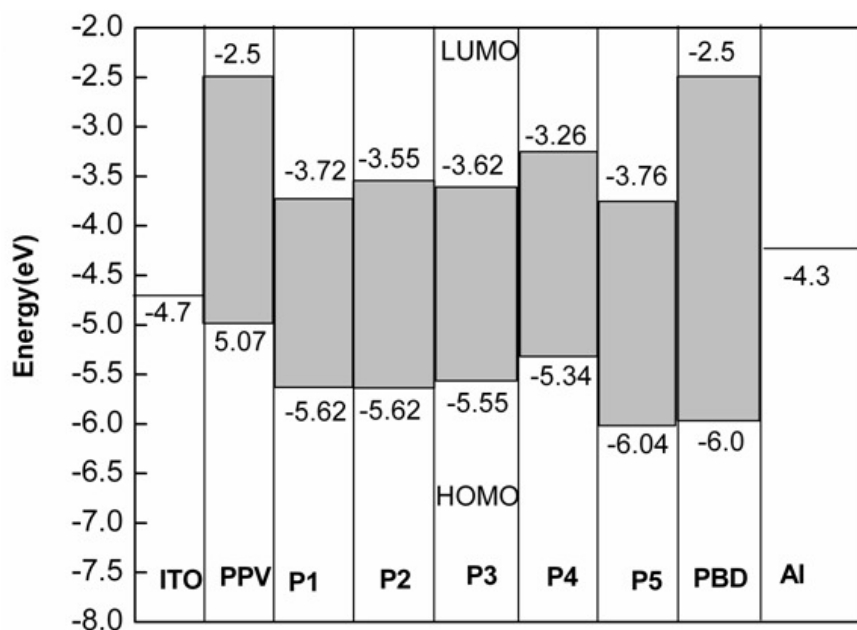


Figure 5.12: Band diagram of polymers **P1-P5** with aluminum and ITO electrodes

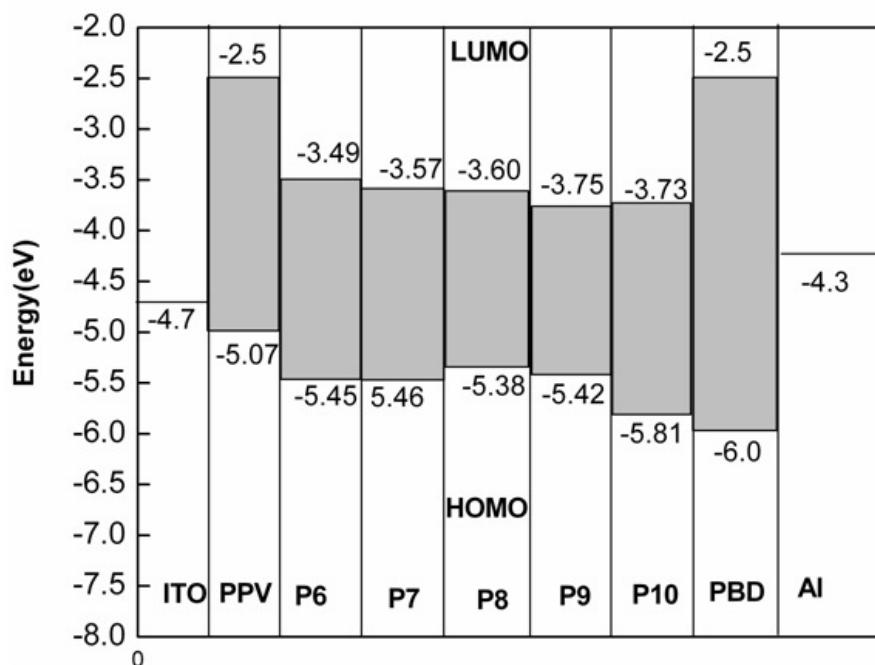


Figure 5.13: Band diagram of polymers **P6-P10** with aluminum and ITO electrodes

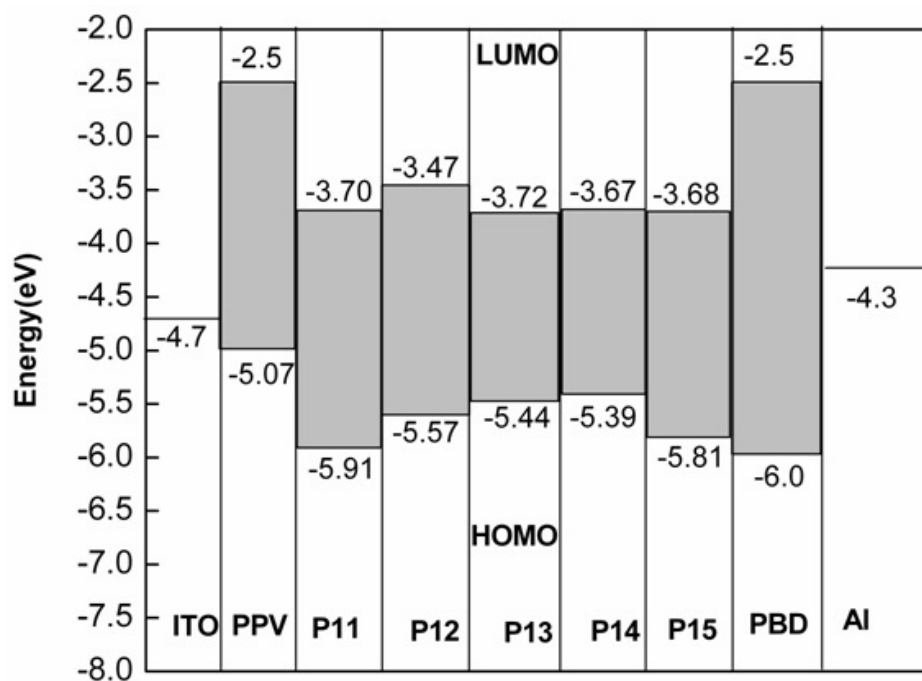


Figure 5.14: Band diagram of polymers P11-P15 with aluminum and ITO electrodes

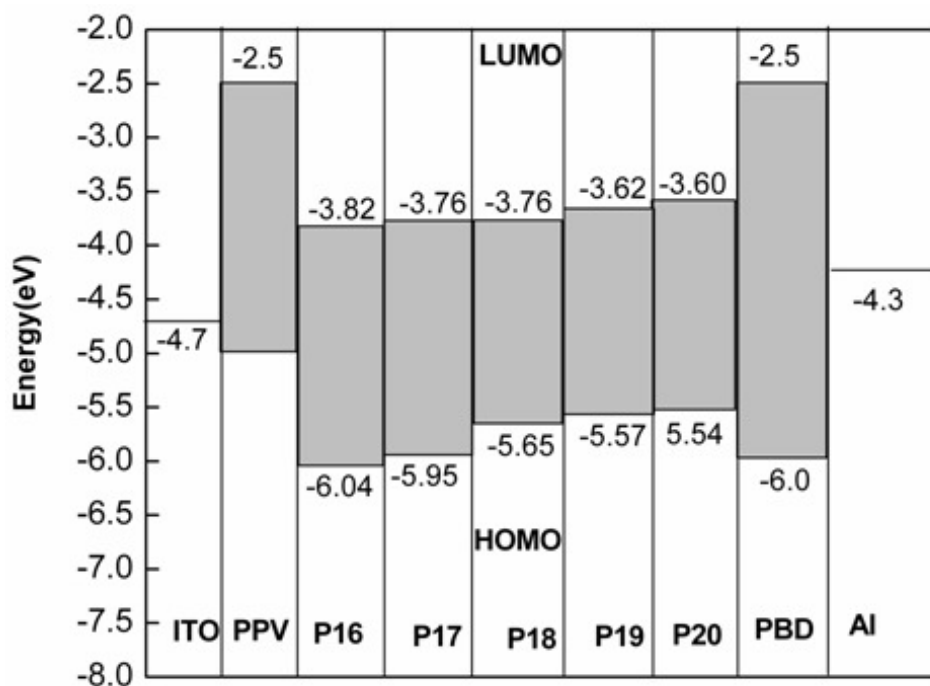


Figure 5.15: Band diagram of polymers P16-P20 with aluminum and ITO electrodes

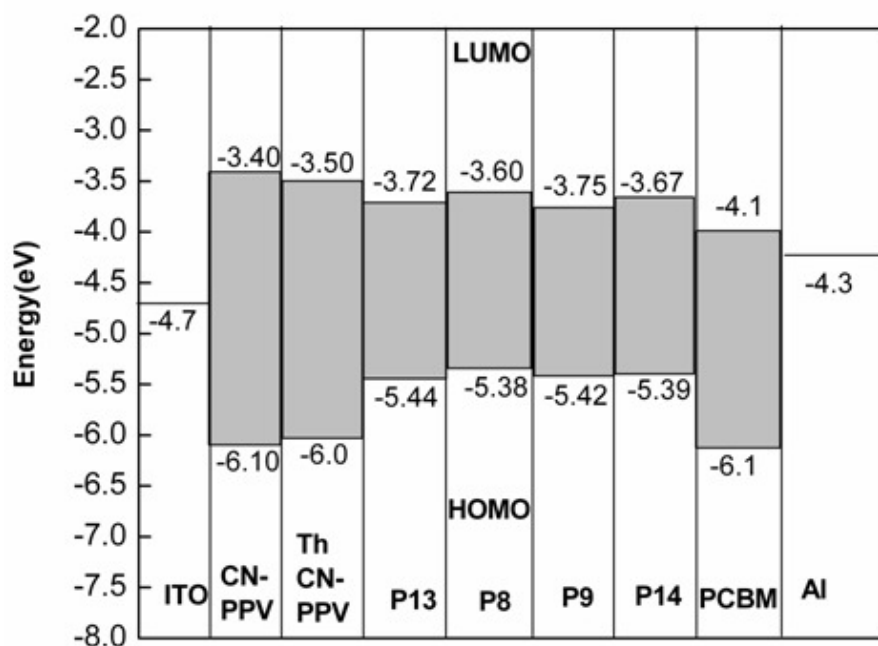


Figure 5.16: Band diagram of **P8**, **P9**, **P13**, **P14**, CN-PPV, Th-CN-PPV, PCBM Aluminum and ITO electrodes

From the results it is clear that new D-A type conjugated polymers **P1-P20** demonstrate ΔE_c lower than those of PPV (1.80 eV) and some other reported p-type polymers (**Table 5.3**). Further, these polymers also showed higher value of ΔE_h than that of PPV (0.30 eV) and lower than that of PBD (Bradley 1993, Okumoto and Shirota 2001). The variation in these values is mainly attributed to their structural features. In polymers **P1-P5**, **P11-P20** the lower value of ΔE_c is ascribed to the presence of electron affinitive 1,3,4-oxadiazole moiety and the higher value of ΔE_h is due to the occurrence of 3,4-dialkoxy substituted thiophene rings in polymer backbone. Further, polymers **P6-P9** showed low barrier potential values because of the balance electron and hole injection property of the polymers. This behavior may be attributed to the presence of electro-active cyanopyridine unit along the polymer main chain. In the same series, polymer **P10** displayed little higher barrier energy than others. This observed fact may be due to the introduction of diphenylamine moiety, which results in decrease in delocalization of electron in the conjugated system because of the presence of nitrogen bridge in the polymer chain. Further, polymer **P11** showed higher energy barrier than those of **P12** and **P14** owing to presence of an

additional electron releasing thiophene unit in its structure. Similarly, polymers **P13** and **P14** comprising additional electron withdrawing cyanovinylene and cyanopyridine rings along the chain showed decreased barrier energy values. Amongst the studied polymers, **P20** showed the lowest $\Delta E_e - \Delta E_h$ value, which may be due to the enhanced D-A character of the polymer chain resulting from inclusion of 3,4-ditetradecyl/3,4-didodecyloxythiophene units along the imine functionalized backbone.

Table 5.3: Barrier energies of polymers **P1-P20**

Polymer	ΔE_h (eV)	ΔE_e (eV)	$\Delta E_e - \Delta E_h$ (eV)	E_g (eV)
P1	0.82	0.58	0.24	1.90
P2	0.82	0.75	0.07	2.07
P3	0.75	0.68	0.07	1.93
P4	0.54	1.04	0.5	2.08
P5	1.24	0.54	0.7	2.28
P6	0.65	0.81	0.16	1.95
P7	0.66	0.73	0.07	1.89
P8	0.58	0.7	0.12	1.77
P9	0.62	0.55	0.07	1.67
P10	1.01	0.57	0.44	2.00
P11	1.11	0.6	0.51	2.21
P12	0.77	0.83	0.06	2.10
P13	0.64	0.58	0.06	1.72
P14	0.59	0.63	0.04	1.75
P15	1.01	0.62	0.39	2.13
P16	1.24	0.48	0.76	2.22
P17	1.15	0.54	0.61	2.19
P18	0.85	0.54	0.31	1.84
P19	0.77	0.68	0.09	1.95
P20	0.74	0.7	0.04	1.94

5.6. CONCLUSIONS

The results of electrochemical studies of polymers **P1-P20** revealed that their HOMO energy levels are in the range of -5.34 - -6.04 eV and LUMO energy levels are in the range of -3.26 - -3.82 eV. Further, these polymers showed the bandgaps ranging from 1.67-2.22 eV. Also, study revealed that the bandgap of the polymer can be tuned by changing the donor strength as well as conjugation path length through structural variations. Since polymers **P8, P9, P13** and **P14** showed very low bandgap, they are potential candidates for solar cell applications. Further, as polymers **P2, P3, P9, P12, P13, P14** and **P20** displayed very low barrier energies ($\Delta E_e - \Delta E_h$) values with balanced electron as well as hole injection behavior, these polymers are expected to provide enhanced charge-carrying properties for the development of efficient PLEDs. In conclusion, donor-acceptor approach with appropriate donor and acceptor moieties is a very good tool to tune the electrochemical properties of the polymers required for different applications in the field of photonics.

Abstract

This chapter comprises linear and nonlinear optical characterization of new polymers P1-P20. It involves study of both solution phase absorption and fluorescence emission behavior of the polymers. Also it encompasses the solvatochromic studies of selected polymers in their solution state. In addition, it explains the nonlinear behavior of the polymer. A detailed discussion on results of their optical studies has been presented here.

6.1. LINEAR OPTICAL PROPERTIES

Linear optical techniques involve the study of interaction of electromagnetic radiation with the sample. Among various optical techniques, UV-vis absorption spectral study is important, as it provides valuable information regarding material property. It is well-established that study of interaction between polymeric materials and light is essential for their optical characterization. The fluorescence spectroscopy deals with electronic transitions from the excited state to the ground state, while absorption spectroscopy involves the electronic transitions from ground state to the excited state. The results of linear optical studies are useful to evaluate the important parameters like optical band gap and fluorescent quantum yield of the polymers. These are valuable parameters for selecting such polymers for optoelectronic device applications.

6.1.1. UV-visible absorption and fluorescence emission spectral studies of polymers P1-P20

Generally, the observed electronic transitions in absorption spectroscopy of conjugated polymers are attributed to electronic excitation from π to π^* states while transitions in emission spectroscopy is due relaxation from π^* to π states. Upon electronic excitation of the polymer by photons, a number of photo-physical processes take place, viz. fluorescence, phosphorescence, or radiation-less decay, which result in acquisition of some interesting photonic properties.

Fluorescence is an optical phenomenon that explains the behavior of a material under the irradiation of photon. In principle, when a photon is incident on a conjugated polymer molecule, if its energy matches with the bandgap energy of polymer, that photon can be absorbed under the formation of an electron-hole pair

(exciton) (**Figure 6.1**). After the absorption of the photon, polymer reaches to the excitation state (Frank-Condon principle), then the excited molecule relaxes to the lowest energy level to attain stability (Bassler et al. 2003 and Arkhipov et al. 2004). After a short span of time, when the formed exciton diffuses to a certain distance, it recombines and decays, either radiatively under the emission of a photon (in a process called fluorescence) or non-radiatively as heat. Emission processes in conjugated polymers are schematically represented in **Figure 6.1**.

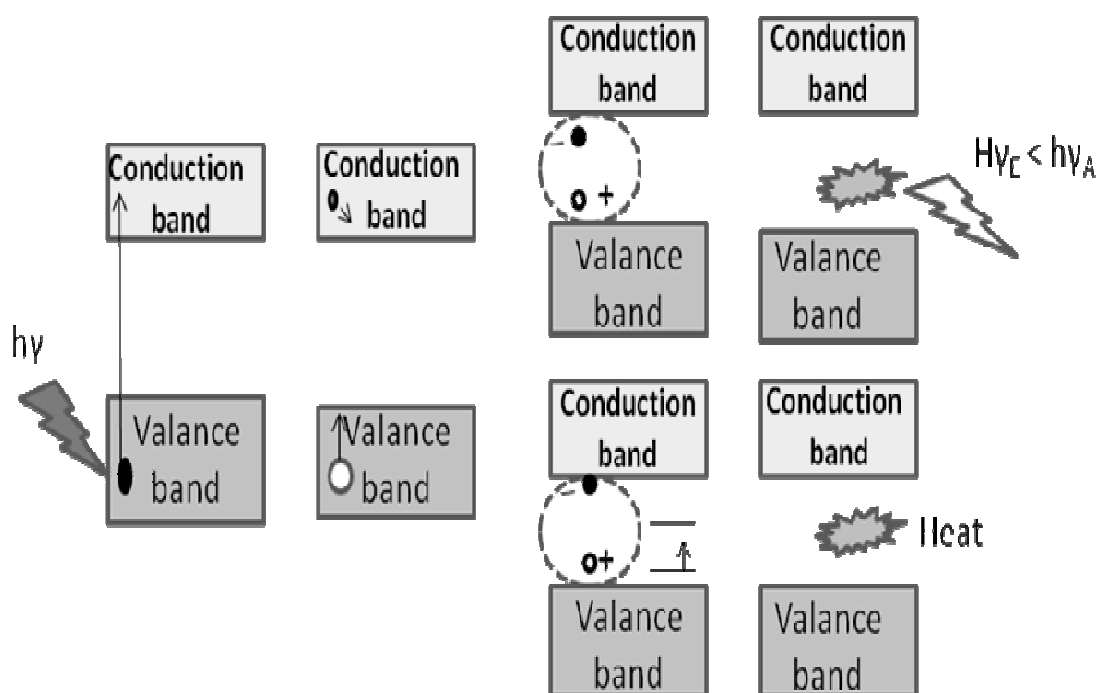


Figure 6.1: Fluorescence emission process in conjugated polymers

6.1.1.1. Instrumentation, materials and methods

The UV-visible spectra of polymers **P1-P20** were measured using Perkin Elmer Lambda-750 UV-visible spectrophotometer and Ocean optics fiber optics spectrometers. The absorption of these polymers was recorded at lab temperature in dilute THF (analytical grade) solutions. Fluorescence emission spectra of polymers **P1-P20** were recorded using Jasco FP-2600 spectrofluorometer. Studies were carried out in dilute THF solutions (10^{-5} M). The emission spectra were obtained by irradiative excitation at the wavelength of their absorption maxima. The fluorescence quantum yields of the polymers were calculated against the standard, viz. quinine sulfate, by taking quantum yield of quinine sulfate in 0.1 M H_2SO_4 as 58%. Selected

polymers were subjected to solvatochromic studies in different polar solvents in order to explore their variable fluorescence behavior.

6.1.1.2. Results and discussion

The linear optical properties of the polymers were studied by UV-visible absorption and fluorescence emission spectroscopic techniques. Spectra of the polymers of **Series 1, 2, 3, 4** and **5** are given in **Figures 6.2, 6.3, 6.4, 6.5** and **6.6**, respectively and their analysis data are summarized in **Table 6.1**. Series-wise spectral results are discussed in the following section.

Polymers **P1-P5** (Series 1)

The UV-visible absorption and fluorescence emission spectra of polymers **P1-P5** are provided in **Figures 6.2a** and **6.2b**. Polymers **P1-P5** showed higher absorption and emission maxima than those of thiophene-oxadiazole based D-A type conjugated systems reported in the literature. This is mainly due to introduction of various electron donating moieties such as thiophene, naphthyl, isophthalyl, vinylenyl and pyrazole units along the polymer backbone, which results in increase in conjugation and reduction in steric hindrance of the bulky alkoxy side chains (Andersson et al. 1999).

Among five polymers, **P1** showed the highest absorption and emission maxima because in **P1** un-substituted thiophene is present as electron donating moiety as well as conjugated spacer, which is a stronger donating moiety than that of naphthyl, phenyl, pyrazole or vinylenyl moiety. Generally, the introduction of thiophene unit along a polymeric backbone leads to the enhancement in its conjugation path length (Cho et al. 2002). This results in broadening of conduction and valence band and hence it leads to red shift in absorption maxima as well as emission maxima of the resulting polymer. Also, it is observed that increase in the donor strength has led to enhancement in the absorption as well as emission maxima of polymers of the series. Also, polymers showed high quantum yields; this could be attributable to the rigid structure of the polymer in which relaxation from the excited state through non-radiative (E.g. thermal) processes is less.

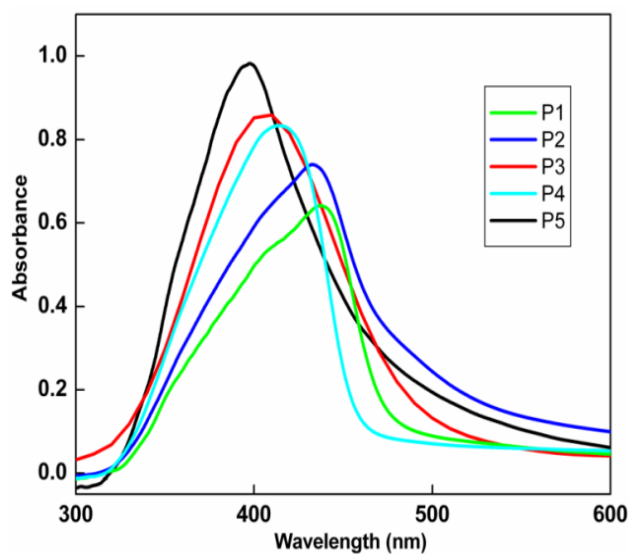


Figure 6.2a: UV-vis absorption spectra of polymers **P1-P5** in THF solution

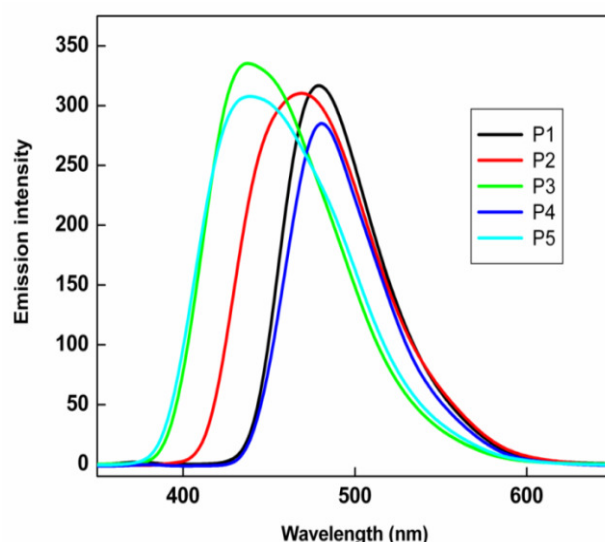


Figure 6.2b: Fluorescence emission spectra of polymers **P1-P5** in THF solution

Polymers **P6-P10** (Series 2)

The UV-vis absorption and fluorescence emission spectra of polymers **P6-P10** are given in **Figures 6.3a** and **6.3b**. UV-vis absorption spectra, polymers **P6-P10** showed broad absorption in the range of 300-600 nm. The absorption/emission maxima of polymer **P7** is greater than that of **P6** because of the presence of electron donating carbazole unit in **P7**. Due to its bent structure, it has enhanced the photochemical properties of polymer **P7** (Grazulevicius et al. 2003). Also, **P8** showed the highest absorption as well as emission maxima in this series owing to the

enhanced D-A nature of it by the presence of strong electron donating 3,4-dialkoxy thiophene units. Polymer **P9** displayed higher absorption maxima than that of polymer **P7**, because it contains highly electron donating tricyclic phenothiazine ring, which is a stronger electron donating moiety than carbazole. It is observed that absorption maxima of polymers **P6-P10** has redshifted with the increase in the donor strength (phenyl < carbazole < diphenylamine < phenothiazine < 3,4-dialkoxythiophene). As donor strength increases, the delocalization also increases thereby causing red shift in its spectrum. Amongst **P6-P10**, phenothiazene based conjugated polymer **P9** showed the highest emission maxima. In this series of polymers, **P10** showed good fluorescence quantum efficiency due to the presence of highly fluorescent diphenylamine unit along the polymer backbone.

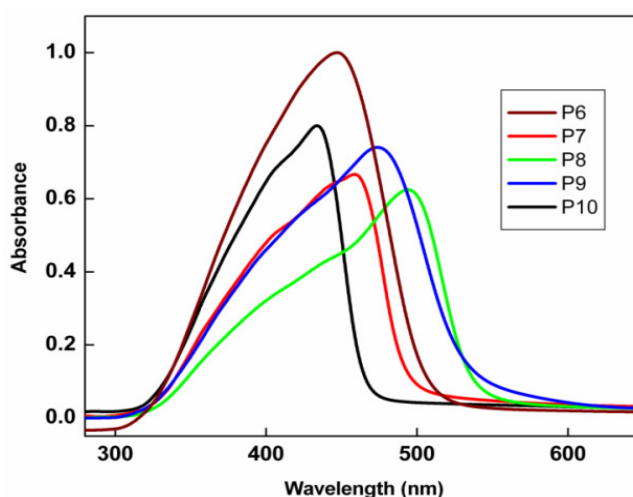


Figure 6.3a: UV-vis absorption spectra of polymers **P6-P10** in THF solution

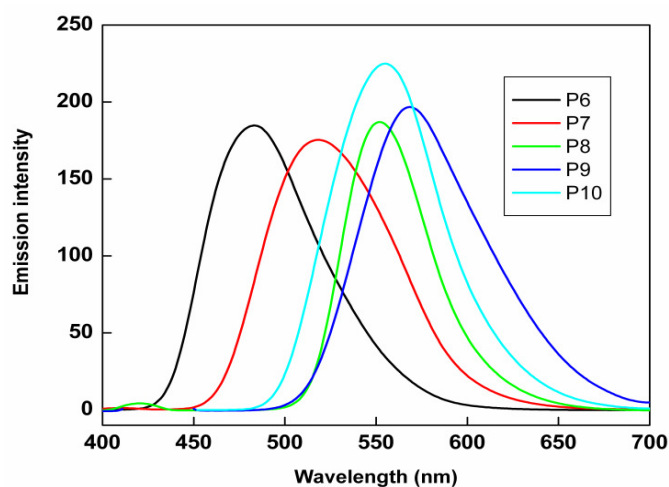


Figure 6.3b: Fluorescence emission spectra of polymers **P6-P10** in THF solution

Polymers P11-P14 (Series 3)

UV-vis absorption and fluorescence emission spectra of polymers **P11-P14** are depicted in the **Figures 6.4a** and **6.4b**. It is observed that polymers **P11** and **P14** showed almost same absorption/emission maxima, which is mainly attributed to the presence of electron withdrawing 1,3,4-oxadiazole and cyanopyridine moieties, respectively. Amongst this series, polymer **P12** showed the lowest absorption and emission maxima; this may be ascribed to the presence of nitrogen bridge containing diphenylamine units along the polymer strands. Polymer **P13** displayed the highest absorption/emission maxima due to the presence of strong electron withdrawing cyanovinylene units along the polymeric backbone (Waltman et al. 1983). The results indicate that on increasing donor and acceptor strength in the polymer backbone, there is significant enhancement in the absorption as well as emission maxima of the resulting polymers. The broad absorption spectrum of **P13** indicates that it is a suitable candidate for the preparation of polymer solar cells.

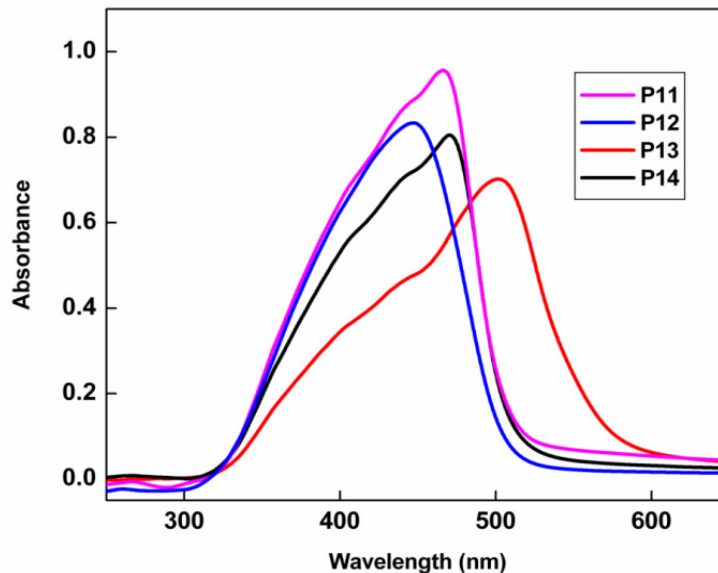


Figure 6.4a: UV-vis absorption spectra of polymers **P11-P14** in THF solution

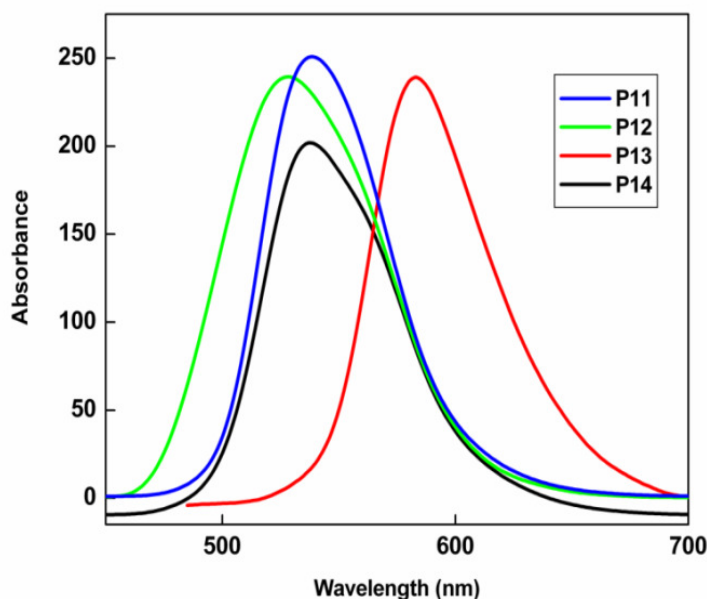


Figure 6.4b: Fluorescence emission spectra of polymers **P11-P14** in THF solution

Polymers P15-P16 (Series 4)

UV-vis absorption and fluorescence emission spectra of polymers **P15** and **P16** are depicted in **Figures 6.5a** and **6.5b**. Polymers of this series showed high absorption maxima when compared to the poly(amide)s reported in the literature. This is due to the presence of strong D-A nature induced by the 3,4-dialkoxythiophene and 1,3,4-oxadiazole moieties along the backbone. Also, polymer **P16** displayed a red shift of 15 nm when compared to that of polymer **P15**, which is attributed to the enhancement in conjugation path length brought about by the additional phenyl ring containing carbonyl functionality. Further, these polymers were found to be strongly emissive with high quantum yields. This could be attributable to the rigid structure of the polymeric backbone tendered by the introduction of cyclic imides. Because of this, relaxation from the excited state through non-radiative (e.g., thermal) processes has been reduced resulted in higher fluorescence quantum yield. Hence, these polymers are potential candidates for their applications in electroluminescent devices.

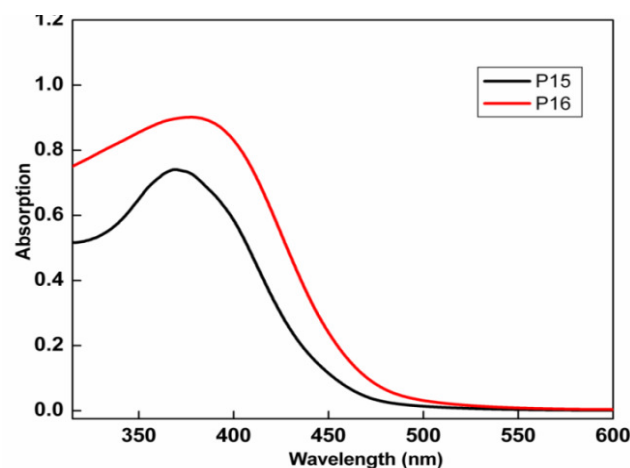


Figure 6.5a: UV-vis absorption spectra of polymers **P15-P16** in THF solution

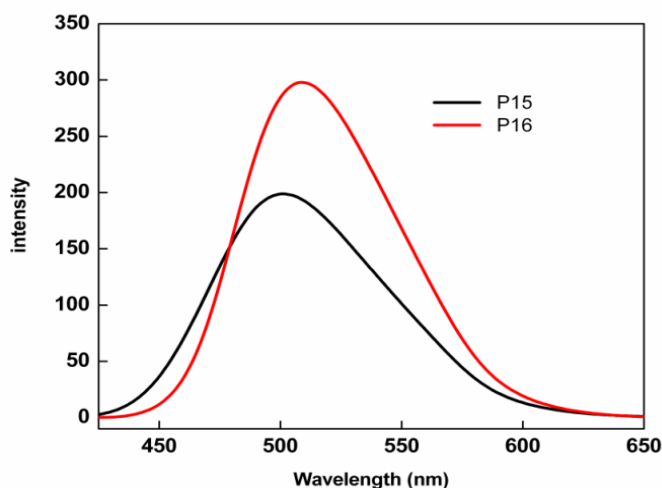


Figure 6.5b: Fluorescence emission spectra of polymers **P15-P16** in THF solution

Polymers **P17-P20** (Series 5)

Records of UV-visible absorption and fluorescence emission spectra of polymers **P17-P20** are given **Figures 6.6a** and **6.6b**. The spectral data indicate that their absorption maxima (λ_{max}) increased in the order of the donor strength, i.e. isophthalyl < phenyl < diphenylamine < didodecyloxythiophene, respectively. It is well documented that insertion of thiophene in the conjugated segments results in better conjugation which in-turn enhances the absorption maxima (Rao et al. 1993 and 1994). Therefore, polymer **P20** showed the highest absorption maxima amongst polymers **P17-P20**. Also, polymers of the series showed good fluorescence emission behavior with high fluorescence quantum yield. Here, the observed fluorescence property is due to the existence of photo-induced intramolecular charge transfer (ICT)

phenomenon from the donor (3,4-dialkoxythiophene) to the acceptor (1,3,4-oxadiazole) moieties in their structure, which in-turn enhances the donor-acceptor strength of the macromolecular system (Wu et al. 2006 and Qin et al. 2007). Also, the presence of bulky alkyl/alkoxythiophene groups in between oxadiazole facilitates to attain trans form resulting in improved planarity and rigidity in the resulting polymer chains. Furthermore, presence of imine (-C=N-) functionality along the backbone has enhanced its fluorescence property. It is observed that polymers **P17**, **P18** and **P20** showed almost same emission maxima, while polymer **P19** displayed a blue shift which may be attributed to the less rigidity of the core structure containing diphenylamine moiety.

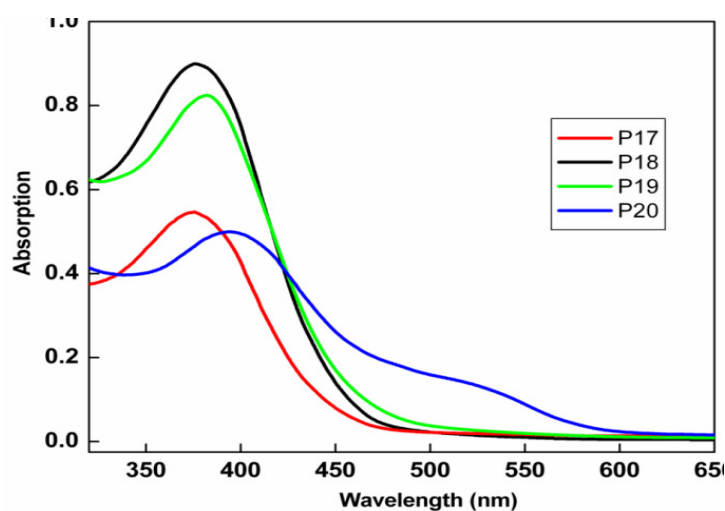


Figure 6.6a: UV-Vis absorption spectra of polymers **P17-P20** in THF solutions

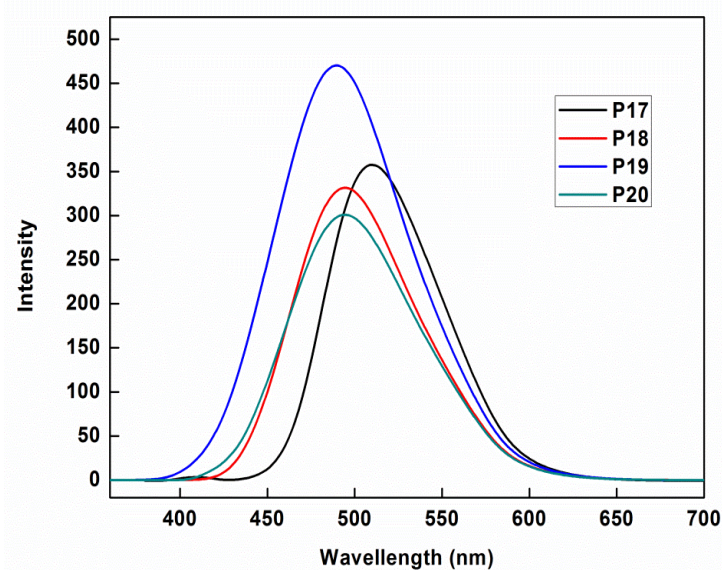


Figure 6.6b: Fluorescence emission spectra of polymers **P17-P20** in THF solutions

Table 6.1 Linear optical characterization data of polymers **P1-P20**

Sl. No	Polymers	UV-visible absorption maxima in THF (in nm)	Fluorescence emission maxima in THF (in nm)	Quantum Yields *
1	P1	437	487	38 %
2	P2	433	468	35 %
3	P3	413	435	30 %
4	P4	407	480	32 %
5	P5	397	436	30 %
6	P6	434	484	36 %
7	P7	458	517	42 %
8	P8	494	551	38 %
9	P9	474	567	41 %
10	P10	472	570	44 %
11	P11	431	538	35 %
12	P12	448	536	39 %
13	P13	502	582	42 %
14	P14	471	538	44 %
15	P15	368	511	29 %
16	P16	378	501	31 %
17	P17	374	496	36 %
18	P18	379	505	38 %
19	P19	384	492	44 %
20	P20	396	495	40 %

*Quantum yield relative to quinine sulfate (10^{-5} M quinine sulfate in 0.1 M H_2SO_4)

6.1.2 Solvatochromism study of cyanopyridine based polymers (P6-P10)

The term solvatochromism is used to describe the change in position and sometimes intensity of UV-visible absorption and fluorescence emission spectra with a change in polarity of the solvent in which the polymer is dissolved. Generally, solvatochromism is induced by a conformational change in the conjugated polymer backbone driven by both intra-chain steric hindrance and inter-chain interactions (attractive interactions, π - π interactions, excitons etc.) that accompany the formation

(or disruption) of small aggregates (Politis et al. 1999). This conformational change leads to a modification of the effective conjugation length, which induces optical shifts in conjugated polymers. Also, conformational changes in the backbone enhance the planarity, which induces red-shift of the absorption as well as emission maxima. In fact, solvatochromic properties of the polymers are quite useful to explore their applications in the field of sensors as well as smart materials (Bernier et al. 2002).

For the solvatochromic study of the polymers, the same experimental set up as described for the fluorescence measurements was employed. Here, polymers were dissolved in different polar solvents (CHCl_3 , THF, DMF and DMSO) at same concentration and fluorescence emission spectra of them were recorded at room temperature. Cyanopyridine based polymers were used for the study because of their excellent fluorescent behavior. The results of the study are summarized in **Table 6.2** and their spectra are depicted in **Figures 6.7a** and **6.7b**.

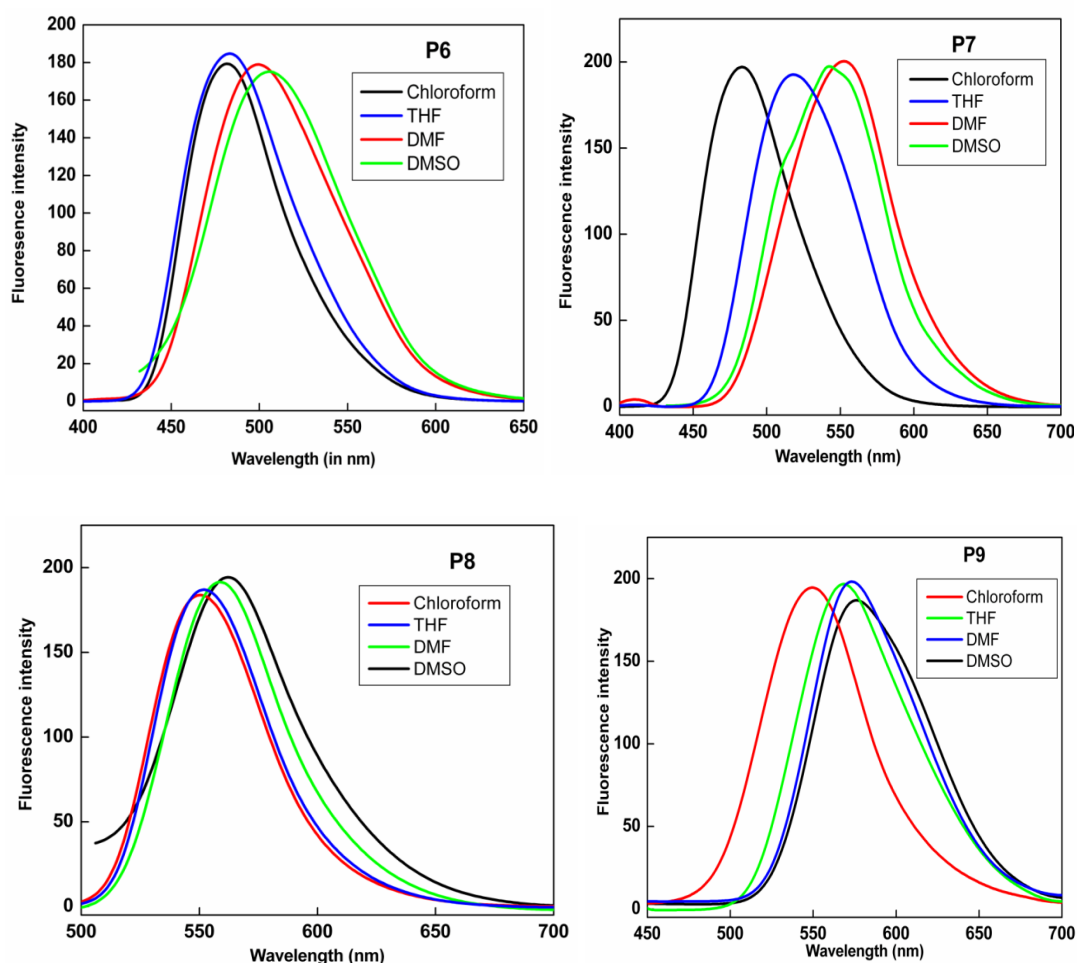


Figure 6.7a: Fluorescence emission spectra of **P6** and **P9** in different polar solvents

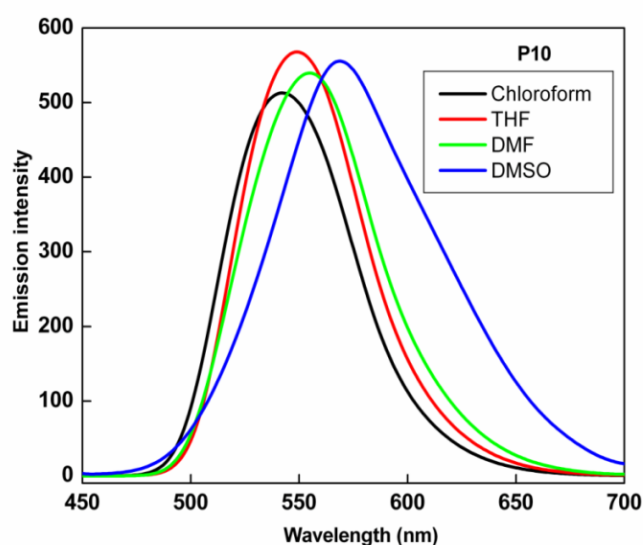


Figure 6.7b: Fluorescence emission spectra of **P6-P10** in different polar solvents

The polymers showed strong solvatochromic effect in different polar solvents (chloroform (CHCl_3), tetrahydrofuran (THF), dimethylformamide (DMF) and dimethylsulfoxide (DMSO), because of the presence of highly fluorescent cyanopyridine ring in their structure (Alessandro et al. 1997). From the results, it is observed that emission maxima of the polymers were red shifted as the polarity of the solvent was increased. The solvatochromism can be explained on the basis of their electronic transitions across various energy levels. In highly polar solvent such as DMF and DMSO, the emissive S_1 state of intra-molecular charge transfer (ICT) is strongly solvated and its energy is hence dramatically lowered. Consequently, the energy gap between excited states (S_1 , S_2) and the ground state is enlarged so that the coupling of the S_1 state directly to the ground state stays opened and the intersystem crossing from S_1 to T state is enhanced. The high electron releasing character of carbazole, thiophene, phenothiazine and diphenylamine moieties lead to a red shift (lower energy) of the emission relative to the absorption. This phenomenon is caused by energy losses due to dissipation of vibrational energy during the decay. In fact, solvatochromic effect is influenced by interaction between the fluorophore and the solvent molecules through the excited dipole, hydrogen bonding or formation of charge complexes.

Among the polymers studied, carbazole containing conjugated polymer **P7** showed maximum solvatochromic behavior, i.e, 68 nm red shift in emission maxima from chloroform solution to DMSO solution. This is mainly attributed to the bent structure of the fluorescent carbazole unit in polymer backbone.

Table 6.2 Solvatochromic behavior of polymers **P6-P10**

Sl. No	Polymers	Fluorescence in different polar solvents (nm)			
		CHCl ₃	THF	DMF	DMSO
1	P6	481	484	499	505
2	P7	484	517	541	552
3	P8	550	551	558	562
4	P9	549	567	573	575
5	P10	540	548	555	570

6.2. NONLINEAR OPTICAL PROPERTIES

In recent years, a great deal of interest has been focused on the synthesis of novel π -conjugated polymers, because of their intriguing third-order non-linear optical properties. In addition, the search for novel nonlinear optical (NLO) materials have found a new horizon with the development of organic materials since they have the advantages of synthetic flexibility, high damage resistance and large optical nonlinearities. More efforts have been focused on the third-order NLO properties particularly of D-A type polymeric molecules, which are promising materials for photonic switching and optical limiting applications. Since these molecules typically possess delocalized π -electrons, they are believed to be a potential source of fast nonlinearity.

6.2.1 Z-scan technique

The “open aperture” Z-scan is normally used for measurement of nonlinear optical properties. The technique is particularly useful when the nonlinear refraction is accompanied by nonlinear absorption. The technique relies on the principles of self focusing and defocusing of an optical beam by a thin medium. In this technique a

Gaussian laser beam is used for molecular excitation, and its propagation direction is taken as the z axis. The beam is focused using a convex lens, and the focal point is taken as $z = 0$. The experiment is done by placing the polymer solution in the beam at different positions with respect to the focus and measuring the corresponding transmission. The beam will have maximum energy density at the focus, which will symmetrically reduce towards either side of it. For the positive and negative values of z , sample experiences different laser intensity at each z position. Here the medium acts like an intensity dependent thin lens. As polymeric sample moved along the path, its effective focal length will be changed since the light intensity within the sample is changing. This change will be reflected in the optical power measured at the aperture in the far field. A schematic representation of Z-scan set up is given in the **Figure 6.8**.

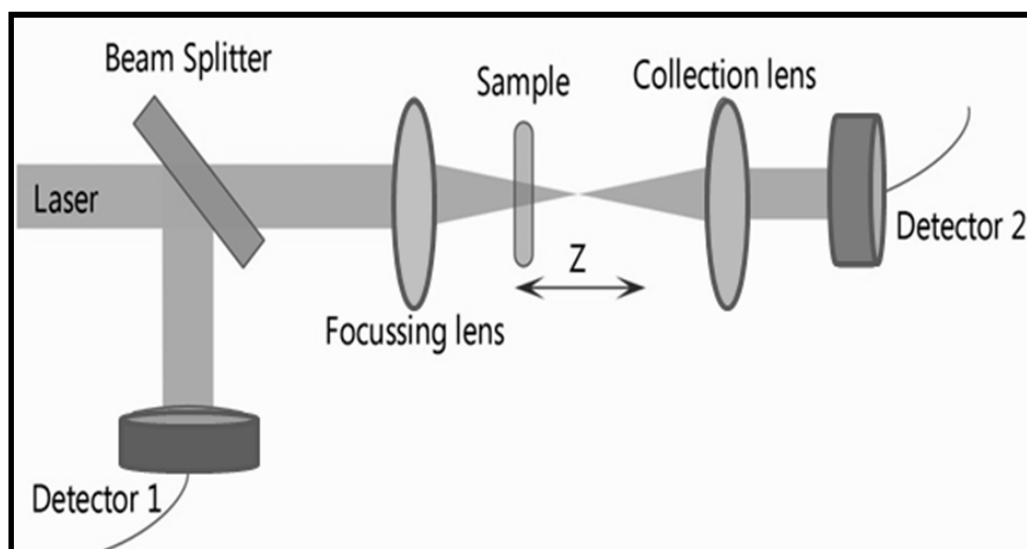


Fig 6.8: Experimental setup of Z-scan technique

6.2.2 Instrumentation, materials and method

In the present study, the second harmonic output from a Q-switched Nd:YAG nanosecond laser (Quanta Ray, Spectra Physics) was used for the measurements. The laser used has a nominal pulse width of 7 nanoseconds and laser pulse energy of 15 micro joules was used for the experiments. The output of the laser possessed almost a Gaussian Intensity profile. The sample was taken in a 1 mm cuvette. The transmission of the sample at each point was measured by means of two pyro-electric energy probes (Rj7620, Laser Probe Inc.). One energy probe monitors the input energy, while

the other monitors the transmitted energy through the sample. The pulses were fired in the “single shot” mode, allowing sufficient time between successive pulses to avoid accumulative thermal effects in the sample (Sheik-Bahae et al. 1990).

All NLO measurements were carried out in the solutions state at room temperature. The polymers were dissolved in NLO inactive organic solvent (THF) and used for the study. The concentration of the samples has a linear transmission of about 60-70% at the excitation wavelength. Therefore, strong two-step excited state absorption will happen along with weak genuine two-photon absorption (TPA) in the present case. The net effect is then known as an “effective” TPA process. The nonlinear transmission behavior of the present samples can therefore be modeled by defining an effective nonlinear absorption coefficient $\alpha(I)$, given by

$$\alpha(I) = \frac{\alpha_0}{1 + \left(\frac{I}{I_s}\right)} + \beta I \dots \dots \dots \text{(Eq 6.1)}$$

where α_0 is the unsaturated linear absorption coefficient at the wavelength of excitation, and I_s is the saturation intensity (intensity at which the linear absorption drops to half of its original value). β is the effective TPA coefficient. For calculating the output laser intensity for a given input intensity, first we numerically evaluated the output intensity from the sample for each input intensity by solving the propagation equation,

$$\frac{dI}{dz'} = - \left[\left(\frac{\alpha_0}{1 + \frac{I}{I_s}} \right) + \beta I \right] I \dots \dots \dots \text{(Eq 6.2)}$$

using the fourth order Runge-Kutta method. Input intensities for the Gaussian laser beam for each sample position in the Z-scan were calculated from the input energy, laser pulse width and irradiation area. Here ‘z’ indicates the propagation distance within the sample. The normalized transmittance is then calculated by dividing the output intensity by the input intensity and normalizing it with the linear transmittance. Further the intensity of the light coming out from the polymeric solution at various laser intensities were plotted against position of the sample gives us open aperture Z-scan traces. Furthermore, these values were fitted to the theoretical equations to obtain effective TPA coefficients (β). There was good agreement between the experimental data and numerical simulation for polymers **P1-P20**. The approximate energy of the

laser was made around 100 mJ. Polymers under the study showed reverse saturable absorption with two-photon absorption process.

6.2.3 Results and discussion

The results of third order nonlinear optical studies of polymers **P1-P20** are discussed in the following section.

Nonlinear optical properties of polymers **P1-P5** (Series 1)

The two-photon absorption (TPA) coefficients of the polymers **P1**, **P2**, **P4** and **P5** were found to be 0.181×10^{-10} , 0.110×10^{-10} , 0.210×10^{-10} and 22.652×10^{-10} m/W respectively. These values of effective TPA coefficient values are comparable to those of good NLO materials like copper (Cu) nanocomposite glasses (10^{-10} to 10^{-12} m/W, Karthikeyan et al. 2008), functionalized carbon nanotubes (3×10^{-11} m/W, Nan et al. 2009), bismuth (Bi) nanorods (0.53×10^{-10} m/W, Sivaramakrishnan et al. 2007) and cadmium sulphide (CdS) quantum dots (1.9×10^{-9} m/W, Kurian et al. 2007). Also, many π -conjugated polymers showed similar TPA coefficients (Samoc et al. 2000) in the order of 10^{-10} m/W.

In conjugated polymeric system, electrons can move in large molecular orbitals which results from the linear superposition of the carbon p_z atomic orbitals, leading to a very high optical nonlinearity, which increases with the conjugation length. In polymers **P1-P5** introduction of strong electron accepting 1,3,4-oxadiazole along with electron releasing 3,4-dilakoxythiophene units significantly enhanced NLO response because of its increased D-A strength (Cassano et al. 2001). The enhanced third order nonlinearity in **P1-P5** is due to the high electron density along the polymer backbone which is easily polarizable as a result of D-A type of arrangements. Further, the incorporation of electron releasing thophene, naphthalene, phenyl, vinylene, and pyrazole units enhanced the electron donating ability as well as conjugation path length. Introduction of such chromophores along the chain enhanced the optical nonlinearity of the system. Amongst the studied polymers, **P5** showed the highest optical limiting efficiency with two-photon absorption process. This enhancement may be attributed to presence of the pyrazole nucleus which is a good electron donating hetero-cycle. In this molecule, presence of lone pair on the nitrogen atom participates in the enhancement of conjugation which leads to the improvement

in the molecular hyperpolarizability. The graphical representation of open aperture Z-Scan traces of polymers **P1**, **P2**, **P4** and **P5** is depicted in **Figures 6.9a** and **6.9b**, respectively.

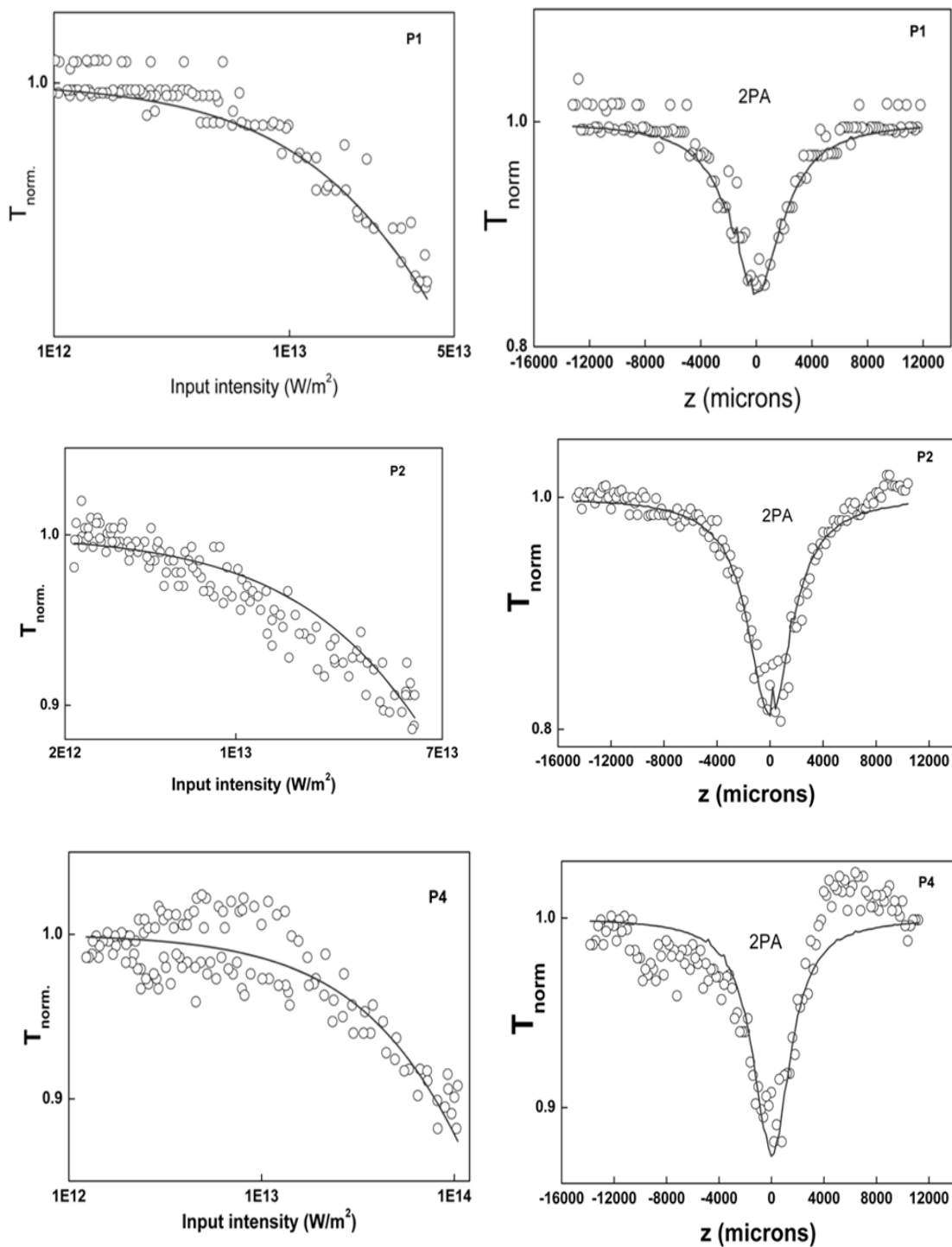


Figure 6.9a: Open aperture Z-scan traces of polymers **P1**, **P2** and **P4**

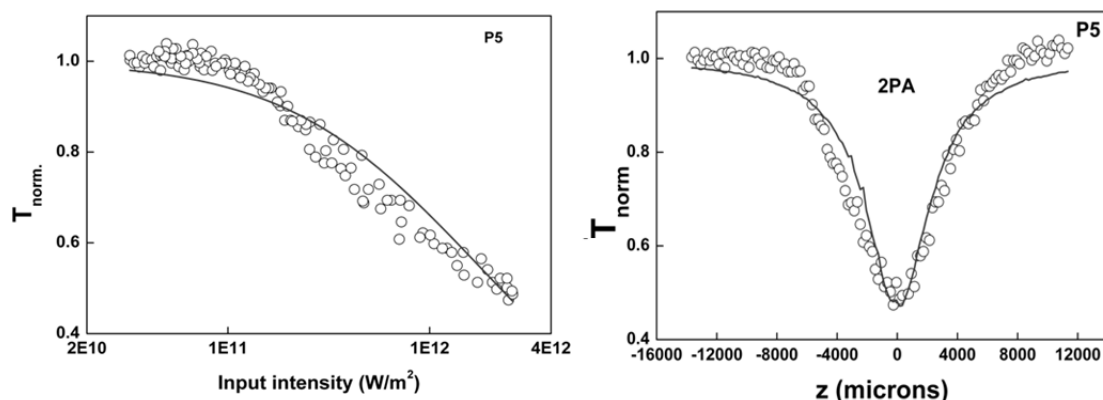


Figure 6.9b: Open aperture Z-scan trace of polymer **P5**

Nonlinear optical properties of polymers **P6-P10** (Series 2)

The experimentally measured TPA coefficients of the polymers **P6**, **P7**, **P8**, **P9** and **P10** were found to be 0.134×10^{-10} , 0.124×10^{-10} , 0.304×10^{-10} , 0.185×10^{-10} and 0.212×10^{-10} m/W, respectively. These values are almost same as those of good optical limiting materials reported in the literature. The results are comparable to that of functionalised carbon nanotubes (3×10^{-11} m/W) and some of dye functionalized polymers (Samoc et al. 2000). Introduction of electron deficient cyanopyridine in between highly electron donating moieties has enhanced the D-A strength of the resulting polymers and hence extent of delocalization in the chain. As a result, the optical nonlinearity of polymers **P6-P10** has increased considerably. It is well-known that increase in planarity and rigidity of polymer chain helps to enhance third-order susceptibilities as it optimizes the overlap of π -orbitals, resulting in enhanced electron delocalization. Also, the third-order optical nonlinearity can be enhanced by increasing π -delocalized electron density and the carrier transport (Yu et al. 1989). In the present study polymers **P7** and **P8** showed (Nan et al. 2009) promising optical limiting behavior with increased effective TPA values. The enhanced behavior of polymer **P7** is due to the presence of highly electron-donating alkyl substituted carbazole ring, which brings about rigid structure and bent shape to the resulting polymer chain (Qiu et al. 2006). The maximum NLO property of polymer **P8** is mainly attributed to the presence of highly electron donating 3,4-dialkoxythiophene and a strong electron accepting cyanopyridine unit in the polymer chain. Further, presence of extended conjugation, easy polarizability of the molecule due to D-A type arrangement and presence of chromophores are responsible for enhanced optical

nonlinearity in polymer **P8**. The open aperture Z-scan traces of polymers **P6-P10** are depicted in **Figures 6.10a** and **6.10b**.

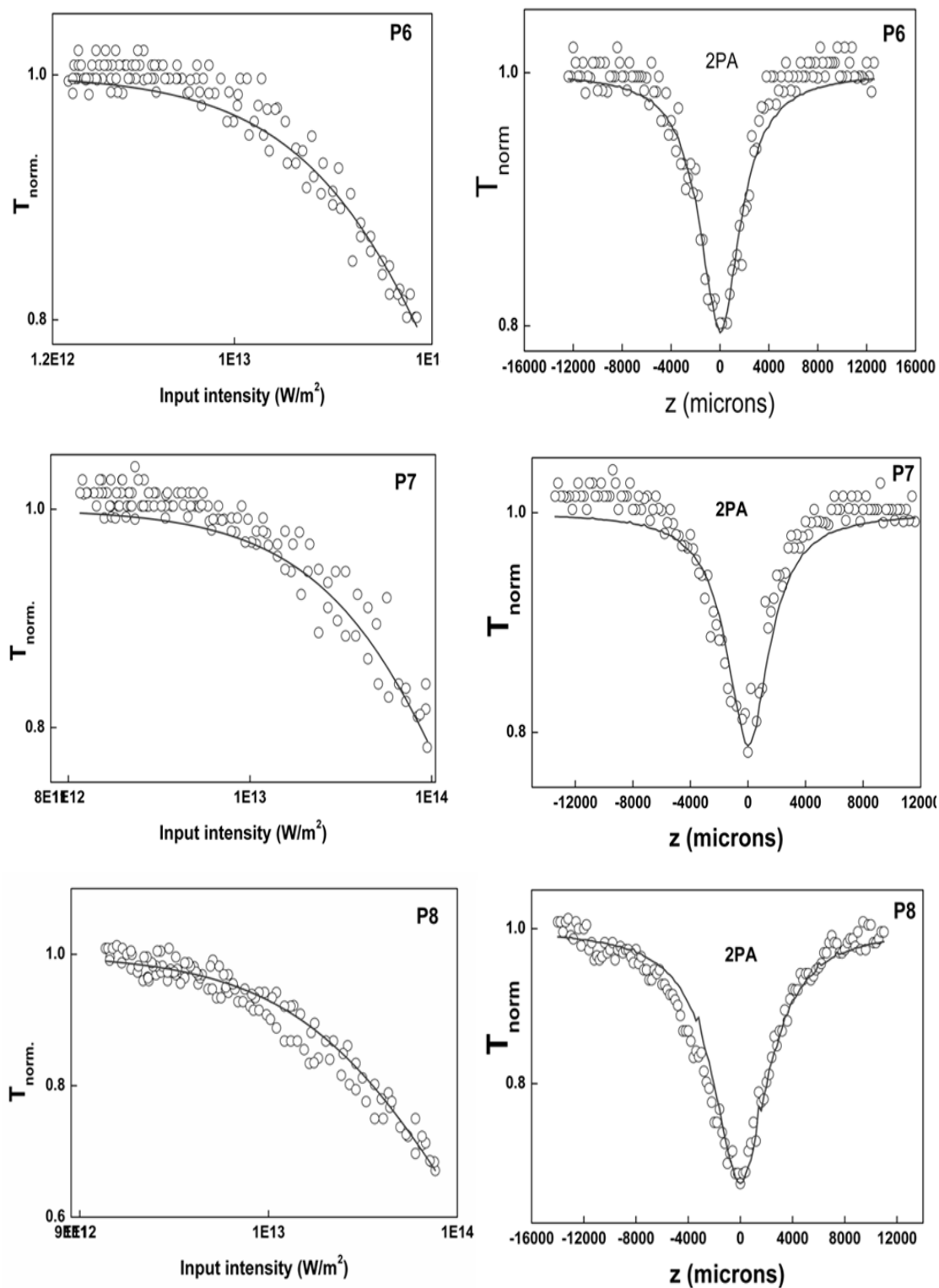


Figure 6.10a: Open aperture Z-scan traces of polymers **P6** and **P8**

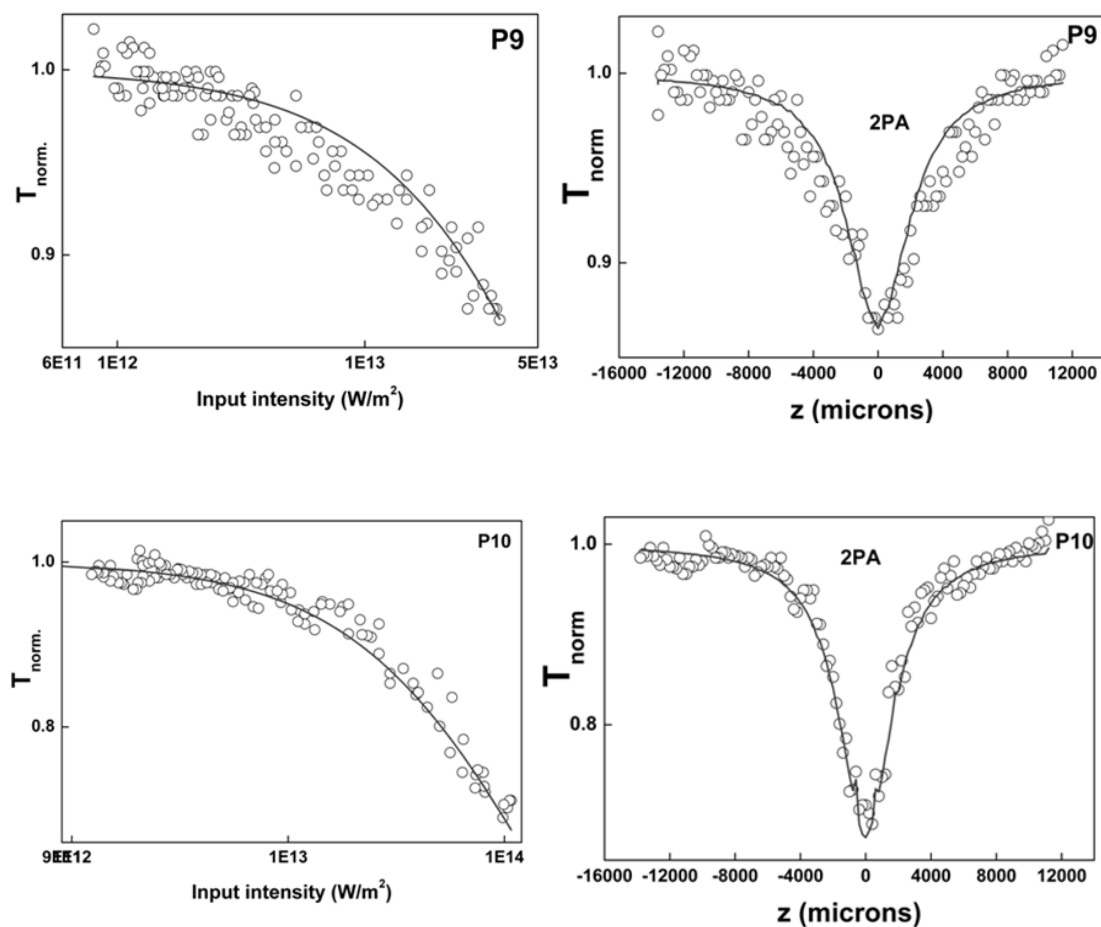


Figure 6.10b: Open aperture Z-scan traces of polymers **P9** and **P10**

Nonlinear optical properties of polymers **P11-P14** (Series 3)

The experimentally measured effective TPA coefficients of polymers **P11**, **P12**, **P13** and **P14** were determined to be 0.300×10^{-10} , 0.645×10^{-10} , 0.091×10^{-12} and 0.210×10^{-10} m/W, respectively. These values are comparable with those of reported polymers (Samoc et al. 2000). Amongst polymers in the series, polymer **P11** showed maximum optical limiting behavior. This is attributed to the enhancement in the conjugation path length with the incorporation of additional thienylvinylene units along the main chain (Pina et al. 2006). Polymer **P14** displayed fairly good TPA coefficient, which is mainly due to the presence of highly electron-withdrawing cyanopyridine unit along the polymer backbone. The occurrence of cyanopyridine moiety in between the thienylvinylene units enhanced the D-A strength of the polymer as well as conjugation path length, when compared to other polymers of the series. The Z-scan traces of polymers **P11- P14** are depicted in **Figure 6.11**.

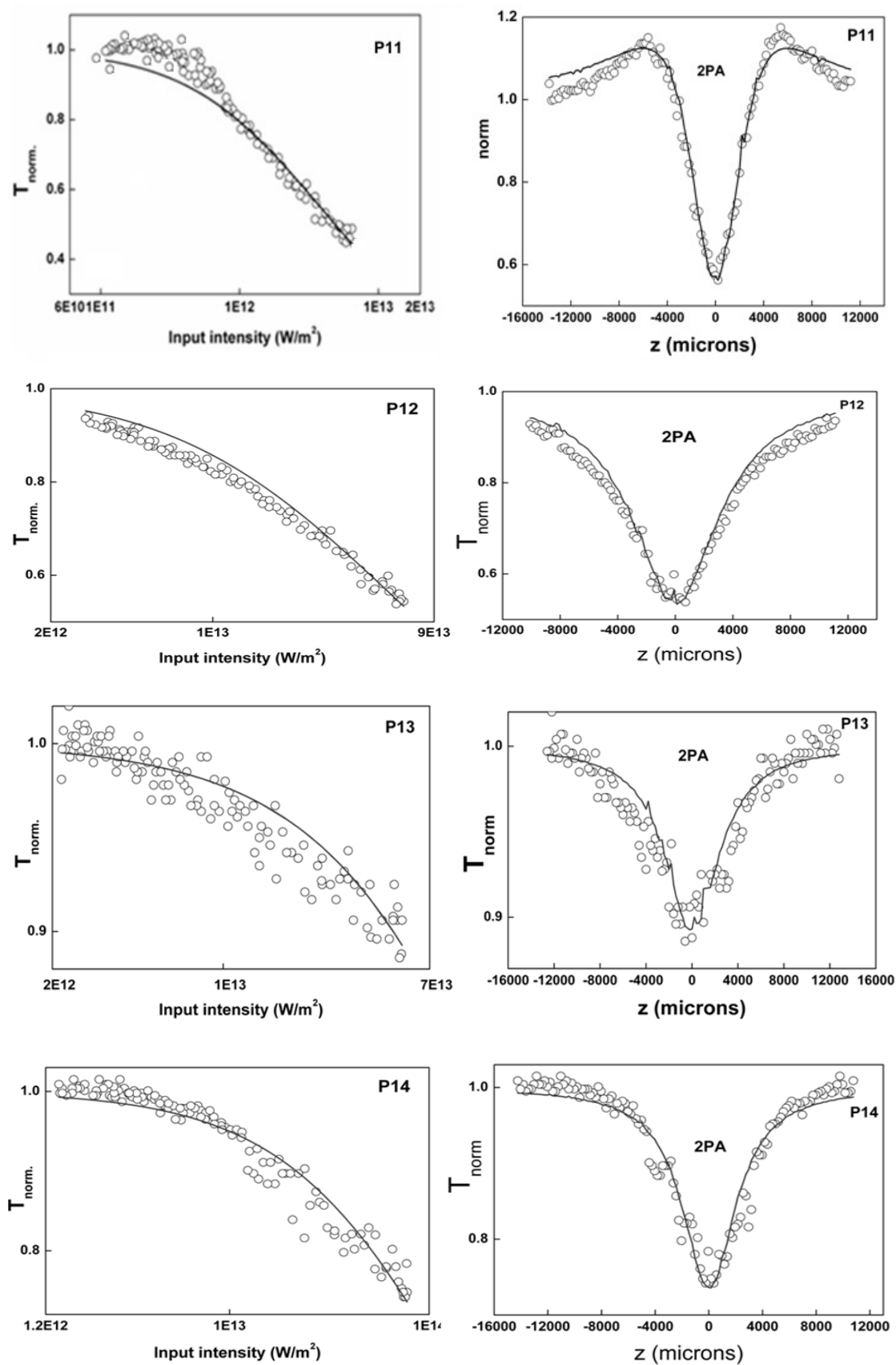


Figure 6.11: Open aperture Z-scan traces of polymers P11-P14

Nonlinear optical properties of polymers P15-P16 (Series 4)

The experimentally measured TPA coefficients of the polymers **P15** and **P16** were found to be 0.343×10^{-10} and 2.031×10^{-10} m/W, respectively. The enhanced nonlinearity of these polymers is mainly attributed to the increase in the conjugation path length due to the presence of sterically rigid cyclic imides (He et al. 2009) and the occurrence of D-A nature in the polymeric back bone (Tembe et al. 2009). These cyclic imides reduced the steric strain between bulky alkoxy side chains of polymer backbone. Further, the presence of highly electron withdrawing oxadiazole unit enhanced molecular hyperpolarizability which in-turn increased the optical limiting behavior of the resulting polyimides (Wang et al. 2008). In conclusion, **P15** and **P16** are good NLO materials, as they fulfill the most of the requirements. The open aperture Z-scan traces of polymers **P15-P16** are depicted in **Figure 6.12**.

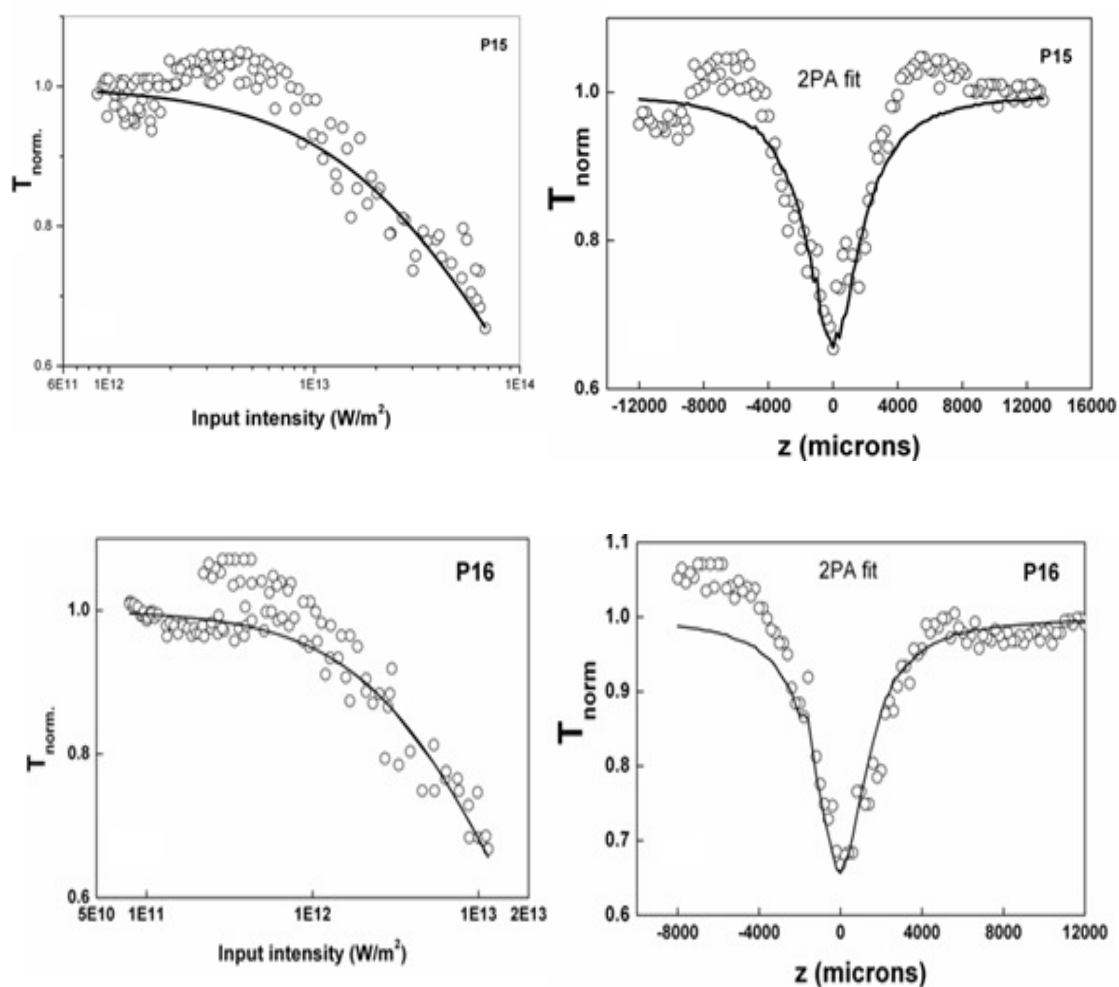


Figure 6.12: Open aperture Z-scan traces of polymers **P15** and **P16**

Nonlinear optical properties of polymers P17-P20 (Series 5)

The experimentally measured effective TPA coefficients of the polymers **P17**, **P18**, **P19** and **P20** were estimated to be 3.401×10^{-10} , 4.402×10^{-10} , 10.402×10^{-10} and 7.312×10^{-10} m/W, respectively. The open aperture Z-scan traces of polymers **P17-P18** and **P19-P20** are depicted in **Figure 6.13** and **Figure 6.14** respectively.

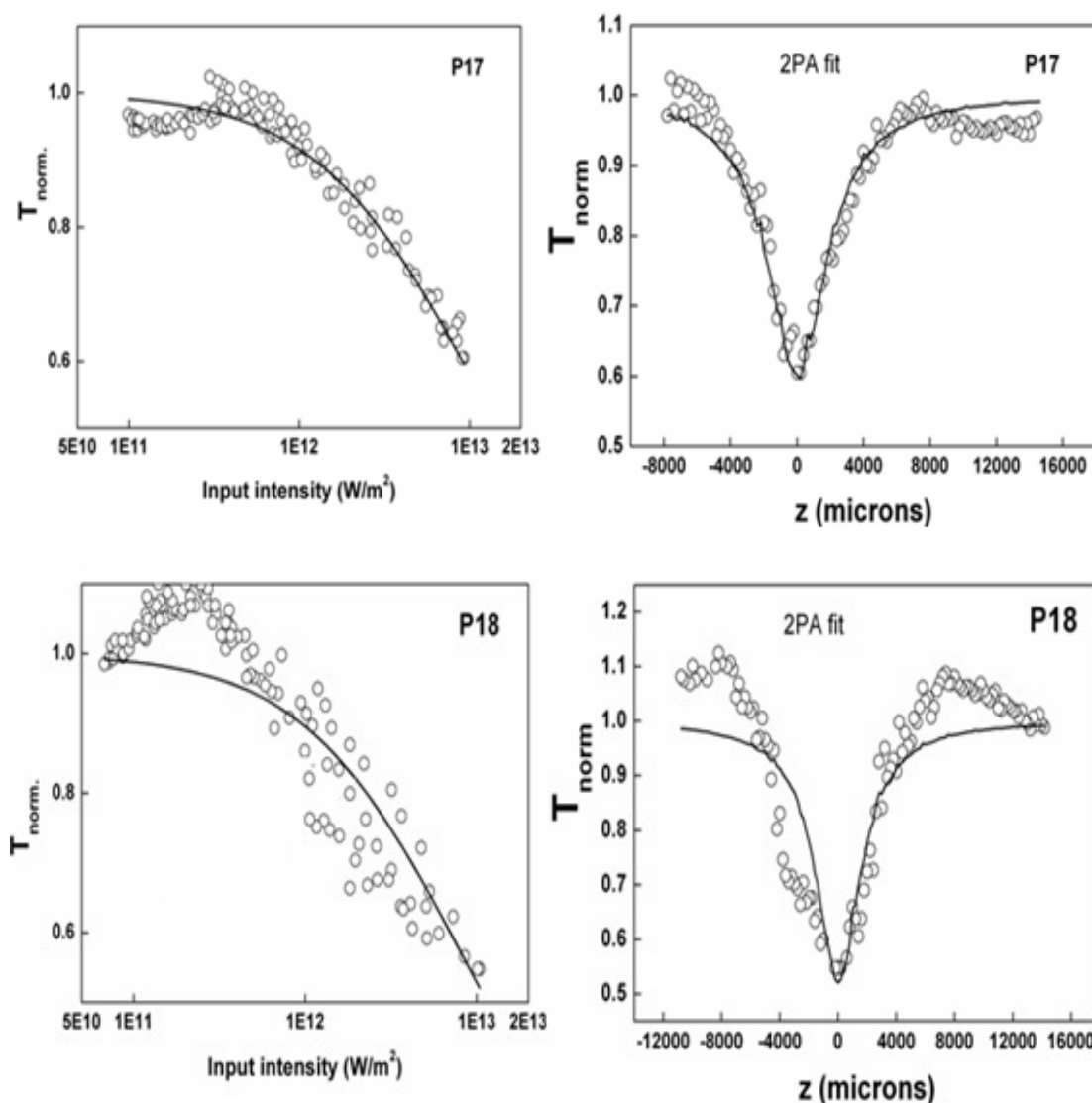


Figure 6.13: Open aperture Z-scan traces of polymers **P17** and **P18**

As discussed earlier, planarity and rigidity of the polymers play an important role in the enhancement of molecular hyper polarizability and hence causes enhancement of the NLO/optical limiting response of the resulting polymers. Polymers of **Series 5** showed good optical limiting behavior compared to that of reported polymers. The observed NLO property is due to the presence of rigid imine

functionality in the chain. Out of studied polymers, **P19** and **P20** showed promising optical limiting behavior with good effective TPA values. The enhanced optical limiting property of polymer **P19** is mainly attributed to the presence of highly electron-donating alkyl substituted diphenylamine ring, which brings about linear structure. The maximum NLO property of polymer **P20** is mainly ascribed to the presence of highly electron donating 3,4-dialkoxy thiophene and a strong electron accepting oxadiazole units in the architecture. In this molecule, presence of strong D-A nature has increased the molecular hyperpolarizability which in-turn enhanced the optical nonlinearity. The open aperture Z-scan traces of polymers **P19-P20** and are depicted in **Figure 6.14**.

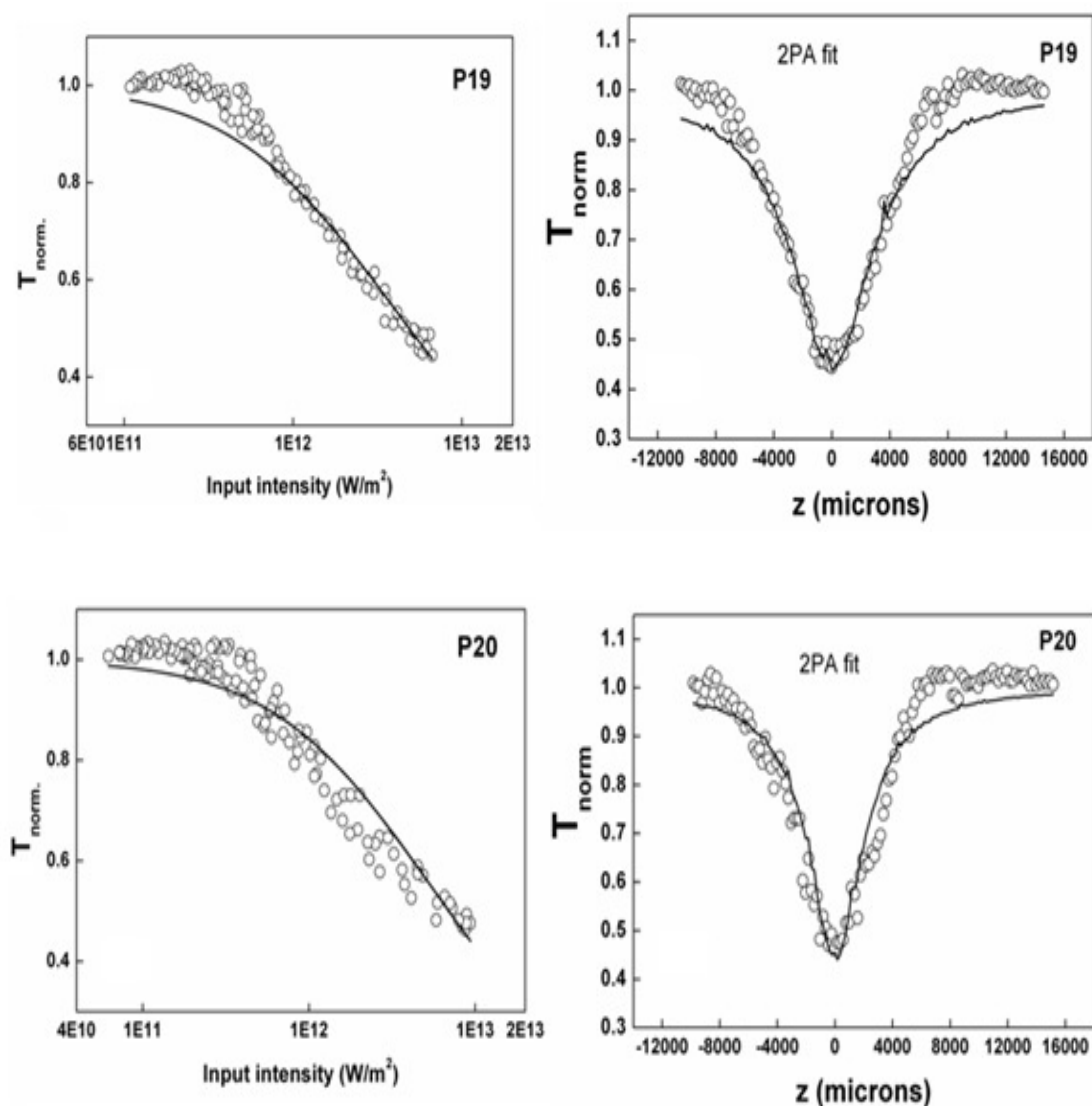


Figure 6.14: Open aperture Z-scan traces of polymers **P19-P20**

6.3 CONCLUSIONS

In summary, the results of linear optical characterization of polymers **P1-P20** indicate that polymer containing cyanovinylene unit (**P13**) displayed the highest absorption maxima of 506 nm and hence it is a potential candidate for its application in solar cells. Further, canopyridine containing polymers **P6-P10** showed good solvatochromic behavior. So, they may be useful as ion sensor materials. Furthermore, third order NLO results of polymers **P1-P20** reveal that most of the studied polymers are good optical limiting materials with enhanced TPA coefficients and the operating mechanism is reverse saturable absorption type. Polymer **P5** with pyrazole unit exhibited the highest optical nonlinearity with high **2PA** coefficient of 22.65×10^{-10} m/W. The observed NLO results are comparable with those of good NLO materials like copper, nanocomposite glasses, bismuth, cadmium sulphide, quantum dots etc. Thus, these polymers are the promising materials for optical limiting device applications.

Abstract

This chapter covers the summary of the entire research work carried out along with important conclusions drawn from the present systematic studies. Scope for the future work has also been included in the end.

7.1. SUMMARY

In recent years, a great deal of interest has been focused on the synthesis of novel π -conjugated polymers, because of their intriguing properties such as electrical conductivity, electroluminescence, third-order non-linear optical properties and chemical sensing. These polymers easily form relatively stable radical cations (holes) and also possess high-charge carrier mobility. As a result, they achieve high thermal as well as photochemical stability. Amongst various classes of conjugated polymers, D-A type polymers are under an extensive investigation in recent years due to their unique optical and electrochemical properties in addition to thermal stability.

During last decade lots of attentions have been dedicated towards the development of new D-A type polymers with desired properties through proper structural modifications. Also, D-A type polymeric materials have been identified as strong candidates for use in a variety of NLO applications. The promise of D-A type NLO active polymers lies in their fortuitous combination of exceptional optical quality, low cost and ease of fabrication into device structures. This juxtaposition of technologically favorable aspect has led to considerable research activities towards the development of new NLO active polymers for commercial applications. Although several D-A type of conjugated polymers were reported in the literature, still there are ample of scopes to explore new D-A type polymers with desired optical and photonic properties.

Based on the literature review, it has been aimed at designing and synthesizing new series of D-A type conjugated polymers with possible applications in photonics. Accordingly, five new series of D-A type conjugated polymers (**P1-P20**) carrying substituted 3,4-dialkoxythiophene, naphthalene, carbazole, phenylenevinylene, diphenylamine, imine and pyrazole as electron donors and 1,3,4-oxadiazole, cyanopyridine, cyanovinylene and cyclic-imide as electron acceptor moieties have been designed.

To obtain newly designed conjugated polymers, seven series of bi-functional monomers have been successfully prepared using appropriate synthetic procedures from simple molecules and structures of new intermediates and monomers have been evidenced using FTIR, ^1H NMR, spectral analysis, followed by elemental analysis. Starting from these monomers following five new series of target polymers (**P1-P20**) have been successfully synthesized and their synthetic protocols have been established.

- (i) Poly(3,4-ditetradecyloxythiophene)s carrying thiophene, naphthalene, isophthalyl, vinyl and pyrazole moieties as π -conjugated spacers (**Series 1, P1-P5**)
- (ii) Poly(cyanopyridines) containing phenyl, carbazole, alkoxythiophene phenothiazine and diphenyl amine based electron donating bridges (**Series 2, P6-P10**)
- (iii) Poly(3,4-ditetradecyloxythiophene)s involving vinylene π -conjugated spacers (**Series 3, P11-P14**)
- (iv) Poly(3,4-ditetradecyloxythiophene)s carrying aromatic conjugated cyclic imides (**Series 4, P15 and P16**)
- (v) Poly(3,4-ditetradecyloxythiophene)s with imine functionalized electron donors as π -conjugated bridges (**Series 5, P17-P20**)

Structures of newly synthesized conjugated polymers **P1-P20** have been established by different spectroscopic techniques. Their molecular weights have been determined by gel permeation chromatography (GPC) technique using polystyrene standards. Further the thermal stability of these polymers has been determined using thermogravimetric analysis. Electrochemical properties of these polymers have been studied using cyclic voltammetric experiments in order to investigate their hole-carrying and electron-transporting properties. The UV-visible absorption and fluorescence emission characteristics of new polymers **P1-P20** have been studied by UV-visible absorption and fluorescence emission spectroscopy. Their fluorescent quantum yields have been estimated. Also, solvatochromic behavior in various polar solvents has been determined using spectrofluorimeter. Finally, third-order NLO properties of new polymers **P1-P20** have been investigated using open aperture Z-scan technique in order to investigate their optical limiting behavior.

7.2. CONCLUSIONS

On the basis of experimental results, following important conclusions have been drawn.

- Based on literature survey, eleven new monomers and twenty new D-A type conjugated polymers **P1-P20** have been successfully designed
- Seven series of required monomers and five series of newly designed D-A type polymers **P1-P20** have been successfully synthesized, their synthetic methods and structures have been established by spectral studies
- Their molecular weights has been estimated to be in the range of 5000-30000, as determined by GPC technique
- The new polymers have been found to be thermally stable up to 300° C. Polymers **P6**, stable up to 340 °C. The extra stability is accounted for the absence of alkyl/alkoxy side-chains in polymer **P6**
- The electrochemical bandgaps of the polymers has been determined to be in the range of 1.6-2.3 eV. Polymer **P9** carrying phenothiazine and cyanopyridine rings shows the lowest bandgap of 1.67 eV because of its enhanced D-A nature
- The experimental electrochemical data of polymers are comparable to those of standard materials reported in the literature. Their results indicate that their bandgap decreases with increase in their D-A nature
- Polymers **P8**, **P9**, **P13** and **P14** have emerged as low bandgap materials with broad absorption spectrum indicating their suitability in polymer solar cells
- The observed low barrier energy difference ($\Delta E_e - \Delta E_h$) values for majority of polymers indicate that they are potential candidates for the preparation of PLED devices
- Cyanopyridine based conjugated polymers exhibit maximum solvatochromic behavior due to fluorescent nature of electron withdrawing cyanopyridine moiety.
- The quantum yields of the new polymers have been found to be in the range 32-43 % indicating their efficiency as electroluminescent materials

- The enhanced absorption maxima of new polymers are attributed to the presence of 3,4-dialkoxythiophene units along the chain
- An optical limiting behavior has been observed in all the tested polymers (**P1-P20**), which results from a combined action of reverse saturable absorption and excited state absorption
- The observed nonlinearity of the new polymers are comparable with C₆₀, inorganic semiconductors, metal nano-clusters, phthalocyanines and some fluorene derivatives
- Pyrazole containing conjugated polymer **P5** possesses the highest effective TPA coefficient (β) of 22.65×10^{-10} m/W
- The polymers **P16, P17, P18, P19** and **P20** exhibit very good optical nonlinearity with good β values, which is attributed to the strong D-A type arrangement and rigid structure of polymer architecture
- The NLO results of polymers reveal that introduction of thiophene moieties along the D-A type chain enhances the molecular hyperpolarizability and hence increases their β values
- Nonlinear optical response of the polymers enhance with the increase in the conjugation path length as well as strength of donors and acceptors
- No direct relationship exists between the bandgap and the NLO performance of the polymer
- NLO studies suggest that the new polymers are effective optical limiting materials for photonic switching applications

7.3. SCOPE FOR FUTURE WORK

The new D-A type polymers with variable electrochemical and optical properties are potent material for their applications in photonic devices. From the results of UV-vis absorption and fluorescence emission spectral study, polymers **P1-P20** can be considered as good luminescent materials and their high quantum yield suggest that they can be used in PLEDs. Further, excellent solvatochromic behavior of

polymers **P6-P10** offers their applications in the construction of electro-chromic windows and sensors. Their good charge carrying properties indicate their suitability in the design of LED, super-capacitors etc. Further, the low bandgap polymers **P8, P9, P13** and **P14** possessing good charge carrying property may find their applications in designing solar cells. The active polymers can be further studied for detailed NLO properties in their thin film form with various concentrations and as composites, particularly with carbon nanotubes, fullerene, metal oxides, metal nano-particles. The new composites are expected to show excellent optical limiting behavior with possible applications in eye sensor protection devices, optical switching and modulations.

REFERENCES

- Akcelrud, L. (2003). "Electroluminescent polymers." *Prog. Polym. Sci.* 28, 875-962.
- Akoudad, S. and Roncali, J. (1998). "Electro-generated poly(thiophenes) with extremely narrow band-gap and high stability under n-doping cycling." *Chem. Commun.*, 2081-2082.
- Alessandro, A., Silvia, B., Antonio, F. and Giorgio, A.P. (1997). "Facile, regioselective synthesis of highly solvatochromic thiophene-spaced N-Alkyl pyridinium dicyano methanides for second-harmonic generation." *J. Org. Chem.*, 62(17), 5755-5765.
- Andersson, M.R., Thomas, O., Mammo, W., Svensson, M., Theander, M. and Inganäs, O. (1999). "Substituted poly(thiophene)s designed for optoelectronic devices and conductors." *J. Mater. Chem.* 9, 1933-1940.
- Arkhipov, V.I., Emelianova, E.V., and Bassler, H. (2004). "Quenching of excitons in doped disordered organic semiconductors." *Phys. Rev. B.*, 70(20), 205205-205212.
- Babudri, F., Cardone, A., Farinola, G.M., Naso, F., Cassano, T., Chiavarone, C. and Tommasi, R. (2003). "Synthesis and optical Properties of a copolymer of tetrafluoro- and dialkoxy-Substituted poly(p-phenylenevinylene) with a high percentage of fluorinated units." *macromolecular chemistry and physics.* *Macromol. Chem. Phys.*, 204(13), 1621-1627.
- Baek, M.J., Fei, G., Lee, S.H., Zong, K. and Lee, Y.S. (2009). "Poly(2,5-dihexyloxyphenylene vinylene-*alt*-2,2-dibutylpropylenedioxythiophene): Synthesis and characterization for photovoltaic applications." *Synth. Met.*, 159(13), 1261-1266.
- Baibarac, M., Lira-Cantu, M., Oro´ Sol, J., Baltog I., Casan-Pastor, N. and Gomez-Romero, P. (2007). "Poly(N-vinylcarbazole) and carbon nanotubes based composites and their application to rechargeable lithium batteries." *Compos. Sci. Technol.*, 67(11-12), 2556-2563.

Bässler, H., Arkhipov, V.I., Emelianova, E.V., Gerhard, A., Hayer, A., Im, C. and Rissler, J. (2003). "Excitons in π -conjugated polymers." *Synth. Met.*, 135-136(4), 377-382.

Batista, R.M.F., Costa, S.P.G., Belsley, M. and Raposo, M.M. (2007). "Synthesis and second-order nonlinear optical properties of new chromophores containing benzimidazole, thiophene, and pyrrole heterocycles." *Tetrahedron*, 63(39), 9842-9849.

Becker, M.W., Sapochak, L.S., Ghosen, R., Xu, C., Dalton, L.R., Shi, Y., Steier, Y.H. and Jen, A.K.Y. (1994). "Large and stable nonlinear optical effects observed for a polyimide covalently incorporating a nonlinear optical chromophore." *Chem. Mater.*, 1994, 6(2), 104-106.

Bernier, S., Garreau, S., Béra-Abérem, M., Gravel, C. and Leclerc, M. (2002). "A versatile approach to affinity chromic polythiophenes." *J. Am. Chem. Soc.* 124(42), 12463-12468.

Bhuiyan, M.D.H., Teshome, T., Gainsford, G.J., Ashraf, M., Clays, K., Asselberghs, I. and Kay, A.J. (2010). "Synthesis, characterization, linear and non-linear optical (NLO) properties of some Schiff's bases." *Opt. Mat.*, 32(6), 669-672.

Bradley, D.D.C. (1993). "Conjugated polymer electroluminescence." *Synth. Met.*, 54(1-3), 401-415.

Bredas, J.L. (1985). 1985. "Relationship between band gap and bond length alteration in organic conjugated polymer." *J. Chem. Phys.*, 82, 3808-3812.

Bredas, J.L., Themans, B., Andre, J.M., Chance, R. and Silbey, R. (1984). "The role of mobile organic radicals and ions (Solitons, polarons and bipolarons) in the transport properties of doped conjugated polymers." *Synth. Met.*, 9(2), 265-274.

Bundgaard, E. and Krebs, F.C. (2007). "Large-area photovoltaics based on low band gap copolymers of thiophene and benzothiadiazole or benzo-bis(thiadiazole)." *Sol. Energy Mater. Sol. Cells.*, 91(11) 1019-1025.

Carella, A., Castaldo, A., Centore, R., Fort, A. and Sirigu, A. (2002). "Synthesis and second order nonlinear optical properties of new chromophores containing 1,3,4-oxadiazole and thiophene rings." *J. Chem. Perkin.Trans.2.*, 1791-1795.

Cassano, T., Tommasi, R., Babudri, F., Cardone, A., Farinola, G.M. and Naso, F. (2002). "High third-order nonlinear optical susceptibility in new fluorinated poly(*p*-phenylenevinylene) copolymers measured with the Z-scan technique." *Opt. Lett.*, 27(24), 2176-2178.

Chan, H.S.O and Ng, S.C. (1998) "Synthesis, characterization and applications of thiophene based functional polymers." *Prog. Polym. Sci.*, 23(7), 1167-1231.

Chen, H., Huang, H., Tian, Z., Shen, P., Zhao, B. and Tan, S. (2010). "Synthesis and photovoltaic performances of 2,5-dioctyloxy-1,4-phenylenevinylene and terthiophene copolymers with di(*p*-tolyl)phenylamine and oxadiazole side groups." *Eur. Polym. J.*, 46(4), 673-680.

Chen, T., Jen, A.K.Y. and Cai, Y. (1995). "Facile approach to nonlinear optical side-chain aromatic polyimides with large second-order nonlinearity and thermal stability." *J. Am. Chem. Soc.*, 117(27), 7295-7296.

Chen, Y., Liao, C. and Wu, T. (2002) "Synthesis and characterization of luminescent copolyethers with alternate stilbene derivatives and aromatic 1,3,4-oxadiazoles." *Polymer*, 43, 4545-4555.

Chi, S.H., Hales, J.M., Fuentes-Hernandez, C., Tseng, S.Y., Cho, J.Y., Odom, S.A., Zhang, Q.S., Barlow, Schrock, R.R., Marder, S.R., Kippelen, B. and Perry, J.W. (2008). "Thick optical-quality films of substituted poly-acetylenes with large, ultrafast third-order nonlinearities and application to image correlation." *Adv. Mater.*, 20(17), 3199-3203.

Cho, B.R., Kim, Y.H., Son, K.W., Khalil, C., Kim, Y.H. and Jeon, S. (2002). "Synthesis and nonlinear optical properties of 1,3,5-tricyano-2,4,6-tris [2-(thiophen-2-yl)vinyl] benzene derivatives." *Bull. Korean Chem. Soc.*, 23(9), 1253-1256.

Choon, S.N., Lu, H.F., Chan, H.S.O., Fujii, A., Laga, T. and Yoshino, T. (2001). "Novel efficient blue fluorescent polymers comprising alternating phenylene pyridine repeat units: Their syntheses, characterization, and optical properties." *Macromolecules*, 34(20), 6895-6903.

Chung, I.S. and Kim, S.Y. (1997). "Synthesis and characterization of wholly aromatic polyamides containing pendent amino and cyano groups." *Polym. Bull.*, 38(6), 635-642.

Colladet, K., Fourier, S., Cleij, T.J., Lutsen, L., Gelan, J., Vanderzande, D., Nguyen, L.H., Neugebauer, H., Sariciftci, S., Aguirre, A., Janssen, G. and Goovaerts, E. (2007). "Low band gap donor-acceptor conjugated polymers toward organic solar cells applications." *Macromolecules*, 40(1), 65-72.

Danel, A., He, Z., Harry, G., Milburna, W. and Tomasik, P. (1999). "Electroluminescence from novel pyrazole-based polymer systems." *J. Mater. Chem.*, 9, 339-342.

de Leeuw, D.M., Simenon, M.M.J., Brown, A.R. and Einerhand, R.E.F. (1997). "Stability of n-type doped conducting polymers and consequences for polymeric microelectronic devices". *Synth. Met.* 87, 53-59.

Diaz, A.F., Kanazawa, K. and Gardini, G.P. (1979). "Electrochemical polymerization of pyrrole." *J. Chem. Soc., Chem. Commun.*, 632-635.

Dyer, A.L., Craig, M.R., Babiarz, J.E., Kiyak, K. and Reynolds, J.R. (2010). "Orange and red to transmissive electrochromic polymers based on electron-rich dioxythiophenes." *Macromolecules*, 43(10), 4460-4467.

Elsenbaumer, R.L., Jen, A.K.Y. and Oboody, R. (1986). "Processible and environmentally stable conducting polymers." *Synth. Met.*, 15(2-3), 169-174.

Emilie, M.G., Kim, Y.G., Jeremiah, K.M., Jones, A.G., McCarley, T.D., Vishal S., Yang, Y. and Reynolds, J.R. (2006). "Optimization of Narrow Band-Gap Propylenedioxythiophene: Cyanovinylene Copolymers for Optoelectronic Applications". *Macromolecules* 39, 9132-9142.

Epstein, A.J., Blatchford, J.W., Wang, Z.H., Jessen, S.W., Gebler, D.D., Lin, L.B., Gustafson, T.L., Wang, H.L., Park, Y.W., Swager, T.M. and MacDiarmid, A.G. (1996). "Poly(*p*-pyridine)- and poly(*p*-pyridyl vinylene)-based polymers: Their photo physics and application to SCALE devices." *Synth. Met.*, 78(3), 253-261.

Franz, E., Frank, W. and Felix, S. (1995). "Synthesis and solvatochromic properties of donor-acceptor-substituted oligothiophenes." *J. Org. Chem.*, 60(7), 2082-2091.

Galand, E.M., Kim, Y.G., Mwaura, J.K., Jones, A.G., McCarley, T.D., Shrotriya, V., Yang, Y. and Reynolds, J.R. (2006). "Optimization of narrow band-gap propylenedioxythiophene: cyanovinylene copolymers for optoelectronic applications." *Macromolecules*, 39(26), 9132-9142.

Grazulevicius, J.V., Strohriegl, P., Pielichowski, J. and Pielichowski, K. (2003). "Carbazole-containing polymers: synthesis, properties and applications." *Prog. Polym. Sci.*, 28(9), 1297-353.

Grigoras, M. and Antonoaia, N.C. (2005). "Synthesis of isoelectronic polyazomethine and poly(arylene vinylene) by a palladium-catalyzed Suzuki coupling method." *Polym. Int.*, 54(12), 1641-1646.

Günes, S., Neugebauer, H. and Sariciftci, S. N. (2007). "Conjugated polymer-based organic solar cells." *Chem. Rev.*, 107, 1324-1338.

Hao, J., Han, M.J., Guo, K., Zhao, Y., Qiu L., Shen, Y. and Meng, X. (2008). "A novel NLO: Synthesis azothiophene-based chromophore, characterization, thermal stability and optical nonlinearity." *Mater. Lett.*, 62(6-7), 973-976.

He, M., Zhou, Y., Dai, J., Liu, R., Cui, Y. and Zhang, T. (2009). "Synthesis and nonlinear optical properties of soluble fluorinated polyimides containing hetarylazo chromophores with large hyperpolarizability." *Polymer*, 50(16), 3924-3931.

Heeger, A.J. (2000). "Semiconducting and metallic polymers: The fourth generation of polymeric materials." *Nobel lecture*, December 8.

Hegde, P.K., Adhikari, A.V., Manjunatha, M.G., Poornesh, P. and Umesh, G. (2009). "Third-order nonlinear optical susceptibilities of new copolymers containing alternate

3,4-dialkoxythiophene and (1,3,4-oxadiazolyl)pyridine moieties." *Opt. Mater.*, 31(6), 1000-1006.

Hongli, W., Zhen, L., Bin, H., Zuoquan, J., Yanke, L., Hui, W., Jingui, Q., Gui, Y. Yunqi, L. and Yinglin, S. (2006). "Synthesis, light-emitting and optical limiting properties of new donor-acceptor conjugated polymers derived from 3,5-dicyano-2,4,6-tristyrylpyridine." *React. Funct. Polym.*, 66(9), 993-1002.

Hu, J.L., Li, B., Meng, F.S., Ding, F., Qian, S.X. and Tian, H. (2004). "Two-photon absorption properties of hyperbranched conjugated polymers with triphenylamine as the core." *Polymer*, 45(21), 7143-7149.

Izumi, T., Kobashi, S., Takimiya, K., Aso, Y. and Otsubo, T. (2003). "Synthesis and spectroscopic properties of a series of α -blocked long oligothiophenes up to the 96-mer: reevaluation of effective conjugation length", *J. Am. Chem. Soc.*, 125, 5286-5287.

Janietz, S. and Wedel, A. (1997). "Electrochemical redox behavior and electroluminescence in the mixed energy-sufficient system thianthrene and 2-(4-Biphenyl)-5-(4-*tert*-butylphenyl)-1,3,4-oxadiazole." *Adv. Mater.*, 9(5), 403-407.

Jen, K., Maxfield, M., Shacklette, L.W. and Elsenbaumer, R.L. (1987). "Highly-conducting, poly(2,5-thienylene vinylene) prepared via a soluble precursor polymer." *J. Chem. Soc., Chem. Commun.*, 309-311.

Jumin, H., Mei-Juan, H., Kunpeng, G., Yuxia, Z., Ling, Q., Yuquan, S. and Xiaoguang, M. (2008). "A novel NLO azothiophene-based chromophore: Synthesis, characterization, thermal stability and optical nonlinearity." *Mater. Lett.*, 62(6-7), 973- 975.

Jung, M. S., Lee, T.W., Hyeon-Lee, J., Sohn, B.H. and Jung, I. (2006). "Synthesis and characterizations of a polyimide containing a triphenylamine derivative as an interlayer in polymer light-emitting diode." *Polymer*, 47(8), 2670-2676.

Junjian, L., Shen, P., Zhao, B., Yao, B., Xie, Z., Liu, E. and Tan, S. (2008). "Two novel triphenylamine-substituted poly (p-phenylenevinylene) derivatives: synthesis, photo- and electroluminescent properties." *Eur. Polym. J.*, 44(7), 2348-2355.

Karthikeyan, B., Anija, M., Sandeep, S.C.S., Nadeer, M.T.M. and Philip, R. (2008) "Optical and nonlinear optical properties of copper nano-composite glasses annealed near the glass softening temperature." *Opt. Commun.*, 281(10), 2933-2937.

Kim, D., Kim, S., Zyung, T., Kim, J., Cho, I. and Choi, S.K. (1996). "Synthesis of a new Class of processable electroluminescent poly(cyanoterephthalylidene) derivative with a tertiary amine linkage." *Macromolecules*, 29(10), 3657-3660.

Kim, J. H. and Lee, H. (2003). "Efficient poly (*p*-phenylenevinylene) derivative with 1,2-diphenyl-2-cyanoethene for single layer light-emitting diodes." *Synth. Met.*, 139(2), 471-478.

Kim, J., Seo, Y., Lee, W., Hong, Y., Lee, S.K., Shinc, W.S., Moonc, S. and Kanga, I. (2011). "Synthesis and properties of phenothiazylene vinylene and bithiophene-based copolymers for organic thin film transistors." *Synth. Met.*, 161(1-2), 72-78.

Kim, J.H. (2008). "Synthesis and electro-optical properties of poly(*p*-phenylenevinylene) derivative with conjugated 1,3,4-oxadiazole pendant and its AC electroluminescence." *Synth. Met.*, 158(21-24), 1028-1036.

Kim, K., Hong, Y.R., Lee, S.W., Jin, J.I., Park, Y., Sohn, B.H., Kim, W.H and Park, J.K. (2001). "Synthesis and luminescence properties of poly(*p*-phenylenevinylene) derivatives carrying directly attached carbazole pendants." *J. Mater. Chem.*, 11, 3023-3030.

Koecelberghs, G., Sioncke, S., Verbiest, T., Persoons, A. and Samyn, C. (2003). "Synthesis and properties of chiral helical chromophore functionalized polybinaphthalenes for second-order nonlinear optical application." *Polymer*, 44(14), 3785-3794.

Kohler, A., Wilson, J.S. and Friend, R.H. (2002). "Fluorescence and phosphorescence in organic materials." *Adv. Mater.*, 14(10), 701-707.

Kroon, R., Lenes, M., Hummelen, J.C., Blom, P.W.M. and de-Boer, B. (2008). "Small band gap polymers for organic solar cells (Polymer material development in the Last 5 years)". *Polym. Rev.*, 48, 531-582.

- Kurian, P.A., Vijayan, C., Sathiyamoorthy, K., Sandeep, S.C.S. and Philip, R. (2007). "Exitonic transitions and off-resonant optical limiting in CdS quantum dots stabilized in a synthetic glue metrics." *Nano. Res. Lett.* 2(11), 561-568.
- Leng, W.N., Zhou, Y.M., Xu, Q.H. and Liu, J.Z. (2001). "Synthesis of nonlinear optical polyimides containing benzothiazoe moiety and their electro-optical and thermal properties." *Polymer*, 42(22), 9253-9259.
- Levi, M.D., Fisyuk, A.S., Demadrille, R., Markevich, E., Gofer, Y., Aurbacha, D. and Pron, A. (2006). "Unusually high stability of a poly(alkyl quaterthiophene-alt-oxadiazole) conjugated copolymer in its n and p-doped states." *Chem. Commun.*, 3299-3301.
- Li, Y., Li, H., Xu, B., Li, Z., Chen, F., Feng, D., Zhang, J. and Tian, W. (2010). "Molecular structure-property engineering for photovoltaic applications: Fluorene-acceptor alternating conjugated copolymers with varied bridged moieties." *Polymer*, 51(8), 1786-1795.
- Liang, Y., Feng, D., Guo, J., Szarko, J.M., Ray, C., Chen, L.X. and Yu, L. (2009). "Regioregular oligomer and polymer containing thieno[3,4-*b*]thiophene moiety for efficient organic solar cells." *Macromolecules*, 42(4), 1091-1098.
- Ling, Q., Liaw, D., Zhu, C., Chan, D.S., Kang, E. and Neoh, K. (2008). "Polymer electronic memories: Materials, devices and mechanisms." *Prog. Polym. Sci.*, 33(10), 917-978.
- Liu, B., Yu, W.L., Lai, Y.H. and Huang, W. (2001). "Blue-light-emitting fluorene-based polymers with tunable electronic properties." *Chem. Mater.*, 13(16), 1984-1991.
- Liu, G., Ling, Q.D., Kang, E.T., Neoh, K.G., Liaw, D.J. and Chang, F.C. (2007). "Bistable electrical switching and write-once read-many-times memory effect in a donor-acceptor containing polyfluorene derivative and its carbon nanotube composites." *J. App. Phy.*, 102(2), 024502-024510.
- Lowe, J.P. and Kafafi, S.A. (1984). "Effects of chemical substitution on polymer band gaps: transferability of band-edge energies." *J. Am. Chem. Soc.*, 106(20), 5837-5841.

Manjunatha, M.G., Adhikari, A.V. and Hegde, P.K. (2009). "Design and synthesis of new donor-acceptor type conjugated copolymers derived from thiophenes." *Eur. Polym. J.*, 45(3), 763-771.

Manjunatha, M.G., Adhikari, A.V., Hegde, P.K., Suchand-sandeep, C.S. and Philip, R. (2009). "A new nonlinear optically active donor-acceptor type conjugated polymer: Synthesis and electrochemical and optical characterization." *J. Electron. Mater.*, 39(12), 2711-2719.

Michelle, S.L., Jiang, X., Sen, L., Petra, H., and Alex, K.Y.J. (2002). "Effect of cyano substituents on electron affinity and electron-transporting properties of conjugated polymers." *Macromolecules*, 35(9), 3532-3538.

Michinobu, T., Okoshi, K., Osako, H., Kumazawa, H. and Shigehara, H. (2008). "Band-gap tuning of carbazole-containing donor-acceptor type conjugated polymers by acceptor moieties and p-spacer groups." *Polymer*, 49(1), 192-199.

Mikroyannidis, J.A., Damouras, P.A., Maragos, V.G., Tsai, L.R. and Chen, Y. (2009). "Synthesis, photophysics and electroluminescence of new vinylene-copolymers with 2,4,6-triphenylpyridine kinked segments along the main chain." *Eur. Polym. J.*, 45(1), 284-294.

Miller, G.G., Ronald, L. and Elsenbaumer. (1986). "Highly conducting, soluble, and environmentally-stable poly (3-alkylthiophenes)." *J. Chem. Soc., Chem. Commun.*, 1346-1349.

Mircea, G. and Nicoleta, C.A. (2005) "Synthesis and characterization of some carbazole-based imine polymers ." *Eur. Polym. J.*, 41(5), 1079-1089.

Mori, T. and Kijima, M. (2009). "Synthesis and electroluminescence properties of carbazole-containing 2,6-naphthalene-based conjugated polymers." *Eur. Polym. J.*, 45(4), 1149-1157.

Myung-Jin, B., Lee, S.H., Zong, K. and Lee, Y. (2010). "Low band gap conjugated polymers consisting of alternating dodecylthieno[3,4-b]thiophene-2-carboxylate and

one or two thiophene rings: Synthesis and photovoltaic property.” *Synth. Met.*, 160(11-12), 1197-1203.

Nan, H., Yu, C., Jinrui, B., Jun, W., Werner, J.B. and Jinhui, Z. (2009). “Preparation and optical limiting properties of multi-walled carbon nanotubes with π -conjugated metal-free phthalocyanine moieties.” *Phys. Chem. C.*, 113(30), 13029-13035.

Ojha, U.P., Krishnamoorthy and Anilkumar. (2003). “Synthesis and characterization of aromatic polyoxadiazoles containing 3,4-alkylenedioxythiophenes.” *Synth. Met.*, 132(3), 279-283.

Okumoto, K. and Shirota, Y. (2001). “Development of high-performance blue-violet-emitting organic electroluminescent devices”. *Appl. Phys. Lett.*, 79(9), 1231-1233.

Ong, B.S., Wu, Y., Liu, P. and Gardner, S. (2004). “High-performance semiconducting polythiophenes for organic thin-film transistors.” *J. Am. Chem. Soc.*, 126(11), 3378-3379.

Pai, C.L., Liu, C.L., Chen, W.C and Jenekhe, S.A. (2006). “Electronic structure and properties of alternating donor-acceptor conjugated copolymers: 3,4-Ethylenedioxythiophene (EDOT) copolymers and model compounds.” *Polymer*, 47(2), 699-708.

Pal, B., Yen, W.Y., Yang, J.S. and Su, W.F. (2007). “Substituent effect on the optoelectronic properties of alternating fluorene-thiophene copolymers.” *Macromolecules*, 40(23), 8189-8194.

Paoli, M.D. and Gazotti, W.A. (2002). “Electrochemistry, polymers and optoelectronic devices: A combination with a future.” *J. Braz. Chem. Soc.*, 13(4), 410-424.

Peng, Q., Lu, Z.Y., Huang, Y., Xie, M.G., Xiao, D., Han, S.H., Peng, J.B. and Cao, Y. (2004). “Novel efficient green electroluminescent conjugated polymers based on fluorene and triarylpyrazoline for light-emitting diodes.” *J. Mater. Chem.*, 14, 396-401.

Perzon, E., Wang, X., Admassie, S., Inganäs, O. and Andersson, M.R. (2006). "An alternating low bandgap polyfluorene for optoelectronic devices." *Polymer*, 47(12), 4261-4268.

Pina, J., Melo, J.S., Burrows, H.D, Bilge, A., Farrell, A., Forster, M. and Scherf, U. (2006). "Spectral and photophysical studies on cruciform oligothiophenes in solution and the solid state" *J. Phys. Chem., B*. 110(31), 15100-15106.

Politis, J.K., Somoza, F., Kampf, J.W. and Curtis, M.D. (1999). "A comparison of structures and optoelectronic properties of oxygen- and sulfur-containing heterocycles: conjugated nonylbisoazole and nonylbithiazole oligomers." *Chem. Mater.*, 1999, 11(8), 2274-2284.

Qian, Y., Meng, K., Lu, C.G., Lin, B., Huan, W. and Cui, Y. (2009). "The synthesis photophysical properties and two-photon absorption of triphenylamine multipolar chromophores." *Dyes Pigm.*, 80(1), 174-180.

Qian, Y., Xiao, G., Wang, G., Sun, Y., Cui, Y. and Yuan, C. (2006). "Synthesis and third-order optical nonlinearity in two-dimensional A- π -D- π -A carbazole-cored chromophores." *Dyes Pigm.*, 71(2), 109-117.

Qin, A., Jim, C.K.W., Lu, W., Lam, J.W.Y., Häussler, M., Dong, Y., Sung, H.H.Y., Williams, I.D., Wong, K.L.G. and Tang, B.Z. "Click polymerization: Facile synthesis of functional poly(aroyltriazole)s by metal-free, region-selective 1,3-dipolar polycycloaddition." *Macromolecules*, 40(7), 2308-2317.

Qiu, F., Zhou Y., Liu, J. and Zhang, X. (2006). "Preparation, morphological and thermal stability of polyimide/silica hybrid material containing dye NBDPA." *Dyes Pigm.*, 71(1), 37-42.

Rao, V.P., Cai, Y.M. and Jen, A.K.Y. (1994). "Ketene dithioacetal as a π -electron donor in second-order nonlinear optical chromophores." *Chem. Soc., Chem. Commun.*, 1689-1690.

Rao, V.P., Jen, A.K.Y., Wong, K.Y and Drost, K.J. (1993). "Novel push-pull thiophenes for second order nonlinear optical applications." *Tetrahedron Lett.* 34(11), 1747-1750.

Rao, V.P., Jen, A.K.Y., Wong, K.Y. and Drost, K.J. (1993). "Dramatically enhanced second-order nonlinear optical susceptibilities in tricyanovinylthiophene derivatives." *J. Chem. Soc., Chem. Commun.*, 1118-1120.

Roncali, J., Garreau, R., Yassar, A., Marque, P., Garnier, F. and Lemaire, M. (1987). "Effects of steric factors on the electro-synthesis and properties of conducting poly(3-alkylthiophenes)." *J. Phys. Chem.*, 91(27), 6706-6714.

Rosa, M.F.B., Susana, P.G.C., Belsley and Manuela, M.R. (2007) "Synthesis and second-order nonlinear optical properties of new chromophores containing benzimidazole, thiophene, and pyrrole heterocycles." *Tetrahedron*, 63(39), 9842-9849.

Rosso, P.G.D., Almassio, M.F., Palomar, G.R. and Garay, R.O. (2011). "Nitroaromatic compounds sensing. Synthesis, photophysical characterization and fluorescence quenching of a new amorphous segmented conjugated polymer with diphenylfluorene chromophores." *Sens. Actuators, B*, 160(1), 524-532.

Saadeh, H., Gharavi, A., Yu, D. and Yu, L. (1997). "Polyimides with a diazo chromophore exhibiting high thermal stability and large electro-optic coefficients." *Macromolecules*, 1997, 30(18), 5403-5407.

Samoc, M., Samoc, A. and Davies, B.L. (1998) "Femto second Z-scan and degenerate four-wave mixing measurements of real and imaginary parts of the third-order nonlinearity of soluble conjugated polymers." *J. Opt. Soc. Am. B.*, 15(2) 817-825.

Samoc, M., Samoc, A. and Davies, B.L. (2000). "Two-photon and one-photon resonant third-order nonlinear optical properties of π -conjugated polymers." *Synth. Met.*, 109(1-3), 79-83.

Schroeder, B.C., Nielsen, C.B., Kim, Y.J., Smith, J., Huang, Z., Durrant, J., Watkins, S. E., Song, K., Anthopoulos, T.D. and McCulloch, I. (2011). "Benzotrithiophene co-

polymers with high charge carrier mobilities in field-effect transistors." *Chem. Mater.*, 23(17), 4025-4031.

Seung, W.K., Jung, B.J., Ahn, T. and Shim, H.K. (2002). "Novel poly(*p*-phenylenevinylene)s with an electron-withdrawing cyanophenyl group." *Macromolecules*, 35(16), 6217-6223.

Sheik-Bahae, M., Said, A.A. and Wei, T. (1990). "Sensitive measurement of optical nonlinearities using a single beam." *IEEE. J. Quantum. Electron.*, 26(4), 760-769.

Shin, W.S., Kim, S.C., Lee, S., Jeon, S., Kim, M., Naidu, B.V.K., Jin, S., Lee, J., Lee J.W. and Gal, Y. (2007). "Synthesis and photovoltaic properties of a low-band-gap polymer consisting of alternating thiophene and benzothiadiazole derivatives for bulk-heterojunction and dye-sensitized solar cells." *J. Polym. Sci. A, Polym. Chem.*, 45(8), 1394-1402.

Sim, J.H., Ueno, E., Natori, I., Ha, J. and Sato, H. (2008). "Oxidation polymerization of *N*-butyl-*N,N*-diphenylamine (BDPA) and *N*-4-butylphenyl-*N,N*-diphenylamine (BTPA). *Synth. Met.*, 158(8-9), 345-349.

Sivaramakrishnan, S., Muthukumar, V.S., Sivasankara, S., Venkataramanaiah, S.K., Reppert, J., Rao, A.M., Anija, M., Philip, R. and Kuthirummal, N. (2007). "Nonlinear optical scattering and absorption in bismuth nanorod suspensions." *Appl. Phys. Lett.*, 91(9), 093104-093107.

Smela, E. (2003). "Conjugated polymer actuators for biomedical applications." *Adv. Mater.*, 15(6), 481-494.

Sonar, P., Zhang, Z., Grimsdale, A.C., Mullen, K., Surin M., Lazzaroni, R., Leclere, P., Tierney, S., Heeney, M. and Mc-Culloch, I. (2004). "4-Hexylbithieno[3,2-*b*:2c3c-]pyridine: An efficient electron-accepting unit in fluorene and indenofluorene copolymers for light-emitting devices." *Macromolecules*, 37(3), 709-715.

Sonmez, G., Meng, H. and Wudl, F. (2003). "Very stable low band gap polymer for charge storage purposes and near-infrared applications." *Chem. Mater.*, 15(26), 4923-4929.

Spanggaard, H. and Krebs, F.C. (2004). "A brief history of the development of organic and polymeric photovoltaics." *Sol. Energy Mater. Sol. Cells*, 83(2-3), 125-146.

Strukelj, M., Papadimitrakopoulos, F., Miller, T.M. and Rotheberg, L.J. (1995). "Design and application of electron-transporting organic materials." *Science*, 267(5206), 1969-1972.

Tambe, S.M., Kittur, A.A., Inamdar, S.R., Mitchell, G.R. and Kariduraganavar, M.Y. (2009). "Synthesis and characterization of thermally stable second-order nonlinear optical side-chain polyimides containing thiazole and benzothiazole push-pull chromophores." *Opt. Mater.*, 31(6), 817-825.

Tameev, A.R., Heb, Z., Milburn, G.H.W., Danel, A., Tomasik, P. and Vannikova, A. V. (2004) "Drift mobility of electrons in pyrazoline-containing copolymers." *Russ. J. Electrochem.*, 40(3), 359-363.

Tarkka, R.M., Zhang, X. and Jenekhe, S.A. (1996). "Electrically Generated Intramolecular Proton Transfer: Electroluminescence and Stimulated Emission from Polymers." *J. Am. Chem. Soc.*, 118(39), 9438-9439.

Tourillon. (1986). *Handbook of Conducting Polymers*; T. A. Stotheim, Ed. Marcel Dekker: New York, 294.

Tsutsumi, N., Morishima, M. and Sakai, W. (1998). "Nonlinear optical (NLO) polymers. NLO polyimide with dipole moments aligned transverse to the imide linkage." *Macromolecules*, 31(22), 7764-7769.

Udayakumar, D. and Adhikari, A.V. (2006). "Synthesis and characterization of new light-emitting copolymers containing 3,4-dialkoxythiophenes." *Synth. Met.*, 156(18-20), 1168-1173.

Udayakumar, D., Kiran, A.J., Adhikari, A.V., Chandrasekharan, K., Umesh, G. and Shashikala, H.D. (2006). "Third-order nonlinear optical studies of newly synthesized polyoxadiazoles containing 3,4-dialkoxythiophenes." *Chem. Phys.*, 331(1), 125-130.

- Viehbeck, A., Goldberg, M.J. and Kovac, C.A. (1990). "Electrochemical properties of polyimides and related imide compounds." *J. Electrochem. Soc.* 137(5), 1460-1466.
- Waltman, R.J., Bargon, J. and Diaz, A.F., (1983). "Electrochemical studies of some conducting polythiophene films." *J. Phys. Chem.* 87(8), 1459-1463.
- Walton, D.J. (1990). "Electrically conducting polymers." *Mater.Des.*, 11(3), 142-152.
- Wang, H., Li, Z., Huang, B., Jiang, Z., Liang, Y., Wang, H., Qin, J., Yu, G., Liu, Y. and Song, Y. (2006). "Synthesis, light-emitting and optical limiting properties of new donor-acceptor conjugated polymers derived from 3,5-dicyano-2,4,6-tristyrylpyridine." *React. Funct. Polym.*, 66(9), 993-1002.
- Wang, K.L., Liaw, D.J., Liou, W.T and Chen, W.T. (2008). "A novel fluorescent poly(pyridine-imide) acid chemosensor." *Dyes Pigm.*, 78(2) 93-100.
- Wang, K.L., Liaw, D.J., Liou, W.T and Huang, S.T. (2008). "High glass transition and thermal stability of new pyridine-containing polyimides: Effect of protonation on fluorescence." *Polymer*, 49(6), 1538-1546.
- Wang, X., Li, Y.F., Ma, T., Zhang, S. and Gong. C. (2006). Synthesis and characterization of novel polyimides derived from 2,6-bis[4-(3,4-dicarboxyphenoxy)benzoyl]pyridine dianhydride and aromatic diamines." *Polymer*, 47, 3774-3783.
- Wienk, M.M., Struijk, M.P. and Janssen, R.A.J. (2006). "Low band gap polymer bulk heterojunction solar cells." *Chem. Phys. Lett.*, 422(4-6), 488-491.
- Wu, C.W., Liu and Chen, C.L. (2006). "Synthesis and characterization of new fluorene-acceptor alternating and random copolymers for light-emitting applications." *Polymer*, 47(2), 527-530.
- Wu, X., Liu, Y. and Zhu, D. (2001). "Synthesis and characterization of a new conjugated polymer containing cyano substituents for light-emitting diodes." *J. Mater. Chem.*, 11, 1327-1331.

Xu, S., Yang, M. and Cao, S. (2005). "A fluorescent co-polyimide containing perylene, fluorene and oxadiazole units in the main chain." *React. Funct. Polym.*, 66(4), 471-478.

Xue, J., Uchida, S., Rand, B.P. and Forrest, S.R. (2004). "4.2 % efficient organic photovoltaic cells with low series resistances." *Appl. Phys. Lett.*, 84(16), 3013-3015.

Yanamao, D., Lu, J., Xu, Q., Yan, F., Xia, X., Wang, L. and Hu, L. 2010. "Effects of substituents on the third-order nonlinear optical properties of poly(3-alkoxythiophene) derivatives." *Synth. Met.* 160(5-6), 409 - 412.

Yang, B., Li, G., Zhang, X., Shu, X., Wang, A., Zhu, X. and Zhu, J. (2011). "Hg²⁺ detection by aniline-based conjugated copolymers with high selectivity." *Polymer*, 52(12), 2537-2541.

Yin, S.G., Wedel, A., Janietz, S., Krueger, H., Sainova, D., Arlt, K., Kuechlr, F. and Fischer, B., (2003). Synthetic and electroluminescent properties of polymer containing phenothiazene and oxadiazole units." *Synth. Met.*, 137(1-3), 1145-1466.

Yoon, K.R., Byun, N.M. and Lee, H. (2007). "Synthesis and characterization of carbazole based nonlinear optical polymers possessing chromophores in the main or side chains." *Synth. Met.*, 157(16-17), 603-610.

Yu L.P. and Dalton L.R. (1989). "Synthesis and characterization of new electro-active polymers ." *Synth. Met.*, 29(1), 463-470.

Yu, C.Y., Ko, B.T., Ting, C. and Chen, C.P. (2009). "Two-dimensional regioregular polythiophenes with conjugated side chains for use in organic solar cells." *Sol. Energy Mater. Sol. Cells*, 93(5), 613-620.

Yu, L., Bao, Z. and Cai, R. (1993). "Conjugated, liquid crystalline polymers." *Angew. Chem. Int. Ed.*, 32(9), 1345-1347.

Yu, W.L., Meng, H., Pei, J. and Haung, W. (1998). "Tuning redox behavior and emissive wavelength of conjugated polymers by p-n diblock structures." *J. Am. Chem. Soc.*, 120(45), 11808-11809.

Zhan, X., Liu, Y., Wu, X., Wang, S. and Zhu, D. (2002). "New series of blue-emitting and electron-transporting copolymers based on fluorene." *Macromolecules*, 35(7), 2529-2537.

Zhang, H., Li, Y., Jiang, Q., Xie, M., Peng, J. and Cao, Y. (2007). "Novel green-emitting polymer containing fluorene and 1-(2-benzothiazolyl)-3,5-diphenylpyrazoline." *J. Mater. Sci.*, 42(12), 4476-4479.

Zhang, S., He, C., Liu, Y., Zhan, V.X and Chen, J. (2009). "Synthesis of a soluble conjugated copolymer based on dialkyl-substituted dithienothiophene and its application in photovoltaic cells." *Polymer*, 50(15), 3595-3599.

Zhao, B., Liu, D., Peng, L., Li, H., Shen, P., Xiang, N., Liu, Y. and Tan, S. (2009). "Effect of oxadiazole side chains based on alternating fluorene-thiophene copolymers for photovoltaic cells." *Eur. Polym. J.* 45(7), 2079-2086.

Zhao, W., Cai, W., Xu, R., Yang, W., Gong, X., Wu, H. and Cao, Y. (2010). "Novel conjugated alternating copolymer based on 2,7-carbazole and 2,1,3-benzoselenadiazole." *Polymer*, 51(14), 3196-3202.

Zoombelt, A.P., Mark, A.M., Fonrodona, M., Nicolas, Y., Wienk, M.M., Rene, A.J. and Janssen, R.A.J. (2009). "The influence of side chains on solubility and photovoltaic performance of dithiophene-thienopyrazine small band gap copolymers." *Polymer*, 50(19), 4564-4570.

Zou, Y., Peng, B., Liu, B., Li, Y., He, Y., Zhou, K. and Pan, C. (2009). "Conjugated copolymers of cyano substituted poly(p-phenylene vinylene) with phenylene ethynylene and thienylene vinylene moieties: Synthesis, optical, and electrochemical properties." *J. Appl. Polym. Sci.*, 115(3), 1480-1488.

PUBLICATIONS

PAPERS PUBLISHED IN INTERNATIONAL JOURNALS

1. **Vishnumurthy, K.A.**, Adhikari, A.V., Sunitha, M.S., Ann Mary, K.A. and Philip, R. (2011). "Design and synthesis of a new thiophene based donor-acceptor type conjugated polymer with large third order nonlinear optical activity." *Synthetic Metals*, 161(15-16), 1699-1706.
2. **Vishnumurthy, K.A.**, Sunitha, M.S., Safakath, K., Philip, R. and Adhikari, A.V. (2011). "Synthesis, electrochemical and optical studies of new cyanopyridine based conjugated polymers as potential fluorescent materials." *Polymer*, 52(19), 4174-4183.
3. **Vishnumurthy, K.A.**, Sunitha, M.S., Philip, R. and Adhikari, A.V. (2011). "New diphenylamine-based donor-acceptor-type conjugated polymers as potential photonic materials." *Reactive and Functional polymers*, 71(12), 1119-1128.
4. **Vishnumurthy, K.A.**, Adhikari, A.V., Sunitha M.S. and Philip, R. (2011). "Synthesis and Characterization of a New Conjugated Polymer Bearing Pyrazole and Thiophene Moieties as Potent NLO Material." *Phenomena, Materials, Devices, and Characterization AIP Conf. Proc.*, 1391, 652-654.
5. **Vishnumurthy, K.A.**, Sunitha, M.S. and Adhikari, A.V. (2012). "New optical limiting polymeric materials with different π -electron conjugation bridge structures: Synthesis and characterization." *European Polymer Journal*, 48(9), 1575-1585.
6. **Vishnumurthy, K.A.**, Sunitha, M.S. and Adhikari, A.V. (2012). "Synthesis and Characterization of Thiophene Based Donor-Acceptor Type Polyimide and Polyazomethines for Optical Limiting Applications." *Polymer Bulletin*, (Accepted, DOI 10.1007/s00289-012-0789-8).

PAPERS PRESENTED IN NATIONAL / INTERNATIONAL CONFERENCES

1. **Vishnumurthy K.A.**, Sunitha M.S. and Adhikari, A.V. "Synthesis and characterization of new thiophene based conjugated polymer bearing 1,3,4-oxadiazole moieties as potential light emitting material". Paper presented in **National conference on recent trends in chemistry, NCRTCR 2010**. National Institute of Technology Karnataka, Surathkal, March 8-9, 2010.
2. **Vishnumurthy. K.A.**, Hegde, P.K., Adhikari, A.V. and Manjunatha M.G, "New Thiophene based Conjugated Polymers Bearing 1,3,4-Oxadiazolyl-naphthalene moieties as potential Light emitting and NLO materials", "**The Polymer Congress-APA-2009**", Indian Institute of Technology Delhi, New Delhi, India, December 17-20, 2009.
3. **Vishnumurthy K.A.**, Adhikari, A.V., Sunitha M.S., Smijesh, N. and Philip, R. "Design and synthesis of a new donor acceptor type conjugated polymer bearing oxadiazole, naphthalene and thiophene moieties as potent NLO material". "**International conference on Recent Trends in material science and technology**, Tiruvananthapuram, October 18-21, 2010.
4. **Vishnumurthy, K.A.**, Adhikari, A.V., Sunitha, M.S. and Philip, R. "Synthesis and Characterization of a New Conjugated Fluorescent Polymer Bearing Pyrazole and Thiophene Moieties as Potent NLO Material". **OPTICS-II**, NIT Calicut, Kerala, India, May 23-25, 2011.
5. **Vishnumurthy K.A.**, Sunitha M.S. and Adhikari, A.V. "Design and synthesis of thiophene based conjugated polymer with cyanopyridine spaces as potent optical limiting material". **International Conference on Synthetic & Structural Chemistry ICSSC-2011**, Mangalore University, Mangalore India, December 8-10, 2011.

CURRICULUM VITAE

Present address

Vishnumurthy K. A
Research Scholar
Department of chemistry
National Institute of Karnataka
Srinivasnagar, Mangalore
Karnataka, India-575025
Email: vishnukanive@gmail.com
Phone: +919741211557

Permanent Address

Vishnumurthy K. A.
Kanivebagilu
Haniya Post
Hosanagara Taluk
Shivamogga District
Karnataka, India-577415
Email: vishnukanive@gmail.com
Phone: +919741211557,

Research Experience:

12/2008-present: **Research scholar**
Department of Chemistry
National Institute of Technology Karnataka, India
Research: Design and synthesis of conjugated polymers for photonic applications

06/2007-12/2008 **Scientist**
Syngene International (<http://www.syngeneintl.com>)
Biocon Limited.
Research Area: Synthesis and characterization of medicinally important hetero-cyclic drug molecules

Education:

12/2008-present: **Ph.D** (Polymer chemistry)
Department of Chemistry
National Institute of Technology Karnataka, India
Title: 'Design and synthesis of new conjugated polymers for photonic applications'
Supervisor: Prof A. V. Adhikari

06/2005-12/2007: **M.Sc.** (Industrial chemistry)
Department of Industrial Chemistry
Jnana Sahyadri Shankaraghatta
Kuvempu University, Shimoga, Karnataka, India

06/2003-12/2005: **B.Sc.** (Chemistry)
Tungamahavidyalaya Thirthahalli
Kuvempu University, Thirthahalli Shimoga, Karnataka, India

Honors:

2011: Best poster award “**International conference on Recent Trends in material science and technology**, Tiruvananthapuram, 18-21, October 2010.

2007: First rank award in **M. Sc.** (Industrial chemistry) with **Prof. Gajendraghad Goldmedal** from Kuvempu University.

Publications

1. **K.A. Vishnumurthy**, A. Vasudeva Adhikari, M.S. Sunitha, K.A. Ann Mary, Reji Philip. “Design and synthesis of a new thiophene based donor–acceptor type conjugated polymer with large third order nonlinear optical activity.” *Synthetic Metals*, 161 (2011) 1699-1706.
2. **K.A. Vishnumurthy**, M.S. Sunitha, K. Safakath, Reji Philip, Airody Vasudeva Adhikari. “Synthesis, electrochemical and optical studies of new cyanopyridine based conjugated polymers as potential fluorescent materials.” *Polymer*, 52 (2011) 4174-4183.
3. **K.A. Vishnumurthy**, M.S. Sunitha, Reji Philip, Airody Vasudeva Adhikari. “New diphenylamine-based donor–acceptor-type conjugated polymers as potential photonic materials.” *Reactive & Functional Polymers*, 71(2011) 1119–1128.
4. **K.A. Vishnumurthy**, A. Vasudeva Adhikari, M.S. Sunitha, Reji Philip. “Synthesis and Characterization of a New Conjugated Polymer Bearing Pyrazole and Thiophene Moieties as Potent NLO Material.” *Phenomena, Materials, Devices, and Characterization AIP Conf. Proc.* 1391, 652-654 (2011); doi: 10.1063/1.3643638.
5. **K.A. Vishnumurthy**, M.S. Sunitha, A. Vasudeva Adhikari. “New optical limiting polymeric materials with different π -electron conjugation bridge structures: Synthesis and characterization.” *European Polymer Journal* . 48(9),(2012) 1575-1585.
6. **K.A. Vishnumurthy**, M. S. Sunitha, A. Vasudeva Adhikari. Synthesis and Characterization of Thiophene Based Donor-Acceptor Type Polyimide and Polyazomethines for Optical Limiting Applications. *Polymer bulletin*. (Accepted DOI: **10.1007/s00289-012-0789-8**)

7. Sunitha M. S, Airody Vasudeva Adhikari, **Vishnumurthy K. A**, Safakath Karuthedathb, Reji Philip. "Large third order nonlinearity of new π -conjugated donor-acceptor polymers with substituted thiophene and 1,3,4-oxadiazole moieties" *International journal of polymeric materials*. 61(2012), 1-22.
8. M.S. Sunitha, A.V. Adhikari, **K.A. Vishnumurthy**, N. Smijesh N, R. Philip. "Electrochemical and nonlinear optical properties of new D-A type π -conjugated polymers carrying 3,4-benzyloxythiophene, oxadiazole and 3,4-alkoxythiophene systems." *Chemistry Letters*, 41 (2012) 234-236.
9. M.S. Sunitha, A.V. Adhikari, **K.A. Vishnumurthy**, R. Philip. "Nonlinear optical properties of a newly synthesized thiophene based conjugated polymer" *AIP Conf. proc.*, 1391 (2011) 703-705.

LIST OF CONFERENCE PAPERS

- i. **Vishnumurthy, K.A.**, Hegde, P.K., Adhikari, A.V. and Manjunatha M.G, "New Thiophene based Conjugated Polymers Bearing 1,3,4-Oxadiazolyl-naphthalene moieties as potential Light emitting and NLO materials." "*The Polymer Congress-APA 2009*", December 17-20, 2009, Indian Institute of Technology Delhi, New Delhi, India
- ii. **Vishnumurthy K. A.**, Adhikari, A.V., Sunitha, M.S., Smijesh, N. and Philip, R. "Design and synthesis of a new donor acceptor type conjugated polymer bearing oxadiazole, naphthalene and thiophene moieties as potent NLO material." "*International conference on Recent Trends in material science and technology*, Tiruvananthapuram, 18-21, October 2010.
- iii. **Vishnumurthy, K.A.**, Adhikari, A.V., Sunitha, M.S. and Philip, R. "Synthesis and Characterization of a New Conjugated Fluorescent Polymer Bearing Pyrazole and Thiophene Moieties as Potent NLO Material." *OPTICS'11: NIT Calicut, Kerala, INDIA*, May 23-25, 2011.
- iv. **Vishnumurthy K. A.**, Sunitha, M.S. and Adhikari, A.V. "Design and synthesis of thiophene based conjugated polymer with cyanopyridine spaces as potent optical limiting material." *International Conference on Synthetic & Structural Chemistry ICSSC-2011*, December 8-10, 2011 held a Mangalore University.
